ANALYSIS OF THE SUBUNIT INTERACTIONS IN α-ACTININ

Thesis submitted for the degree of Doctor of Philosophy at

the University of Leicester

by

GEOFFREY JOSEPH FLOOD B.Sc. (LIVERPOOL)

Department of Biochemistry and the National Centre for Macromolecular Hydrodynamics, University of Leicester

February 1997

ProQuest LLC
789 East Eisenhower Parkway
P.O. Box 1346
Ann Arbor, MI 48106-1346

ACKNOWLEDGEMENTS

I would like to thank a number of people for their help with this project. Firstly, I wish to acknowledge the fellow members of the laboratories I have worked in for useful discussion. These include Mark Holt, Dr. Lance Hemmings, Dr. Olwyn Byron, Alistair Clewlow, and Helena Silkowski. I also wish to thank Bipin Patel, Anil Pancholi, Nima Mistry, Evie Roberts, Stefan Hyman, and Dr. Edith Kahana (King's College, Drury Lane, London) for technical contributions. I would like to acknowledge Dr. Clive Bagshaw for guidance throughout my Ph.D. as a member of my committee. I would especially like to thank Professor Walter Gratzer (King's College, Drury Lane, London) for invaluable advice and discussion. I acknowledge support by a University of Leicester studentship. Finally, I would like to thank and acknowledge Dr. Arthur Rowe and Professor David Critchley, as my supervisors, for their essential assistance throughout my studies in the department.

This thesis is dedicated to my parents, without whose support this would have been impossible, and to Marion, for putting up with me.

ABBREVIATIONS

^{35}S ATP	^{35}S labelled adenosine triphosphate
α^{LELY}	human low-expression allele
A	adenine
$\overset{o}{A}$	angstrom
AAC1_HUMAN	human placental α-actinin
AAC2_HUMAN	human skeletal muscle α-actinin
AAC3_HUMAN	human skeletal muscle α-actinin
AACN_CHICK	chicken brain α-actinin
AACS_CHICK	chicken skeletal muscle α-actinin
AACT_CHICK	chicken smooth muscle α-actinin
AACT_DICDI	*Dictyostelium discoideum* α-actinin
AACT_DROME	*Drosophila melanogastor* α-actinin
ABD	actin-binding domain
ABP	actin-binding protein
ABS	actin-binding site
AJ	adherens junction
Ala	alanine
A_0	absorbance at reference radius r_0
APS	ammonium persulphate
A_r	absorbance at radius r
Arg	arginine
AUC	analytical ultracentrifuge
B	second virial coefficient
BM	excluded volume
BMD	Becker muscular dystrophy
bp	base pair
c	concentration of solute
C	cytosine
CALM_SCHPO	*Schizosaccharomyces pombe* calmodulin
CD	circular dichroism
cDNA	copy deoxyribonucleic acid
CH domain	calponin homology domain
cm^{-1}	per centimetre
c_0	initial concentration
c_p	concentration in the plateau region
C-terminal	carboxy-terminal

$\Delta G(H_2O)$	free energy of unfolding
DAG	diacylglycerol
DGC	dystrophin glycoprotein complex
DMD	Duchenne muscular dystrophy
DMD_CHICK	chicken dystrophin
DMD_HUMAN	human dystrophin
DMD_MOUSE	mouse dystrophin
DNA	deoxyribonucleic acid
DMS	dimethylsuberimidate
DTT	dithiothreitol
E	baseline offset
ECM	extra-cellular matrix
EDTA	diaminoethanetetra acetic acid
EF	EF-hand
EGTA	ethyleneglycol-bis (β-aminoethyl ether) N,N,N',N'-tetra acetic acid
exp	exponent
f	frequency of oscillation
f/f_0	frictional ratio
F-actin	filamentous actin
FPLC	fast protein liquid chromatography
g	gram
G	guanine
Glu	glutamate
GST	glutathione S-transferase
GTP	guanosine triphosphate
$\eta_{20,w}$	viscosity of water at 20 °C
η_s	solvent viscosoity
$\eta_{T,w}$	viscosity of water at the temperature of the experiment
η_w	viscosity of water
HEV	high endothelial venules
His	histidine
hrs	hours
ICAM	intercellular ahesion molecule
IP3	inositol 1,4,5-trisphosphate
IPTG	isopropylthio-β-D-galactoside
K_2PO_4	potassium phosphate
K_a	association constant
Ka_2HPO_4	potassium dihydrogen phosphate

kb	kilo-base
KCl	potassium chloride
K_d	dissociation constant
kDa	kilo-Dalton
k_s	concentration-dependence coefficient
kV	kilo-volt
l	litre
lb in^{-2}	pound per square inch
Leu	leucine
LFA-1	lymphocyte function-associated antigen-1
ln	natural logarithm
Lys	lysine
(-Δ8)	8-residue deletion
μM	micromolar
M	molar
M^{-1}	per mole
mA	milli-ampere
M_{app}	apparent molar weight,
MCS	multiple-cloning site
$MgCl_2$	magnesium chloride
$MgSO_4$	magnesium sulphate
mm	milimetre
mM	milimolar
MOPS	3-(N-morpholino) propane-sulphonic acid
M_w	weight-average molecular mass
Na_2ATP	disodium adenosine triphosphate
Na_2CTP	disodium cytosine triphosphate
Na_2HPO_4	disodium hydrogen phosphate
Na_2GTP	disodium guanosine triphosphate
Na_2TTP	disodium thiamine triphosphate
NaCl	sodium chloride
NaH_2PO_4	sodium dihydrogen phosphate
$NaHCO_3$	sodium hydrogen carbonate
NaOH	sodium hydroxide
$(NH_4)_2SO_4$	ammonium sulphate
NH_4Cl	ammonium chloride
NH_4CO_3	ammonium carbonate
nm	nanometre
nM	nanomolar

NM	non-muscle
NMDA	N-methyl-D-aspartate
NMJ	neuromuscular junction
NOE	nuclear Overhauser effect
NRM	nemaline rod myopathy
N-terminal	amino-terminal
ω	angular velocity
o	degree
^oC	degrees celcius
OD	optical density
PAGE	polyacrylamide gel electrophoresis
PBS	phosphate buffered saline
PCR	polymerase chain reaction
PDGF	platelet-derived growth factor
PEG 8000	polyethylene glycol 8000
pH	-log $[H^+]$
PH domain	pleckstrin-homology domain
PI 3-kinase	phosphatidylinositol 3-kinase
PIP_2	phosphatidylinositol 4,5-bisphosphate
PKC	protein kinase C
PLC	phospholipase C
pM	picomolar
PM	plasma membrane
PMSF	phenylmethyl-sulphonyl fluoride
Pro	proline
ρ	solvent density
$\rho_{20,w}$	density of water at 20 ^oC
$\rho_{T,s}$	solvent density at the temperature of the experiment
R	gas constant
$RbCl_2$	rubidium chloride
r_{bnd}	radial position of boundary
r_m	radial position of meniscus
RNAse	ribonuclease
rpm	revolutions per minute
s	sedimentation coefficient
S	Svedberg
s^0	sedimentation coefficient extrapolated to zero concentration
$s_{20,w}$	sedimentation coefficient expressed in terms of the standard solvent of water at 20 ^oC;

s^{-1}	per second
SDS	sodium dodecylsulphate
Ser	serine
SH domain	Src homology domain
s_{obs}	measured sedimentation coefficient
SP14_DROME	*Drosophila melanogastor* spectrin α14
SPCA_DROME	*Drosophila melanogastor* α-spectrin
SPCA_HUMAN	human erythroid α-spectrin
SPCB_DROME	*Drosophila melanogastor* β-spectrin
SPCB_HUMAN	human erythroid β-spectrin
SPCN_CHICK	chicken non-erythroid α-spectrin
SV 40	simian virus 40
$(\theta)_{222}$	molar residue ellipticity at 222 nm
T	thymine
TEM	transmission electron microscopy
TEMED	N.N.N',N'-tetramethyl ethylenediamine
T_m	temperature at the mid-point of the transition
TMV	tobacco mosaic virus
Tris	tris ((hydroxymethyl) amino methane)
Trp	tryptophan
UTRO_HUMAN	human utrophin
UV	ultraviolet
$\bar{v}$	partial specific volume
V_s	hydrated volume
v/v	volume per volume
W->I	tryptophan to isolecine substitution
W->R	tryptophan to arginine substitution
w/v	weight per volume
WT	wild-type
WW	di-tryptophan motif
Z	charge term
$ZnCl_2$	zinc chloride

GEOFFREY JOSEPH FLOOD

ANALYSIS OF THE SUBUNIT INTERACTIONS IN α-ACTININ.

Recombinant fragments of the chicken smooth muscle α-actinin rod domain, which contains 4 spectrin-like repeats, were used in an endeavour to discriminate between aligned and staggered models of the α-actinin homodimer. The results indicate that deletion of either of the terminal repeats, 1 or 4, drastically reduces the dimer formation, and an aligned rather than a staggered model most accurately explains these observations. This model was further confirmed by the demonstration of an interaction between the individual terminal repeats 1 and 4, which in a staggered model would seem to be futile. Mutation of a conserved tryptophan in repeat 1 of a polypeptide spanning the α-actinin rod domain resulted in a decrease in dimer stability compared to the native rod, although dissociation of the dimer still required denaturing conditions. When the effect of this mutation was examined in the isolated single repeat 1, a significant change in solubility was observed, and assumed to reflect a more drastic conformational alteration. A similar result was obtained when a predicted 8-residue insertion was deleted from the N-terminal region of the same repeat. A deletion of a predicted 8-residue insertion from the N-terminal region of repeat 4 also affected conformational stability, and eliminated the heterologous interaction with native repeat 1. However, when the predicted 8-residue insert in repeat 1 was deleted, in a polypeptide spanning the entire rod domain, no decrease in stability or dimer-forming ability was detected.

CHAPTER 1.

INTRODUCTION

1.1 THE α-ACTININ FAMILY OF ACTIN-BINDING PROTEINS

α-Actinin is a protein that belongs to a family of ubiquitous, cytoskeletal, actin-binding proteins which includes spectrin, dystrophin, and utrophin. These proteins play major structural roles in various cell-types, by interacting with filamentous actin and assisting in the maintenance of the cellular architecture, which is vital for structure and function of cells.

1.1.1 α-Actinin

α-Actinin was first identified as a component of the Z-line of skeletal muscle which promotes contraction of actomyosin gels and increases the viscosity of F-actin solutions (Ebashi *et al.*, 1964; Masaki *et al.*, 1967). It has subsequently been identified in many other tissues including intestinal epithelial cells (Craig and Pardo, 1979), lymphocytes (Hoessli *et al.*, 1980), macrophages (Bennet *et al.*, 1984), HeLa cells (Burridge and Feramisco, 1981), bovine blood platelets (Jockusch *et al.*, 1977), human blood platelets (Rosenberg and Stracher, 1981), chicken smooth muscle (Singh *et al.*, 1977), and chicken lung (Imamura and Masaki, 1992).

α-Actinin is an actin-binding and crosslinking protein, found where actin is anchored to a variety of intracellular structures (Figure 1). It is a homodimer with a subunit molecular mass of 94-103 kDa (Endo and Masaki, 1982; Landon *et al.*, 1985; Baron *et al.*, 1987). Electron microscopy of antibody-labelled molecules demonstrated the subunits are antiparallel in orientation (Wallraff *et al.*, 1986). It appears as a rod-shaped molecule in the electron microscope, 3-4 nm by 30-40 nm (Podlubnaya *et al.*, 1975; Bretscher *et al.*, 1979; Imamura *et al.*, 1988).

Sequence alignments suggest that α-actinin is composed of three domains: (1) an N-terminal actin-binding domain (ABD) of molecular weight 27-36 kDa, that is present in the proteins of the spectrin/filamin/fimbrin family (Sheterline *et al.*, 1995; Hartwig, 1995), and which also contains two calponin-homology (CH) domains (Castresana and Saraste, 1995); (2) four internal 122 amino acid repeats of molecular weight 55 kDa (Mimura and Asano, 1987; Imamura *et al.*, 1988); (3) and a C-terminal calmodulin-like region containing two EF-hand calcium binding motifs.

A number of distinct isoforms have been characterised. These include *Dictyostelium discoideum* (Noegel *et al.*, 1987; Witke *et al.*, 1986), *Drosophila* (Fyrberg *et al.*, 1990), nematode (Barstead *et al.*, 1991), chicken fibroblast/smooth muscle (Baron *et al.*, 1987), chicken skeletal muscle (Arimura *et al.*, 1988), chicken brain (Waites *et al.*, 1992), human cytoskeleton (Youssoufian *et al.*, 1990), human placenta (Millake *et al.*, 1989), and two human skeletal muscle isoforms (Beggs *et al.*, 1992). A major functional difference between the

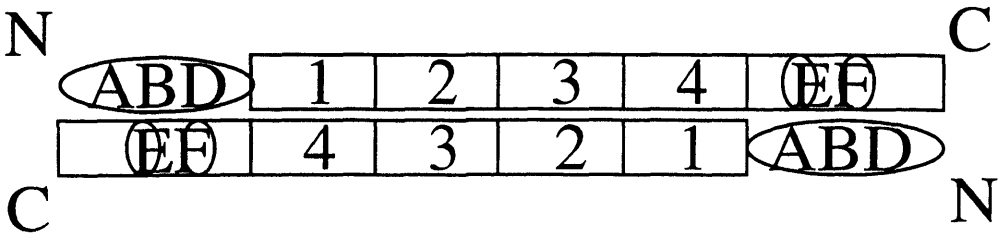

Figure 1: Proposed structure of the α-actinin homodimer. The actin-binding domain (ABD) contains two calponin-like motifs, and the EF-hands (EF) are similar to calmodulin.

muscle and non-muscle isoforms is that only the latter is calcium-sensitive in respect of actin-binding (Blanchard *et al.*, 1989).

Comparison of the sequence of α-actinin with other proteins shows extensive homology with erythroid and non-erythroid (fodrin) spectrins (Baron *et al.*, 1987; Wasenius *et al.*, 1987; Davison *et al.*, 1989) and with the protein encoded by the gene at the Duchenne muscular dystrophy locus, dystrophin (Koenig *et al.*, 1988; Hammonds, 1987; Davison and Critchley, 1988). The spectrin repeat is the predominant element in these members although the length of the repeat is slightly longer and less conserved in α-actinin and dystrophin.

1.1.2 Spectrin

Spectrin is a flexible, elongated, actin-cross-linking molecule (Figure 2). Most of the molecule is comprised of contiguous, homologous repeats approximately 106 residues in length (Speicher *et al.*, 1984; Speicher, 1985). 280 kDa α- and 246 kDa β-subunits associate side-to-side in an antiparallel orientation (Speicher *et al.*, 1982) to produce heterodimers that associate to form tetramers. It is a major component on the cytoplasmic face of the red cell membrane. However, non-erythroid spectrin is a ubiquitous structural protein which is present in most vertebrate tissues as well as in non-vertebrates such as *Drosophila* (Byers *et al.*, 1992; Dubreil *et al.*, 1989), *Dictyostelium* (Bennett and Condeelis, 1988), *C. elegans* (Bennett and Gilligan, 1993), echinoderms (Wessel and Chen, 1993) and possibly in higher plants (Maude *et al.*, 1991). The membrane skeleton of the human erythrocyte consists of a network of proteins that associates with the inner surface of the cell membrane and imparts structural integrity and flexibility to circulating erythrocytes. Spectrin tetramers cross-link short actin oligomers, an association modulated by band 4.1, to form a dynamic two-dimensional submembranous latticework (Bennett and Lambert, 1991; Morrow, 1989).

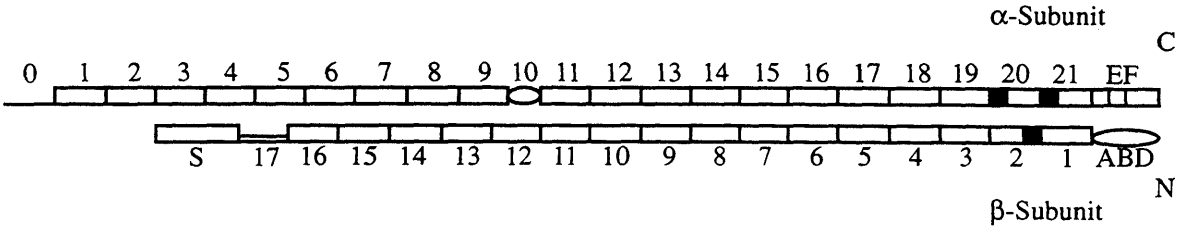

Figure 2: Model of spectrin structure. Black squares, 8-residue inserts; S: serine-rich region. Repeats α0 and β17 represent partial repeats involved in tetramer formation, and α10 consists of a Src-homology 3 (SH3) domain.

In the erythrocyte isoform, the β-subunit contains an N-terminal ABD, 16 complete spectrin repeats, an ankyrin-binding site in repeat 15, a partial spectrin repeat implicated in tetramerisation, and a serine-rich region at the C-terminus which is phosphorylated (Harris and Lux, 1980). The corresponding α-chain has a partial spectrin repeat at the N-terminus, 20 complete spectrin repeats, a Src-homology 3 (SH3) domain, which bind short proline-rich sequences (Ren *et al.*, 1994; Yu *et al.*, 1994), inserted inside the repeat number 9, and a calmodulin-like domain at the C-terminus. The non-erythroid β-subunit contains an additional proline/serine-rich region and a pleckstrin-homology (PH) domain, suggested to be involved in protein-protein or lipid-protein interactions, prior to the serine-rich C-terminal region. The vertebrate non-erythroid α-subunit contains an additional calmodulin-binding region inside repeat 10 (including the cleavage site for calcium-activated protease) (Harris *et al.*, 1988; Leto *et al.*, 1989), whilst in *Drosophila* this occurs in repeat 15 (Dubreuil *et al.*, 1989).

1.1.3 Dystrophin

Dystrophin is a 427 kDa protein encoded by a gene, which encompasses more than 65 exons spread over two million base pairs, on the Xp21 chromosome (Hoffman *et al.*, 1987; Koenig *et al.*, 1987; Koenig *et al.*, 1988; van Ommen *et al.*, 1987; Burmeister *et al.*, 1988). It is expressed in a wide range of tissues (Figure 3). Alternatively spliced forms of dystrophin exist. The longest molecule is made up of 3 domains: (1) a globular ABD at the N-terminal end; (2) a rod, comprising 24 degenerate spectrin-like repeating units (Davison and Critchley, 1988; Koenig *et al.*, 1988), separated by 4 proline-rich hinge regions (Koenig and Kunkel, 1990; Cross *et al.*, 1990); (3) and a C-terminal end comprising of a WW domain, two EF-hands, a cysteine-rich domain, and a helical region. In the sarcolemma, dystrophin is associated with six proteins, which bind at the C-terminal region, collectively called the dystrophin glycoprotein complex (DGC) (Ervasti *et al.*, 1991). The DGC apparently links the actin cytoskeleton to the extra-cellular matrix (ECM) (Ervasti and Campbell, 1993).

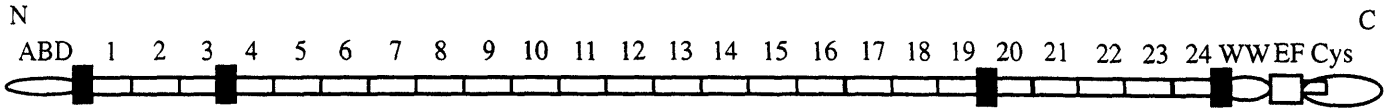

Figure 3: Domain structure of dystrophin: Black rectangles, hinge regions; WW, WW domain; Cys, cysteine-rich domain. The β-dystroglycan binding domain is located within the C-terminal end (WW-EF-Cys) of the protein.

Boys suffering from the recessive Duchenne muscular dystrophy (DMD), first described in the mid-1800s (Meryon, 1852; Duchenne, 1868) have severe muscle wasting manifesting after 3 to 5 years of age and leaving affected individuals wheel-chair bound by the age of 11. Early death due to respiratory failure ensues, and the disease is sometimes associated with mental retardation (30% incidence) (Zellweger and Hanson, 1967). Whereas total absence of dystrophin leads to severe (Duchenne) muscular dystrophy (Hoffman *et al.*, 1987), affecting approximately 1 in 3,500 males, many types of mutation result in much milder or intermediate forms of the disease (Becker) (BMD) (Moser, 1984). These are degenerative diseases caused by mutations of a single locus, the dystrophin gene. Thus, whereas deletions of the C-terminal or cysteine-rich domains invariably cause DMD, loss of the actin-binding domain or of large proportions of the rod are often associated with BMD (Ahn and Kunkel, 1993; Ohlendieck, 1996).

1.1.4 Utrophin

Utrophin, a 395 kDa dystrophin-related protein, is an autosomal homologue of dystrophin (Tinsley *et al.*, 1992). Unlike dystrophin, the utrophin gene is located on chromsome 6 (Love *et al.*, 1989). The protein is ubiquitously expressed (Nguyen *et al.*, 1991, 1992; Khurana *et al.*, 1992; Ohlendieck *et al.*, 1991; Pons *et al.*, 1991; Love *et al.*, 1991) and in muscle tissues the expression is developmentally regulated, occurring in foetal and regenerating muscle, where it could play a similar role to dystrophin in early development (Clerk *et al.*, 1993; Helliwell *et al.*, 1992; Khurana *et al.*, 1992; Takemitsa *et al.*, 1991). In normal adult muscle, utrophin is found primarily at the neuromuscular junction (NMJ), whilst it has been detected in the sarcolemma outside the NMJ in DMD and dystrophic (*mdx*) mouse (Khurana *et al.*, 1991; Man *et al.*, 1991; Takemitsu *et al.*, 1991). Since utrophin has a similar domain structure to dystrophin, lacking only 2 repeats and 2 hinges, it has been suggested that it could substitute for dystrophin in dystrophic muscle. One aproach would be to up-regulate expression of utrophin in patients suffering from DMD, since it has been shown that utrophin is found throughout the sarcolemma in small-calibre skeletal muscles and cardiac muscle of adult *mdx* mice (Karpati and Carpenter, 1986; Karpati *et al.*, 1988). It has been recently demonstrated in mice that utrophin can effectively rescue dystophin-deficient muscle (Tinsley *et al.*, 1996). Like

dystrophin, utrophin has been shown to localise to the membrane (Khurana *et al.*, 1992; Man *et al.*, 1991, 1992), and to be associated with a membrane-bound glycoprotein complex (Matsumura *et al.*, 1992).

1.2 ACTIN-BINDING DOMAINS OF THE α-ACTININ FAMILY

1.2.1 α-Actinin

α-Actinin has been shown to bind F-actin by actin co-sedimentation (Meyer *et al.*, 1990) and viscosity measurements (Goll *et al.*, 1972; Holmes *et al.*, 1971). This binding interaction is temperature dependent and affected by tropomyosin (Holmes *et al.*, 1971; Goll *et al.*, 1972; Maruyama, 1976; Rosenberg *et al.*, 1981; Bennet *et al.*, 1984; Landon *et al.*, 1985; Goll *et al.*, 1991). Under saturating conditions one α-actinin molecule binds for every 10 to 13 actin monomers (Goll *et al.*, 1972; Landon *et al.*, 1985). This corresponds to one α-actinin cross-link per turn of the actin filament helix.

The cytoskeleton is composed of three major classes of filaments, the microtubules, the intermediate filaments, and the microfilaments. Actin filaments, which are a double helix, form a large number of cytoskeletal structures under the influence of various cross-linking proteins. Actin bundles are closely cross-linked parallel arrays of actin filaments. *In vivo*, actin bundles are found in microvilli, stereocilia, and the acrosomal process among other places (Taylor and Taylor, 1994). Actin gels are much looser aggregations of randomly orientated filaments that occur as a supporting structure under the plasma membrane. Actin bundles and gels are formed by separate classes of proteins (Pollard and Cooper, 1986), but some proteins, such as α-actinin, are capable of forming both gels and bundles depending on conditions.

It has been shown that different isoforms of α-actinin have different actin-binding properties. Thus, chicken gizzard, *Dictyostelium*, and *Acanthamoeba* α-actinins are able to cross-link F-actin into networks, but *Dictyostelium* α-actinin is unable to bundle F-actin. Chicken gizzard and *Dictyostelium* α-actinins cross-link actin filaments in an antiparallel fashion, a characteristic unique of α-actinin, whereas *Acanthamoeba* cross-links in a parallel fashion (Meyer and Aebi, 1990). Interestingly, it has also been shown that different α-actinins have different dimensions. The length of α-actinin was shown to be 35 nm for chicken gizzard, 44 nm for *Acanthamoeba*, and 31 nm for *Dictyostelium* α-actinin (Meyer and Aebi, 1990). The length of α-actinin when bound to actin filaments was shown to be 36 nm for chicken gizzard and 35 nm for *Acanthamoeba*, a molecular length roughly coinciding with the cross-over repeat of the two-stranded F-actin helix, but only 28 nm for *Dictyostelium* α-actinin (Meyer and Aebi, 1990). The minimal longitudinal spacing between cross-linking α-actinin molecules along the adjacent actin filaments was 36 nm for both smooth muscle and *Acanthamoeba* α-actinin, but only 31

nm for *Dictyostelium* α-actinin (Meyer and Aebi, 1990). This suggests that the length of α-actinin may determine its spacing along the actin filament, and hence F-actin bundle formation may require one α-actinin molecule after the other, with their long axis parallel to the actin filament axes rather than twisting around the filaments (Meyer and Aebi, 1990).

Contradictory evidence suggests that chicken gizzard α-actinin can form bundles of parallel unipolar actin filaments (Taylor and Taylor, 1994). However, chicken gizzard α-actinin may cross-link both parallel and antiparallel actin filaments. In smooth muscle, α-actinin is localised to both adhesion plaques and cytoplasmic dense bodies (Schollmeyer *et al.*, 1976; Geiger *et al.*, 1981). Adhesion plaques are sites where actin filaments bind to the cell membrane, whereas cytoplasmic dense bodies are anchoring points for antiparallel actin filaments (Bond and Somlyo, 1982; Tsukita *et al.*, 1983). Since actin filaments typically originate from cell membranes in a unipolar orientation (Mooseker and Tilney, 1975, Begg *et al.*, 1978; Small *et al.*, 1978), if α-actinin localised to these regions is functioning as an actin filament cross-linker, it would have to be cross-linking unipolar filaments. Other α-actinin isoforms also probably differ in the specificity and orientation of their actin filament cross-links. Skeletal muscle I-segments treated with high salt to remove tropomyosin bind chicken gizzard α-actinin throughout their length, with 2 α-actinins per cross-link. This suggests self-association of α-actinin molecules (Sanger *et al.*, 1984), and unipolar cross-linking (Taylor and Taylor, 1994). In striated muscle α-actinin is found in the Z-disks (Masaki *et al.*, 1967; Lazarides and Granger, 1978), but not in the terminal segments of frog skeletal muscle where actin filaments are attached to the membrane (Tidball, 1987), suggesting a tendency to bundle antiparallel actin filaments. In the body wall muscle of the nematode, a protein immunologically related to α-actinin is localised to dense bodies but not to adhesion plaques of the same fibrils (Francis and Waterson, 1985).

Vertebrate α-actinins isolated from various non-muscle cells also exhibit large differences in their ability to assemble actin filaments. α-Actinin from HeLa cells (Burridge and Feramisco, 1981), rat liver (Kuo *et al.*, 1982; Ohtaki *et al.*, 1985), and macrophages (Bennett *et al.*, 1984) was found to have a gelation activity, or capacity to form actin networks instead of bundles, approximately 10-fold higher than α-actinin from brain (Duhaiman and Bamburg, 1984) and platelets (Landon *et al.*, 1985).

The ABD of α-actinin was located initially by proteolytic digestion. A 27 kDa thermolytic fragment of α-actinin was shown to retain F-actin-binding ability (Mimura and Asano, 1986). The binding of this fragment was calcium insensitive unlike the binding of the intact non-muscle isoform of α-actinin. At saturation, 1 ABD was bound to 3.2 actin monomers. α-Chymotrypsin produces a fragment of 36 kDa that also retained actin-binding ability (Imamura

```
AACT_CHICK    1 ------------------MDHHYDPQQ-TNDYMQPEEDWDRDL------LLDPAWEKQ-
AACN_CHICK    1 ------------------MDHHYDPQQ-TNDYMQPEEDWDRDL------LLDPAWEKQ-
AAC1_HUMAN    1 -------------------MDHYDSQQ-TNDYMQPEEDWDRDL------LLDPAWEKQ-
AAC3_HUMAN    1 -------MMMVMQPEGLGAGEGRFAGGGGGGEYMEQEEDWDRDL------LLDPAWEKQ-
AACS_CHICK    1 -------MNSMNQIETNMQYTYNYEED----EYMTQEEEWDRDL------LLDPAWEKQ-
AAC2_HUMAN    1 ----------MNQIEPGVQYNYVYDED----EYMIQEEEWDRDL------LLDPAWEKQ-
AACT_DROME    1 -------------MMMENGLSMEYGDG-----YMEQEEEWEREG------LLDPAWEKQ-
AACT_DICDI    1 ----------------------MSEE-------PTPVSGNDKQ------LLNKAWEIT-
SPCB_HUMAN    1 MTSATEFENVGNQPPYSRINARWDAPDDELDNDNSSARLFERSR------IKALADEREV
SPCB_DROME    1 --MTTDISIVRWDP--SQGPGNEYIDEYEYDGGNSSSRLFERSR------IKALAEERES
UTRO_HUMAN    1 ---------------------------MAKYGEHEASPDNGQNEFSDIIKSRSDEHND
DMD_CHICK     1 ------------------------MSAHVLWYEEVEDDYER----------------ED
DMD_HUMAN     1 ---------------------------MLWWEEVEDCYER----------------ED
DMD_MOUSE     1 ---------------------------MLWWEEVEDCYER----------------ED

                  ___ABS1___
AACT_CHICK   34 -QRKTFTAWCNSHLRKAG-TQIENIEEDFRDGLKLMLLLEVISGERLAKPERG--KMRVH
AACN_CHICK   34 -QRKTFTAWCNSHLRKAG-TQIENIEEDFRDGLKLMLLLEVISGERLAKPERG--KMRVH
AAC1_HUMAN   33 -QRKTFTAWCNSHLRKAG-TQIENIEEDFRDGLKLMLLLEVISGERLAKPERG--KMRVH
AAC3_HUMAN   47 -QRKTFTAWCNSHLRKAG-TQIENIEEDFRNGLKLMLLLEVISGERLPRPDKG--KMRFH
AACS_CHICK   43 -QRKTFTAWCNSHLRKAG-TQIENIEEDFRNGLKLMLLLEVISGERLPKPDRG--KMRFH
AAC2_HUMAN   40 -QRKTFTAWCNSHLRKAG-TQIENIEEDFRNGLKLMLLLEVISGERLPKPDRG--KMRFH
AACT_DROME   36 -QKKTFTAWCNSHLRKAG-TAIDNIEEDFRNGLKLMLLLEVISGETLPKPDRG--KMRFH
AACT_DICDI   23 -QKKTFTAWCNSHLRKLG-SSIEQIDTDFTDGIKLAQLLEVISNDPVFKVNKTPKLRRIH
SPCB_HUMAN   55 VQKKTFTKWVNSHLARVS-CRITDLYKDLRDGRMLIKLLEVLSGEMLPKPTKG--KMRIH
SPCB_DROME   51 VQKKTFTKWVNSHLCRVN-CRIADLYVDMRDGKHLIKLLEVLSGERLPKPTKG--KMRIH
UTRO_HUMAN   32 VQKKTFTKWINARFSKSGKPPINDMFTDLKDGRKLLDLLEGLTGTSLPKERGS---TRVH
DMD_CHICK    20 VQKKTFTKWINAQFAKCGRRCIEDLFNDFRDGRKLLELLECLTGQKIAKEKGS---TRVH
DMD_HUMAN    16 VQKKTFTKWVNAQFSKFGKQHIENLFSDLQDGRRLLDLLEGLTGQKLPKEKGS---TRVH
DMD_MOUSE    16 VQKKTFTKWINAQFSKFGKQHIDNLFSDLQDGKRLLDLLEGLTGQKLPKEKGS---TRVH
                 *.**** * *.. .     *  .  *   *  *  *** ...  . .        * *

                                  ___________ABS2___________              __
AACT_CHICK   90 KISNVNKALDFIASKGVKLVSIGAEEIVDGNVKMTLGMIWTIILRFAIQDISVEET----
AACN_CHICK   90 KISNVNKALDFIASKGVKLVSIGAEEIVDGNVKMTLGMIWTIILRFAIQDISVEET----
AAC1_HUMAN   89 KISNVNKALDFIASKGVKLVSIGAEEIVDGNVKMTLGMIWTIILRFAIQDISVEET----
AAC3_HUMAN  103 KIANVNKALDFIASKGVKLVSIGAEEIVDGNLKMTLGMIWTIILRFAIQDISVEET----
AACS_CHICK   99 KIANVNKALDYIASKGVKLVSIGAEEIVDGNVKMTLGMIWTIILRFAIQDISVEET----
AAC2_HUMAN   96 KIANVNKALDYIASKGVKLVSIGAEEIVDGNVKMTLGMIWTIILRFAIQDISVEET----
AACT_DROME   92 KIANVNKALDFIASKGVHLVSIGAEEIVDGNLKMTLGMIWTIILRFAIQDISVEEM----
AACT_DICDI   81 NIQNVGLCLKHIESHGVKLVGIGAEELVDKNLKMTLGMIWTIILRFAIQDISIEEL----
SPCB_HUMAN  112 CLENVDKALQFLKEQRVHLENMGSHDIVDGNHRLVLGLIWTIILRFQIQDIVVQTQEGRE
SPCB_DROME  108 CLENVDKALQFLREQRVHLENIGSHDIVDGNASLNLGLIWTIILRFQIQDITIEEVDNKE
UTRO_HUMAN   89 ALNNVNRVLQVLHQNNVELVNIGGTDIVDGNHKLTLGLLWSIILHWQVKDVMKDVMSDLQ
DMD_CHICK    77 ALNNVNKALQILQRNNVDLVNIGSSDIVDGNHKLTLGLIWNIILHWQVKDVMKNIMAGLQ
DMD_HUMAN    73 ALNNVNKALRVLQNNNVDLVNIGSTDIVDGNHKLTLGLIWNIILHWQVKNVMKNIMAGLQ
DMD_MOUSE    73 ALNNVNKALRVLQKNNVDLVNIGSTDIVDGNHKLTLGLIWNIILHWQVKNVMKTIMAGLQ
                  . **   *  .    * *  .*  ..** *  . **..* ***.  .. .

                  ______ABS3______
AACT_CHICK  146 --SAKEGLLLWCQRKTAPYKNVNIQNFHISWKDGLGFCALIHRHRPELIDYGKLRK-DDP
AACN_CHICK  146 --SAKEGLLLWCQRKTAPYKNVNIQNFHISWKDGLGFCALIHRHRPELIDYGKLRK-DDP
AAC1_HUMAN  145 --SAKEGLLLWCQRKTAPYKNVNIQNFHISWKDGLGFCALIHRHRPELIDYGKLRK-DDP
AAC3_HUMAN  159 --SAKEGLLLWCQRKTAPYRNVNVQNFHTSWKDGLALCALIHRHRPDLIDYAKLRK-DDP
AACS_CHICK  155 --SAKEGLLLWCQRKTAPYRNVNIQNFHLSWKDGLGLCALIHRHRPDLIDYSKLNK-DDP
AAC2_HUMAN  152 --SAKEGLLLWCQRKTAPYRNVNIQNFHTSWKDGLGLCALIHRHRPDLIDYSKLNK-DDP
AACT_DROME  148 --TAKEGLLLWCQRKTAPYKNVNVQNFHLSFKDGLAFCALIHRHRPDLIDYAKLSK-DNP
AACT_DICDI  137 --SAKEALLLWCQRKTEGYDRVKVGNFHTSFQDGLAFCALIHKHRPDLINFDSLNK-DDK
SPCB_HUMAN  172 TRSAKDALLLWCQMKTAGYPHVNVTNFTSSWKDGLAFNALIHKHRPDLIDFDKLKD-SNA
SPCB_DROME  168 TKSAKDALLLWCQMKTAGYHNVNVRNFTTSWRDGLAFNAIIHKHRPDLVQFEKLSK-TNA
UTRO_HUMAN  149 QTNSEKILLSWVRQTTRPYSQVNVLNFTTSWTDGLAFNAVLHRHKPDLFSWDKVVK-MSP
DMD_CHICK   137 QTNSEKILLSWVRQSTRNYPQVNVINFTSSWSDGLAFNALLHSHRPDLFDWNAVASQQSP
DMD_HUMAN   133 QTNSEKILLSWVRQSTRNYPQVNVINFTTSWSDGLALNALIHSHRPDLFDWNSVVCQQSA
DMD_MOUSE   133 QTNSEKILLSWVRQSTRNYPQVNVINFTSSWSDGLALNALIHSHRPDLFDWNSVVSQHSA
                   .   ** * .  *  *  * . **  *  ***   *..* *.*.*     .
```

```
AACT_CHICK  203 LTNLNTAFDVAEKYLDIPKMLDAEDIVGTARPDEKAIMTYVSSFYHAFSGAQKAETAANR
AACN_CHICK  203 LTNLNTAFDVAEKYLDIPKMLDAEDIVGTARPDEKAIMTYVSSFYHAFSGAQKAETAANR
AAC1_HUMAN  202 LTNLNTAFDVAEKYLDIPKMLDAEDIVGTARPDEKAIMTYVSSFYHAFSGAQKAETAANR
AAC3_HUMAN  216 IGNLNTAFEVAEKYLDIPKMLDAEDIVNTPKPDEKAIMTYVSCFYHAFAGAEQAETAANR
AACS_CHICK  212 IGNINLAMEIAEKHLDIPKMLDAEDIVNTPKPDERAIMTYVSCFYHAFAGAEQAETAANR
AAC2_HUMAN  209 IGNINLAMEIAEKHLDIPKMLDAEDIVNTPKPDERAIMTYVSCFYHAFAGAEQAETAANR
AACT_DROME  205 LENLNTAFDVAEKYLDIPRMLDPDDLINTPKPDERAIMTYVSCYYHAFQGAQQAETAANR
AACT_DICDI  194 AGNLQLAFDIAEKELDIPKMLDVSDMLDVVRPDERSVMTYVAQYYHHFSASRKAETAGKQ
SPCB_HUMAN  231 RHNLEHAFNVAERQLGIIPLLDPEDVFTE-NPDEKSIITYVVAFYHYFSKMKVLAVEGKR
SPCB_DROME  227 IHNLNNAFDVAEDKLGLAKLLDAEDVFVE-HPDEKSIITYVVTYYHYFSKLKQETVQGKR
UTRO_HUMAN  208 IERLEHAFSKAQTYLGIEKLLDPEDVAVR-LPDKKSIIMYLTSLFEVLP-----------
DMD_CHICK   196 VQRLDHAFNIARQHLGIEKLLDPEDVATA-CPDKKSILMYVTSLFQVLPQQVTMEA----
DMD_HUMAN   192 TQRLEHAFNIARYQLGIEKLLDPEDVDTT-YPDKKSILMYITSLFQVLPQQVSIEA----
DMD_MOUSE   192 TQRLEHAFNIAKCQLGIEKLLDPEDVATT-YPDKKSILMYITSLFQVLPQQVSIEA----
                   .  *   *   * .  .**  *.     ** .... *.   .

AACT_CHICK  262 ICKVL
AACN_CHICK  262 ICKVL
AAC1_HUMAN  261 ICKVL
AAC3_HUMAN  275 ICKVL
AACS_CHICK  271 ICKVL
AAC2_HUMAN  268 ICKVL
AACT_DROME  264 ICKVL
AACT_DICDI  253 VGKVL
SPCB_HUMAN  289 VGKVI
SPCB_DROME  285 IGKVV
UTRO_HUMAN      -----
DMD_CHICK       -----
DMD_HUMAN       -----
DMD_MOUSE       -----
```

Figure 4: Sequence alignment of actin-binding domains using Clustal V. Chicken smooth muscle α-actinin (AACT_CHICK, residues 1-267) (Baron *et al.*, 1987; J03486), chicken brain α-actinin (AACN_CHICK, 1-267) (Waites *et al.*, 1992; M74143), human placental α-actinin (AAC1_HUMAN, 1-266) (Millake *et al.*, 1989; X15804), human skeletal muscle α-actinin (AAC3_HUMAN, 1-280) (Beggs *et al.*, 1992; M86407), chicken skeletal muscle α-actinin (AACS_CHICK, 1-276) (Arimura *et al.*, 1988; X13874), human skeletal muscle α-actinin (AAC2_HUMAN, 1-273) (Beggs *et al.*, 1992; M86406), *Drosophila* α-actinin (AACT_DROME, 1-269) (Fyrberg *et al.*, 1990; X51753), *Dictyostelium* α-actinin (AACT_DICDI, 1-258) (Noegel *et al.*, 1987; Y00689), human erythroid β-spectrin (SPCB_HUMAN, 1-294) (Winkelmann *et al.*, 1990; J05500), *Drosophila* β-spectrin (SPCB_DROME, 1-290) (Byers *et al.*, 1989; M92288), human utrophin (UTRO_HUMAN, 1-255) (Tinsley *et al.*, 1992; X69086), chicken dystrophin (DMD_CHICK, 1-251) (Lemaire *et al.*, 1988; X13369), human dystrophin (DMD_HUMAN, 1-247) (Koenig *et al.*, 1988; X06179), mouse dystrophin (DMD_MOUSE, 1-247) (Koenig *et al.*, 1987; M18025). Star denotes conservation of residue and dot indicates chemical similarity. Actin-binding sites determined in chicken smooth muscle α-actinin are bold and underlined, whilst those in human dystrophin are bold and underlined, and labelled ABS1-3.

et al., 1988), and it was shown that this fragment was derived from the N-terminus of α-actinin (Singh *et al.*, 1977; Baron *et al.*, 1987; Imamura *et al.*, 1988).

A thermolysin-sensitive cut site is present near the centre of the ABD (Hemmings *et al.*, 1992) suggesting the presence of two domains. Later studies showed that the actin-binding site was located between residues 108 and 189 (Hemmings *et al.*, 1992), and was further localised to residues 120-134 (Kuhlman *et al.*, 1992) (Figure 4). Amino acid substitutions within this region indicate that several highly conserved hydrophobic residues are involved in binding to F-actin, and binding between α-actinin and F-actin is relatively independent of salt concentration suggesting the interaction is predominantly hydrophobic in nature (Kuhlman *et al.*, 1992). The 27 kDa actin-binding fragment of chicken α-actinin has been shown to bind at two sites of actin, the first between residues 1-12, the second involving residues spanning 86-119 or 123 (Mimura and Asano, 1987). In decorated filaments, the lower half of the ABD rests on the front face of actin whereas the upper portion is orientated more towards the back of actin (Figure 5). Because of its size, the ABD overlaps the top portion of subdomain 1 of actin on the same monomer as well as the bottom portion of the subdomain 1 on the next monomer up the two-start helix (McGough *et al.*, 1994). Gelsolin binds actin filaments at the fast-growing (barbed) end and nucleates polymerisation (Doi and Frieden, 1984). It has been shown that gelsolin binds two actin monomers which are diagonally adjacent along the short-pitch helix of actin (Doi, 1992). The orientation of monomers in the gelsolin nucleator is across the actin filament (McLaughlin *et al.*, 1993). In contrast, α-actinin binds two monomers along the long-pitch helix and does not nucleate polymerisation. However, interestingly, the ABD can functionally replace S2-3, an F-actin-binding domain in gelsolin (Way et al., 1992).

Actin bundling is favoured by high actin concentrations with an α-actinin/actin molar ratio in excess of 0.05:1, and an apparent binding constant of 0.4 μM for the interaction between chicken gizzard smooth muscle α-actinin and F-actin at 22 °C has been estimated (Meyer and Aebi, 1990). The actin saturated at a stoichiometry of 0.07 mol α-actinin/mol actin monomer. An equilibrium constant of 0.59 μM with a stoichiometry of 1 mol/mol under comparable conditions has also been deduced (Wachsstock *et al.*, 1993). Using the ABD of chicken smooth muscle α-actinin the equilibrium binding constant was estimated to be 4.7 μM (Way *et al.*, 1992). More recently, it was shown that ABD binds to F-actin yielding second order rate constants for association of 2×10^5, 1.8×10^6 and 4×10^6 M^{-1} s^{-1} at 5 °C, 15 °C and 25 °C, respectively (Kuhlman *et al.*, 1994). At the latter two temperatures, the dissociation rate constants were 1.5 and 9.6 s^{-1}, giving equilibrium constants of 0.83 and 2.4 μM, respectively. A reduction in binding affinity with increasing temperature also implicates hydrophobic interactions in the binding of α-actinin to F-actin.

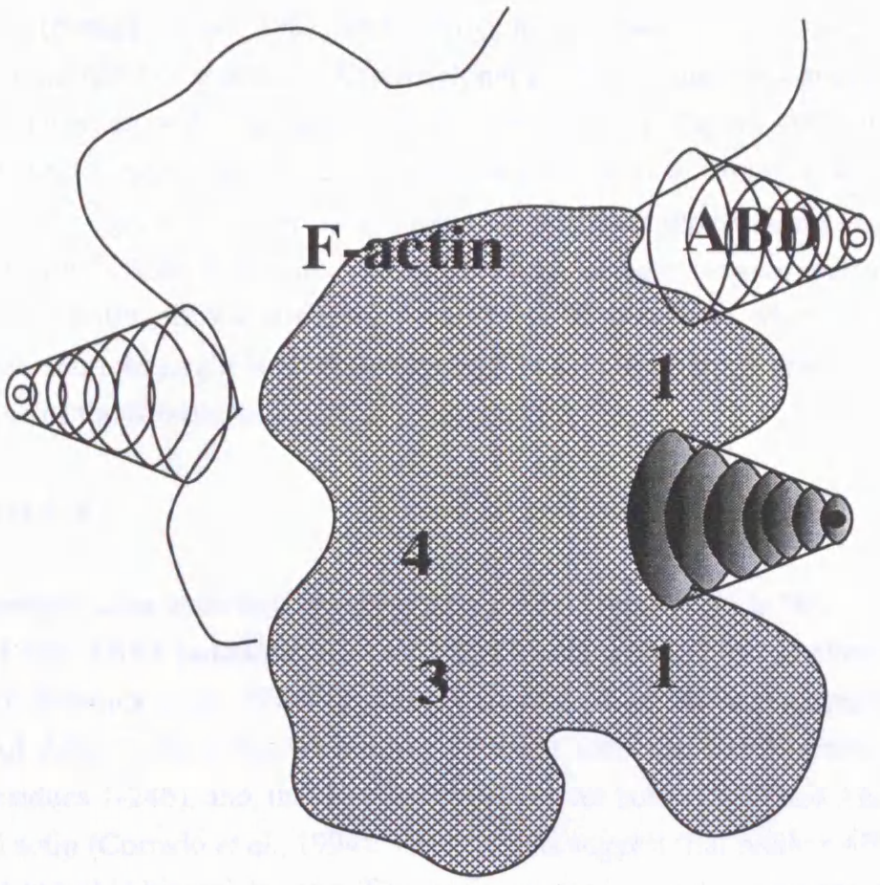

Figure 5: Orientation of the monomeric actin-binding domain of α-actinin along the F-actin filament. Numbers represent the subdomains of actin monomers. The lower part of the ABD makes contact with the interface between actin subdomains 1 and 2 (where subdomain 2 is obscured by the ABD), whilst the upper portion interacts with subdomain 1 of the next actin monomer in the filament (adapted from McGough *et al.*, 1994).

It has been proposed that the ABD of α-actinin is homologous to the N-terminal domain of calponins (Vancompernolle *et al.*, 1990). Calponins are a family of proteins, mainly involved in the regulation of smooth muscle contraction. Calponins consist of a unique N-terminal domain followed by one to three calponin repeats. Both α-actinin actin-binding subdomains share significant homology with the calponin domain. The structure of the CH domain is mainly α-helical with four α-helices (Rost and Sander, 1994). The structural and functional independence of the CH domain is demonstrated by a neuronal protein which appears to be exclusively made of this domain, and by a protein of unknown function that contains a single CH domain which seems to be evolutionarily closely related to the second domain in α-actinin (Castresana and Saraste, 1995).

There is a high degree of sequence similarity between the ABD in different species and isoforms (Figure 4). The N-terminal 250 amino acids of the 120 kDa *Dictyostelium* actin

gelation factor (Noegel *et al.*, 1987) and *Drosophila* β-spectrin have been shown to be homologous to the ABD of α-actinin. A monoclonal antibody which recognises an epitope in the ABD of chicken smooth α-actinin also cross-reacts with filamin (Mimura and Asano, 1986). Inspection of the aligned N-terminal regions of the α-actinins, dystrophin and the *Dictyostelium* actin gelation factor have shown 66 positions where amino acid identity is absolutely conserved (Blanchard *et al.*, 1989). Similarly, in the extensive sequence alignment of the α-actinin family, shown in Figure 4, there are 57 positions where amino acids are identical. These residues might be directly involved in actin-binding or they might define the overall structure of the N-terminal region of these proteins.

1.2.2 Dystrophin

Dystrophin contains three actin-binding sites (ABS): ABS1 (amino acids 18-27), ABS2 (amino acids 91-117) and ABS3 (amino acids 131-148) (Levine *et al.*, 1992; Levine *et al.*, 1990; Higuchi, 1990; Bresnick *et al.*, 1991) (Figure 4). It has been shown that a synthetic 27 amino acid peptide of ABS2 fails to inhibit binding between actin and the N-terminal domain of dystrophin (residues 1-246), and, that a constuct deleted for both ABS2 and ABS3 retains the ability to bind actin (Corrado *et al.*, 1994). These results suggest that neither ABS2 nor ABS3 is critical for dystrophin binding to actin. The results are similar to those observed for α-actinin in which the first 107 amino acids were shown to bind actin in the absence of ABS2 (Kuhlman *et al.*, 1992). However, in the case of α-actinin, the binding between ABS1 and actin appears to be weaker than that of ABS2 and actin, whereas for dystrophin, the construct containing ABS1 alone exhibited an actin-binding activity similar to that of the construct containing all three binding sites. Deleting the highly conserved amino acids KTFT, of ABS1 in dystrophin has little effect on the ability of dystrophin residues 1-90 to bind actin (Corrado *et al.*, 1994). This is consistent with results from mutational analysis of this same region of α-actinin where it was shown that the same amino acids, KTFT, were not essential for its binding to actin (Hemmings *et al.*, 1992). In the α-actinin study, the actin-binding site ABS2 was still present in the KTFT deletion construct, possibly accounting for its actin-binding ability. It has been reported that amino acids 1-68 of dystrophin are capable of binding actin, and it has been suggested that there is an inhibitory effect of the ABS2 site on the ABS1 site (Fabbrizio *et al.*, 1993). The fact that residues 1-90 displays a greater binding affinity than residues 1-130 (Corrado *et al.*, 1994) suggests that the latter may contain a region that inhibits binding to actin in the absence of amino acids 131-246.

A variety of studies have demonstrated binding of bacterial expressed dystrophin protein fragments with F-actin in vitro. Proposed K_d for this interaction range from 44 μM to 100 nM (Way *et al.*, 1992; Fabbrizio *et al.*, 1993; Corrado *et al.*, 1994). Several groups have studied the binding of full-length dystrophin to actin. A K_d for purified dystrophin in the nM range has

been detected (Senter *et al.*, 1993), and it has been demonstrated that dystrophin-enriched membranes or the dystrophin-glycoprotein complex are able to bind actin (Fabbrizio *et al.*, 1993; Ervasti and Campbell, 1993). While these results support the idea that actin and dystrophin form a direct interaction, they do not rule out the possibility that other proteins facilitate this interaction.

The sites identified by sequence homology may not all behave similarly with respect to their actin-binding activity. It has been shown that α-actinin does not inhibit the binding of purified dystrophin to actin (Senter *et al.*, 1993). This suggests that the sites on actin with which the two proteins interact are independent and presents the possibility that dystrophin and α-actinin interact with actin by different mechanisms, perhaps requiring additional binding sites and/or other interacting proteins.

1.2.3 Utrophin

Expressed regions of the predicted actin-binding domain in the N-terminus of utrophin are able to bind to F-actin in vitro (Winder *et al.*, 1995). The utrophin ABD was also able to associate with actin-containing structures, stress fibres and focal contacts, when microinjected into chicken embryo fibroblasts. The N-terminal 261 amino acid domain of utrophin has an affinity for skeletal F-actin, midway between that of the corresponding domains of α-actinin and dystrophin. Thus in non-muscle and developing muscle, utrophin performs the same predicted spacer or shock absorber role as dystrophin in mature muscle tissues, suggesting that utrophin could replace dystrophin functionally in dystrophic muscle (Winder *et al.*, 1995).

1.3 STRUCTURE OF THE ROD DOMAIN OF THE α-ACTININ FAMILY

1.3.1 α-Actinin

Chymotryptic cleavage of chicken gizzard smooth muscle α-actinin results in a rod-shaped, 55 kDa fragment, of size 25 x 4 nm, containing four spectrin-like repeats (Imamura *et al.*, 1988). Circular dichroism demonstrated that the α-helical content of this fragment was 14% higher than that of native gizzard α-actinin. Cross-linking generated a 110 kDa fragment from two 55 kDa fragments, indicating that it is the repeats that are responsible for dimer formation. It has also been shown that the fragment exists in solution as an extremely stable dimer, which is dissociated only under denaturing conditions, with the association constant not less than 10^{11} M^{-1} (Kahana and Gratzer, 1991). Hence it is thought that this region of the protein is responsible for the formation of the antiparallel dimer. The central region of α-actinin contains four internal repeats of about 122 amino acids, homologous to the 106 residue repeats in spectrin (Speicher *et al.*, 1984) and the approximately 110 residue repeats found in dystrophin

(Davison and Critchley, 1988; Koenig *et al.*, 1988). Each repeat has a molecular weight of about 12.5 kDa. Cross-linking results suggest that a site somewhere in repeats 1 and/or 2 of one subunit interact with repeat 4 of the other subunit (Imamura *et al.*, 1988).

A number of models have been advanced for the structure of these repeats. A bundle of three α-helices of similar length, connected by a flexible loop to the next bundle to form a rodlike domain, was first proposed for α-spectrin (Speicher and Marchesi, 1984). Analysis of the repeats of dystrophin (Koenig *et al.*, 1988) led to a modification of this scheme, such that the motif consisted of one long helix followed by a β-turn, followed by a short helix and another β-turn. A three-α-helix motif was then generated from this arrangement by each motif incorporating part of the long helix from the successive repeat. A similar scheme for spectrin and α-actinin was advanced (Dubreil *et al.*, 1989). It has also been recognised that the α-helical regions in the spectrin superfamily contain a heptad substructure (Stewart and McLachlan, 1975; McLachlan and Stewart, 1975; McLachlan and Karn, 1983) of the form $(a\text{-}b\text{-}c\text{-}d\text{-}e\text{-}f\text{-}g)_n$ where *a* and *d* are generally occupied by apolar residues (Cohen and Parry, 1986; Koenig *et al.*, 1988; Cross *et al.*, 1989). Such a pattern is characteristic of proteins in which two or three right-handed α-helices wind around one another in a left-handed manner to generate a coiled-coil stabilised by optimal knob-hole packing of the apolar residues in the *a* and *d* positions (Cohen and Parry, 1986, 1990). A structural model for the members of the spectrin superfamily was then postulated where the α-helical segments pack together in a common way involving antiparallel coiled-coils, and differences in the chemical repeat length were localised to the linking regions. The precise boundaries of these repeats were initially unidentified, although tentative boundaries based on the initial sequence alignments of the four repeats in chicken smooth muscle α-actinin were made (Baron *et al.*, 1987). Repeat 1 was predicted to begin at approximately residue 245. The N-terminal sequences of 50-55 kDa polypeptides liberated from α-actinin by several proteases suggested that the repeats started in the vicinity of residue 266 (Imamura *et al.*, 1988; Davison *et al.*, 1989), approximately 21 residues C-terminal to the predicted start point. Interestingly, it was demonstrated that the repeats in spectrin started 26 residues C-terminal to the site predicted by multiple sequence alignments (Winograd *et al.*, 1991). The criteria for an independently folding unit was resistance to proteolysis and the high α-helicity characteristic of the native protein. The repeat boundaries established in this way for α-actinin differed from those originally deduced from sequence alignments. The N-terminal boundaries of the repeats were 14-24 residues nearer the C-terminus than predicted (Gilmore *et al.*, 1994). These studies have revealed a stable, highly α-helical segment very closely similar in sequence to the motif predicted for the spectrin superfamily (Parry *et al.*, 1992). The N- and C-termini of these fragments correspond almost exactly to the motif between two C/A junctions. The number of structural repeats (complete triple-helices) forming the rod domains in α-spectrin and α-actinin will be one less than the number of chemical repeats (coordinates based upon sequence alignment). This results from the partial structural repeat comprising the

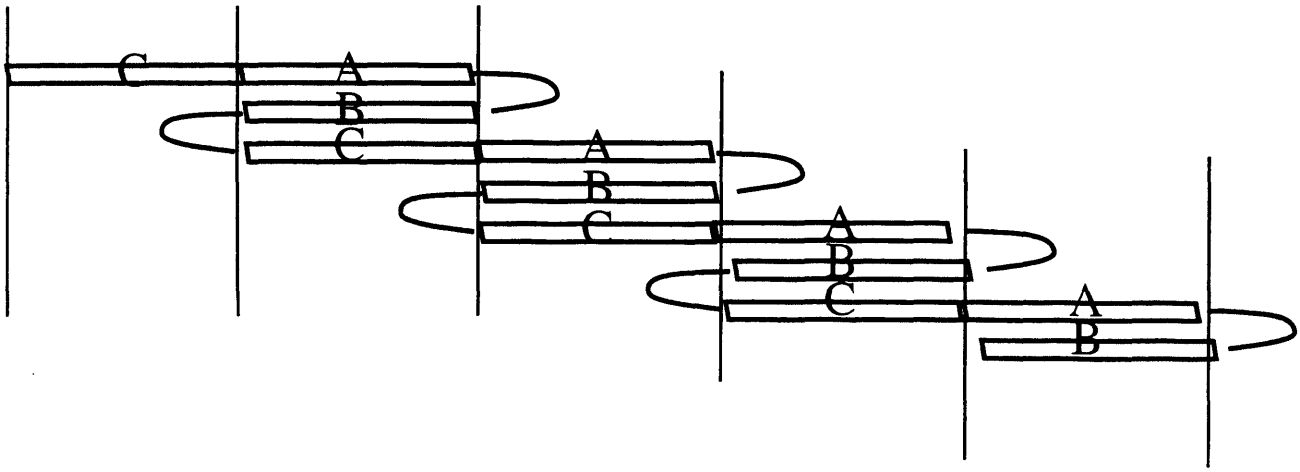

Figure 6: Structural model for the repeating units of the α-actinin family. The number of chemical repeats (C-A-B) in monomeric conformation is one more than the number of structural repeats (A-B-C). When a dimer forms, the helix C of one molecule would pair with helices A and B of the other, generating two more complete structural repeats.

C helix at the N-terminal end of the rod, and the A and B helices at the C-terminal end. However, when a dimer forms, the C helix of molecule 1 could pair with the A and B helices of molecule 2. This arrangement would generate two more 3-α-helix motifs than in a single molecule (Parry *et al.*, 1992) (Figure 6).

Alignment of the individual repeats across species found in α-actinin have shown that repeat 1 displays a greater level of identity than repeats 2-4 (Blanchard *et al.*, 1989) (Figure 7). Also the C-terminal part of repeat 3 displays a greater divergence than the N-terminal region. Analysis of the repeats has revealed that the level of identity between a given repeat across species is greater than that between the four repeats within the same species. The residues in each repeat which are highly conserved across species suggest that they fulfil some critical function.

The consensus sequence for the repeats in the α-actinin family shows no positions where amino acid identity is absolutely conserved, but there are 45 positions where the physicochemical property of the amino acid is maintained (Davison *et al.*, 1989). The spectrin repeats have 56, and the dystrophin repeats 67 such positions. Comparison of the α-actinin and spectrin repeats show that they share 25 positions where residues of similar property are conserved. Of these, 16 are conserved in the first 10 dystrophin repeats. Further inspection shows that the dystrophin consensus is no more similar to the spectrin consensus than to the α-actinin consensus (Blanchard *et al.*, 1989).

The positions of the conserved residues in both the α-actinin and spectrin repeats show a distinct clustering. Inspection of the level of amino acid identity between all possible

REPEAT 1 (β1)

```
AACT_CHICK  268 AVNQENEQLMEDYEKLASDLLEWIRRTIPWLENRAPENTMQAMQQKLEDFRDYRRLHKPP
AACN_CHICK  268 AVNQENEQLMEDYEKLASDLLEWIRRTIPWLENRAPENTMQAMQQKLEDFRDYRRLHKPP
AAC1_HUMAN  267 AVNQENEQLMEDYEKLASDLLEWIRRTIPWLENRVPENTMHAMQQKLEDFRDYRRLHKPP
AACS_CHICK  277 AVNQENERLMEEYERLASELLEWIRRTIPWLENRTPEKTMQAMQKKLEDFRDYRRKHKPP
AAC2_HUMAN  274 AVNQENERLMEEYERLASELLEWIRRTIPWLENRTPEKTMQAMQKKLEDFRDYRRKHKPP
AAC3_HUMAN  281 AVNQENEKLMEEYEKLASELLEWIRRTVPWLENRVGEPSMSAMQRKLEDFRDYRRLHKPP
AACT_DROME  270 KVNQENERLMEEYERLASDLLEWIRRTMPWLNSRQADNSLAGVQKKLEEYRTYRRKHKPP
AACT_DICDI  259 DTFMLLEQTKSDYLKRANELVQWINDKQASLESRDFGDSIESVQSFMNAHKEYKKTEKPP
SPCB_DROME  291 GIAMENDKMVHDYENFTSDLLKWIETTIQSLGEREFENSLAGVQGQLAQFSNYRTIEKPP
SPCB_HUMAN  295 DHAIETEKMIEKYSGLASDLLTWIEQTITVLNSRKFANSLTGVQQQLQAFSTYRTVEKPP
                      ..    *   . .*. **      *  *    ..  .*  .     *.   ***

AACT_CHICK  328 KVQEKCQLEINFNTLQTKLRLSNRPAFMPSEGKMVSDINNAWGGLEQAEKGYEEWLLNEI
AACN_CHICK  328 KVQEKCQLEINFNTLQTKLRLSNRPAFMPSEGKMVSDINNAWGGLEQAEKGYEEWLLNEI
AAC1_HUMAN  327 KVQEKCQLEINFNTLQTKLRLSNRPAFMPSEGRMVSDINNAWGCLEQVEKGYEEWLLNEI
AACS_CHICK  337 KVQEKCQLEINFNTLQTKLRISNRPAFMPSEGKMVSDIAGAWQRLEQAEKGYEEWLLNEI
AAC2_HUMAN  334 KVQEKCQLEINFNTLQTKLRISNRPAFMPSEGKMVSDIAGAWQRLEQAEKGYEEWLLNEI
AAC3_HUMAN  341 RIQEKCQLEINFNTLQTKLRLSHRPAFMPSEGKLVSDIANAWRGLEQVEKGYEDWLLSEI
AACT_DROME  330 RVEQKAKLETNFNTLQTKLRLSNRPAYLPTEGKTVSDISNSWKGLELAEKGFEEWLLAET
AACT_DICDI  319 KGQEVSELEAIYNSLQTKLRLIKREPFVAPAGLTPNEIDSTWSALEKAEQEHAEALRIEL
SPCB_DROME  351 KFVEKGNLEVLLFTLQSKMRANNQKPYTPKEGKMISDINKAWERLEKAEHERELALREEL
SPCB_HUMAN  355 KFQEKGNLEVLLFTIQSRMRANNQKVYTPHDGKLVSDINRAWESLEEAGYRRELALRNEL
                    .  .   **    ..*...*   .  .    *    .*  .*  **         *  *
```

REPEAT 2 (β2)

```
AACT_CHICK  388 RRLERLDHLAEKFRQKASIHESWTDGKEAMLQQKDYETATLSEIKALLKKHEAFESDLAA
AACN_CHICK  388 RRLERLDHLAEKFRQKASIHESWTDGKEAMLQQKDYETATLSEIKALLKKHEAFESDLAA
AAC1_HUMAN  387 RRLERLDHLAEKFRQKASIHEAWTDGKEAMLRQKDYETATLSEIKALLKKHEAFESDLAA
AACS_CHICK  397 RRLERLEHLAEKFRQKASTHEQWAYGKEQILLQKDYESASLTEVRAMLRKHEAFESDLAA
AAC2_HUMAN  394 RRLERLEHLAEKFRQKASTHETWAYGKEQILLQKDYESASLTEVRALLRKHEAFESDLAA
AAC3_HUMAN  401 RRLQRLQHLAEKFRQKASLHEAWTRGKEEMLSQRDYDSALLQEVRALLRRHEAFESDLAA
AACT_DROME  390 MRLERLEHLAQKFKHKADAHEDWTRGKEEMLQSQDFRQYKLNELKALKKKHEAFECDLAA
AACT_DICDI  379 KRQKKIAVLLQKYNRILKKLENWATTKSVYLGSNE-TGDSITAVQAKLKNLEAFDGECQS
SPCB_DROME  411 IRQEKLEQLAARFDRKASMRETWLS-ENQRLVSQDNFGFDLAAVEAAAKKHEAIETDIFA
SPCB_HUMAN  415 IRQEKLEQLARRFDRKAAMRETWLN-ENQRLVAQDNFGYDLAAVEAAKKKHEAIETDTAA
                    *  ..  *  .. .    * *      *   .     .  . *  .  ** . .  .

AACT_CHICK  448 HQDR-VEQIAAIAQELNELDYYDSPSVNARC-QKICDQWDNLGALTQKRREALER
AACN_CHICK  448 HQDR-VEQIAAIAQELNELDYYDSPSVNARC-QKICDQWDNLGALTQKRREALER
AAC1_HUMAN  447 HQDR-VEQIAAIAQELNELDYYDSPSVNARC-QKICDQWDNLGALTQKRREALER
AACS_CHICK  457 HQDR-VEQIAAIAQELNELDYHDAASVNDRC-QKICDQWDSLGTLTQKRREALER
AAC2_HUMAN  454 HQDR-VEQIAAIAQELNELDYHDAVNVNDRC-QKICDQWDRLGTLTQKRREALER
AAC3_HUMAN  461 HQDR-VEHIAALAQELNELDYHEAASVNSRC-QAICDQWDNLGTLTQKRRDALER
AACT_DROME  450 HQDR-VEQIAAIAQELNTLEYHDCVCVNARC-QRICDQWDRLGALTQRRRTALDE
AACT_DICDI  439 LEGQSNSDLLSILAQLTELNYNGVPELTERKDTFFAQQWTGVKSSAETYKNTLLA
SPCB_DROME  471 YEER-VQAVVAVCDELESERYHDVKRILLRK-DNVMRLWTYLLELLRARRMRLEI
SPCB_HUMAN  475 YEER-VRALEDLAQELEKENYHDQKRITARK-DNILRLWSYLQELLQSRRQRLET
                    . .    . .  .*    *     .  *        *  .       .  *
```

REPEAT 3 (α20)

```
AACT_CHICK   501 TEKLLETIDQLYLEYAKRAAPFNNWMEGAMEDLQDTFIVHTIEEIQGLTTAHEQFKATLP
AACN_CHICK   501 TEKLLETIDQLYLEYAKRAAPFNNWMEGAMEDLQDTFIVHTIEEIQGLTTAHEQFKATLP
AAC1_HUMAN   500 TEKLLETIDQLYLEYAKRAAPFNNWMEGAMEDLQDTFIVHTIEEIQGLTTAHEQFKATLP
AACS_CHICK   510 TEKLLETIDQLHLEFAKRAAPFNNWMEGAMEDLQDMFIVHSIEEIQSLISAHDQFKATLP
AAC2_HUMAN   507 MEKLLETIDQLHLEFAKRAAPFNNWMEGAMEDLQDMFIVHSIEEIQSLITAHEQFKATLP
AAC3_HUMAN   514 MEKLLETIDQLQLEFARRAAPFNNWLDGAVEDLQDVWLVHSVEETQSLLTAHDQFKATLP
AACT_DROME   503 AERILEKIDILHLEFAKRAAPFNNWLDGTREDLVDMFIVHTMVEIQGLIQAHDQFKATLG
AACT_DICDI   494 ELERLQKIEDSLVEFAKRAAQLNVWIEAADDHVFDPINVDSVQGVQEIQEKFDAFLHDQS
SPCA_DROME  2030 MQEQFRQIEELYLTFAKKASAFNSWFENAEEDLTDPVRCNSIEEIRALRDAHAQFQASLS
SPCA_HUMAN  2033 KQLPLQKAEDLFVEFAHKASALNNWCEKMEENLSEPVHCVSLNEIRQLQKDHEDFLASLA
                          .   . .*..*.  * * .   . . .    ..   . .      *
```

```
AACT_CHICK   561 DADKERQAILGIHNEVSKIVQTYHVNMAGTNPYTTITPQEINGKWEHVRQLVPR
AACN_CHICK   561 DADKERQAILGIHNEVSKIVQTYHVNMAGTNPYTTITPQEINGKWEHVRQLVPR
AAC1_HUMAN   560 DADKERLAILGIHNEVSKIVQTYHVNMAGTNPYTTITPQEINGKWDHVRQLVPR
AACS_CHICK   570 EADGERQAILSIQNEVEKVIQSYSMRISASNPYSTVTVEEIRTKWEKVKQLVPQ
AAC2_HUMAN   567 EADGERQSIMAIQNEVEKVIQSYNIRISSSNPYSTVTMDELRTKWDKVKQLVPI
AAC3_HUMAN   574 EADRERGAIMGIQGEIQKICQTYGLRPCSTNPYITLSPQDINTKWDMVRKLVP-
AACT_DROME   563 EADKEFNLIVNLVREVESIVKQHQIPGGLENPYTTLTANDMTRKWSDVRQLVPQ
AACT_DICDI   554 QQFAELEALA----ALTQQLRELGRSE---NDYSVISYDELSAKWNNLLAGIEE
SPCA_DROME  2090 SAEADFKALA----ALDQKIKSFNVGP---NPYTWFTMEALEETWRNLQKIIEE
SPCA_HUMAN  2093 RAQADFKCLL----ELDQQIKALGVPS---SPYTWLTVEVLERTWKHLSDIIEE
                     .   .      .   .           *   .   .   *   .   .
```

REPEAT 4 (α21)

```
AACT_CHICK   615 RDQALMEEHARQQQNERLRKQFGAQANVIGPWIQTKMEEIGRIS-IEMHGTLEDQLNHLR
AACN_CHICK   615 RDQALMEEHARQQQNERLRKQFGAQANVIGPWIQTKMEEIGRIS-IEMHGTLEDQLNHLR
AAC1_HUMAN   614 RDQALTEEHARQQHNESVRKQFGAQANVIGPWIQTKMEEIGRIS-IEMHGTLEDQLSHLR
AACS_CHICK   624 RDQSLQEELARQHANERLRRQFAAQANVIGPWIQTKMEEIARSS-IEMTGPLEDQMNQLK
AAC2_HUMAN   621 RDQSLQEELARQHANERLRRQFAAQANAIGPWIQNKMEEIARSS-IQITGALEDQMNQLK
AAC3_HUMAN   627 RDQTLQEELARQQVNERLRRQFAAQANAIGPWIQAKVEEVGRLA-AGLAGSLEEQMAGLR
AACT_DROME   617 RDQTLANERRKQQNNEMLRRQFAEKANIVGPWIERQMDVVTPLV-WDLQGSLEDQLHRLK
AACT_DICDI   600 RKVQLANELTTQTNNDVLCQSFSVKANEISDYVRVTLDAISQNT----SSDPQEQLNNIR
SPCA_DROME  2137 RDGELAKEAKRQEENDKLRKEFAKHANLFHQWLTETRTSMMEG-----SGSLEQQLEALR
SPCA_HUMAN  2140 REQELQKEEARQVKNFEMCQEFEQNASTFLQWILETRAYFLDGSLLKETGTLESQLEANK
                 *   *  *   *  *  . . *   *       .                  . *.   .
```

```
AACT_CHICK   674 QYEKSIVNYKPKIDQLEGDHQQIQEALIFDNKHTNYTMEHIRVGWEQLLTTIARTINEVE
AACN_CHICK   674 QYEKSIVNYKPKIDQLEGDHQQIQEALIFDNKHTNYTMEHIRVGWEQLLTTIARTINEVE
AAC1_HUMAN   673 QYEKSIVNYKPKIDQLEGDHQLIQEALIFDNKHTNYTMEHIRVGWEQLLTTIARTINEVE
AACS_CHICK   683 QYEQNIINYKHNIDKLEGDHQLIQEALVFDNKHTNYTMEHIRVGWELLLTTIARTINEVE
AAC2_HUMAN   680 QYEHNIINYKNNIDKLEGDHQLIQEALVFDNKHTNYTMEHIRVGWELLLTTIARTINEVE
AAC3_HUMAN   686 QQEQNIINYKTNIDRLEGDHQLLQESLVFDNKHTVYSMEHIRVGWEQLLTSIARTINEVE
AACT_DROME   676 EYEQAVHAYKPNIEELEKIHQAVQESMIFENRYTNYTMETLRVGWEQLLTSINRNINEVE
AACT_DICDI   656 AIITAHAEKKPELDELYTIRSQLEEAQVVDNKHTQHSLESLKLKWDKLNTLAKKNEQVVE
SPCA_DROME  2192 VKATEVRARRVDLKKIEELGALLEEHLILDNRYTEHSTVGLAQQWDQLDQLSMRMQHNLE
SPCA_HUMAN  2200 RKQKEIQAMKRQLTKIVDLGDNLEDALILDIKY---STIGLAQQWDQLYQLGLRMQHNLE
                         .  .  .     ...  . . .   .  .  *. *    .    .*
```

```
AACT_CHICK   734 NQILTRDAKGISQEQM
AACN_CHICK   734 NQILTRDAKGISQEQM
AAC1_HUMAN   733 NQILTRDAKGISQEQM
AACS_CHICK   743 TQILTRDAKGITQEQM
AAC2_HUMAN   740 TQILTRDAKGITQEQM
AAC3_HUMAN   746 NQVLTRDAKGLSQEQL
AACT_DROME   736 NQILTRDSKGISQEQL
AACT_DICDI   716 GEILAKQLTGVTAEEL
SPCA_DROME  2252 QQIQARNHSGVSEDSL
SPCA_HUMAN  2257 QQIQAKDIKGVSEETL
                  .. ..   *.. . .
```

Figure 7: Sequence alignment of repeats 1-4 of α-actinin and the homologous repeats β1-2 and α20-21 of spectrin. Chicken smooth muscle α-actinin (AACT_CHICK, residues 268-749), chicken brain α-actinin (AACN_CHICK, 268-749), human placental α-actinin (AAC1_HUMAN, 267-748), chicken skeletal muscle α-actinin (AACS_CHICK, 277-758), human skeletal muscle α-actinin (AAC2_HUMAN, 274-755), human skeletal muscle α-actinin (AAC3_HUMAN, 281-762), *Drosophila* α-actinin (AACT_DROME, 270-751), *Dictyostelium* α-actinin (AACT_DICDI, 259-732), *Drosophila* β-spectrin (SPCB_DROME, 291-523), human erythroid β-spectrin (SPCB_HUMAN, 295-527), *Drosophila* α-spectrin (SPCA_DROME, 2030-2267), human erythroid α-spectrin (SPCA_HUMAN, 2033-2272). Conserved tryptophans are bold and underlined, and conserved lysine-proline-proline motif in repeat 1 is bold.

combinations of the α-actinin repeats have shown that repeats 1 and 4 are much less similar than other repeats (Blanchard *et al.*, 1989). This appears to be consistent for all isoforms of α-actinin. Should the interaction between repeat units 1 and 4 be important in dimer formation, it might be expected that they would show significant divergence in order to minimise charge similarities.

Despite the low level of identity between the repeats in spectrin, dystrophin, and α-actinin, antibodies to a synthetic peptide covering residues 48-70 in the chicken α-spectrin repeats cross-reacted with α-actinin (Narvanen *et al.*, 1987). Similarly, antibodies to the repeats in dystrophin cross-reacted with α-actinin (Hoffman *et al.*, 1989).

1.3.2 Spectrin

Electron microscopy of spectrin dimers shows flexible 100 nm long rod-like molecules, whilst dimers *in situ* are only about 30 nm in length (Ursitti *et al.*, 1991). This ability of the spectrin molecule to shorten and extend, as well as its flexibility, have been attibuted to the repeat segments initially identified by partial peptide sequence (Speicher and Marchesi, 1984) and confirmed by complete sequencing of cDNAs for the α-subunit (Sahr *et al.*, 1990) and β-subunit (Winkelmann *et al.*, 1990).

Rotary shadowed images of native spectrin dimers have shown strong side-to-side interactions only at the ends of the dimers (Shotton *et al.*, 1979), while peptide mapping indicated multiple points of attachment along the two subunits (Morrow *et al.*, 1980). A HPLC gel filtration assay was used to locate peptides that could associate, and this indicated that heterodimer assembly was initiated at a single region on each subunit (Speicher *et al.*, 1992) (Figure 8). The adjacent EF-hand region on the α-subunit and the adjacent ABD on the β-subunit were not involved in

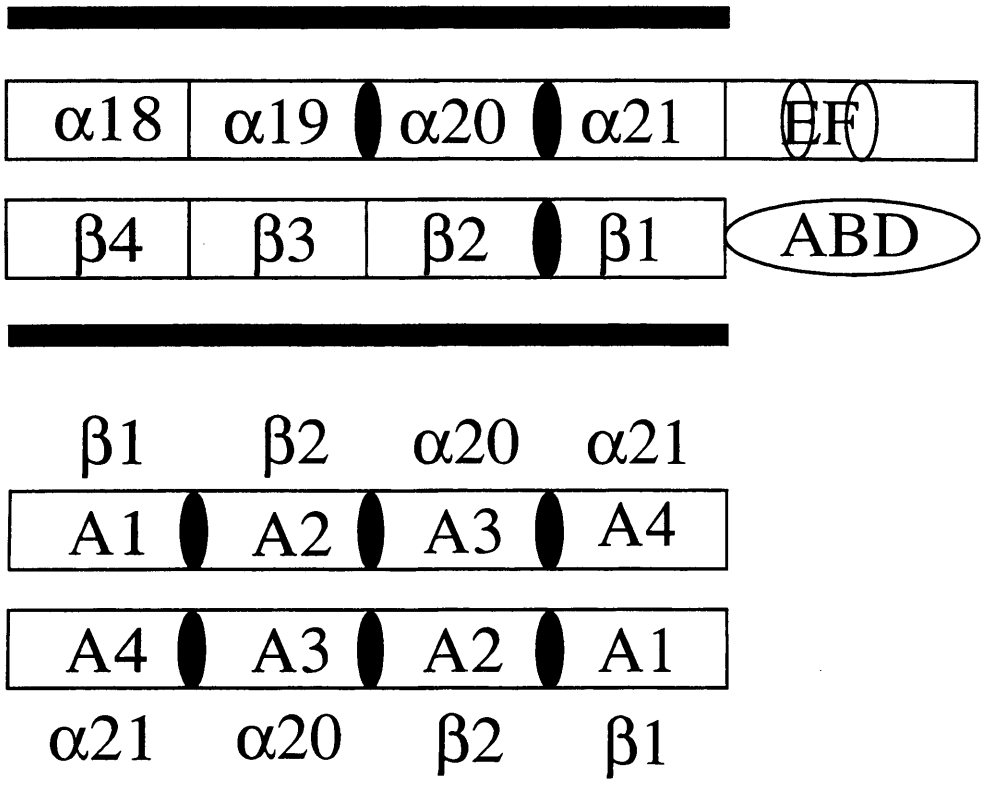

Figure 8: Nucleation region of human erythroid spectrin and its similarity to α-actinin. The minimum dimerisation site of spectrin consists of α18-21 and β1-4 (indicated by black lines). In α-actinin, repeats A1-4 are most homologous with β1-2 and α20-21 of spectrin respectively. Therefore, the α-actinin dimer resembles two spectrin nucleation regions side-by-side, with each homologous repeat being separated from the next by an 8-residue insert (black oval).

assembly. A zipper-type mechanism was proposed, where only the few homologous segments, the dimer nucleation site, had an appropriate conformation that initiated dimer assembly and defined the lateral pairing of repeats. After initial association of the nucleation sites, a conformational change is propagated along the full length of both chains, probably involving supercoiling of the two subunits to form a rope-like structure (McGough and Josephs, 1990). After initial binding of this region, the remainder of the monomers rapidly paired with the appropriate complimentary segment since complete dimer assembly occurred within seconds, even at 0 °C (Speicher *et al.*, 1992). This nucleation region contains repeats most homologous to those in α-actinin, and three of the repeats have an 8-residue insertion in the normal 106-residue repeat unit, also similar to α-actinin. As α-actinin has been shown to exist as a tightly associated dimer, it suggests these inserts may have a role in dimer formation.

Spectrin heterodimers can assemble further in a head-to-head orientation to form tetramers with a contour length twice that of dimers (Figure 9). The association is concentration- and

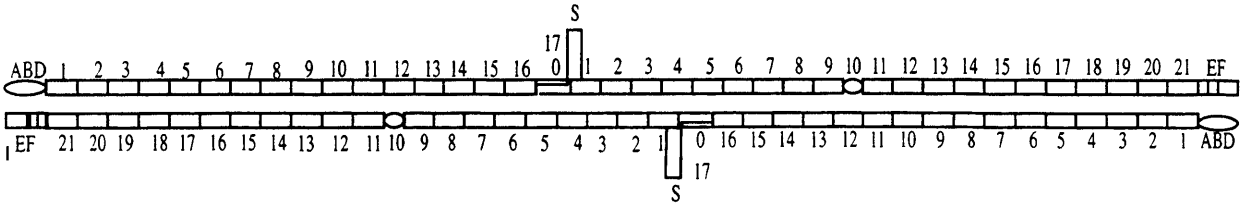

Figure 9: Tetramer conformation of spectrin. The partial repeats of α0 and β17 from different spectrin molecules assemble to form two additional complete triple-helical motifs.

temperature-dependent with little interconversion of dimers and tetramers below 30 °C (Kam *et al.*, 1977; Ungewickell and Gratzer, 1978). Higher oligomers can also form by insertion of additional dimers at the tetramer site, to form branched or star shaped structure (Morrow and Marchesi, 1981). A similar internal head-to-head α-β interaction in dimers was initially suggested by electron microscopy images (Shotton *et al.*, 1979). It has also been described recently for equine erythrocyte spectrin (Bobich and Wallis, 1996). Opening the head-to-head αβ site in closed dimers was recently identified as the rate-limiting step for tetramer formation (DeSilva *et al.*, 1992). This step is responsible for the normal temperature threshold of about 30 °C which is required for interconversion between dimers and tetramers. Conversion of open dimers to a closed form through formation of the internal head-to-head α-β association occurred on a timescale of hours at 0 °C (Speicher *et al.*, 1993).

It has been demonstrated that the A and B helices contained in the 60 residues of the partial segment found near the C-terminus of β-spectrin forms a three-helix bundle by packing against the potential C helix in the 30 residues of the partial segment found at the N-terminus of α-spectrin (Tse *et al.*, 1990) (Figure 9). It has been found that many functionally important consequences arise from deletions and mutations within these regions. These effects can, in general, be attributed to a weakening or breakdown of the spectrin network as a result of tetramer interchain binding defects. The binding site within β-spectrin for the lone C helix near the N-terminus of α-spectrin can be recreated within any β-spectrin repeating segment by deleting the segment's C helix (Kennedy *et al.*, 1994). This suggests that interchain binding depends on the same helix-helix interactions that produce the three-helix bundle of the other α-spectrin and β-spectrin repeats. But, although there is no doubt that the C helix contributed by α-spectrin is necessary for interchain binding, it is not sufficient (Kotula *et al.*, 1993).

Homodimers of the 14th segment of *Drosophila* α-spectrin have been crystallised and its structure determined. Helices A and B form a hairpin, but helix C is continuous with helix B. In place of helix C, helix C' (residues from the second polypeptide chain in the dimer) pack against helices A and B to create the anticipated three-helix bundle (Yan *et al.*, 1993) (Figure 10). Because the intact molecule has an extended structure whose N- and C terminal ends lie at

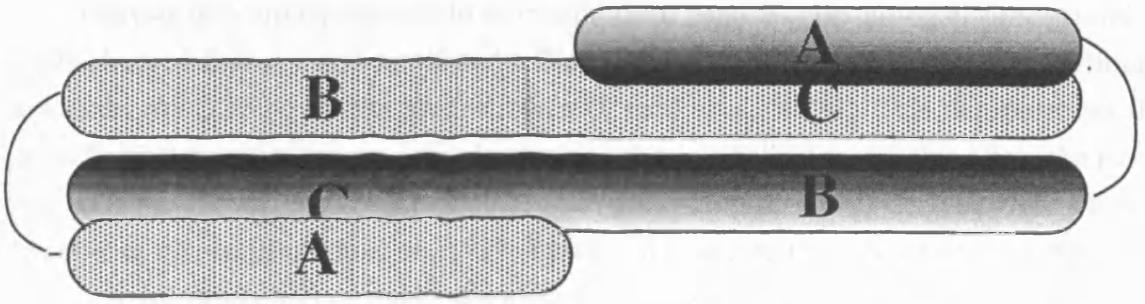

Figure 10: Homodimer of *Drosophila* spectrin α14. The B-C helix is straight in both repeats, and the three-helix bundle is formed by the C-helix of one repeat, and the A-B helices of the other.

opposite ends, the N- and C-terminal ends of a segment must extend in opposite directions. Therefore, the C helix of each segment must fold back against helices A and B. Thus, although the residues between helices B and C maintain a continuous α-helical conformation in the crystalline dimer, in the intact spectrin chain these residues must form a small loop (Yan *et al.*, 1993). This model has since been shown by NMR to apply equally to a single repeat of chicken brain α-spectrin (Pascual *et al.*, 1996). A model was also given for the disposition of successive repeats along the polypeptide chain, in which one long α-helix forms part of two contiguous three-helix bundles (Yan *et al.*, 1993).

The spectrin segment used for the crystallographic analysis has since been shown to undergo reversible dimerisation (G. Ralston, T. Cronin, D. Branton, private communication). Equilibrium between monomer and dimer populations occurs fairly rapidly above 20 °C, but at a negligible rate at 5 °C. The fact that the equilibriation process is temperature dependent is consistent with the requirements for extensive disruption of helix-helix packing as the reaction proceeds in either direction. Dimerisation of the 14th repeat in the α-chain of *Drosophila* spectrin (Yan *et al.*, 1993) may be an unusual function of the particular amino acid sequence of the loop between the B and C helices in this repeat, and not in others, especially since helix-breaking residues are relatively abundant in the inferred loop segments throughout the rod domain (Winder *et al.*, 1995).

A frictional ratio of 1.2 for the monomer of α-spectrin repeat 14 has been obtained (G. Ralston, T. Cronin, D. Branton, private communication), indicating a relatively globular structure, consistent with the model developed (Yan *et al.*, 1993). A frictional ratio of 1.5 for the dimer was also close to that predicted for a model based on the actual crystal structure of the dimer. Both the dimer of α14 and the monomer of α14-15 appeared to be twice the length of the α14 monomer, while the frictional ratio of the α14-15 dimer is consistent with four end-to-end triple α-helical domains (G. Ralston, T. Cronin, D. Branton, private communication). In

contrast, analysis of hydrodynamic radii of recombinant peptides containing differing numbers of motifs showed that a single motif had a Stokes radius of 2.35 nm, while each additional motif added only 0.85 nm to the Stokes radius (Ursitti *et al.*, 1996). This demonstrates that spectrin's flexibility arises from regions between each triple helical motif, that allow the motifs to pleat and fold as suggested by models (Bloch and Pumplin, 1992) derived from electron microscopic evidence (Shotton *et al.*, 1979; Byers and Branton, 1985; Shen *et al.*, 1986; Liu *et al.*, 1987; Ursitti *et al.*, 1991), rather than from within the segment itself which is relatively rigid in solution as might be expected for triple helical bundles with strong inter-helix interactions.

1.3.3 Dystrophin

In dystrophin, early work demonstrated that a heptad pattern of hydrophobic residues was preserved across all repeats, and that each repeat consisted of a constant-length core helix of 54 residues, coupled via a short linker to a weakly conserved variable-length helix, and then via a second linker to the next core (Cross *et al.*, 1990). The variable-length helix appeared truncated in repeats 10 and 13 and extended in repeats 4 and 20. The extension of repeat 20 is particularly interesting since it corresponds to a hotspot of dystrophy-inducing mutations (Love *et al.*, 1989). Parts of this repeat are unusually proline-rich, and strongly hydrophobic, suggesting they may fold into a globular subdomain, rather than having an extended rod structure (Cross *et al.*, 1990). This region could represent a binding site for some other components of the cytoskeleton.

It has been found that the critical length for repeat folding in dystrophin is 117 residues, and shortening the chain by 1 residue results in loss of the capacity to form a defined tertiary structure (Kahana and Gratzer, 1995). Replacement of glutamine residue 117 by a methionine residue did not impair the ability of the chain to enter the folded conformation, implying that it is the length of the C-terminal α-helix, rather than any specific side-chain interaction, that is critical in determining the stability of the native structure. Model building (Cross *et al.*, 1990; Parry and Cohen, 1991) suggests that the helix bundles which make up the dystrophin rod may be nested and hence there would then be no structural discontinuity between successive repeats. A fragment of 119 residues forms a significantly more stable structure than that of 117 (Calvert *et al.*, 1996), suggesting the minimum unit capable of forming the native fold extends some residues into the adjoining sequence repeat. Extending the chain by a further six residues also results in a large increase in conformational stability, which is not related to a change in association state of the polypeptide (Calvert *et al.*, 1996).

Little is known about the organisation of the dystrophin-containing complex on the membrane, but most published models have assumed that dystrophin forms an antiparallel dimer, like other

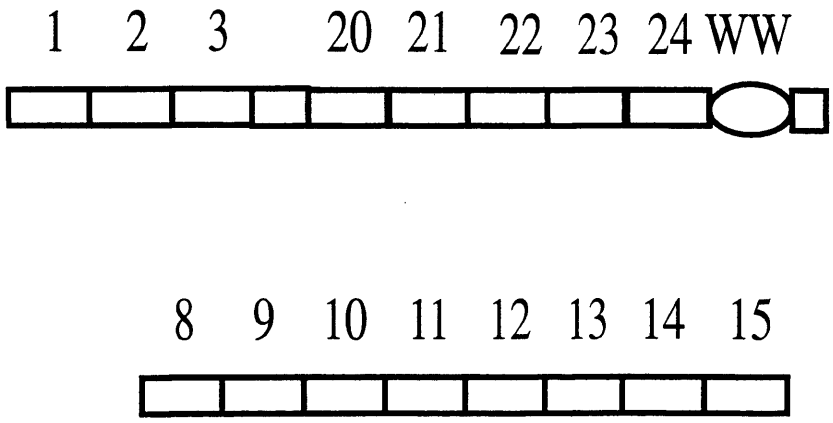

Figure 11: Constructs used for investigation of dimer formation in dystrophin. Neither portion of the rod domain was demonstrated to associate.

known proteins of the spectrin class. This would allow a two-dimensional network to be generated at the membrane surface.

Experimental data that bear on the association state of native, intact dystrophin stem mainly from electron microscopy, which concluded that preparations contained mainly monomers with some dimers (Pons *et al.*, 1990). Later data (Sato *et al.*, 1992) should probably be disregarded because of the authors' subsequent doubts concerning the identity of the material (Kake *et al.*, 1994). It has also been claimed that alkali treated dystrophin sedimented at a size consistent with a dystrophin dimer (Ervasti *et al.*, 1991).

Analysis has shown that there are more conserved residues in the aligned spectrin sequences than in dystrophin and utrophin (Winder *et al.*, 1995). The lengths of the helices in the spectrins are more consistent and well defined and contain considerably fewer insertions than do those in dystrophin and utrophin. The insertions in the A helix would be especially unfavourable for antiparallel dimer formation due to the insertions putting the helices out of register. α- and β-Spectrin are known to form antiparallel dimers, so surface residues should be conserved in the dimer interface. There are 21 extra residues conserved in each spectrin repeat and they map to one external face of the domain structure, consisting of helix A and half of helix B (Winder *et al.*, 1995). Therefore this region is likely to be the dimer interface. By contrast, all of the conserved residues in dystrophin and utrophin map exclusively to core or interface positions with none available to form a surface dimer interface as in spectrin. Moreover, the presumptive self-association sites, present in all erythroid spectrin repeats occur in only a few dystrophin repeats, and of these all but two are out of register in an antiparallel alignment (Winder *et al.*, 1996).

Results have demonstrated that neither the middle portion of the rod nor the ends, which would interact by pairs in an antiparallel dimer, are able to self-associate measurably (Kahana *et al.*, in press) (Figure 11). The rod domain is thus unlike those of erythroid spectrin and α-actinin in its behaviour. It is possible that dystrophin and utrophin may dimerise in an end-to-end arrangement via the C-terminal coiled-coil regions or possibly by a staggered overlap involving a short region of dimerisation in the coiled-coil region.

Interestingly, recently, it has been shown that the cysteine-rich sequences of dystrophin binds to full length dystrophin suggesting that these sequences may be important in dystrophin dimerisation (Madhavan and Jarrett, 1995).

1.4 EF-HANDS OF THE α-ACTININ FAMILY

1.4.1 α-Actinin

Calmodulin is a small, ubiquitous and highly conserved calcium-binding protein with diverse cellular functions (Strynadka and James, 1989, 1991; Heizmann and Hunziker, 1991). It contains four calcium-binding sites, which are present in two distant domains connected by a long α-helix (Figure 12). Two pairs of sites in the N-terminal and C-terminal domains bind calcium in a cooperative manner with affinities in the micromolar range. Each binding site is formed by a long loop connecting two helices, called the EF-hand which are classified in two main sub-families (Kawasaki and Kretsinger, 1994). In both cases, the liganding oxygens build a pentagonal bipyramid around the calcium ion. In all the structures determined so far, EF-hands occur in side-to-side pairs which form either one or two globular units (Kawasaki and Kretsinger, 1994). Each unit can bind up to two calcium ions, one in each helix-loop-helix motif. EF-hand structures are found in two conformations, often referred to as "closed" and "open" (Hertzberg *et al.*, 1986). Generally, the closed and open conformations correspond to calcium-free and calcium-bound states respectively. In the absence of calcium, the four helices (EF-1-4) would pack in pairs forming a very compact structure. Upon binding of calcium, the two helices of each EF-hand would be pushed apart inducing the exposure of hydrophobic residues otherwise involved in helix-helix packing in the calcium-free form. These residues would then become available for interaction with the target protein. The C-terminus of α-spectrin has a domain with a calmodulin fold and two calcium-binding sites (Trave *et al.*, 1995). Sequence alignments suggest that the related domains in α-actinin, and possibly in dystrophin, may share the same calmodulin-like structure. In some cases (Dubreil *et al.*, 1991; Lundberg *et al.*, 1992; Wallis *et al.*, 1992; Witke *et al.*, 1993) but not all (Waites *et al.*, 1992; Pacaud and Harricane, 1993), the regions of α-actinin and spectrin that contain these motifs have been found to bind calcium with high affinity. Only non-muscle α-actinins appear to have

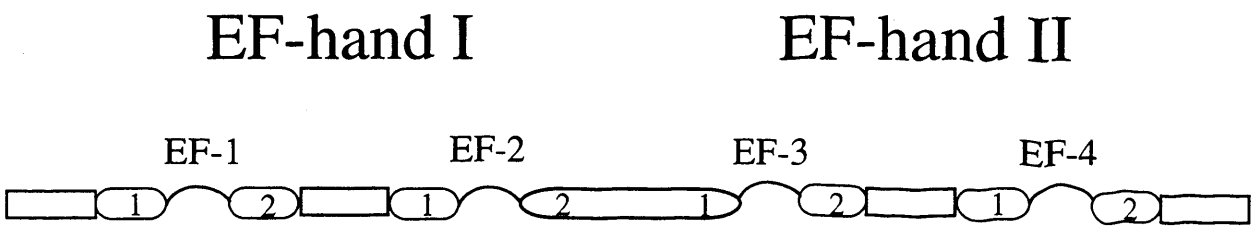

Figure 12: The structure of typical EF-hands. Four calcium-binding sites (EF-1-4) are present in two domains (EF-hand I and II) separated by an α-helix (cylinders). Each site consists of a loop connecting two helices (labelled 1 and 2).

one or two EF-hands with the calcium-binding consensus, and a strict consensus is not found in the muscle α-actinins or dystrophins.

In all known α-actinin sequences two EF-hands with different degress of conservation are found in the C-terminal region despite the fact that only non-muscle type α-actinins are regulated by calcium (Burridge and Feramisco, 1981). Comparison of the EF-hand sequences present in α-actinins have suggested that most of these regions are defective and probably do not bind calcium. An ideal EF-hand structure is present in the first EF-hand of *Drosophila* muscle α-actinin, and an almost complete set of liganding oxygens can be found in EF-hands I of chicken fibroblast α-actinin (Arimura *et al.*, 1988) and brain α-actinin (Waites *et al.*, 1992).

Functional EF-hands typically contain amino acids with oxygen-containing side chains at the X, Y, Z, -X and -Z in the loop between helices (Tufty and Kretsinger, 1975; Kretsinger, 1980) (Figure 13). The N-terminal EF-1 of chicken lung α-actinin, characterised as having a decreased sensitivity to calcium, lacks two oxygen-containing amino acid residues in the loop region, where Cys and Gly are found instead at the Z and -Y vertices (Imamura *et al.*, 1994). However, Gly is also found at -Y position in the EF-1 of non-muscle α-actinin, which is predicted to be functional for calcium binding (Arimura *et al.*, 1988). This suggests that the Cys residue at the Z position is the residue responsible for the decreased calcium sensitivity of the lung α-actinin. In the C-terminal EF-2 of the lung α-actinin, one oxygen-containing calcium-chelating amino acid side chain is defective, where Ala is found at the -Z position (Imamura *et al.*, 1994). However, EF-2 may not be essential for calcium sensitivity in the interaction with F-actin because this amino acid replacement is also found in the calcium-sensitive non-muscle α-actinin (Arimura *et al.*, 1988).

Studies show that the smooth muscle and fibroblast isoforms of chicken α-actinin are 98% identical, differing only in the second half of the first EF-hand. The critical difference within this region of the two isoforms appears to be at the Y coordinate, with the smooth muscle

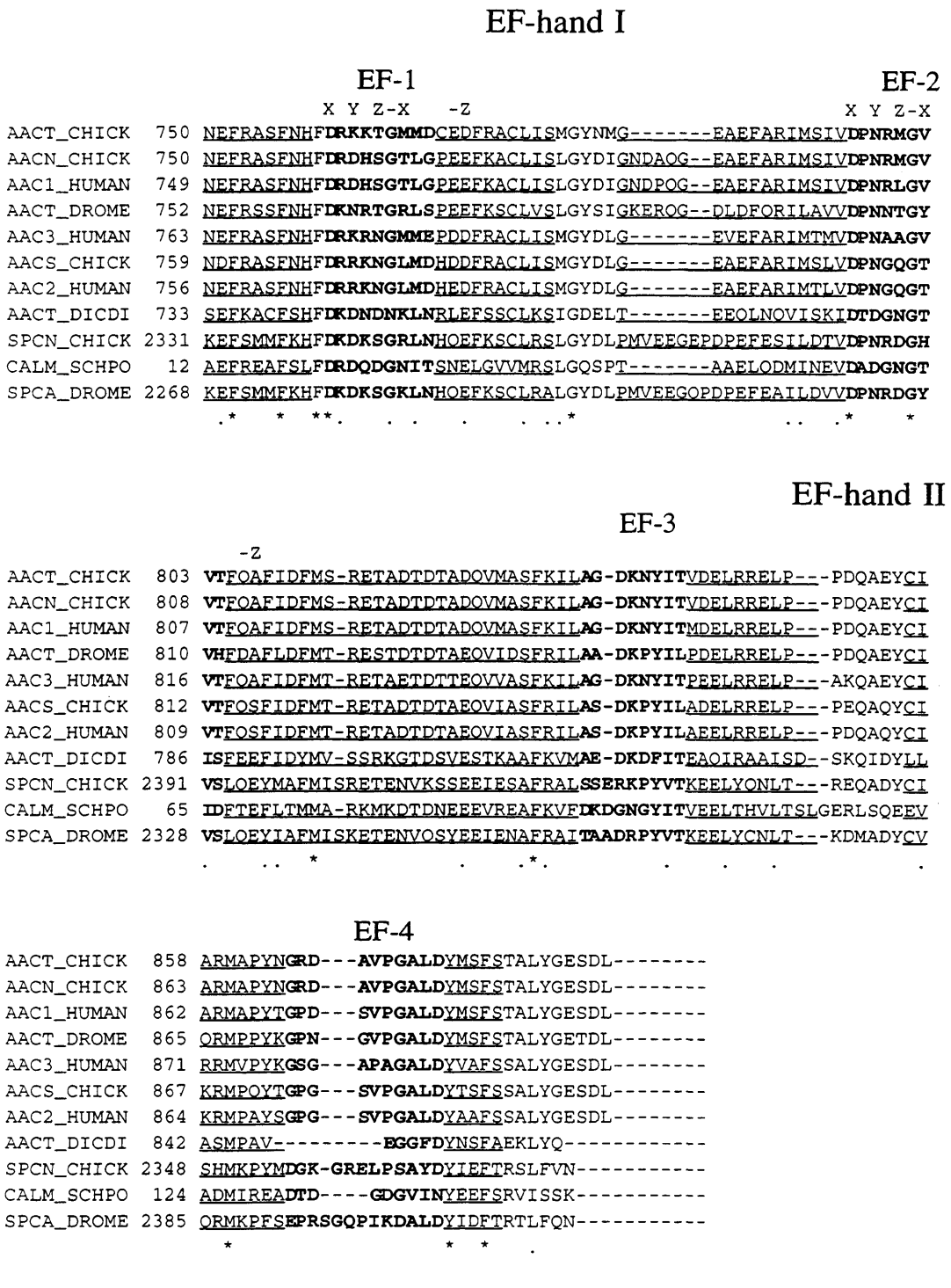

Figure 13: Sequence alignment of EF-hands. Chicken smooth muscle α-actinin (AACT_CHICK, residues 750-888), chicken brain α-actinin (AACN_CHICK, 750-893), human placental α-actinin (AAC1_HUMAN, 749-892), *Drosophila* α-actinin (AACT_DROME, 752-895), human skeletal muscle α-actinin (AAC3_HUMAN, 763-901), chicken skeletal muscle α-actinin (AACS_CHICK, 759-897), human skeletal muscle α-actinin (AAC2_HUMAN, 756-894), *Dictyostelium* α-actinin (AACT_DICDI, 733-862), chicken non-erythroid α-spectrin (SPCN_CHICK, 2331-2477) (Wasenius *et al.*, 1989; X14518), *Schizosaccharomyces pombe* calmodulin (CALM_SCHPO, 12-150) (Takeda and Yamamoto, 1987; M16475), *Drosophila* α-spectrin (SPCA_DROME, 2268-2415). Helical regions are

underlined, loop regions are in bold, and the calcium coordinating residues are labelled in EF-1 and 2.

protein possessing a lysine residue which is unlikely to be able to participate in coordinating a calcium ion (Blanchard *et al.*, 1989).

At calcium concentrations below 10^{-7} M and pH values of 6.6-6.8, *Dictyostelium* α-actinin is highly active in crosslinking actin filaments. Micromolar concentrations of calcium and pH above 7 inhibit the cross-linking activity (Condeelis and Vahey, 1982; Fechheimer *et al.*, 1982). Inactivation of EF-1 has been shown to abolish completely the F-actin cross-linking activity of *Dictyostelium* α-actinin, but calcium binding by EF-2 was still observed (Witke *et al.*, 1993). In contrast, after mutation of EF-2 the molecule was still active, but required 500-fold more calcium for inhibition. This suggests that EF-1 has a low affinity for calcium, implying a regulatory function of EF-1 in the inhibition of F-actin cross-linking activity. A comparison of the EF-hands in *Dictyostelium* α-actinin suggests that EF-1 is unsuitable for calcium-binding, whilst EF-2 has the ideal structure of a calcium-specific site (Witke *et al.*, 1993). This is consistent with the findings showing a high-affinity calcium-specific site in EF-2 and a low affinity regulatory site in EF-1. Similar results have also been obtained more recently for *Dictyostelium* α-actinin (Janssen *et al.*, 1996). This might explain why fibroblast and brain α-actinin with an almost ideal EF-1 are calcium-sensitive but because of the lack of an intact EF-2 the sensitivity towards calcium is lowered. The idea that EF-1 is the key regulatory calcium-binding site in α-actinin is consistent with the observation that this is a region of alternative splicing in the chicken α-actinin gene described by Waites *et al.* (1992). This results in expression of a smooth and non-muscle isoform from a single gene.

It has been shown that any mutation introduced in the EF-hand regions lowers the cross-linking activity of the mutated α-actinins as compared to wild type protein (Witke *et al.*, 1993). This suggests that the actin-binding site of one strand requires an EF-hand domain from the second subunit for high affinity binding to F-actin. A peptide containing only the F-actin-binding domain exhibited a reduced affinity for F-actin (Harris and Morrow, 1990). This might explain why all α-actinins whose sequences are known possess EF-hands irrespective of exhibiting calcium-regulated or -unregulated cross-linking activity. Similarly, cleavage of the fodrin α-chain by the protease calpain alters the calcium-sensitivity of fodrin, with regard to F-actin cross-linking, indicative of an interaction between the opposing actin-binding site and EF-hand structures (Harris and Morrow, 1990).

1.4.2 Spectrin

The sequence of the non-repetitive segment at the C-terminus of α-spectrin is homologous to the C-terminus of α-actinin (Figure 13). *In vitro*, only the N-terminal domain binds calcium, and it does so with low affinity (Trave *et al.*, 1995). In the absence of calcium, EF-1 α-helices are tightly packed, whereas the EF-2 helices are less compact and are involved in side-to-side interactions with the EF-1 helices. Calcium binding causes a redistribution of hydrophobic interactions within EF-1, resulting in an opening of the helix-turn-helix structure that is propagated to EF-2 (Trave *et al.*, 1995). These conformational changes may modify the interface between the EF-hands and the ABD, and may in particular modify the loop structure between EF-1 and EF-2, which plays an important role in interchain binding at the tail end of the *Drosophila* spectrin subunits (Viel and Branton, 1994). The importance of the EF-hands has been further demonstrated *in vivo*. In *Drosophila*, a deletion of the carboxyl terminus of the EF-hands, which includes the deletion of EF-2-4, is lethal (Lee *et al.*, 1993), but this deletion does not affect interchain binding (Viel and Branton, 1994).

1.5 CALCIUM BINDING IN α-ACTININ

Calcium is a second messenger in eukaryotic cells. At the molecular level, this implies that calcium is expected to generate conformational changes in some, if not all, of its target proteins. Signal transduction often elicits a change in the intracellular concentration of calcium, either by mobilisation of internal calcium stores or by altered calcium flux across the membrane. Transmission of the calcium signal inside the cell may be accomplished by binding to the target protein directly, or in an indirect manner by binding to and concomitant activation of a regulatory protein, which in turn will regulate the target process.

A principle feature that differentiates muscle from non-muscle, e.g. brain, platelet and macrophage α-actinins, is the ability of the latter to bind actin in a calcium sensitive manner (Bennett *et al.*, 1984; Duhaiman and Bamburg, 1984; Landon *et al.*, 1985). At calcium concentrations of $<10^{-7}$ M, such non-muscle α-actinins increase F-actin viscosity significantly, an effect abolished by the presence of $>10^{-7}$ M calcium. Similar results have been obtained using Hela cell α-actinin (Burridge and Feramisco, 1981). The affinity of macrophage α-actinin for calcium is 4×10^{6} M^{-1} with a capacity of four calcium ions per molecule (Bennett *et al.*, 1984).

The mechanism by which calcium inhibits actin-binding by the non-muscle isoform of α-actinin is unknown. Given the antiparallel orientation of the two subunits, it is likely that binding of calcium to the EF-hands of one subunit inhibits actin-binding by the neighbouring

subunit. It is possible that calcium binding induces a conformational change in the EF-hands such that they sterically inhibit actin-binding.

In the evolution of α-actinin, it is possible the ancestral gene encoded a calcium sensitive isoform, whilst the calcium insensitive forms arose with the development of muscle tissue, where the interaction with actin was required to be independent of fluctuations in calcium levels, since muscle contraction is associated with an increase in calcium concentration from 10^{-7} M to 10^{-5} M (Blanchard *et al.*, 1989). In non-muscle isoforms, α-actinin has been detected at or very close to structures intimately associated with membranes, e.g. in zonula adherens, and in the terminal web of intestinal epithelial cells (Craig and Pardo, 1979; Geiger *et al.*, 1981; Drenckhahn and Mannherz, 1983). In lymphoid cells, α-actinin co-caps with a number of surface antigens, while in cultured fibroblasts it is found in adhesion plaques (Lazarides and Burridge, 1975). It is possible that a calcium sensitive isoform localised to the membrane may allow the reversible dissociation of actin/membrane interaction in response to external signals which regulate intracellular calcium levels (Blanchard *et al.*, 1989).

There is much indirect evidence suggesting calcium is involved in the initiation of cytoskeletal reorganisation in macrophages and neutrophils in response to chemotractant or phagocytic stimuli (Sklar *et al.*, 1985; Howard and Oresajo, 1985; Omann *et al.*, 1987). Interestingly, it has been demonstrated that macrophage α-actinin is not a calcium-modulated actin-binding protein (Pacaud and Harricane, 1993). This could be predicted from the primary sequence of the two EF-hands in the α-actinin monomer (Arimura *et al.*, 1988) based on the crucial role of some calcium-binding residues demonstrated by point mutations in calcium-binding sites of calmodulin (Haiech *et al.*, 1991). Calcium also does not affect the behaviour of macrophage α-actinin in actin gel networks from cytosolic extracts (Pacaud and Harricane, 1987).

1.6 CALMODULIN-BINDING IN THE α-ACTININ FAMILY

1.6.1 Dystrophin

It has been shown that dystrophin binds calmodulin with an apparent affinity in the range of 6-60 nM, and it was suggested that the calmodulin binding sites were located in both the N- and C-terminal domains of dystrophin (Madhavan *et al.*, 1992). It has also been shown that a bacterially expressed N-terminal domain of dystrophin binds calmodulin in a calcium-dependent manner (Bonet-Kerrache *et al.*, 1994). The N-terminal domain contains more than one calmodulin-binding site, but the apparent affinity here was about 2 μM (Jarrett and Foster, 1995). Additionally, calmodulin has been found to competitively inhibit F-actin-binding (Jarrett and Foster, 1995). It is interesting to note that calmodulin inhibits F-actin interactions with spectrin (Sobue *et al.*, 1981; Kakiuchi *et al.*, 1981) and utrophin (Winder and Kendrick-Jones,

```
                                                    ABS2
AACT_CHICK    83 RG--KMRVHKISNVNKALDFIASKGVKLVSIGAEEIVDGNVKMTLGMIWTIILRFAIQD
AACN_CHICK    83 RG--KMRVHKISNVNKALDFIASKGVKLVSIGAEEIVDGNVKMTLGMIWTIILRFAIQD
AAC1_HUMAN    82 RG--KMRVHKISNVNKALDFIASKGVKLVSIGAEEIVDGNVKMTLGMIWTIILRFAIQD
AAC3_HUMAN    96 KG--KMRFHKIANVNKALDFIASKGVKLVSIGAEEIVDGNLKMTLGMIWTIILRFAIQD
AACS_CHICK    92 RG--KMRFHKIANVNKALDYIASKGVKLVSIGAEEIVDGNVKMTLGMIWTIILRFAIQD
AAC2_HUMAN    89 RG--KMRFHKIANVNKALDYIASKGVKLVSIGAEEIVDGNVKMTLGMIWTIILRFAIQD
AACT_DROME    85 RG--KMRFHKIANVNKALDFIASKGVHLVSIGAEEIVDGNLKMTLGMIWTIILRFAIQD
AACT_DICDI    72 KTPKLRRIHNIQNVGLCLKHIESHGVKLVGIGAEELVDKNLKMTLGMIWTIILRFAIQD
SPCB_HUMAN   105 KG--KMRIHCLENVDKALQFLKEQRVHLENMGSHDIVDGNHRLVLGLIWTIILRFQIQD
SPCB_DROME   101 KG--KMRIHCLENVDKALQFLREQRVHLENIGSHDIVDGNASLNLGLIWTIILRFQIQD
UTRO_HUMAN    83 GS---TRVHALNNVNRVLQVLHQNNVELVNIGGTDIVDGNHKLTLGLLWSIILHWQVKD
DMD_CHICK     71 GS---TRVHALNNVNKALQILQRNNVDLVNIGSSDIVDGNHKLTLGLIWNIILHWQVKD
DMD_HUMAN     67 GS---TRVHALNNVNKALRVLQNNNVDLVNIGSTDIVDGNHKLTLGLIWNIILHWQVKN
DMD_MOUSE     67 GS---TRVHALNNVNKALRVLQKNNVDLVNIGSTDIVDGNHKLTLGLIWNIILHWQVKN

                        * . **   *  .    * *  .*  ..** *  . **..* ***.  ..
```

Figure 14: Sequence alignment of the predicted calmodulin-binding domains in chicken smooth muscle α-actinin (AACT_CHICK), human dystrophin (DMD_HUMAN), and human utrophin (UTRO_HUMAN) (underlined and bold) with other isoforms, and spectrin. Chicken brain α-actinin (AACN_CHICK), human placental α-actinin (AAC1_HUMAN), human skeletal muscle α-actinin (AAC3_HUMAN), chicken skeletal muscle α-actinin (AACS_CHICK), human skeletal muscle α-actinin (AAC2_HUMAN), *Drosophila* α-actinin (AACT_DROME), *Dictyostelium* α-actinin (AACT_DICDI), human erythroid β-spectrin (SPCB_HUMAN), *Drosophila* β-spectrin (SPCB_DROME), chicken dystrophin (DMD_CHICK), mouse dystrophin (DMD_MOUSE).

1995). While calmodulin-binding seqences are not strictly homologous, they do all share the chemical characteristics of being cationic, hydrophobic, and aromatic-rich sequences (Jarrett and Madhaven, 1991). Calmodulin is abundant in most mammalian tissues, often reaching concentrations as high as 10 μM (Watterson *et al.*, 1980). The concentration present at the sarcolemma where dystrophin resides is not known but is likely to be of a similar order. Calmodulin binding potentially could regulate actin-binding in response to the increase in intracellular calcium which accompanies muscle contraction. This could allow the cytoskeleton to rearrange during contraction to reduce stresses on the membrane during muscle shortening.

1.6.2 Utrophin

Calmodulin can regulate the F-actin-binding activity of utrophin in a calcium-dependent manner (Winder and Kendrick-Jones, 1995). This suggests there is regulation of the utrophin-actin interaction via a calmodulin-dependent mechanism, and the putative C-terminal calcium binding domain of utrophin may itself be able to regulate F-actin-binding in the adjacent N-terminal ABD if utrophin exists as an antiparallel dimer. Given the low cellular concentration of utrophin (Ohlendieck and Campbell, 1991) and relatively high concentrations of calmodulin, the concentration of calmodulin required to regulate utrophin-actin-binding is easily obtainable

within most cells (Winder and Kendrick-Jones, 1995). The organisation of the F-actin-utrophin-membrane glycoprotein complex can therefore be considered to be dynamic, with modulation by calcium-calmodulin allowing for the redistribution of utrophin in response to cell division, cell movement and external factors such as agrin which induces the clustering of acetylcholine receptors via the utrophin glycoprotein complex (Sealock and Froehner, 1994).

Analysis of the amino acid sequences of α-actinin, dystrophin and utrophin for putative calmodulin-binding basic amphiphilic α-helices, reveals a 15-16 residue region in all three proteins (Winder and Kendrick-Jones, 1995) (Figure 14). In each case the predicted region is N-terminal of ABS2, the largest F-actin-binding region in these proteins. In α-actinin a region of 16 amino acids was predicted to bind calmodulin, but the mean hydrophobicity and hydrophobic moment was low. A similar region was also predicted to bind calmodulin in dystrophin, but the aggregate hydrophobic moment was also low. The identical region in utrophin had a high average hydrophobicity and a considerably higher hydrophobic moment (Winder and Kendrick-Jones, 1995).

1.7 ISOFORMS OF α-ACTININ

Invertebrate α-actinin genes have been characterised in a number of species including *Dictyostelium*, *C. elegans*, and *Drosophila* (Noegel *et al.*, 1987; Barstead *et al.*, 1991; Fyrberg *et al.*, 1990). In vertebrates, two chicken genes have been identified, one encoding a skeletal muscle isoform and one encoding the smooth muscle isoform (Baron *et al.*, 1987; Arimura *et al.*, 1988; Baron *et al.*, 1987). In humans, three genes have been identified. The non-muscle cytoskeletal isoform (AACT1) maps to chromosome 14q22-q24 (Millake *et al.*, 1989; Youssoufian *et al.*, 1990), and two skeletal muscle genes located on chromosomes 1q42-q43 (AACT2) and 11q13-q14 (AACT3) (Beggs *et al.*, 1992). AACT2 is expressed in both skeletal and cardiac muscle, but AACT3 expression is limited to skeletal muscle.

Although the ABD of smooth and skeletal muscle α-actinin isoforms are closely similar, the extreme N-terminal region of the skeletal isoform has an additional 9 residues when compared to the smooth and non-muscle isoforms, and a totally novel sequence over the following 12 amino acids (Figure 4). The extreme N-terminal region of dystrophin also differs between the brain and muscle isoforms (Nudel *et al.*, 1989; Feener *et al.*, 1989), and is quite different to that found in α-actinin isoforms. The C-terminal half of the skeletal isoform of α-actinin is also notably divergent from the smooth and non-muscle isoforms (Blanchard *et al.*, 1989). Since the skeletal isoform of α-actinin is specifically localised to the Z-disc, it has been suggested that these regions of the protein are involved in interactions with other Z-disc components, and the assembly of the Z-disc itself. Interestingly, one *Drosophila* mutant at the α-actinin locus, *fliA*^{3}

is unable to form Z discs in the jump muscle, although it retains the capacity to assemble thick and thin filaments into fibrils (Fyrberg, 1990).

A chicken skeletal-muscle α-actinin gene has been shown to give rise to 2 alternatively spliced isoforms which differ in EF-hand I (Parr *et al.*, 1992). The 22 residues found in the skeletal-muscle isoform were replaced by a stretch of 26 unique residues in the variant. Although this α-actinin splice variant is expressed in non-muscle tissues, neither of the two EF-hands would be predicted to be functional, making it unlikely to be a typical non-muscle isoform. In addition, vertebrate non-muscle α-actinins have a spacer of five amino acids between the two EF-hands, whereas in the variant, the spacer is just four residues in length (Parr *et al.*, 1992).

In cultured skeletal muscle cells two distinct isoforms of α-actinin are present after myoblast fusion, although they are found at separate locations within the cell (Endo and Masaki, 1984). Antibodies to the skeletal muscle isoform stained only Z discs, whereas an antibody for the smooth muscle isoform stained membrane associated structures. It is interesting that cDNAs encoding fibroblast (Arimura *et al.*, 1988) and smooth muscle isoforms of α-actinin have been isolated from chicken skeletal muscle cDNA libraries. cDNAs encoding both smooth muscle and fibroblast isoforms have been isolated from a chicken fibroblast cDNA library (Baron *et al.*, 1987). Chicken smooth muscle and non-muscle α-actinins arise by alternative splicing from a single gene, producing polypeptides that differ only in the C-terminal region of the first EF-hand (Baron *et al.*, 1987; Arimura *et al.*, 1988). The extensive sequence difference between smooth and skeletal muscle isoforms and the failure of the respective probes to cross-hybridise indicates that the skeletal isoform is encoded by a separate gene. Targetting must presumably depend on isoform specific sequences which perhaps allow a given isoform to interact with other proteins with a unique distribution within the cell. Expression of the smooth muscle α-actinin cDNA in monkey COS cells results in the protein localising to both stress fibres and adhesion plaques (Jackson *et al.*, 1989). Similarly, microinjection of α-actinin isolated from lymphoid cells and smooth muscle into fibroblasts has also been found to distribute to both stress fibres and adhesion plaques (McKenna *et al.*, 1985). Interestingly, an antibody raised against part of the dystrophin repeats cross-reacts with an α-actinin specific to fast-twitch glycolytic skeletal muscle (Hoffman *et al.*, 1989).

The chicken and human non-muscle and smooth muscle α-actinin isoforms are all highly homologous, but show substantially lower homology to the skeletal muscle isoforms even within the same species. These differences in a single species are probably required to produce the unique properties of that specific isoform. This probably includes unique structural properties of each isoform conferred by the isoform specific sequence regions which prevent formation of α-actinin heterodimers when multiple isoforms are expressed in a single cell. Isoform specific mutations are restricted to small regions of the repeats since 68% of the

positions have been shown to be identical among all chicken and human α-actinin sequences (D.W. Speicher, priveliged communication).

It has been shown that the calcium sensitivity of a chicken lung α-actinin for the interaction with polymerised actin is much lower than those of the other non-muscle α-actinins (Imamura *et al.*, 1994). The deduced amino acid sequence of the lung α-actinin showed 76%, 82% and 83% identity to those of chicken skeletal-muscle, smooth muscle and fibroblast-type α-actinin, respectively. Differences in the structure between the lung-type and the other α-actinins were found in the extreme N- and C-terminal halves, in the third and fourth regions of the repeats, and in the two EF-hand regions (Imamura *et al.*, 1994). It was shown that the lung-type (NM2) α-actinin was expressed not only in non-muscle but also in muscle, including heart, gizzard and pectoralis muscle, and results suggested that the NM2 α-actinin detected in muscle tissues was derived from capillary endothelial cells. Contraction of endothelial cells is caused by inflammatory mediators, histamine and thrombin (Laposata *et al.*, 1983; Wysolmerski and Lagunoff, 1988), and this retraction is regulated by phosphorylation of myosin light chains in a calcium-dependent manner (Wysolmerski and Lagunoff, 1990). Histamine increases the cytosolic calcium concentration to micromolar levels in endothelium (Jacob *et al.*, 1988), hence the occurence of low-calcium-sensitive α-actinin. However, a homologue of the non-muscle type (fibroblast-type) NM1 α-actinin was isolated from a cultured human umbilical-vein endothelial cell cDNA library, suggesting the co-existence of two functionally different isoforms of α-actinin within individual vascular endothelial cells (Imamura and Masaki, 1994). Similarly, an α-actinin was purified from the cytosolic fraction of rabbit alveolar macrophages (Pacaud and Harricane, 1993) and its calcium-sensitivity was shown to be different from that of the macrophage α-actinin that was purified from the cytoskeletal fraction (Bennett *et al.*, 1984).

Human platelet α-actinin, characterised as a non-muscle type, appears to exist as two isoforms which differ in chain length and immunological properties (Gache *et al.*, 1984). Interestingly, the two isoforms differ in their calcium sensitivity with respect to F-actin-binding, and yet show equivalent calcium sensitivity to cross-linking actin filaments (Landon *et al.*, 1985), suggesting that the two isoforms might have distinct functions, or that they are differentially regulated. Like macrophage and brain α-actinins, the platelet variants also exhibit temperature-dependent actin gelation, a reduction in activity being observed at 37 °C (Bennett *et al.*, 1984; Duhaiman and Bamburg, 1984).

1.8 THE EFFECT OF VARYING SALT CONCENTRATION ON THE STRUCTURE OF α-ACTININ

Skeletal muscle α-actinin can take on at least three different conformations depending on the KCl concentration of the solvent (Kuroda *et al.*, 1994). The size, estimated using viscosity data, under low-salt conditions was 3.2 x 74.2 nm, and this changed to 3.4 x 51.3 nm and 4.5 x 40.1 nm, respectively, in intermediate and high salt ranges. The conformational change was reversible and the change was shown to take place through the elongation and/or shortening of the rod domain of the molecule. This isoform was more resistant to proteolysis with increasing KCl, and the conformational change affected the binding ratio between α-actinin and actin (Kuroda *et al.*, 1994).

It has been shown that chicken gizzard α-actinin is able to bind calcium, but that this binding is eliminated in the presence of physiological potassium levels (Wenegieme *et al.*, 1994). α-Actinin contains 3.5 high affinity calcium binding sites per dimer, with a $K_d = 6.4 \times 10^{-6}$ M, and 87.3 lower affinity sites with a $K_d = 1.7 \times 10^{-4}$ M. However, when KCl in the binding buffer was increased to 120 mM, calcium binding was eliminated. Structural changes produced by potassium binding to α-actinin, measured by circular dichroism, proteolysis, and fluorescence, were substantial (Wenegieme *et al.*, 1994). A decrease of calcium affinity with increasing potassium concentration has also been observed for brain spectrin (Wallis *et al.*, 1992). The potassium ions could alter a conformation in the N-terminal ABD of α-actinin which may interact with the EF-hands in the antiparallel homodimer. An increase in fluorescence upon KCl addition indicated greater exposure of hydrophobic areas for bisANS binding (Wenegieme *et al.*, 1994), similar to observations on the effects of cations on the structure of erythrocyte spectrin (Wallis *et al.*, 1993). This could be due to a possible contraction of the α-actinin molecule leading to a formation of more hydrophobic sites. The protein in the presence of physiological KCl was more susceptible to proteolytic digestion. This is also similar to observations on erythrocyte spectrin (Wallis *et al.*, 1993), but interestingly, the reverse to skeletal muscle α-actinin (Kuroda *et al.*, 1994).

Similarly, increasing KCl from 0-120 mM led to a decrease in α-helix conformation for brain, platelet and heart α-actinins (Wenegieme *et al.*, 1996). In 120 mM KCl, calcium produced small changes in the CD spectra of both brain and platelet α-actinin, but had no effect on heart α-actinin. Digestion of brain, platelet and heart α-actinins with α-chymotrypsin showed an increase of proteolytic susceptibility in 120 mM KCl. It was also demonstrated that increasing the concentration of calcium or magnesium led to greater changes in digestion fragment patterns in the absence of KCl than in the presence of 120 mM KCl (Wenegieme *et al.*, 1996). These sudies indicate different isoforms of α-actinin behave differently in the presence of monovalent

and divalent cations, reflecting the electrolyte variations that occur in muscle and non-muscle tissues.

1.9 LIPID BINDING IN α-ACTININ

Phosphatidylinositol 4,5-bisphosphate (PIP_2) is a low abundance phospholipid, which generates two second messengers, inositol 1,4,5-trisphosphate (IP_3) and diacylglycerol (DAG), when phospholipase C (PLC) is activated in response to various hormones and mitogens (Berridge and Irvine, 1984; Nishizuka, 1984). IP_3 and DAG are known to mobilise calcium from the endoplasmic reticulum (ER) and to activate protein kinase C (PKC), respectively (Berridge, 1987; Nishizuka, 1984). PIP_2 dramatically increases the gelating activity of smooth muscle α-actinin (Fukami *et al.*, 1992) and the hydrolysis of PIP_2 on α-actinin by PLC may be important in cytoskeletal reorganisation (Fukami *et al.*, 1994). The decrease in PIP_2 bound to α-actinin induced by addition of platelet-derived growth factor (PDGF) correlates with the depolymerisation of actin (Fukami *et al.*, 1994). This suggests that the amount of PIP_2 regulates the organisation of stress fibres. It has been shown that a proteolytic fragment comprising amino acids 168-184 from striated muscle α-actinin contains a PIP_2-binding site (Fukami *et al.*, 1996). A synthetic peptide composed of the 17 amino acids inhibited the activities of PLC-γ1 and -δ1. Interestingly, smooth muscle α-actinin is extracted with relatively little bound PIP_2, and has a lower actin-binding affinity (Fukami *et al.*, 1992). Amino acid sequences which contain the PIP_2-binding site in skeletal muscle α-actinin are homologous to that in chicken smooth muscle α-actinin, except for the substitution of a basic amino acid, arginine, to another basic amino acid, lysine. Point mutants in which arginine 172 or lysine 184 of α-actinin were replaced by isoleucine reduced the inhibitory effect of the peptide on PLC mediated PIP_2 hydrolysis by nearly half (Fukami *et al.*, 1996). This region is homologous to sequences in the PIP_2-binding site in spectrin and the PH domains of PLC-δ1 and Grb7. The PH domain is suggested to be involved in protein-protein or lipid-protein interactions, because the PH domain is reported to associate not only with PIP_2 (Harlan *et al.*, 1994), but also with the βγ subunit of trimeric G proteins, which play various roles in cellular signaling processes (Touhara *et al.*, 1994; Tsukada *et al.*, 1994), and PKC (Yao *et al.*, 1994).

Phosphatidylinositol 3-kinase (PI 3-kinase) has been shown to play an important role in the signal transduction pathways that regulate cell growth. It has also been implicated in cytoskeletal reorganisation (Zhang *et al.*, 1992; Eberle *et al.*, 1990; Downes and Macphee, 1990). It has been shown that chicken gizzard α-actinin copurifies with PI 3-kinase (Shibasaki *et al.*, 1994). The antibody against the PI 3-kinase 85 kDa regulatory subunit (p85), which contains two SH2 domains (Koch *et al.*, 1991; Pawson and Gish, 1992; Birge and Hanafusa, 1993), and one SH3 domain, also co-immunoprecipitated α-actinin. In addition, anti-α-actinin antibody coprecipitated PI 3-kinase activity. This coprecipitation was observed even after

depolymerisation of actin fibres, suggesting that PI 3-kinase binds directly to α-actinin. In the absence of PIP_2, α-actinin bound only to the whole p85 construct, but in the presence of PIP_2, α-actinin binds to the truncated proline-rich region of p85 fragments, indicating a conformational change of α-actinin by PIP_2 (Shibasaki *et al.*, 1994). These results suggest that PI 3-kinase binds to α-actinin and regulates cytoskeletal reorganisation.

Where α-actinin is involved in anchoring actin filaments to membrane associated structures, the link to the membrane is probably indirect since α-actinin has no notably hydrophobic region which would allow it to intercalate into the lipid bilayer (Blanchard *et al.*, 1989). However, an interaction between certain lipids and α-actinin has been noted (Meyer *et al.*, 1982). Indeed, it has been reported that α-actinin interacts with diacylglycerol and palmitic acid, with a parallel increase in actin bundle formation (Burn *et al.*, 1985). It is interesting that erythrocyte spectrin also binds lipids. However, the apparent distance between α-actinin and the cell membrane would appear to be too great to be compatible with α-actinin serving as a direct link between F-actin and the membrane (Geiger *et al.*, 1979; Chen and Singer, 1982).

However, α-actinin has been shown to insert into bilayers containing acidic phospholipids and an analogue of lecithin (Niggli and Gimona, 1993). α-Actinin was also shown to associate with phosphatidylserine liposomes, and results suggested the formation of a ternary complex consisting of vinculin, α-actinin and phospholipids. In this complex, both proteins could interact at the bilayer, resulting in an altered conformation of the two proteins (Niggli and Gimona, 1993).

1.10 INTRACELLULAR LOCALISATION OF α-ACTININ

1.10.1 The Z-disc

The major actin filament cross-linking protein found in the Z-line is α-actinin. The Z-line anchors the thin filaments from neighbouring sarcomeres and has an ordered lattice structure which is hexagonal in insect flight muscle and tetragonal in vertebrates (Lakey *et al.*, 1993). Knockout of the α-actinin gene in *Drosophila* engenders either lethal or flightless phenotypes (Roulier *et al.*, 1992). The lack of flight, due to weakened flight muscles, indicates that α-actinin has the principle role of stabilising or anchoring the actin filaments once localised within the sarcomere (Roulier *et al.*, 1992). The ability of α-actinin to bind actin filaments with antiparallel orientation is indicated by the structure of the Z-line. A number of skeletal muscle proteins have been identified that interact with α-actinin. Titin has been shown to bind to α-actinin (Small *et al.*, 1992). It is believed to connect the Z-line to the M-band defining the length of the sarcomere. Both kettin and titin act to organise other proteins to produce the regular structure of the sarcomere. Kettin has been shown to bind to both F-actin and α-actinin

(Lakey *et al.*, 1993). α-Actinin has the potential to bind to actin filaments along their entire length, although temperature effects and the competitive binding of tropomyosin probably restricts the binding to the thin filaments in the Z-line. The condensation-extension model of α-actinin implies that α-actinin can act as a molecular spring in situ. According to the physiological studies of muscle contraction, the lattice volume of the sarcomere remains constant during contraction of myofibrils (Huxley, 1953; Elliott *et al.*, 1963). The lateral tension developed at each Z-disc upon contraction could be relieved by the extensible nature of α-actinin.

Although no disease-causing mutations of α-actinin have been demonstrated in humans, there is one inherited muscle disease, nemalin rod myopathy (NRM), that is characterised by abnormalities of α-actinin expression. Skeletal muscle from patients with NRM contains disordered Z-lines and rod-shaped bodies that are composed predominantly of α-actinin (Jockusch *et al.*, 1980). Linkage studies in one large Australian family with NRM established linkage to markers 1q21-q23 (Laing *et al.*, 1992), thus ruling out AACT1, AACT2, and AACT3 as candidate genes for the disease in this family.

1.10.2 Smooth muscle

The cytoplasmic dense bodies found in smooth muscle are rich in α-actinin (Geiger *et al.*, 1981) and are believed to be the interaction sites between the intermediate filament cytoskeleton and the actin cytoskeleton (Small *et al.*, 1992). Actin filaments of opposite polarity are bound in these structures, presumably by α-actinin (Bond and Somlyo, 1982). α-Actinin is also localised to adhesion plaques, which are sites where actin bind to the cell membrane. Here α-actinin functions as a unipolar cross-linker of actin filaments (Taylor and Taylor, 1994).

1.10.3 Non-muscle cells

Non-muscle α-actinin isoforms usually have a submembranous location where they apparently play crucial roles in cell adhesion, motility and transmembrane signaling (Blanchard *et al.*, 1989; Matsudaira, 1991; Stickel and Wang, 1988). Association with clathrin trimers, which aggregate to coat vesicles known to be involved in several key cellular events, suggests a role in regulating certain aspects of cellular trafficking (Merisko *et al.*, 1988). Recently, α-actinin has been shown to colocalise in dendritic spines with N-methyl-D-aspartate (NMDA) receptors, and the α-actinin rod domain was also shown to bind subunits of the NMDA receptor. Additionally, binding of α-actinin to one of the receptor subunits was antagonised by calcium/calmodulin, suggesting a role in the localisation of NMDA receptors and their modulation by calcium for α-actinin (Wyszynski *et al.*, 1997).

The loss of α-actinin in *Dictyostelium* has been shown not to result in any phenotype distinguishable from wild type cells (Witke *et al.*, 1992) and a *Dictyostelium* mutant deficient in α-actinin still retained its ability to undergo amoeboid movement, chemotaxis and capping/patching of surface proteins (Schleicher *et al.*, 1988). It was found that *Dictyostelium* lacking both α-actinin and the actin gelation factor ABP-120 were abnormal in a number of characteristics, suggesting that there was a certain level of redundancy within actin-binding proteins in these cells (Witke *et al.*, 1992). They were motile but strongly impaired in fruiting body formation, the culmination of morphological changes which requires the ordered movement of the prestalk cells during formation of the stalk, thereby lifting the spore mass into the air. This could have been due to the inability of the cells to undergo morphogenetic movement, the lack of positional information, an altered chemotactic motility (Knecht and Loomis, 1988), or a lack of viscoelasticity in the cytoskeleton. Each motile event performed intracellularly might require a distinct level of viscoelasticity that is safeguarded by other actin-binding proteins (Matsudaira, 1991), while during morphological changes in development their functions cannot be substituted. It has also been demonstrated that whilst null mutants for an X-linked *Drosophila* α-actinin gene survive embryogenesis but die in the second day of larval growth, and alleles with missense mutations have abnormal flight muscles (Fyrberg *et al.*, 1990), no obvious non-muscle phenotype was observed (Roulier *et al.*, 1992).

1.10.4 Cellular junctions

α-Actinin has been demonstrated to be a component of adherens junctions (AJs). AJs are found between many cell types, including epithelial cells, cardiac myocytes, and fibroblasts (Volk and Geiger, 1984; Geiger *et al.*, 1987, 1990; Geiger and Ayalon, 1992; Heaysman and Pegrum, 1973). Adherens-type junctions can be subdivided depending on the presence of either the cadherin or integrin family of cell adhesion molecules in the junction. Cadherins, which are involved in calcium-dependent intercellular interactions, are identified in adherens junctions at sites of cell-cell contact whereas integrins are located at sites of cell-ECM contact (Figure 15).

α-Actinin itself has been demonstrated to be capable of interacting with the cytoplasmic domain of the β1 and β3 integrin subunits (Otey, 1990), and this occurrs via its central spectrin-like repeats. Fibroblasts in culture flatten and attach to the culture dish. This attachment is accompanied by the formation of long actin bundles that attach to the plasma membrane at the contact points with the culture dish. α-Actinin is located along the stress fibre and in higher concentration at the sites of attachment to the plasma membrane (Lazarides and Burridge, 1975; Isobe *et al.*, 1988). α-Actinin persists in focal adhesions in the absence of associated stress fibres, suggesting that α-actinin is interacting with another focal adhesion component, such as integrin (Otey, 1990) or perhaps vinculin (McGregor *et al.*, 1994). The interaction of the cell with fibronectin is mediated by a specific membrane receptor which recognizes the RGD

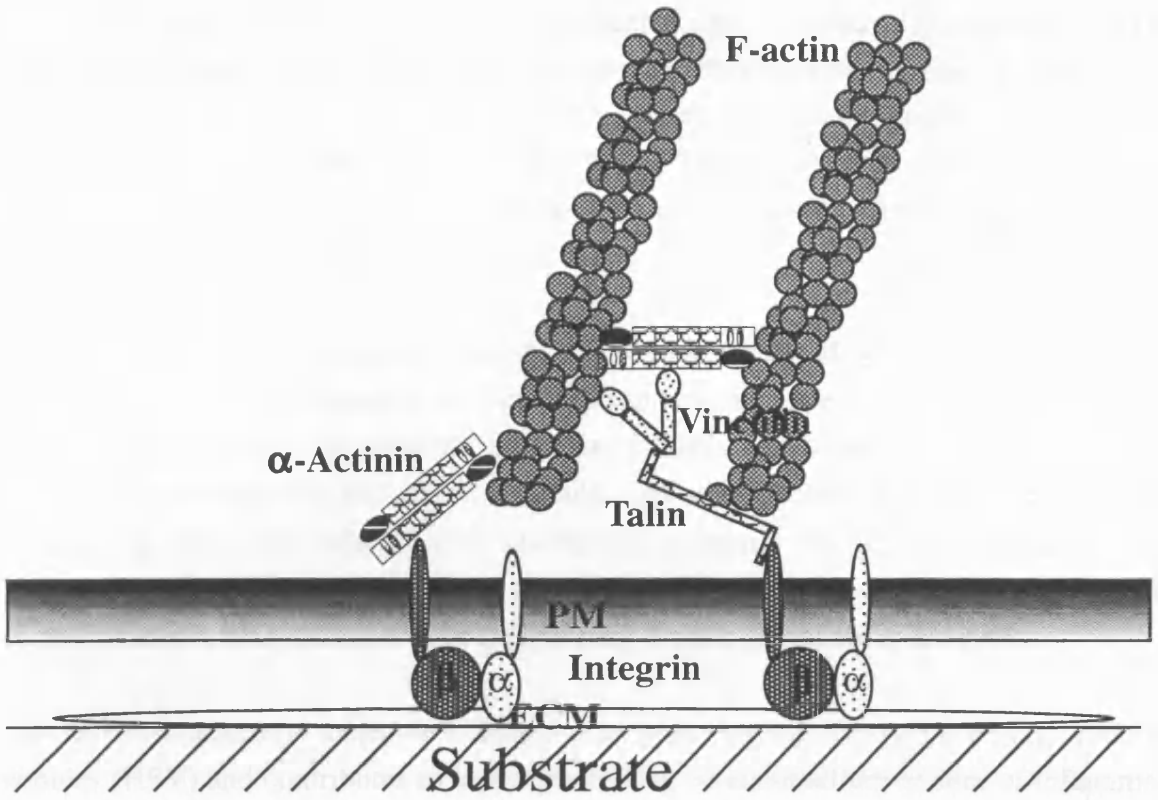

Figure 15: Model of the protein-protein interactions involving α-actinin in focal adhesions determined by *in vitro*-binding experiments and immunolocalisation. ECM, extracellular matrix; PM, plasma membrane.

sequence in fibronectin (Ruoslahti and Pierschbacher, 1987). Data indicate that an early response to the addition of the RGD tripeptide is that α-actinin and vinculin dissociate as a complex from focal contacts, followed by a gradual disappearance of the contact (Stickel and Wang, 1988). It has been shown that at adhesion sites α-actinin mobility is greatly reduced (Geiger *et al.*, 1982, 1984; Stickel and Wang, 1987). It has also been noted that the association of α-actinin with most structures in muscle cells is highly stable when compared with α-actinin in fibroblast stress fibres (McKenna *et al.*, 1985). The localisation of α-actinin to these junctions is a combination of its ability to bind F-actin and the interaction with the other proteins specifically located to these structures. The expression of the ABD of smooth muscle α-actinin in cultured cells resulted in the specific localisation to the adhesion plaques but it did not decorate the stress fibres (Hemmings *et al.*, 1992). The structure of the stress fibre at the contact site with the junction may be subtly different such that the ABD alone is able to preferentially bind to this region. Zyxin binding has been shown to be specific to the ABD of α-actinin (residues 1-265) (Crawford *et al.*, 1992) and may be involved in the localisation of the ABD to the adhesion plaques.

The stability of cell-ECM junctions can be influenced by a number of factors, including small GTP binding proteins, phosphorylation, and calcium. Phorbol ester-induced activation of PKC in epithelial cells (e.g. African Green Monkey kidney cells) causes α-actinin and vinculin to disperse from adhesion plaques (Meigs and Wang, 1986). α-Actinin binding of actin in non-muscle cells is known to be calcium sensitive (Blanchard *et al.*, 1989), suggesting a role for calcium in focal adhesion regulation.

Cadherins localise to the cell-cell adherens junctions in epithelial cells and cardiomyocytes. α-Actinin colocalises extensively with E-cadherin and catenins in epithelial cells (Knudsen *et al.*, 1995). α-Actinin also co-immunoprecipitates specifically with α- and β-catenin from N- and E-cadherin-expressing cells, but only if α-catenin is present. Evidence has been presented that α-actinin can associate with the cadherin/catenin complex via actin (Rimm *et al.*, 1994). However, it has been demonstrated that α-actinin co-immunoprecipitates with the N-cadherin/catenin complex in an actin-independent manner (Knudsen *et al.*, 1995).

The leukocyte adhesion molecule L-selectin mediates binding to lymph node high endothelial venules (HEV) and contributes to leukocyte rolling on endothelium at sites of inflammation. The cytoplasmic domain of L-selectin interacts with cytoskeletal proteins via α-actinin, but receptor positioning in microvilli does not require interaction with α-actinin (Pavalko *et al.*, 1995). F-actin in combination with α-actinin promotes expansion of pseudopods in leukocytes, whereas myosin combined with F-actin promotes contraction (Keller and Niggli, 1993). Mac-1 and lymphocyte function-associated antigen (LFA)-1, members of the leukocyte or CD18 integrin subfamily of adhesion molecules, rapidly change from a low avidity to a high avidity state on activation of neutrophils by various agonists. Activation of neutrophils results in an α-actinin-mediated association between CD18 integrins and actin filaments (Pavalko and Laroche, 1993).

α-Actinin may also be important in cell-cell adhesion, because of its ability to bind the cytoplasmic domain of intercellular ahesion molecule (ICAM)-1 (CD54), an integral membrane protein that functions as a counter-receptor for leukocyte integrins (CD11/CD18) (Carpen *et al.*, 1992). In addition, α-actinin has been shown to colocalise with ICAM-2, which functions as a ligand for LFA-1 and is involved in leukocyte adhesion. Several sites on α-actinin were also demonstrated to bind a cytoplasmic peptide of ICAM-2 (Heiska *et al.*, 1996).

α-Actinin may also have a role in cell proliferation. The expression of α-actinin is rapidly elevated in growth-activated quiescent cells and in regenerating liver (Gluck *et al.*, 1992), and is reduced in simian-virus 40 (SV40)-transformed 3T3 cells and various differentiating cell types (Gluck *et al.*, 1993). Cells overexpressing α-actinin by 40-60% displayed a significant reduction in cell motility. 3T3 cells in which the expression of α-actinin was reduced to 25-

60% of control levels had an increased cell motility. Moreover, such α-actinin-deficient 3T3 cells formed tumors upon injection into nude mice (Gluck and Benzeev, 1994). Likewise, α-actinin cDNA transfected into SV40-transformed 3T3 cells suppresses tumourigenicity (Gluck *et al.*, 1993). Since α-actinin is a major structural component of microfilaments and adherens junctions, it may exert its effect on cellular properties by influencing microfilament organisation and/or cell adhesion and motility. AJs are dynamic structures whose components are present in assembled or unassembled soluble pools between which a dynamic equilibrium is maintained (Kreis *et al.*, 1984). Modulations in this equilibrium in one direction or the other will result in junction disassembly and decreased adhesion or, conversely, in the formation of extended junctions and increased adhesion. Studies with truncated integrin and cadherin transmembrane receptors lacking the extracellular domain have shown that these receptors are still recruited to adhesion plaques and cell-cell junctions, provided their cytoplasmic domain is intact (LaFlamme *et al.*, 1992; Geiger *et al.*, 1992; Fujimori and Takeichi, 1993). This suggests a potentially important role for cytoplasmic plaque components in the recruitment and assembly of adhesion receptors, and their binding to the actin-cytoskeleton by an "inside-out" mechanism (Takeichi *et al.*, 1992; Geiger *et al.*, 1992). The nature of the signal transmitted by alterations in the organisation of this cell adhesion-microfilament complex has been suggested to involve phosphorylation and dephosphorylation of plaque proteins by resident kinases and phosphatases (Volberg *et al.*, 1992; Burridge *et al.*, 1992; Guan and Sholloway, 1992; Takeichi *et al.*, 1992; Juliano and Haskill, 1993). In addition, α-actinin is known to bind, in adhesion plaques, to regulatory molecules such as the LIM domain proteins zyxin and cCRP, which may act in transcriptional regulation (Sadler *et al.*, 1992). It has been suggested that signals for growth control are transmitted through integrins and require an organised association of the microfilaments with these adhesion sites, since in transformed cells that have a disorganised microfilament system these signaling pathways are constitutively activated (Schwartz, 1992; Guan and Shalloway, 1992; Ben-Ze'ev, 1992; Juliano and Haskill, 1993). Junctional plaque proteins such as α-actinin may play an important role in the maintenance of this adhesion-related signaling system by acting as effective tumour supressors (Tsukita *et al.*, 1993).

1.11 FUNCTION AND LOCALISATION OF SPECTRIN

Over-expression of the actin-binding N-terminus of β-spectrin, or of the region containing the ankyrin-binding domain, causes loss of epithelial cell morphology, loss of membrane-associated endogenous β-spectrin, and altered Na^+/K^+-ATPase distribution. Spectrin is essential for the normal morphology of cells in monolayer culture. The dissociation of β-spectrin from the plasma membrane does not affect the localisation of α-spectrin (Hu *et al.*, 1995).

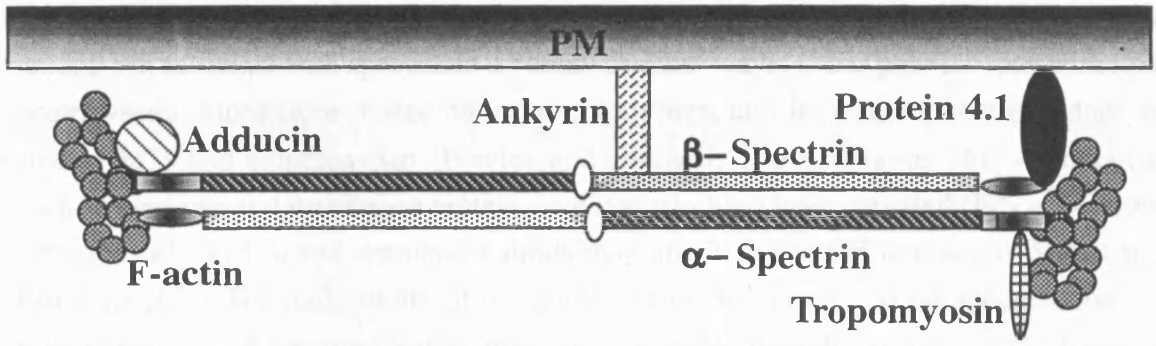

Figure 16: Spectrin and its association with the erythrocyte cytoskeleton. White ovals represent sites of phosphorylation in β-spectrin.

The tail-end region of spectrin includes several binding sites that appear to overlap or be closely juxtaposed to one another. For example, the N-terminus of β-spectrin associates with protein 4.1 and, through protein 4.1, with the cell membrane (Bennett and Gilligan, 1993) (Figure 16). From the position of the Kissimmee mutation in β1 (Becker *et al.*, 1993), a mutation which diminishes spectrin's capacity to bind protein 4.1, it appears that the 4.1-binding region is immediately adjacent to the actin-binding domain and may overlap with the interchain binding site (Viel and Branton, 1994; Becker *et al.*, 1993; Karinch *et al.*, 1990). This overlap may explain the stabilising action of protein 4.1 on the spectrin-actin binary complex (Discher *et al.*, 1995).

The N-terminus of brain β-spectrin also associates directly with integral membrane proteins. The membrane-binding site of spectrin has been suggested to be in segment β1, and that the conserved five-residue motif of β1 is a membrane-binding site (Lombardo *et al.*, 1994). Alternatively, it has been concluded that the membrane-binding sites are located in a larger region that includes segments β2-4 and β6-7 (Davis and Bennett, 1994). In both studies, those synthetic polypeptides with the highest affinity for the membrane contained the conserved octamer between β1 and β2 that is required for interchain binding (Viel and Branton, 1994). This octamer may also constitute a membrane protein-binding site. If so, it may explain why non-conservative substitutions in this octamer do not affect interchain binding (Viel and Branton, 1994). The conserved residues in the octamer may be required in a sequence-independent manner to define the register of neighbouring segments that contain the interchain-binding sites (Viel and Branton, 1994). The presence of a similar octamer between α20 and α21 implies that α-spectrin chains could also independently associate with the cell membrane. The presence of this octamer in α-spectrin may explain the association of α-chains with the periphery of epithelial cells lacking β-subunits (Hu *et al.*, 1995).

In addition to its association with spectrin via ankyrin (Bennett and Gilligan, 1993), the plasma membrane can associate with spectrin in a variety of other ways. Other proteins may participate in spectrin-actin interactions, based on *in vitro* activities, and include adducin (Gardner and Bennett, 1987) and tropomyosin (Fowler and Bennett, 1984) (Figure 16). Associations between several integral membrane proteins and spectrin have been reported (Iida *et al.*, 1994; Pollerberg *et al.*, 1987), and membrane lipids may attach to the PH domain in β19 of non-erythroid spectrin. The multiplicity of membrane-association domains on spectrin, together with the variability of spectrin ligands, may be responsible for selective targeting of spectrin isoforms to functionally distinct plasma membrane domains. An erythroleukemic cell line lacking α-spectrin was generated from spectrin-deficient mice (Dahl *et al.*, 1994). The effects of α-spectrin deficiency were apparent in the cells' irregular shape and fragility, and in their susceptibility to capping by lectins or antibodies. A series of experiments demonstrated the association of a β-spectrin isoform with the Golgi membrane, and show that this association is dependent on a functional Golgi apparatus (Beck *et al.*, 1994). Results also suggested that the spectrin membrane skeleton is part of the protein sorting machinery. Therefore, spectrin appears to regulate the mobility of integral membrane proteins both at the plasma membrane and in intracellular membrane systems such as the Golgi (Viel and Branton, 1996).

1.12 FUNCTION OF DYSTROPHIN

The precise function of dystrophin is a matter of debate. Interestingly, in the case of *mdx* mice, only the diaphragm displays the muscle pathology typical of human DMD patients (Stedman *et al.*, 1991). In the absence of dystrophin, the capacity of the membrane to withstand mechanical stress is greatly impaired, and the degeneration of the mouse diaphragm is presumably due to the large work rate performed which overcomes the relative protection of the smaller fibre size of the mouse limb muscles (Petrof *et al.*, 1993). The membranes osmotic fragility is also increased (Hutter *et al.*, 1991) and myotubes exhibit a large diminuition in stiffness (Pasternak *et al.*, 1995). Dystrophin is mainly located in specialised zones of the sarcolemma, the costameres, surrounding the Z-discs of the myofibrils (Porter *et al.*, 1992; Straub *et al.*, 1992). These probably represent the sites of mechanical coupling between the sarcolemma and the contractile system. It serves as a link between the transmembrane glycoprotein complex that in turn connects the membrane to the ECM and to the cortical actin cytoskeleton (Figure 17) (Ahn and Kunkel, 1993). Dystrophin is presumed to protect the membrane against the shearing stresses to which it is subjected, in much the same way as the spectrin lattice stabilises the red cell membrane. Spectrin is responsible for the elasticity of the membrane with which it associates, and the dystrophin rod domain, with its spectrin-related sequence (Koenig and Kunkel, 1990) and conformation (Kahana *et al.*, 1994), may be supposed to exert a similar effect.

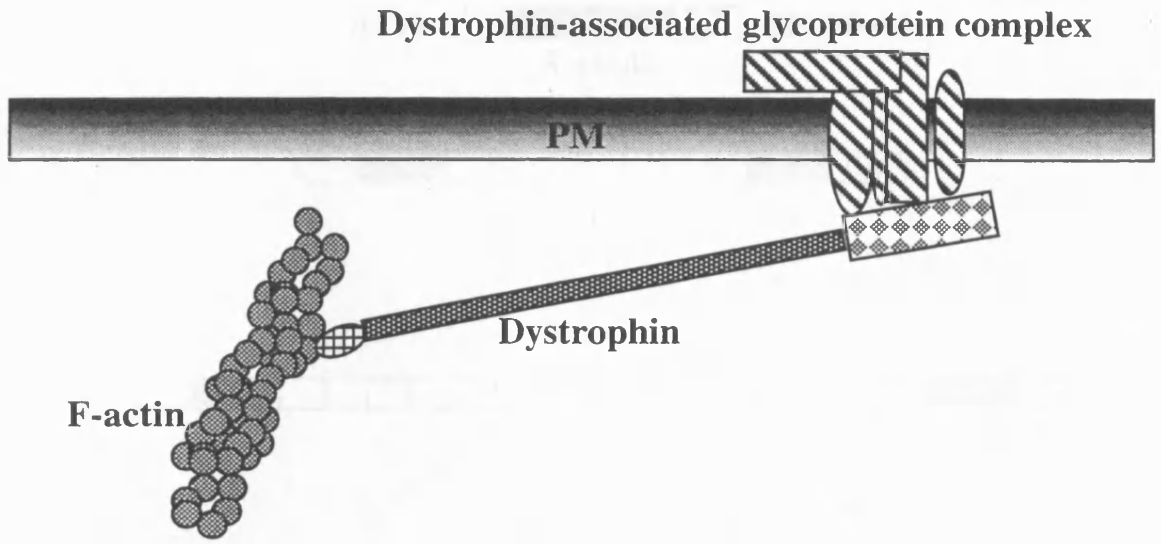

Figure 17: Interactions of dystrophin. Dystrophin associates with actin at its N-terminal region, and the dystrophin associated glycoprotein complex near the C-terminal end.

1.15 EVOLUTION OF THE SPECTRIN FAMILY

The structural similarity of spectrin, and α-actinin homologues shows that these genes existed in much the same form before the split between vertebrates and invertebrates. The relationship of spectrin subunits with α-actinin suggests that they are evolutionary related through a simple set of genetic mechanisms. These mechanisms probably include unequal crossing over between segments (Smith, 1973), such that α-actinin and spectrin arose from the other, or from a common precursor. While other events appear to complicate the relation of dystrophin to α-actinin and the spectrin subunits, it is clear that the members of the spectrin superfamily arose from the shuffling of a common set of domains very early in the evolution of the cell.

The evolutionary scheme probably began with an α-actinin-like molecule with multiple 114-residue segments (Figure 18). The duplication of 114-residue segments may have preceded the modification and multiplication of 106-residue segments since the former have diverged from one another more extensively then the latter (Dubreuil *et al.*, 1989). The formation of separate α- and β-spectrin subunits probably occurred after duplication of the 106-residue repetitive segment. Additional duplication events probably account for the expansion of the repetitive domains of spectrin, perhaps through unequal crossing over of ancestral genes. It is likely that the insertion of a transcriptional promoter inside the genomic region coding for the ancestor of the tetramerisation repeat caused the splitting of that repeat into the partial repeats β17 and α0, and the separation of spectrin into the ancestral β- and α-subunits (Pascual *et al.*, unpublished observations). The fact that segment 10 is not repeated in the α-spectrin sequence suggests that it was also acquired relatively late in the evolution of α-spectrin, after multiplication of the

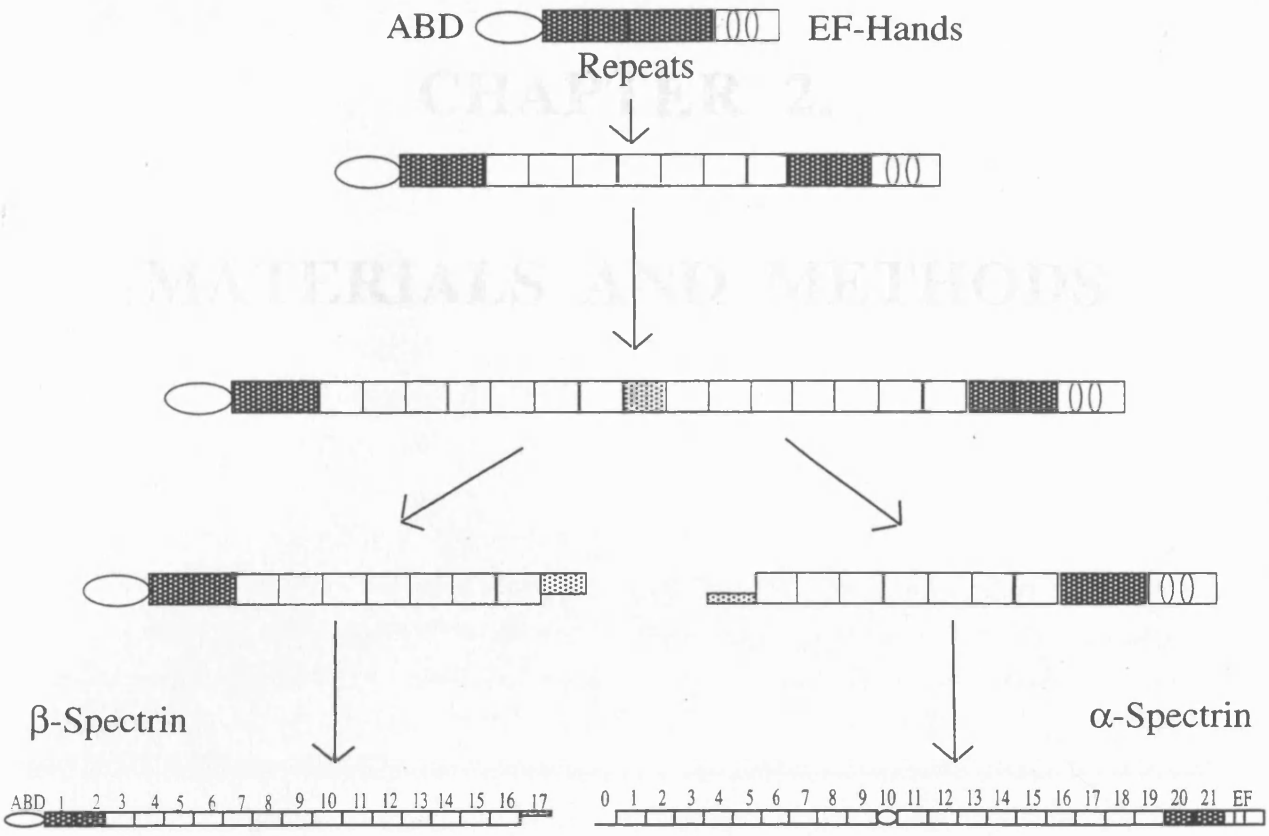

Figure 18: Evolution of spectrin from an α-actinin precursor. Elongation and duplication events were different for each spectrin subunit, resulting in diversity between the two (adapted from Pascual *et al.*, unpublished manuscript).

repetitive segments. The dystrophin repeats are the most diverse and difficult to align with those of the other two proteins, suggesting that the evolutionary line leading to dystrophin and utrophin separated earlier.

CHAPTER 2.

MATERIALS AND METHODS

2.1 REAGENTS

Rubidium chloride ($RbCl_2$), sodium hydrogen carbonate ($NaHCO_3$), dithiothreitol (DTT), 3-(N-morpholino) propane-sulphonic acid (MOPS), ethidium bromide, ampicillin, tris ((hydroxymethyl) amino methane) (Tris), polyethylene glycol 8000 (PEG 8000), ammonium persulphate (APS), 2-mercaptoethanol, phenylmethyl-sulphonyl fluoride (PMSF), isopropylthio-β-D-galactoside (IPTG), Triton X-100, glutathione, disodium adenosine triphosphate (Na_2ATP), disodium cytosine triphosphate (Na_2CTP), disodium guanosine triphosphate (Na_2GTP), disodium thiamine triphosphate (Na_2TTP) were all supplied by Sigma (Sigma chemical company, Poole, England).

Sodium chloride (NaCl), sodium hydroxide (NaOH), disodium hydrogen phosphate (Na_2HPO_4), potassium dihydrogen phosphate (KH_2PO_4), magnesium sulphate ($MgSO_4$), zinc chloride ($ZnCl_2$), potassium chloride (KCl), potassium phosphate (K_2PO_4), ammonium sulphate ($(NH_4)_2SO_4$), sodium dihydrogen phosphate (NaH_2PO_4),glycerol, diaminoethanetetra acetic acid (EDTA), ethyleneglycol-bis (β-aminoethyl ether) N,N,N',N'-tetra acetic acid (EGTA), phenol, chloroform, isoamylalcohol, ethanol, glycine, methanol, glacial acetic acid were all supplied by Fisons (Fisons of Loughborough, U.K.).

Ammonium chloride (NH_4Cl), magnesium chloride ($MgCl_2$), and sodium azide were supplied by BDH Ltd. (BDH Ltd., Poole, England).

Sodium dodecylsulphate (SDS) and urea were supplied by USB (United States Biochemical Corp., Cleveland, Ohio, U.S.A.).

Bacteriological agar, yeast extract, bacto tryptone supplied the Unipath Ltd. (Unipath Ltd., Basingstoke, Hampshire, U.K.).

The restriction enzymes *Bam*HI and *Eco*RI were supplied by Cambio (Cambridge Biolabs, Cambridge, U.K.).

High melting point agarose was supplied by Flowgen (Flowgen Instruments Ltd., Kent, U.K.).

30% acrylamide/0.8% bisacrylamide and high purity sequencing grade 40% acrylamide/0.8% bisacrylamide were supplied by National Diagnostics (National Diagnostics, Atlanta, Georgia, U.S.A.).

The DNA ligase was supplied by New England Biolabs (New England Biolabs Ltd., Ontario, Canada).

The Taq polymerase was supplied by Boehringer Mannheim (Boehringer Mannheim U.K., Lewes, East Sussex, U.K.).

The ^{35}S labelled adenosine triphosphate (^{35}S ATP) was supplied by Amersham (Amersham International p.l.c., Amersham, Bucks., U.K.).

The N.N.N',N'-tetramethyl ethylenediamine (TEMED) was supplied by Serva (Serva Feinbiochemica Gmbh and co., Heidelberg, Germany).

2.2 α-ACTININ cDNA CLONES

All cDNAs used (except chicken brain EF-hands) were generated by amplifying regions of full-length chicken smooth muscle α-actinin cDNA C17 (Baron *et al.*, 1987) by polymerase chain reaction (PCR).

Some of the the cDNA clones used in this study have been described previously: cDNAs encoding repeat 1 (amino acid residues 267 to 387, cloned into pGEX-3X), repeat 2 (residues 385-499, pGEX-2T), repeat 3 (residues 497-631, pGEX-2T), repeat 4 (residues 614-749, pGEX-2T), repeats 1-4 (267-749, pGEX-3X) and repeats 2-4 (385-749, pGEX-2T) (Gilmore *et al.*, 1994). A construct encoding repeats 1-3 (267-631, pGEX-3X) was also generated by Andrew Gilmore. The ABD of α-actinin (residues 1-269) was cloned into pGEX-2T by Alastair McGregor. The EF-hands of chicken brain (713-893) and smooth muscle isoforms (residues 713-888) were cloned into pGEX-1 by David Millake (Waites *et al.*, 1992). Constructs containing repeat 1 were generated using primers containing an *Eco*RI site, due to the presence of an internal *Bam*HI site, and the products were subcloned into the *Eco*RI site of either pGEX-2T or pGEX-3X. All other constructs were amplified using a 5' primer containing a *Bam*HI site and a 3' primer containing an *Eco*RI site, and the products were subcloned into *Bam*HI/*Eco*RI-cut pGEX-1, or 2T.

Constructs spanning the rod domain (residues 218-749, pGEX-3X), and mutants containing a tryptophan mutation (W->I, W->R, pGEX-3X) in repeat 1 were generated by Andrew Blanchard.

Mutant constructs consisting of repeats 1-4 (267-749), repeat 1, and repeat 4, lacking an 8-residue insertion from the N-terminal region were generated by Lance Hemmings and cloned into pGEX-2T.

2.3 BACTERIOLOGICAL HANDLING PROCEDURES

2.3.1 Growth of *E. coli* on solid media

Transformed bacterium (MC1061) were maintained on a solid medium, supplemented with ampicillin at a concentration of 100 μg ml^{-1}, consisting of- 10 g bacto tryptone, 5 g yeast extract, 10 g NaCl, 16 g bacteriological agar/litre of distilled water. The media was sterilised by autoclaving at 15 lb in^{-2} for fifteen minutes, and ampicillin added after cooling to approximately 55 °C to avoid degradation. The molten media was then dispensed into 9 cm petri dishes (Bibby Sterlin Ltd., Staffordshire, U.K.) and allowed to solidify. These were then stored at 4 °C, and dried in a 37 °C incubator for one hour before use. After inoculation, the plates were grown at 37 °C overnight (16 hrs) and then stored at 4 °C for up to three weeks. Single colonies were subsequently used to inoculate cultures in liquid media.

2.3.2 Growth of *E. coli* in liquid media

Liquid cultures were grown in 2TY broth, consisting of 1.6% bacto tryptone, 1% yeast extract, 0.5% NaCl. Cells transformed with pGEX plasmids were grown in the presence of 100 μg ml^{-1} ampicillin. Overnight cultures were grown in plastic disposable universal tubes (Bibby Sterilin Ltd., Staffordshire, U.K.) and then back diluted into plastic universals for volumes less than 20 ml, or glass conical flasks (250 ml flasks for 100 ml cultures, 500 ml flasks for 200 ml cultures, 2 l flasks for 750 ml cultures). Cultures were grown with aeration at 37 °C in an orbital shaker at 250 rpm.. Bacterial growth was followed by changes in the optical density at 600 nm in a LKB Biochrom Ultraspec 4050 spectrometer.

2.3.3 Storing *E. coli* as glycerol stocks

Long term storage of bacterial strains and transformed cells was at -70 °C in 20% glycerol (v/v). Overnight cultures were mixed with glycerol in a cryotube (Sarstedt, Numbrecht, Germany) and subsequently frozen. Reclaimation was achieved by transfer of some of the frozen culture to 1 ml of medium in a 1.5 ml Eppendorf tube, grown for 1 hour at 37 °C, followed by inoculation of an agar plate.

2.3.4 Generation of competent *E. coli*

Bacterial cells were prepared for the receipt of plasmid DNA by incubation with $CaCl_2$ and $RbCl_2$. 50 μl of an overnight culture was back diluted into 5 ml of fresh media and grown to an optical density of 0.5 at 600 nm, within logarithmic phase of growth. The cells were then pelleted by centrifugation at 13,000 rpm in a MSE Microcentaur in 1.5 ml eppindorfs for five

minutes. The pellet was resuspended in 500 µl of ice cold MR buffer (10 mM MOPS pH 7.0, 10 mM $RbCl_2$). The cells were then pelleted and resuspended in 500 µl of ice cold MRC buffer (100 mM MOPS pH 6.5, 10 mM $RbCl_2$, 50 mM $CaCl_2$) and incubated for an hour at 0 °C. Centifugation of the cells was then followed by resuspension in 150 µl of ice cold MRC buffer.

2.4 MOLECULAR BIOLOGY METHODS

2.4.1 Plasmid DNA isolation from bacterial cells

(a) QIAprep spin plasmid kit (QIAGEN Inc., USA)

The QIA-prep Plasmid Kit procedure is based on the modified alkaline lysis method of Birnboim and Doly (Vogelstein and Gillespie, 1979) and the adsorption of DNA on to silica in the presence of high salt (Vogelstein and Gillespie, 1979; Chen and Thomas, 1980). This protocol is designed for preparation of upto 20 µg of high-copy number plasmid DNA from 1-5 ml overnight cultures of *E. coli* in LB or 2TY medium.

The bacterial cells were pelleted at 13,000 rpm by centrifugation in 1.5 ml eppindorfs for five minutes. The cells were resuspended in 250 µl of buffer P1 (50 mM Tris-HCl, pH 8.0, 10 mM EDTA), containing RNAse A (100 µg ml^{-1}), and transferred to a microfuge tube. 250 µl of buffer P2 (200 mM NaOH, 1% SDS) was added, to denature cellular proteins, and chromosomal and plasmid DNA, and the tube gently inverted, to prevent shearing of genomic DNA bound to the cell wall (Birnboim and Doly, 1979; Birnboim, 1983). Lysis time is optimised to give maximum release of plasmid without complete lysis of the cell and release of chromosomal DNA, and to minimise the exposure of the plasmid to denaturing conditions. After the solution became viscous and slightly clear, the lysis was stopped by addition of 350 µl of buffer P3 (3.0 M KAc, pH 5.5), and the tube inverted immediately but gently to avoid localised precipitation until the solution became cloudy and viscous. The high salt concentration causes denatured proteins, chromosomal DNA, cellular debris and SDS to precipitate, while the shorter plasmid DNA renatures correctly and stays in solution. This was then centrifuged for 10 minutes, and the supernatant was added to a QIAprep spin column by decanting. This column was then centrifuged for 60 seconds, and the flow-through discarded. The column was then washed by adding 0.75 ml of buffer PE (1.0 M NaCl, 50 mM MOPS, pH 8.5), containing ethanol (15%), and centrifuged for 60 seconds. The fow-through was once again discarded and the column centrifuged for an additional 60 seconds to remove residual wash buffer. To elute the DNA, 30 µl of distilled water was added to the centre of the column, left to stand for 60 seconds, and then centrifuged into a clean eppindorf tube for 1 minute. This flow-through was then re-added to the column, and centrifugation repeated to elute residual DNA. The DNA was then stored at -20 °C to prevent autocatalytic degradation.

(b) QIAGEN-midi-plasmid purification protocol

This protocol is for up to 500 μg preparations of plasmid DNA from 500 ml cultures of *E. coli.* The plasmid (MC1061) was grown to an A_{600} of 1.0-1.5, and the cells harvested by centrifugation at 7,000 rpm in a Sorvall GSA rotor. The supernatant was removed, and the bacterial pellet resuspended in 10 ml of buffer P1, containing RNAse (100 μg ml^{-1}). 10 ml of buffer P2 was then added, and the solution mixed gently by inversion, to prevent shearing of genomic DNA. After incubation at room temperature for 5 minutes, 10 ml of chilled buffer P3 was added to stop lysis, and mixed gently by inversion. This was incubated on ice for 15 minutes. The sample was then mixed again, and the cloudy, viscous solution centrifuged at 4 °C for 30 minutes at 14,000 rpm in non-glass tubes in a Sorvall SS-34 rotor. Whilst centrifuging, a QIAGEN-tip 500 was equilibriated by applying 10 ml buffer QBT (740 mM NaCl, 50 mM MOPS buffer pH 7.0, 15% EtOH, 0.15% Triton X-100), and allowing the column to empty by gravity. The clear supernatant from the centrifugation was then added onto the QIAGEN-tip and allowed to enter the resin by gravity. The QIAGEN-tip was washed with 2 x 30 ml buffer QC, allowing the wash buffer to move through the QIAGEN-tip by gravity. The DNA was eluted with 15 ml of buffer QF (1.25 M NaCl, 50mM Tris-HCl pH 8.5, 15% EtOH), and the sample collected in a clean 30 ml tube. The DNA was precipitated with 10.5 ml of isopropanol, centrifuged at 8,000 rpm at 4 °C for 30 minutes, and the supernatant carefully removed. The DNA was then washed with 15 ml of cold 70% ethanol, to remove any precipitated salt and to replace the isopropanol making the DNA easier to dissolve. The DNA was recovered by centrifugation and after removal of the ethanol supernatant, the pellet was air dried for 10 minutes before redissolving in 300 μl of distilled water.

2.4.2 Nucleic acid purification

DNA for ligation and sequencing was extracted once with phenol:(chloroform: isoamyl alcohol (24:1 v/v)) (1:1 v/v) by mixing until a uniform colour, and then centrifuged for 5 minutes. The top layer was discarded, and two volumes of 100% ethanol and 1/10 th volume of 3 M sodium acetate (pH 4.8 with acetic acid) added to the lower phase. The DNA was allowed to precipitate overnight at -20 °C. The DNA was pelleted by centrifugation for 10 minutes and resuspended in the appropriate volume of water. DNA for transformation was further purified by precipitation with PEG. 100 μl of DNA was mixed with 36 μl 5 M NaCl and 164 μl 13% PEG 8000 (Sigma), and precipitated by incubating on ice for 30 minutes. Following centrifugation for 10 minutes, the DNA pellet was washed twice with 70% ethanol, dried, and resuspended in 10 μl water.

2.4.3 DNA separation by agarose gel electrophoresis

Agarose (Flowgen) was heated in TAE buffer (40 mM Tris-HCl pH 7.8, 5 mM NaOH, 1 mM EDTA) at 0.8% until the agarose dissolved, and stored at 60 °C until required. Ethidium bromide was added at 0.5 µg/ml to allow visualisation of the DNA by UV light. Gels were formed on either glass plates or in larger plastic gel casters, using plastic combs to produce sample wells of volume 10 µl or 60 µl respectively. The gels were run in TAE buffer, with the DNA migrating towards the anode, across a potential difference of 100 volts. DNA fragment size was estimated by comparison with standard markers generated by digestion of lambda phage DNA by the restriction enzyme *Hind* III (23 kb, 9.4 kb, 6.7 kb, 4.3 kb, 2.3 kb, 2.0 kb, 564 bp). Prior to loading, DNA samples were mixed with loading buffer (0.25% (w/v) bromophenol blue, 0.25% (w/v) xylene cyanol FF, 30% (v/v) glycerol). The position of the bands was visualised on a trans-illuminator and recorded by photography.

2.4.4 Restriction endonuclease digestion of DNA

1-10 µg of DNA (1-10 µl) was digested with restriction endonuclease (1-3 µl) in the manufacturers own buffer (5 µl), with distilled water to a volume of 50 µl. Incubation was at 37 °C for 1-2 hours, and digestion was checked by agarose gel electrophoresis.

2.4.5 DNA ligation

Digested plasmid DNA was phosphatased to remove terminal phosphate groups, and reduce plasmid religation. Following restriction endonuclease digestion, the plasmid DNA was phenol extracted and ethanol precipitated. The pelleted DNA was resuspended in 44 µl of distilled water, 5 µl of calf intestinal alkaline phosphatase buffer (10 mM Tris-HCl (pH 8.3), 1 mM $ZnCl_2$, 1 mM $MgCl_2$) and 1 µl of calf intestinal phosphatase (Pharmacia), and incubated at 37 °C for 1 hour. The phosphatase was subsequently removed by phenol extraction and ethanol precipitation. 5 ng of DNA insert was ligated to 1 ng of plasmid vector DNA in ligase buffer (20 mM Tris-HCl pH 7.6, 5 mM $MgCl_2$, 5 mM dithiothreitol) with 0.5 µl of T4 bacteriophage DNA ligase (New England Biolabs) to a final volume of 10 µl at room temperature overnight (16 hrs). This was then used to transform competent bacteria.

2.4.6 Transformation of competent *E. coli*

Either 10 µl of ligation reaction or 1 µl purified plasmid DNA was added to 150 µl of competent bacteria . This was mixed and incubated on ice for 30 minutes. After heating at 37 °C for 5 minutes, 1 ml of 2TY medium was added, and the bacteria grown at 37 °C for 1 hour. Bacteria were harvested by centrifugation at 13,000 rpm in a MSE Microcentaur for 5 minutes,

and were resuspended in 200 µl of 2TY. An aliquot was spread using a sterile glass spreader on an agar plate containing 100 µg/ml ampicillin, and then incubated at 37 °C overnight (16 hrs) before being stored at 4 °C.

2.4.7 PCR amplification from plasmid DNA

PCR was used to synthesise a region of DNA defined by two oligonucleotide primers from a cDNA template. This was performed to generate a construct consisting of repeat 1, with a tryptophan to isoleucine mutation, from a construct of repeats 1-4 containing the mutation. The primers had been used successfully by L. Hemmings to isolate DNA encoding repeat 1.

```
5'                          ------->
AAA  GAA  TTC  TT    TGC  AAG  GTT  CTG  GCA  G
     ' EcoRI  '       Cys263

3'                    ------->
AAA  GAA  TTC  CCG  GAT  CTC  CAT  TCA  ACA
     ' EcoRI  ' Arg387
```

Taq polymerase enzyme (Boehringer Mannheim) repeatedly synthesises the region of DNA defined by the primers, and incorporation of restriction endonuclease sites in the primers results in easier cloning into plasmid vectors. DNA concentration of primers and template was judged by absorption at 260 nm, where an OD_{260} 1.0 is equivalent to 50 µg ml^{-1} DNA. For the PCR reaction the following amounts were used: 1 µl template DNA (10 ng μl^{-1}), 3 µl 3' primer (100 ng μl^{-1}), 3 µl 5' primer (100 ng μl^{-1}), 5 µl of 10 x PCR buffer (500 mM KCl, 100 mM Tris-HCl pH 8.3), 5 µl NTPs (2 mM Na_2ATP, 2 mM Na_2CTP, 2 mM Na_2GTP, 2 mM Na_2TTP), 1 µl Taq polymerase (Boehringer Mannheim), 1.5 µl $MgCl_2$ (50 mM), upto 50 µl with distilled water. A drop of paraffin oil was added to prevent evaporation of the reaction mixture during PCR, which was carried out in a Biometra Trio-thermoblock PCR machine, using the following program: denaturation at 94 °C for 60 seconds, annealing at 50 °C for 60 seconds, extension at 72 °C for 120 seconds, repeated 24 times and then held at 4 °C. The amplified DNA was purified from the reaction mix by phenol extraction and ethanol precipitation, dried at room temperature and then resuspended in 50 µl of distilled water. 5 µl was checked on a 0.8% agarose gel for the DNA fragment, and then prepared for ligation by appropriate restriction enzyme digestion, phenol extraction and ethanol precipitation.

2.4.8 Double strand sequencing of plasmid constructs

Sequencing was performed using CircumVent ^{35}S Thermocycle sequencing. Into 4 1/2 ml Eppendorfs labelled A, C, G, and T was added the appropriate CircumVent deoxy/dideoxy base mix. Into a separate eppindorf was added 1.5 µl 10 x CircumVent sequencing buffer, 1 µl 30 x Triton X-100, 1 µl of the appropriate single stranded sequencing primer (10 ng μl^{-1}), 8.5 µl of the double stranded template plasmid (1 µg), 2 µl of ^{35}S-dATP (Amersham) and 2 units (1µl) of Vent DNA polymerase. This was mixed and 3.2 µl was aliquoted to each of the four labelled tubes. After mixing and adding a drop of paraffin oil to prevent evaporation, the Eppendorfs were placed in the PCR block and set to cycle as in normal PCR. 4 µl of stop/dye (95% Formamide, 20 mM EDTA, 0.05% bromophenol blue, 0.05% xylene cyanol FF) was added below the oil after PCR, spun, and stored at -20 °C until the gel was run. The samples were then boiled for 10 minutes before being loaded on to a 20 cm x 40 cm x 0.4 mm, 8% acrylamide sequencing gel (42% urea, 2.5 ml 10 x TBE (162 g Tris, 27.5 g boric acid, 9.5 g EDTA/l)). The gel was electrophoresed in TBE buffer at a power of 38 watts until the dye front reached the bottom. The gel was removed and fixed in 10% glacial acetic acid and 10% methanol for 10 minutes. The gel was then backed with 3 mm filter paper and dried using a Biorad gel drier. After one hour, the gel was exposed to Kodak X-ray film overnight (16 hours). The film was then developed using a DuPont Cronex CX-130 developing machine.

2.5 PROTEIN TECHNIQUES

2.5.1 Expression system

The expression system consisted of a plasmid that directs the synthesis of α-actinin fragments as fusions with the Sj26 gene product, a 26 kDa glutathione S-transferase (GST). In certain plasmids the GST carrier can be cleaved from the fusion protein by digestion with site-specific proteases such as thrombin (Sigma) (pGEX-2T) or blood coagulation factor Xa (Promega) (pGEX-3X). The pGEX vector consists of an ampicillin resistant gene, a lac repressor, and an IPTG inducible tac promoter (Figure 19).

2.5.2 Expression and purification of GST-α-actinin fusion proteins

α-Actinin-pGEX constructs were transformed into *E. coli* and maintained on agar plates containing ampicillin. Recombinant fragments were expressed and purified essentially as described by Smith and Johnson (1988). A 10 ml culture was inoculated with the desired bacterial colony and grown overnight in the presence of ampicillin. 5 ml of this was then back-diluted into the desired volume of 2TY and grown until an optical density at 600 nm of 0.5 absorbance units. The culture was then induced by the addition of 0.2 mM IPTG, and grown

(A)

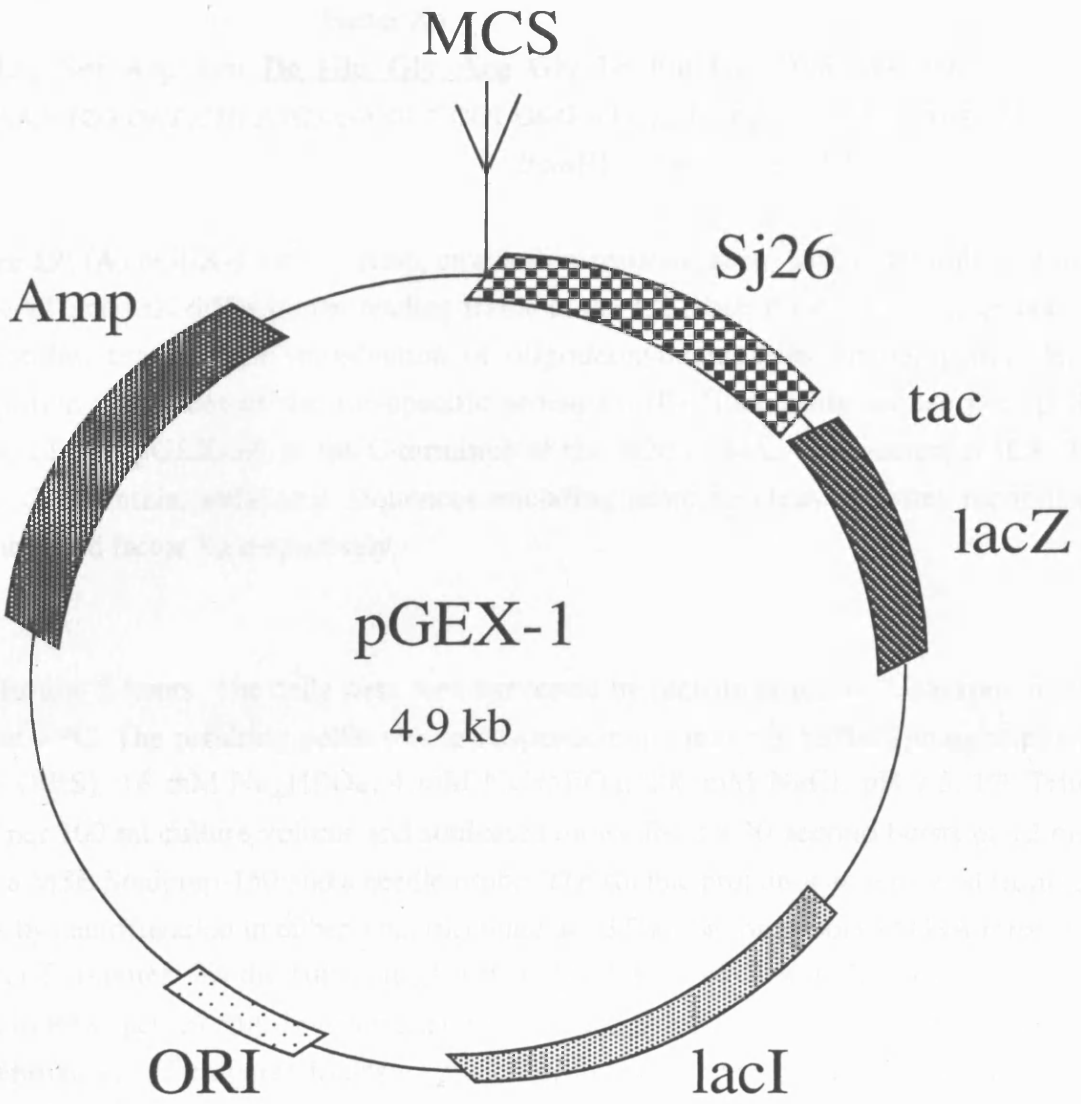

(B)

pGEX-1

Pro Lys Ser Asp Pro Arg Glu Phe Ile Val Thr Asp

CCA AAA TC**G GAT C**CC CGG **GAA TTC** ATC GTG ACT GAC TGA

*Bam*HI *Sma*I *Eco*RI

pGEX-2T

Thrombin

Pro Lys Ser Asp **Leu Val Pro Arg Gly Ser** Pro Gly Ile His Arg Asp

CCA AAA TCG GAT CTG GTT CCG CGT **GGA TC**C CCG **GGA ATT C**AT CGT GAC TGA

*Bam*HI *Sma*I *Eco*RI

pGEX-3X

Factor Xa

Pro Lys Ser Asp Leu **Ile Glu Gly Arg** Gly Ile Pro Gly Asn Ser Ser

CCA AAA TCG GAT CTG ATC GAA GGT CGT **GGG ATC** CCC GGG **AAT TCA** TCG TGA

*Bam*HI *Sma*I *Eco*RI

Figure 19: **(A)** pGEX-1 vector. Amp, ampilcillin-resistant gene; MCS, multiple-cloning site. pGEX-2T and -3X differ by the reading frame at the MCS being shifted by either one or two nucleotides, through the introduction of oligodeoxynucleotides encoding the cleavage-recognition sequences of the site-specific proteases. **(B)** Nucleotide sequence of pGEX-1, pGEX-2T and pGEX-3X at the C-terminus of the Sj26 cDNA. The vectors pGEX-2T and pGEX-3X contain additional sequences encoding protease cleavage sites recognised by thrombin and factor Xa respectively.

for a further 2 hours. The cells were then harvested by centrifugation at 7,000 rpm in a SS-34 rotor at 4 °C. The resulting pellet was re-suspended in 1 ml lysis buffer (phosphate buffered saline (PBS), 16 mM Na_2HPO_4, 4 mM NaH_2PO_4, 200 mM NaCl, pH 7.5, 1% Triton X-100)/ per 100 ml culture volume and sonicated on ice for 2 x 30 second bursts of 12 microns using a MSE Soniprep-150 and a needle probe. The soluble protein was separated from the cell debris by centrifugation in either a microcentaur at 13,000 rpm or a Sorvall GSA rotor at 8,000 rpm for 5 minutes. To the supernatant was added 100 µl of 50% (v/v) glutathione-agarose beads in PBS, per ml culture volume, and was mixed by inversion on a bench rotator at room temperature for 15 minutes to adsorb fusion proteins onto the beads. The beads were then washed three times in PBS by repeated centrifugation, removal of supernatant and then re-suspension, to remove bacterial soluble contamination. The beads were finally re-suspended in three times the volume of PBS, of which 10 µl was subsequently used to assess protein purity and concentration by SDS-polyacrylamide gel electrophoresis (PAGE) (Laemmli, 1970). Depending in which pGEX vector the polypeptide was expressed, the protein of interest was either cleaved from the GST or the fusion consisting of GST-protein was eluted off the GST beads. For liberation of the polypeptides from GST, the beads with bound fusion protein were washed twice in either 100 mM NaCl, 1 mM $CaCl_2$, pH 7.5 (factor Xa cleavage, pGEX-3X) or 150 mM NaCl, 2.5 mM $CaCl_2$, pH 7.5 (thrombin cleavage, pGEX-2T). The beads were then re-suspended in 3 x volume of the appropriate solution and incubated with either factor Xa or thrombin, at a ratio of enzyme to substrate of 1:100. Digestion was carried out on a rotator at room temperaure for 2-3 hours. Elution of the GST-protein fusion was performed by washing the beads twice with 50 mM Tris pH 8.0, followed by resuspension in 3 x volume of 50 mM Tris pH 8.0/ 5 mM reduced glutathione. This was incubated on a rotator for 10 minutes at room temperature, centrifuged and the supernatant removed. The elution was then repeated and the

supernatants pooled. The purity of the liberated polypeptides was again assessed by SDS-PAGE. Expressed proteins were concentrated using Microsep Protein Concentrators (Filtron Technology Corporation, Northborough, M.A.) with a membrane cut-off of 10 kDa. Protein concentrations were determined by absorbance at 280 nm, with extinction coefficients calculated by summation of the extinction coefficients of the chromophoric amino acids (Perkins, 1986) (Table I).When appropriate, concentrations were corrected for nucleotide by approximating the contribution of absorbance (x) at 260 nm ($x = O.D._{260} - O.D._{280}/2$) and subtracting the appropriate absorbance contribution (y) at 280 nm ($y = x/7$).

Table I: Molar extinction coefficients of the chromophoric amino acids.

	Molar Absorption Coefficient (M^{-1} cm^{-1})
Tryptophan	5720
Tyrosine	1380
Cysteine	150

2.5.3 Separation of proteins by SDS-PAGE

Separation of proteins was achieved in approximately one hour using a mini-gel apparatus from Biorad. The concentration of acrylamide depended on the size of proteins to be separated, using the recipes shown in Table II. The apparatus was sealed with 0.8% (w/v) agarose in distilled water, before gel production. The appropriate gel was made, with TEMED added last to initiate polymerisation. The running gel was poured first into the gel apparatus, followed by water saturated n-butanol to level the meniscus. After polymerisation, the gel was washed with distilled water to remove the n-butanol, and then the stacking gel was added. To the stacking gel a plastic comb was inserted to form sample wells after polymerisation. Samples were loaded into the wells after being mixed with an equal volume of sample buffer (1 M Tris-HCl pH 6.8, 15% glycerol, 1.6% SDS, 8% β-mercaptoethanol, 0.2% bromophenol blue) and boiled at 100 °C for 10 minutes. Gels were electrophoresed in running buffer (25 mM Tris, 192 mM glycine, 0.1% SDS) at a current of 45 mA until the dye front reached the gel bottom. The gel was then stained (1% Coomassie blue, 10% methanol, 10% glacial acetic acid) for ten minutes and then destained (10% methanol, 10% glacial acetic acid) until the protein bands were visible.

Table II: Recipes for SDS-PAGE gels.

	Running gel (10%)	Running gel (15%)	Stacking gel
1 M Tris-HCl (pH 8.8)	3.8 ml	3.8 ml	-
1 M Tris-HCl (pH 6.8)	-	-	625 µl
20% SDS	50 µl	50 µl	25 µl
30% acrylamide/ 0.8% bisacrylamide	3.25 ml	4.5 ml	666 µl
distilled water	3.25	1.75	3.75
10% APS	50 µl	50 µl	50 µl
TEMED	20 µl	20 µl	20 µl

2.6 CIRCULAR DICHROISM

The difference in absorption coefficients for an optically active material, measured with left and right circularly polarized light, is known as circular dichroism. Circular dichroism (CD) was measured in a Jobin-Yvon CD6 instrument, in a path length of 0.2 or 0.5 mm at 20 °C (in collaboration with W. Gratzer, King's College, Drury Lane, London). Molar residue ellipticity of expressed fragments was measured at 222 nm, with approximate value of percentage α-helix calculated taking molar residue ellipticity for the α-helix as -36,000 ^{o} cm^2 $dmol^{-1}$ (Greenfield and Fasman, 1969). Polypeptides were dialysed into 100 mM NaCl, 20 mM Na_2HPO_4 and centrifuged to remove aggregated material prior to use.

2.7 SUSCEPTIBILITY TO PROTEOLYSIS

Incubation of expressed proteins with proteolytic enzymes gives useful information concerning the ability of the polypeptides to resist degradation. Resistance to proteolysis suggests a tightly folded conformation. Different proteolytic enzymes have different recognition motifs and hence it is useful to know if digestion is due to general unfolding or to the creation of a specific site. Incubation of purified proteins with the proteolytic enzymes trypsin or thermolysin was at an enzyme to substrate ratio of 1:1000 at 37 °C. Polypeptides exposed to trypsin were in 100 to

150 mM NaCl, 1 to 2.5 mM $CaCl_2$, pH 7.5, whilst those exposed to thermolysin were in 100 mM NH_4CO_3, 5 mM $CaCl_2$. Aliquots were removed at timed intervals, to which were added equal volumes of sample buffer, mixed, and frozen until boiled and separated by SDS-PAGE and stained with Coomassie brilliant blue

2.8 CHEMICAL CROSS-LINKING

One way to learn about the arrangement of components in a protein complex is to see what can be easily cross-linked to what. Bi-functional reagents can react with side chain residues to form cross-links between protein molecules. Cross-linking was performed with the extended cross-linker dimethylsuberimidate (DMS) (24 mM in 0.2 M triethanolamine hydrochloride pH 8.5) (Davis and Stark, 1970), which reacts with lysine residues, at 0 °C. After 1 hour unreacted cross-linker was quenched with an excess of 1 M Tris pH 7.6 and the samples analysed by SDS-PAGE and densitometry of the stained gels (in collaboration with W. Gratzer, King's College, Drury Lane, London).

2.9 UREA DISSOCIATION PROFILES

Chemical cross-linking was performed by adding aliquots of the protein stock solution to urea, followed by cross-linking as described above, to obtain urea denaturation profiles. Samples were analysed by SDS-PAGE.

2.10 THERMAL DENATURATION PROFILES

For thermal melting profiles by CD (in collaboration with W. Gratzer, King's College, Drury Lane, London), the temperature was in general varied between 5 and 70 °C in steps of 5 °C. Molar residue ellipticity was measured at 222 nm. To confirm the results, specific temperatures were chosen, and the measurements were repeated using fresh sample.

2.11 TRANSMISSION ELECTRON MICROSCOPY (TEM)

Proteins were prepared for metal rotary shadowing by mixing with 50% glycerol (v/v) and tobacco mosaic virus (TMV). Samples were sprayed onto freshly cleaved mica using a modified artists air-brush with a nitrogen gas supply. This was then mounted onto a platform in an electron gun evaporation unit which was evacuated to 4×10^{-6} torr, and rotary shadowed with platinum at an angle of 5°. The specimen was then carbon coated and floated onto copper grids for observation. This was performed in a Siemens 102 transmission electron microcope, operating at a potential difference of 80 kV, and at a nominal magnification of 80,000. Actual magnification was obtained by calibration with a diffraction grating replica. Micrographs were

subsequently developed and printed, with axial measurements corrected for shadow cap by comparison with the internal standard, TMV

2.12 ANALYTICAL ULTRACENTRIFUGATION

The analytical ultracentrifuge (AUC) is the most accurate means for determining molecular weights and hydrodynamic and thermodynamic properties of multi-subunit macromolecules. Its applications include examination of sample purity (Albright and Williams, 1967; Schachman, 1959; Soucek and Adams, 1976), molecular weight determination (Van Holde and Baldwin, 1958; Bancroft and Freifelder, 1970), analysis of associating systems (Attri *et al.*, 1991; Correia *et al.*, 1985; Durham, 1972; Herskovits *et al.*, 1990; Mark *et al.*, 1987; Ralston, 1975; Van Holde *et al.*, 1991), detection of conformational changes through sedimentation and diffusion coefficients (Kirschner and Schachman, 1971; Newell and Schachman, 1990; Richards and Schachman, 1959; Smith and Schachman, 1973; Crawford and Waring, 1967; Freifelder and Davison, 1963; Lohman *et al.*, 1980), and ligand binding (Minton, 1990; Steinberg and Schachman, 1966; Bubb *et al.*, 1991; Lakatos and Minton, 1991; Mulzer *et al.*, 1990).

An AUC must spin a rotor at a controlled speed and temperature, and allow the recording of the concentration distribution of the sample at known times. The rotor is spun in an evacuated chamber and should be stable to prevent convection and stirring of the cell contents. The AUC cells must allow the passage of light through the sample so that the concentration distribution can be measured. The sample is contained within a sector-shaped cavity sandwiched between two windows of quartz. The cavity is produced in a centre-piece of re-inforced epoxy resin. Double-sector centre-pieces are used with optical lengths of 3 and 12 mm. Sector-shaped compartments are essential in velocity work since the sedimenting particles move along radial lines and would collide with the walls and cause convective disturbances if sample compartments were parallel-sided. Double-sector cells take account of absorbing components in the solvent and correct for the redistribution of solvent components. A sample of the solution is placed in one sector, and a sample of the solvent is placed in the second sector.

The time required to attain equilibrium is decreased for shorter column lengths of solutions. Hence solution lengths of 1.2 mm are used for equilibrium experiments, rather than the 12 mm for a full sector, used in velocity experiments. Examination of 3 samples at once in 6-channel centre-pieces, in which 3 channels hold 3 different samples, and the 3 channels on the other side hold the respective solvents, can also be performed.

The data obtained from an experiment with an AUC is the concentration distribution with respect to radius, by measuring absorbance at given wavelengths at fixed positions in the cell.

Refractometric methods can also be used for obtaining concentration distributions, where the sample usually has a greater refractive index than the solvent. These consist of schlieren or Rayleigh interference optics.

Sedimentation equilibrium and velocity measurements were performed in a Beckman Optima XL-A analytical ultracentrifuge which is equipped with a four-hole rotor. Three positions are available for sample cells, with one of the holes for the counterbalance with its reference holes to provide calibration of radial distance.

The Optima XL-A utilises absorption optics. A high intensity xenon flash lamp allows the use of wavelengths between 190 and 800 nm. The lamp is fired briefly as the selected sector passes the detector, and cells and individual sectors may be examined in turn with the aid of timing information from a reference magnet in the base of the rotor. The measured light is normalised for variation in lamp output by sampling a reflected small fraction of the incident light. A slit below the sample moves to allow sampling of different radial positions, and to minimise noise multiple readings at a single position are collected and averaged. Wavelength scans are also taken at specified radial positions in the cell allowing discrimination between different solutes.

Protein concentrations, prior to loading, were determined spectrophotometrically, using molar absorptivities at 280 nm, calculated from their composition (Perkins, 1986). Scans were taken using ultraviolet absorption optics at wavelengths between 220 and 280 nm. Partial specific volumes were calculated from amino acid composition, using the partial specific volumes of component residues (Cohn and Edsall, 1943):

$$\bar{v}_c = \frac{\sum_i N_i M_i \bar{v}_i}{\sum_i N_i M_i}$$

where $\bar{v}_c$ is the calculated partial specific volume (ml g^{-1}), N_i the number of residues, M_i the molecular weight of the corresponding component (the residue molecular weight minus 18), and $\bar{v}_i$ the partial specific volume of the component. This was performed using the computer program Biomols. The solvents used were factor Xa and thrombin cleavage buffers.

2.12.1 Sedimentation equilibrium

For sedimentation equilibrium a solution of 1.2 mm was centrifuged at a chosen velocity for 11 hours at 5 °C to equilibrium. As the solute sediments towards the cell bottom (Figure 20), diffusion opposes sedimentation and at equilibrium the chemical potential is equal and opposite to the sedimentation potential. From the Lamm (1929) equation describing movement of molecules in a centrifugal field, it can be derived for a single, thermodynamically ideal solute:

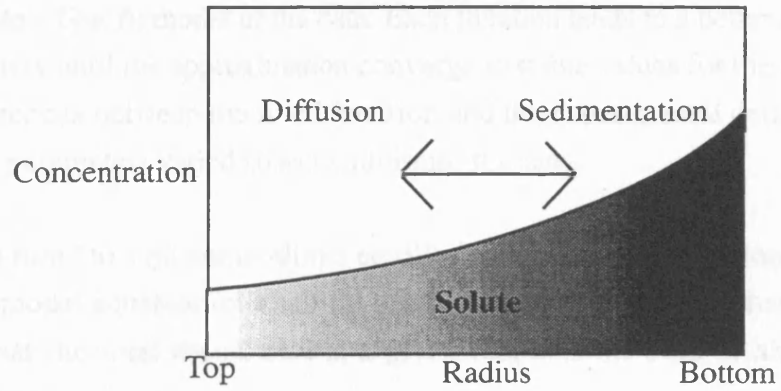

Figure 20: Schematic representation of sedimentation equilibrium.

$$RTdc / dr = \frac{\left[M(1-\bar{v}\rho)\omega^2 rc\right]}{N}$$

where $M(1-\bar{v}\rho)$ is the buoyant molecular weight (M is the solute molar weight (g mol^{-1}), $\bar{v}$ the partial specific volume, and ρ the solvent density (g ml^{-1})), ω the angular velocity of the rotor (radians sec^{-1}), N Avagadro's number, R the gas constant (8.314 J mol^{-1} K^{-1}), T temperature in Kelvin, and c the concentration of the solute (g l^{-1}) at a radial position r from the axis of rotation. Concentration of the solute increases exponentially towards the cell bottom. Plots of absorbance against distance from rotation centre were fitted, using a a non-linear least-squares fit, to the following relation, to yield apparent weight-average molecular weights:

$$A_r = \exp\left(\ln A_0 + \left(\frac{\omega^2}{2RT}\right)M(1-\bar{v}\rho)\left(r^2 - r_0^2\right)\right) + E$$

where A_r is the concentration at radius r, exp the exponent, ln the natural log, A_0 the absorbance at the reference radius r_0, E the baseline offset, and M the molecular weight. Baseline offset results from a difference in the absorbance between the reference and the solvent in which the sample is dissolved. The baseline value can be determined experimentally by a high-speed run where the meniscus is depleted of all sample and the absorbance read directly from the data near the meniscus. This experimental approach is limiting when the meniscus cannot be depleted, but with sufficient data, the baseline can be varied as an additional parameter.

Least-squares methods are a way to obtain a statistical fit of the experimental data to a proposed model and to obtain best estimates for unknown parameters (Johnson, 1992). The major advantage is that data can be analysed directly without transformation. A series of curves is

calculated to locate a best fit model of the data. Each iteration leads to a better approximation of the curve parameters until the approximation converge to stable values for the parameters being varied. The differences between the fitted function and the experimental data are squared and summed, and the parameters varied so as to minimise this sum.

Curves were also fitted to a monomer-dimer equilibrium to obtain association constants where appropriate. The model equation for a self-associating system is similar to that of a single ideal species except that the total absorbance at a given radius is the sum of absorbances of all species at that radius:

$$A_r = \exp\left(\ln A_0 \left(\frac{\omega^2}{2RT} \right) M(1-\bar{v}\rho)\left(r^2 - r_0^2\right) \right)$$

$$+\exp\left(2\ln A_0 + \ln K_a \left(\frac{\omega^2}{2RT} \right) 2M(1-\bar{v}\rho)\left(r^2 - r_0^2\right) \right) + E$$

where A_r is the total absorbance of both species at radius r, A_0 the absorbance of the monomer species at reference radius r_0, M the monomer molecular weight, and K_a the association constant for the monomer-dimer equilibrium. Since data from the analytical ultracentrifuge are in absorbance units, it is assumed that the molar extinction coefficient for a dimer in the monomer-dimer equilibrium is twice that of a monomer in the calculation of association constants expressed in terms of concentration (Becerra *et al.*, 1991; Ross *et al.*, 1991). If the extinction coefficient of the monomer is known:

$$K_{1-2.conc} = \frac{K_{1-2.abs}\varepsilon l}{2}.$$

where $K_{1\text{-}2,conc}$ and $K_{1\text{-}2,abs}$ are the association constants expressed in terms of concentration and absorbance, respectively.

Average dissociation constants were calculated by fitting experimental data to the equation:

$$M_w = \frac{M_1}{c}\left(2c + \left(\frac{K_d - \sqrt{K_d^{\,2} + 8K_d c}}{4} \right) \right) \quad \textbf{Equation 1}$$

where M_w is weight-average molecular mass, M_1 is monomer mass, c is concentration and K_d is the dissociation constant.

2.12.2 Sedimentation velocity

For sedimentation velocity a solution column of 12 mm was centrifuged at 40,000 rpm for 11 hours at 5 °C. This produces a depletion of solute near the meniscus and the formation of a boundary between the depleted region and the sedimenting solute. Scans were performed at 30 minute intervals. Because sector-shaped compartments are used, the solute particles enter a progressively increasing volume as they migrate outwards, and the sample becomes progressively diluted. The concentration in the plateau region, c_p, when the boundary is located at a point, r_{bnd}, is related to the initial concentration, c_0, and the radial position of the meniscus, r_m:

$$c_p = c_0\left(\frac{r_m}{r_{bnd}}\right)^2.$$

where r_m is the radial position of the meniscus. Concentrations were corrected for this radial dilution and sedimentation coefficients were calculated by measuring the rate of movement of the point of inflection, which was taken to be the mid-point of the sedimenting boundary for symmetrical traces:

$$\ln(\frac{r_{bnd}}{r_m}) = s\omega^2 t,$$

The sedimentation coefficient is influenced by the density of the solution and by the solution viscosity. In order to take into account the differences in density and viscosity between different solvents, the experimental sedimentation coefficients were corrected to standard conditions of water at 20 °C:

$$s_{20,w} = s_{obs}\left(\frac{\eta_{T,w}}{\eta_{20,w}}\right)\left(\frac{\eta_s}{\eta_w}\right)\left(\frac{1-\bar{v}\rho_{20,w}}{1-\bar{v}\rho_{T,s}}\right)$$

where $s_{20,w}$ is the sedimentation coefficient expressed in terms of the standard solvent of water at 20 °C; s_{obs} is the measured sedimentation coefficient in the experimental solvent at the experimental temperature, T; $\eta_{T,w}$ and $\eta_{20,w}$ are the viscosities of water at the temperature of the experiment and at 20 °C, respectively; η_s and η_w are, respectively, the viscosities of the solvent and water at a common temperature; $\rho_{20,w}$ is the density of water at 20 °C and $\rho_{T,s}$ is that of the solvent at the temperature of the experiment. These resultant values were plotted against concentration and extrapolated to zero concentration to obtain s^0. Dissociation constants were also estimated when appropriate by comparing calculated plots of sedimentation

coefficient against concentration for selected values of the dissociation constant with experimental data.

2.13 DIGITAL DENSIMETRY

For accurate determination of molecular weights and sedimentation behaviour solvent density needs to be measured. This was done using a digital densimeter, utilising the mechanical oscillator technique (Kratky *et al.*, 1973). A hair-pin shaped gass cell containing the buffer is induced to oscillate which electronically excites a magnetic rod located perpendicular to the glass cell. The measured frequency (f) of the oscillations within the fluid is dependent directly on the sample density inside the tube. The instrument is initially calibrated using samples of known density, air and water, and then the sample is introduced and the time taken measured to reach a fixed number of oscillations. This value of time (T) represents the period (1/f) in units of 10^{-5} secs. Initially the instrument constant (A) was determined:

$$\Delta\rho = A\Delta(T^2)$$

$$\text{Instrument Constant (A)} = \frac{\Delta\rho}{\Delta(T^2)} = \frac{\rho_{H_2O} - \rho_{air}}{(T_{water})^2 - (T_{air})^2}$$

The density of the buffer can then be determined:

$$\rho\text{buffer} = A((\text{Tbuffer})^2 - (\text{Twater})^2) + \rho\text{water}$$

where ρ = density and T is the time for a fixed number of oscillations.

The precision density meter DMA 02C was used with the water bath set to 5 °C. The U-tube in the density meter was thoroughly dried and then calibration was performed using air and distilled water. 1 ml of water was injected into the lower part of the tube to prevent trapping air bubbles and left to equilibriate for 2 or 3 minutes with the ordinary lamp and air pump off. The densimeter was set to the number of counts required, the meter was set to zero and counting was started. This was repeated until a repeatable reading within 1-ten-thousandth of a second was recorded. This was carried out for one ml of factor Xa and thrombin cleavage buffers. Between sample readings the U-tube was cleaned thoroughly with distilled water and alcohol and thoroughly dried.

2.14 VISCOMETRY

In order to take account of different solvents on sedimentation behaviour we require the viscosity of the solvent. The dynamic viscosity of a solution can be determined by measuring

the flow-time of the solution through a capillary relative to the flow-time of pure solvent by means of an Ostwald glass viscometer. This was performed in a Schott Gerate AVS 400. The relative viscosity can be defined as the ratio of solvent to water viscosity:

$$\eta_{rel} = \frac{(tsolv)(\rho solv)}{(twater)(\rho water)}$$

where ρ and t are the density and flow times respectively.

8 ml of distilled water was poured into the wide arm of the viscometer ensuring no air bubbles formed in the capillary tube. The viscometer was immersed in a 5 °C water bath and left to equilibriate for approximately five minutes. The liquid level was raised to above the high level in the viscometer using rubber tubing. The liquid was released and the flow-time for the meniscus to fall from the marked high to the low level was recorded. This was repeated with factor Xa and thrombin buffers.

CHAPTER 3.

ASSOCIATION OF REPEATS IN THE α-ACTININ ROD DOMAIN. ALIGNMENT OF INTER-SUBUNIT INTERACTIONS

3.1 INTRODUCTION

The quaternary structure of dystrophin and utrophin is still uncertain, but the other proteins of the spectrin class all form rod-like, highly elongated antiparallel dimers. In the spectrins these are αβ-heterodimers and in the α-actinins homodimers. The spectrin nucleation sites for dimer assembly include, but are not limited to, several repeat units that are those most similar to α-actinin. The central regions of the available α-actinin sequences were aligned using the program Clustal V (Figure 7), and the identities of the central four repeats with respect to chicken smooth muscle are shown in Table III. The non-muscle and smooth muscle α-actinin isoforms are all highly identical (100-96% identical), but show substantially lower identity to the skeletal muscle isoforms (89-66% identical). Also, as previously noted by others (Fyrberg *et al.*, 1990; Baron *et al.*, 1987; Beggs *et al.*, 1992), the first α-actinin repeat is the most highly conserved between species and isoforms. The four α-actinin repeat sequences were also aligned with all known spectrin dimer nucleation site sequences. In each case, the highest scoring alignments involved pairing of the β1 and β2 repeats of spectrin with the first two α-actinin repeats, A1 and A2, while the A3 and A4 repeats were most homologous to the α20 and α21 repeats, in agreement with published alignments (Ursitti *et al.*, 1996). A schematic arrangement of the α-actinin molecule and the most homologous spectrin repeats would suggest that the two lateral spectrin pairs: β1-α21 and β2-α20 are responsible for dimer assembly, and the α-actinin interaction is stronger since it has two of these unique pairs (Figure 8). Since the isolated α-actinin rod domain exists in solution as a highly stable dimer (Imamura *et al.*, 1988; Kahana and Gratzer, 1991), and defined complimentary repeats of the erythroid spectrin α and β-chains also form a stable 1:1 complex (Speicher *et al.*, 1992), it is implied that the structural repeating elements interact specifically by pairs along the rod. Thus in the case of the α-actinin rod, which consists of four repeats, the antiparallel dimer should be stabilised by interactions between repeats 1 and 4 and between 2 and 3.

However, on the basis of image reconstructions from two-dimensional crystals, Taylor and Taylor (1993) suggested that the chicken gizzard α-actinin structure is staggered, so that repeat 1 is free (or may interact with the terminal globular EF-hands of the protein). Two-dimensional crystals of chicken gizzard α-actinin were formed on positively charged lipid layers, and low resolution three-dimensional projection images were obtained by optical diffraction from electron micrographs of negatively stained crystals. Eight optical density peaks were observed in the central, rod-shaped region, interpreted as the repeats predicted from the amino acid sequence. However, these eight peaks were not arranged in four pairs but, instead, consisted of three central pairs flanked at either end by a single peak, which appeared larger and denser in projection than the three central pairs. The individual α-actinin molecules in projection lacked 2-fold symmetry. This was interpreted as the unpaired density peak corresponded to repeat 1, and the three pairs of density peaks constituted repeats 2 to 4, which would be paired in reverse

Table III: Sequence homology (% identity) of repeats in different isoforms of α-actinin and spectrin with chicken smooth muscle α-actinin.

Isoform	Repeat 1	Repeat 2	Repeat 3	Repeat 4
aacn_chick	100	100	100	100
aac1_human	96	98	98	96
aacs_chick	89	81	72	81
aac2_human	89	81	71	79
aac3_human	84	77	66	72
aact_drome	70	72	56	58
aact_dicdi	37	-	-	28
spcb_human	47 (β1)	37 (β2)	-	-
spcb_drome	45 (β1)	-	-	-
spca_human	-	-	-	29 (α21)
spca_drome	-	-	35 (α20)	29 (α21)

Chicken brain α-actinin (aacn_chick), human placental α-actinin (aac1_human), chicken skeletal muscle α-actinin (aacs_chick), human skeletal muscle α-actinin (aac2_human), human skeletal muscle α-actinin (aac3_human), *Drosophila* α-actinin (aact_drome), *Dictyostelium* α-actinin (aact_dicdi), *Drosophila* β-spectrin (spcb_drome), human erythroid β-spectrin (spcb_human), *Drosophila* α-spectrin (spca_drome), human erythroid α-spectrin (spca_human). Cells with "-" represent identity lower than 20%.

order. Repeat 1 would then share proximity with the C-terminal domain of the other α-actinin molecule. In this model, the greater length of calcium-insensitive isoforms is due to loss of proximity between the calcium- and actin-binding domains. Dimerisation would then result from only three pairwise interactions, viz repeats 2, 3 and 4 of one chain with 4, 3 and 2 of the other (Figure 21B). In an endeavour to discriminate between the aligned and staggered models, deletion mutants of the α-actinin rod domain were used, lacking either of the terminal repeats, 1 and 4, and dimer-forming ability was investigated.

Figure 21. Aligned and staggered models for the α-actinin homodimer. **(A)** Aligned model in which there are four pairwise interactions between repeats. **(B)** Staggered model which predicts only three pairwise interactions between repeats 2 and 4, and between the aligned repeat 3 in each subunit. **(C)** Alternative staggered model which predicts an interaction between repeats 1 and 3, and between the aligned repeat 2 in each subunit.

3.2 RESULTS

3.2.1 Expression and purification of α-actinin polypeptides

The α-actinin rod-domain constructs that were used in this study are shown in Figure 22. The positions of the N- and C-termini were selected to ensure that the sequence encompassed an integral number of homologous repeats, based on the phasing established earlier, which corresponded to within a few residues to that observed in spectrin and dystrophin (Gilmore *et al.*, 1994). The repeats have been shown to constitute independently folding units (Gilmore *et al.*, 1994). α-Actinin polypeptides spanning repeats 1-4 (residues 267-749), repeats 1-3 (residues 267-631) and repeats 2-4 (residues 385-749) were expressed in *E. coli* as soluble GST-fusion proteins and purified on glutathione-agarose beads. Successful purification was determined by SDS-PAGE and observed bands corresponded with expected sizes of 69 kDa for fragments 1-3 and 2-4, and 83 kDa for fragment 1-4. These were then liberated from GST by proteolytic cleavage using either thrombin (fragment 2-4) or factor Xa (fragments 1-3 and 1-4).

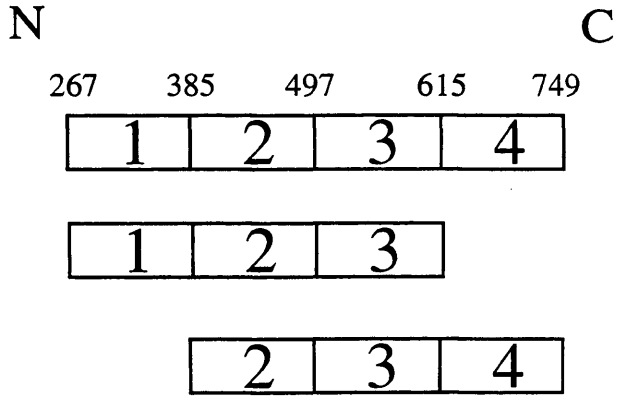

Figure 22. Chicken gizzard α-actinin repeat domain constructs expressed in *E. coli.* The amino acid residues which define the N-terminal boundary of each repeat are indicated (Gilmore *et al.*, 1994). Successive structural repeats begin and end near the centre of the long continuous α-helix that is partitioned between any two contiguous structural repeats.

The polypeptides isolated in this way were >90% pure as analysed by SDS-PAGE (Figure 23 and Figure 24 lanes a, e and i), and observed bands again corresponded with predicted molecular weights of 43 kDa for fragments 1-3 and 2-4, and 57 kDa for fragment 1-4. Yields were determined spectrophotometrically, using calculated absorption coefficients of 1.33, 1.40, and 1.14 cm^{-1} (for 1 mg ml^{-1}) for fragments 1-4, 1-3, and 2-4 respectively (Table IV).

Table IV: Yield of expressed polypeptides determined spectrophotometrically.

	1-4	1-3	2-4
Yield (mg)/ 100 ml culture	0.3	0.4	0.6

3.2.2 Verification of native secondary structure

The ability of rod fragments to enter the native fold has been assessed for α-spectrin (Winograd *et al.*, 1991), dystrophin (Kahana *et al.*, 1994) and α-actinin (Gilmore *et al.*, 1994) in terms of the α-helicity and resistance to proteolysis. The CD spectra, measured at 20 °C (Figure 25), of all the expressed α-actinin polypeptides were characteristic of proteins with a high α-helix content (Table V), and similar to that of the intact rod domain liberated from native chicken smooth muscle α-actinin by proteolysis (Imamura *et al.*, 1988). The bacterially expressed repeat domain polypeptides were also relatively resistant to degradation by trypsin upto 2 hours (Figure 23), a characteristic also of the intact repeat domain liberated from native α-actinin

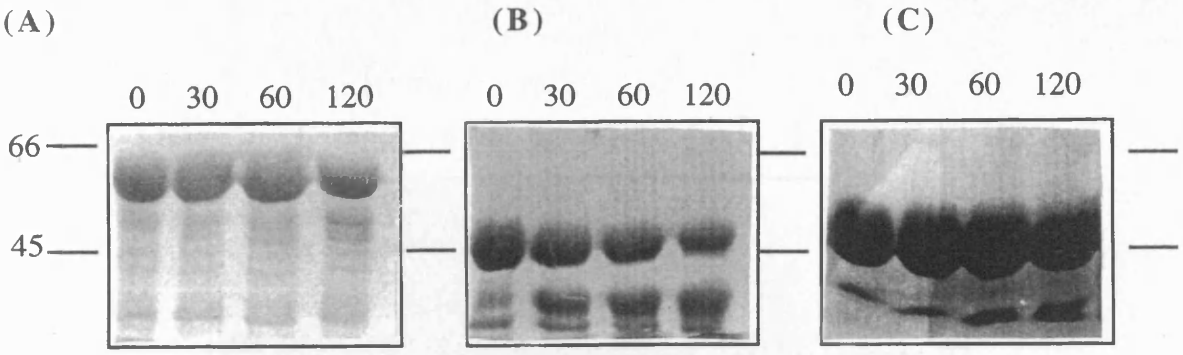

Figure: 23: Trypsin-resistance of the expressed α-actinin repeat domain polypeptides. Purified α-actinin polypeptides were exposed to trypsin (enzyme to substrate ratio 1:1000) for the times shown (mins), in 100-150 mM NaCl containing 1-2.5 mM $CaCl_2$, and the resulting digests analysed by SDS-PAGE. **(A)** Repeats 1-4. **(B)** Repeats 1-3. **(C)** Repeats 2-4. The position of molecular mass standards (kDa) is indicated.

Table V: Formation of covalent dimers by chemical cross-linking of α-actinin polypeptides expressed in *E.coli*..

Fragment	$-[\theta]_{222}$[a]	Helix Content (%)	Concentration (mg ml^{-1})	Cross-Linked Dimer (%)
Repeats 1-4[b]	23,800	66[c]	0.28	67
			0.14	69
			0.03	63
Repeats 1-3	24,800	69	0.40	11
			0.20	9
			0.04	5
Repeats 2-4	24,900	69	0.40	16
			0.20	16
			0.04	7

[a]Molar residue ellipticity (^{o} cm^2 $dmol^{-1}$) at 222 nm.

[b]Cross-linking under identical conditions of the intact rod domain, formed by proteolysis of natural chicken gizzard α-actinin, gave 69% covalent dimers (Kahana and Gratzer, 1991).

[c]Approximate helicity based on a value of $-36,000^o$ for 100% α-helix (Greenfield and Fasman, 1969).

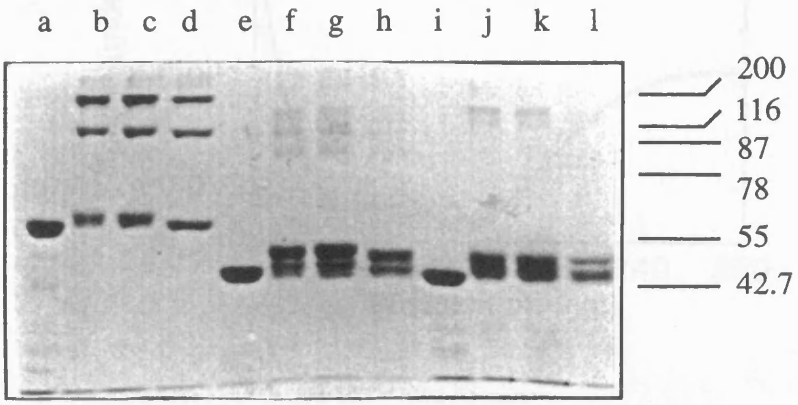

Figure 24: Analysis of the association of α-actinin polypeptides expressed and purified from *E. coli* by chemical cross-linking. Varying concentrations of the α-actinin polypeptides were exposed to the cross-linking reagent dimethylsuberimidate (DMS), as described in Materials and Methods, and the products of the reaction were analysed by SDS-PAGE. The positions of molecular mass standards (kDa) are indicated. Lanes a-d: α-actinin polypeptide containing repeats 1-4, untreated (lane a) and treated with DMS at protein concentrations of 0.28 (b), 0.14 (c), 0.028 (d) mg ml^{-1}. Lanes e-h: α-actinin polypeptide containing repeats 2-4, untreated (lane e) and treated with DMS at protein concentrations of 0.4 (f), 0.2 (g) and 0.04 (h) mg ml^{-1}. Lanes i-l: α-actinin polypeptide containing repeats 1-3, untreated (lane i) and treated with DMS at protein concentrations of 0.4 (j), 0.2 (k) and 0.04 mg ml^{-1} (l).

(A)

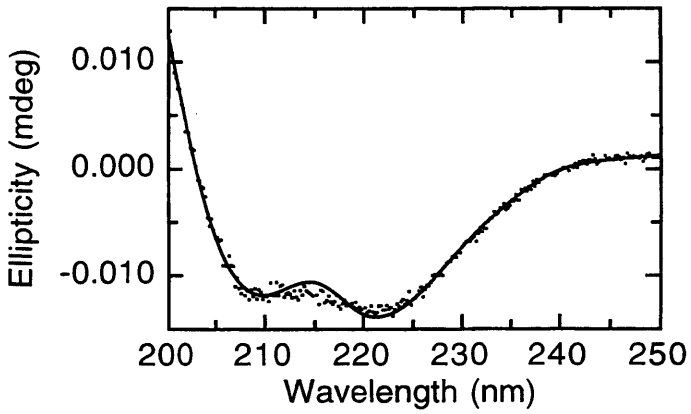

(B)

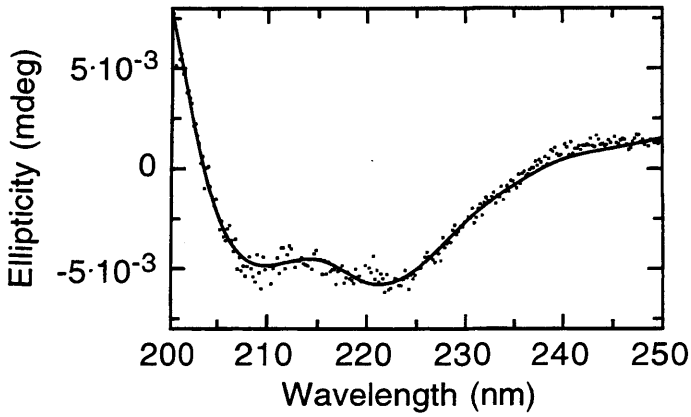

(C)

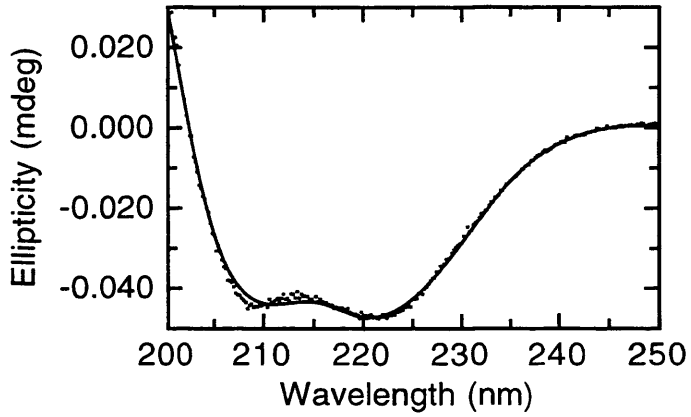

Figure 25: Circular dichroism spectra of expressed α-actinin fragments. **(A)** Repeats 1-4, **(B)** repeats 1-3, and **(C)** repeats 2-4. The spectra are characteristic of proteins with a high α-helical content.

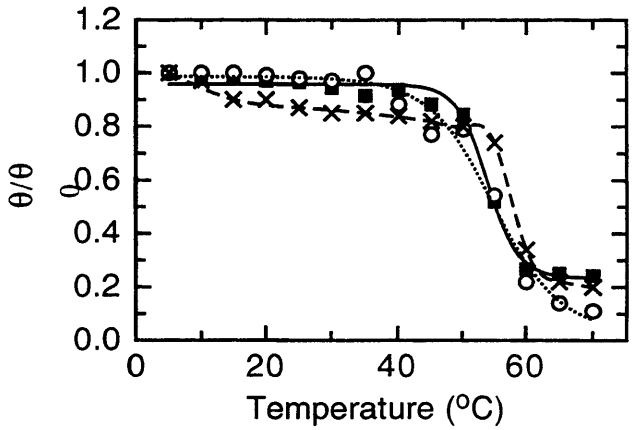

Figure 26: Thermal denaturation profiles of expressed α-actinin rod fragments, determined by circular dichroism. (Unfolding is measured by the ellipticity at 222 nm relative to that at 5 °C): (x, ---) fragment 1-4; (o, ···) fragment 1-3; (■, —) fragment 2-4.

(Imamura *et al.*, 1988; Davison and Critchley, 1988; Gilmore *et al.*, 1994). These results suggest that the bulk of the expressed α-actinin polypeptides were correctly folded.

3.2.3 Thermal stability

Thermal denaturation profiles were measured on the products to allow comparison of the stabilities of the structures (Figure 26). All fragments displayed well-defined sigmoidal transitions, compatible with a two state process, as observed for expressed fragments of dystrophin (Kahana and Gratzer, 1995; Calvert *et al.*, 1996; Kahana *et al.*, in press). However, the truncated rods had decreased thermal stability compared to the intact rod, reflected by a difference of 5 °C in the temperature at the mid-point of the transition, T_m, as observed on separate samples. These show an extended plateau region, in which the structure remained essentially unchanged, followed by a sigmoidal transition to an unfolded state. The conformation was then stable below the transition region. The gradual linear change in ellipticity above the transition region for fragment 1-4 was probably a reflection of the presence of traces of incompletely folded or aggregated material (Pace and Laurents, 1989).

3.2.4 Chemical cross-linking

On reaction with the bifunctional reagent dimethylsuberimidate, the complete rod domain (repeats 1-4) showed extensive cross-linking to a doublet, migrating in the region expected for dimers (Figure 24). The proportion of covalent dimer was essentially unchanged by a tenfold increase in protein concentration (Figure 24 lanes b-d, and Table V), and was the same within error as that formed under identical conditions by the rod domain prepared by proteolysis of

natural chicken gizzard α-actinin (Kahana and Gratzer, 1991). Both truncated rod fragments, containing repeats 1-3 and 2-4 respectively, gave rise to very much smaller proportions of covalent dimer in the cross-linking reaction, the extent of which rose with increasing protein concentration (Figure 24 lanes e-l, and Table V). Whether the cross-linked material represented an equilibrium proportion of dimer or non-specific aggregation cannot be determined from these results. Figure 24 also shows conversion of the monomer zone in the SDS-gel into a doublet or even a triplet by the cross-linker. Such electrophoretic heterogeneity is often generated by bifunctional reagents and results presumably from intra-chain cross-linking, which can perturb both SDS-binding and the dimensions of the hydrodynamic particle migrating in the gel (Griffith, 1972; Nakamura *et al.*, 1991). That this was observed only in the truncated fragments and not with the intact rod domain was taken to be a consequence of the high probability of inter-chain cross-linking in the stable dimer. These results show that the elimination of a repeat from either end of the rod greatly reduced dimerisation.

If the repeats in the antiparallel dimer are aligned, then any association between the polypeptides containing repeats 1-3 or repeats 2-4 would, in both cases, result from two of the four pairwise associations prevailing in the complete rod domain (Figure 21). In a staggered model (Taylor and Taylor, 1993), in which repeat 1 does not participate in inter-chain interactions (Figure 21B), fragment 2-4 would be stabilised by the same three pairwise interactions as occur in the intact rod and should therefore have equal stability. In fragment 1-3 there could be only one such interaction, viz the isologous association between repeats 3 from either chain (Figure 21). The converse would apply for the inverse stagger, with repeat 4 unpaired (Figure 21C). The results of the cross-linking experiments are thus compatible with an aligned structure for the α-actinin dimer but not, in the absence of other structural features, with a staggered structure.

3.2.5 Sedimentation equilibrium

The cross-linking procedure may not give a quantitative reflection of the monomer-dimer equilibrium. This could be due to the reaction being not fully efficient, in consequence probably of competing intra-chain reactions, and it could displace the equilibrium. An analysis of the association by sedimentation equilibrium was therefore undertaken. Molecular weights were calculated using experimentally determined values for the density of the solvents, of 1.00498 and 1.0124 g ml^{-1} for factor Xa and thrombin buffers respectively, and calculated values for the partial specific volumes, of 0.730, 0.729, and 0.730 ml g^{-1} for fragments 1-4, 1-3, and 2-4 respectively. The results shown in Figure 27A and summarised in Figure 28A indicate that the complete rod domain was predominantly or entirely dimeric. Above the distribution is the residual plot, which is the most sensitive graphical representation for goodness of fit, and the best indicator of possible alternative models. A random distribution of points about the zero value is a desired diagnostic for a good fit. The data show no significant dependence of

(A)

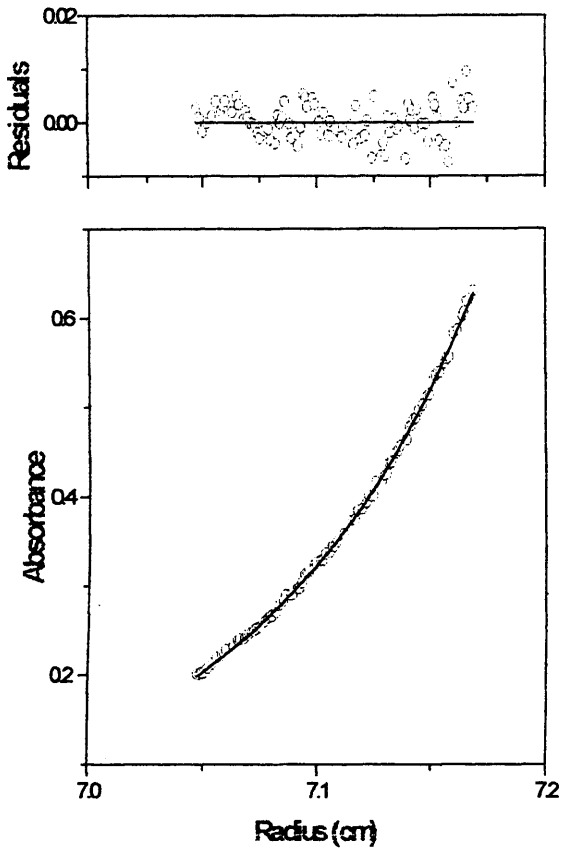
0.02
0.00
Residuals
0.6
0.4
0.2
Absorbance
7.0
7.1
7.2
Radius (cm)

(B)

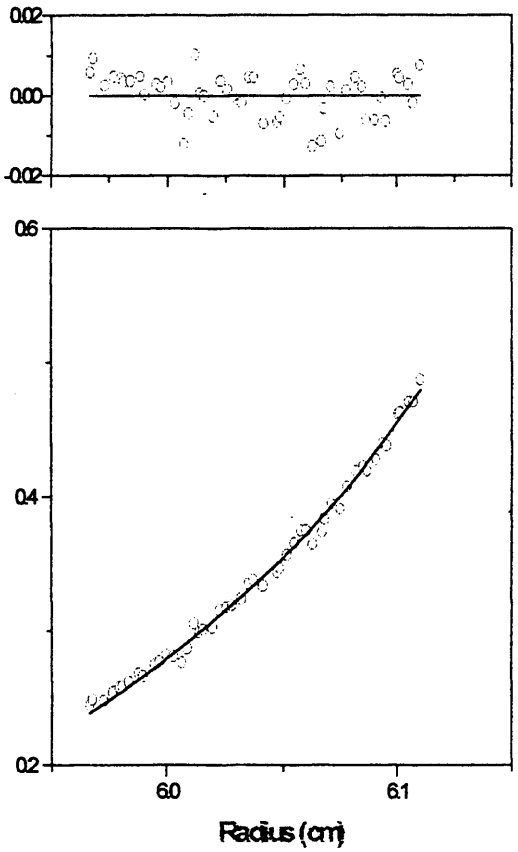
0.02
0.00
-0.02
0.6
0.4
0.2
6.0
6.1
Radius (cm)

(C)

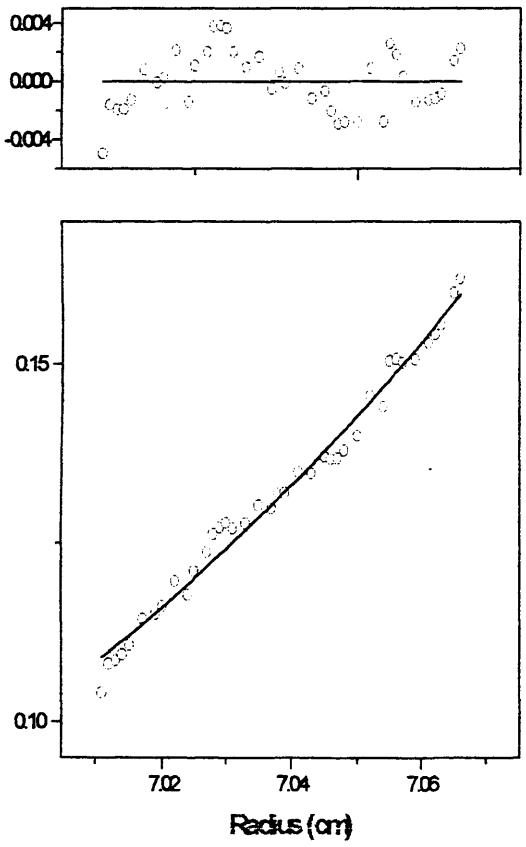
0.004
0.000
-0.004
0.15
0.10
7.02
7.04
7.06
Radius (cm)

Figure 27: Sedimentation equilibrium distributions and residual patterns of α-actinin polypeptides. Absorbance at 280 nm is shown, as a function of distance from the centre of rotation at sedimentation equilibrium. **(A)**: Repeats 1-4 fragment at 0.43 mg ml^{-1}. **(B)**: Repeats 1-3 fragment at 0.28 mg ml^{-1}. **(C)**: Repeats 2-4 fragment at 0.27 mg ml^{-1}. Points are experimental and curves are calculated best fits for a monodisperse solute of M_r 108 kDa **(A)**, monomer-dimer equilibrium with M_r 69 kDa for the monomer and association constant 5 x 10^5 M^{-1} **(B)**, monomer-dimer equilibrium with M_r 60 kDa for the monomer and association constant 10^5 M^{-1} **(C)**. In C the fit was computed for the upper 0.6 mm only of the solution column, so as to disregard the high-molecular weight aggregates appearing near the cell bottom.

molecular mass on concentration. Non-ideality, arising from both the finite size of macromolecules and the charge they carry, tends to reduce the apparent molecular weight. With real solutions of a single solute the measured molecular weight obtained is an apparent molar weight, M_{app}:

$$M_{app} = \frac{M}{(1 + BMc)}$$

where B is termed the second virial coefficient. As the concentration, c, approaches zero, M_{app} approaches M, the true molar weight. The higher the concentration at which the measurement is made, the lower will be the apparent molecular weight. The product BM (l g^{-1} of solute), or excluded volume, is a measure of the volume of solution from which each gram of solute excludes other solute molecules. For globular proteins, the value of BM is smallest, with values near 10 ml g^{-1}. The value of B is increased for expanded molecules that are full of solvent, and for elongated, rod-like molecules, such as double-stranded DNA, and rigid rod-like proteins, such as myosin; the value of BM for myosin is 150 ml g^{-1} (Tanford, 1961). For a species of the size and shape of the α-actinin dimer, the expected second virial coefficient term (BM) was computed, from the sum of the contributions of the excluded volume term, for a particle approximated as a pair of ellipsoids (Rallison and Harding, 1985) of axial ratios 12:2:1 (calculated from rotary shadowed images), and the charge term (Z), at pH 7.5 and ionic strength 0.1 M, given by $Z^2/4mM^2$ (where m is the ionic strength of the solvent and M the molecular weight of the macromolecule), giving a total of 35 ml g^{-1}. A theoretical plot based upon this value is shown in Figure 28A. The experimental results do not differ significantly from this. Whilst a very weak further interaction between dimer molecules (which would act in opposition to the BM term) cannot be excluded, the experimental data do not offer any support for such a hypothesis. The weight-average mass (108 kDa, Figure 27A) was a little lower than the calculated mass of the dimer (114 kDa). The small discrepancy could be due to (i) a difference between the true and calculated partial specific volumes, (ii) the presence of a small

(A)

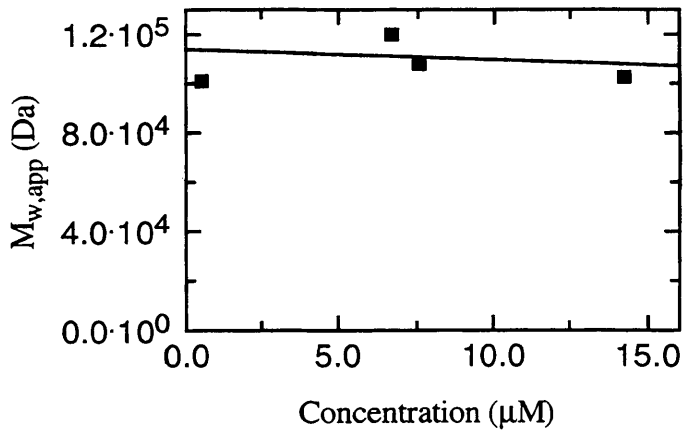

(B)

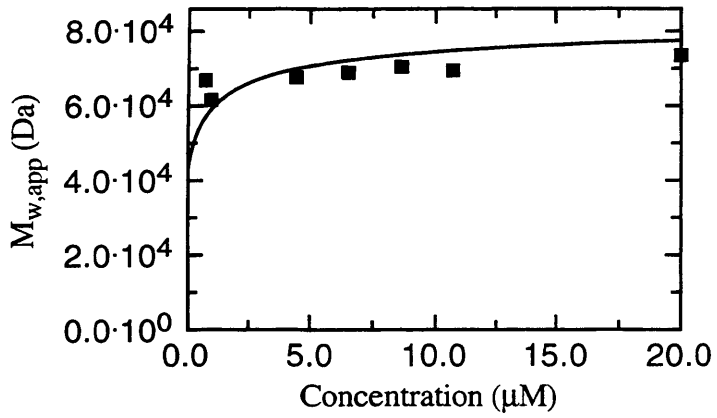

(C)

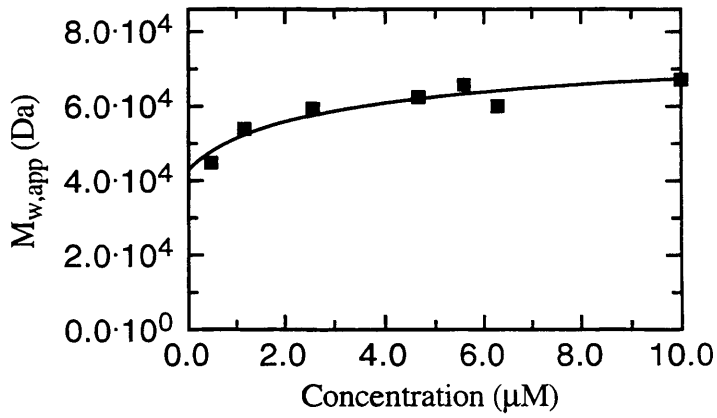

Figure 28: (**A**). Concentration-dependence of apparent weight-average molecular mass for fragment 1-4. (**B**). Concentration-dependence of apparent weight-average molecular mass for fragment 1-3. The curve is based on Equation 1, fixing the monomer mass at the theoretical value. Each experimental point is derived from a sedimentation equilibrium experiment, in which the distribution in all cases conforms satisfactorily to a monomer-dimer equilibrium with

dissociation constants of 0.3-3.8 μM. The curve shown corresponds to a dissociation constant of 2.0 μM. (**C**). Concentration-dependence of weight-average molecular mass for fragment 2-4. The same procedure was followed as in B. The curve of best fit corresponds to a dissociation constant of 6.6 μM. Note that the calculated curves are constrained to approach the monomer molecular mass at infinite dilution. The precision of the data is limited by the quality of the signal obtained at these very low protein concentrations.

proportion of residual, incorrectly folded monomeric material or (iii) perceptible dissociation of the dimer in accordance with a reversible thermodynamic equilibrium. To discriminate between these possibilities a careful analysis was performed on the equilibrium distribution for the highest total polypeptide concentration to determine the apparent values of M_w at a series of radial positions down the solution column. Within experimental error M_w was invariant throughout the column. This would seem to eliminate significant contributions from (ii) and (iii), but a small effect of either is not excluded, the ensuing polydispersity masked possibly by concentration-dependence of the apparent M_w. This is necessarily small, however, and obviously so in view of the lack of any significant dependence of measured M_w values on initial protein concentration (Figure 28A).

By contrast, the polypeptide spanning repeats 1-3 showed evidence of a concentration-dependent association with increasing molecular weight towards the bottom of the solution column (Figure 27B). The polypeptide spanning repeats 2-4 was largely monomeric, but the molecular weight again increases towards the bottom of the cell, indicating concentration-dependent association (Figure 27C). The distribution can be fitted by a monomer-dimer equilibrium, but the apparent association constant increases with initial protein concentrations, suggesting that higher aggregates were formed. The pattern of residuals also showed a typical pattern characteristic of aggregation. Therefore the analysis was confined to the upper part of the solution column. Over a wide range of initial protein concentrations the equilibrium distributions for fragment 1-3 and for the upper part of fragment 2-4 were satisfactorily fitted by a monomer-dimer equilibrium model with dissociation constants in the range 0.3-3.8 and 2.0-11.5 μM respectively. In addition the weight-average molecular masses obtained in these experiments were fitted to a monomer-dimer equilibrium, according to Equation 1 (materials and methods, 2.12.1), based on the theoretical value of the monomer molecular mass. Figure 28 shows the best fits, which correspond to dissociation constants of 2.0 μM for fragment 1-3 and 6.6 μM for 2-4. These are in reasonable agreement with the results from the individual sedimentation equilibria, and confirm the validity of the monomer-dimer model. The sedimentation data thus indicate again a qualitative difference in association state between the intact rod and both fragments, and are thus difficult to reconcile with a simple staggered model.

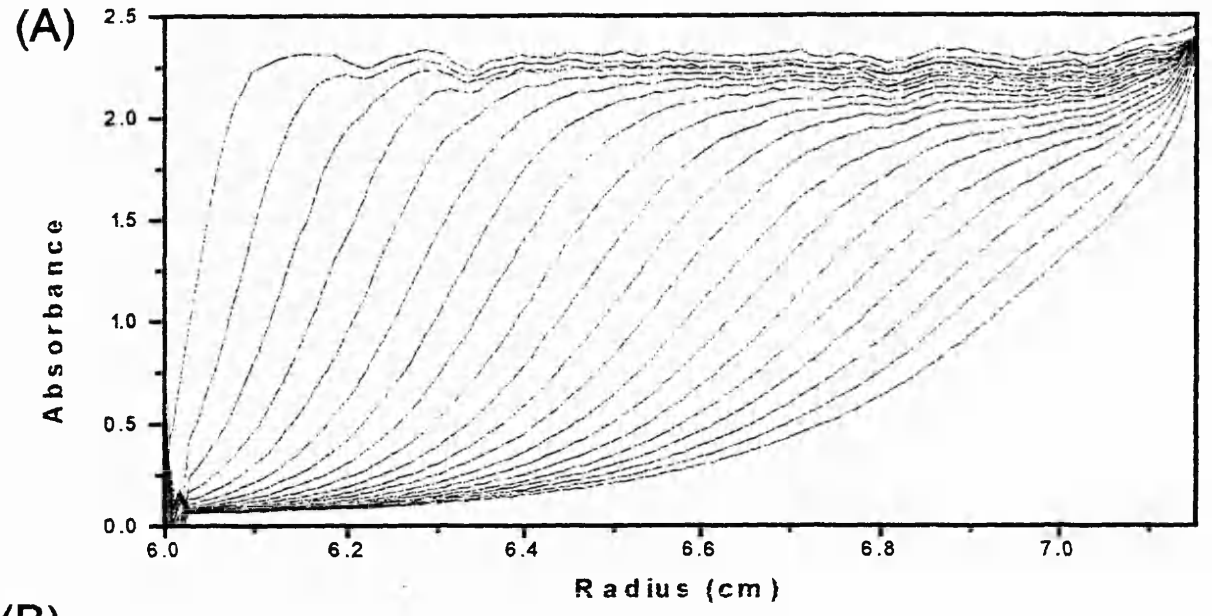
(A)
Absorbance
Radius (cm)

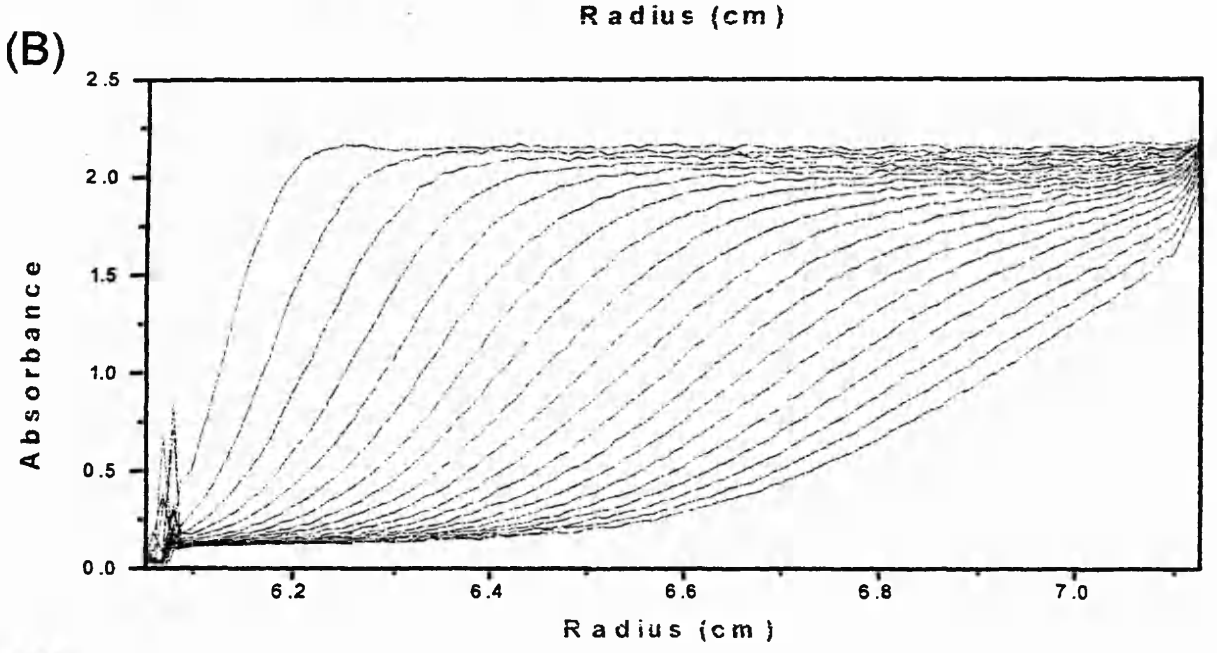
(B)
Absorbance
Radius (cm)

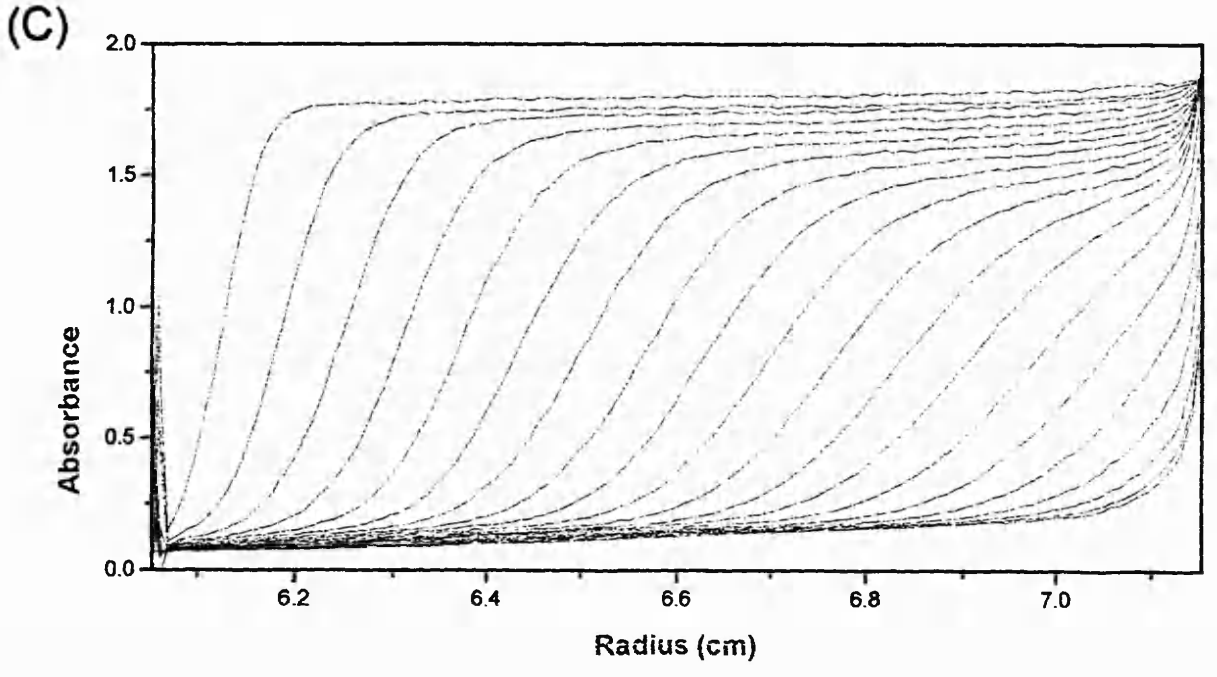
(C)
Absorbance
Radius (cm)

Figure 29: Movement of the boundary in sedimentation velocity experiments of α-actinin constructs. (**A**) Repeats 1-3 at 1.17 mg ml^{-1}; (**B**) repeats 2-4 at 1.39 mg ml^{-1}; (**C**) repeats 1-4 at 0.96 mg ml^{-1}. Sedimentation coefficients of 3.66 S, 3.20 S, and 4.79 S, respectively, were calculated by measuring the rate of movement of the mid-point of the boundary, r_{bnd}, away from the meniscus, r_m (left of each trace).

Additionally, sedimentation equilibrium was performed on a 1:1 mixture of fragments 1-3 and 2-4 to investigate any interaction between the two polypeptides. Values of weight-averaged molecular mass indicated no significant interaction occurred, over affinities observed for the self-interaction of the expressed fragments. If an aligned model was assumed for α-actinin, it would mean that in dimer conformation, repeats 1-3 would be aligned antiparallel with repeats 2-4. Since no interaction was detected between these polypeptides, it suggests that the loss of an interaction between one pair of terminal repeats 1 and 4 is responsible for reduced dimer affinity. Hence, it is likely that an interaction between repeats 1 and 4, at both ends of the rod domain, is required to "bolt" the repeats into a dimer conformation.

3.2.6 Sedimentation velocity

Sedimentation velocity was measured on the expressed polypeptides and sedimentation coefficients were obtained as a function of concentration (Figure 29). The observed sedimentation coefficients were corrected to standard conditions of water at 20 °C. This was achieved by using experimentally determined values for the relative viscosity of the solvents, of 0.9971 and 0.9938 for factor Xa and thrombin buffers respectively. The intact rod made up of repeats 1-4 showed a small decrease in apparent sedimentation coefficient, with diminishing concentration (Figure 30A), characteristic of nonassociating systems:

$$s = \frac{s^0}{(1 + k_s c)}$$

where s^0 is the limiting (ideal) sedimentation coefficient, c is the concentration at which s was determined, and k_s is the concentration-dependence coefficient. The concentration dependence arises from the increased viscosity of the solution at higher concentrations, and from the fact that sedimenting solute particles must displace solvent backwards as they sediment. Both effects become vanishingly small as concentration is decreased. By contrast, the fragments comprising repeats 1-3 and 2-4 both displayed an increase in sedimentation coefficient with increasing concentration, indicative as before of self-association (Figure 30). An estimate of the association constant, assuming a rapid monomer-dimer equilibrium, can then be made, based on the procedure of Gilbert and Gilbert (1973), as modified by Emes and Rowe (1978). It is

(A)

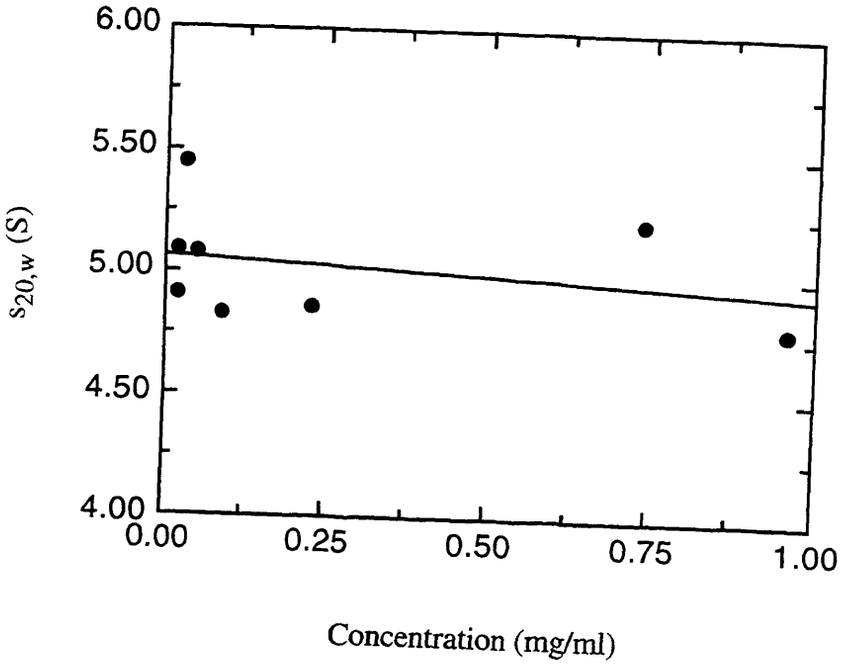
6.00
5.50
5.00
4.50
4.00
$s_{20,w}$ (S)
0.00
0.25
0.50
0.75
1.00
Concentration (mg/ml)

(B)

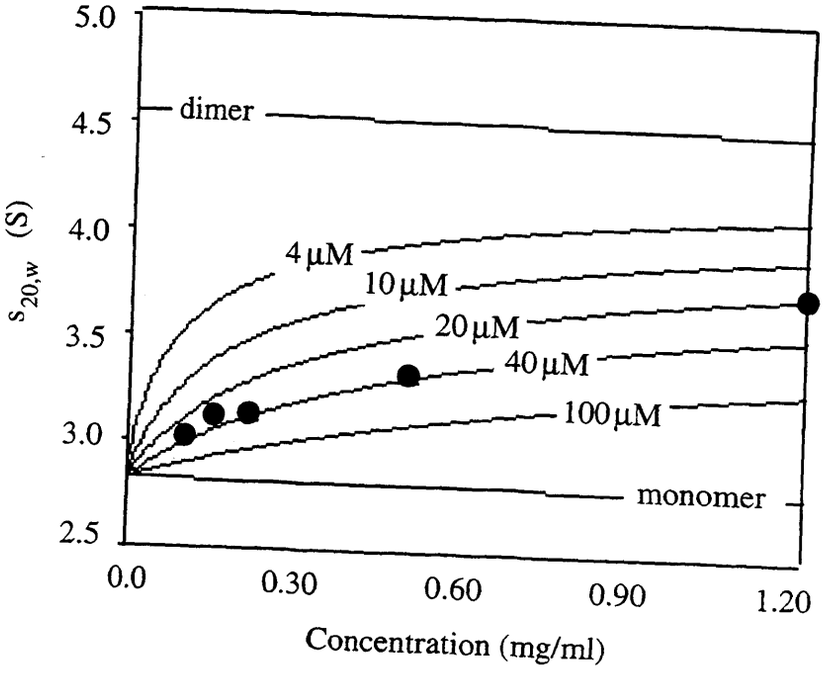
5.0
4.5
4.0
3.5
3.0
2.5
$s_{20,w}$ (S)
dimer
4 μM
10 μM
20 μM
40 μM
100 μM
monomer
0.0
0.30
0.60
0.90
1.20
Concentration (mg/ml)

(C)

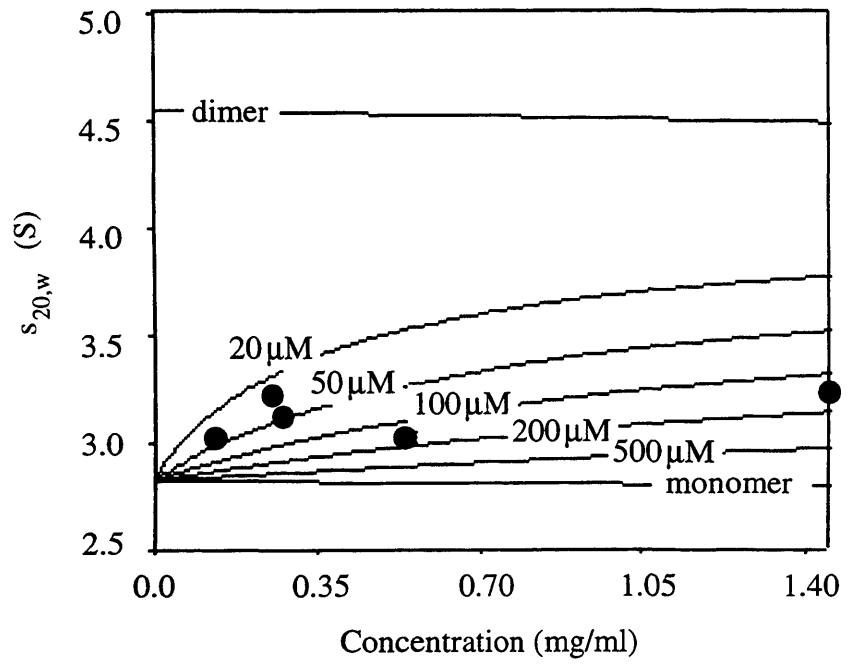

Figure 30: Concentration dependence of sedimentation coefficient for **(A)** fragments 1-4, **(B)** 1-3 and **(C)** 2-4. The curves are calculated for the indicated dimer dissociation constants, and the points are experimental values, yielding apparent dissociation constants of 40 μM and 100 μM.

first necessary to know the concentration-dependence of the sedimentation coefficients of the monomer and dimer, which is assumed to be linear, with a proportionality constant, k_S. This is given by:

$$k_S = 2\bar{v}\left(\left(\frac{V_S}{\bar{v}}\right)+\left(\frac{f}{f_0}\right)^3\right)$$ **Equation 2** (Rowe, 1977)

where $\bar{v}$ is the partial specific volume of the particle, V_S the corresponding hydrated volume and (f/f_0) the frictional ratio (Emes and Rowe, 1978). A value of 0.3 g g^{-1} was assumed for the hydration. Plots of weight-average sedimentation coefficient against protein concentration were then constructed for a series of values of the dimer dissociation constant, K_d, and a match to the experimental data was sought. The best fit (Figure 30) for fragment 1-3 gave a value of ca. 40 μM and that for fragment 2-4 100 μM. These values were larger than those obtained by sedimentation equilibrium, but the method suffers from several drawbacks, in particular that protein association reactions are in general accompanied by a significant volume increase and

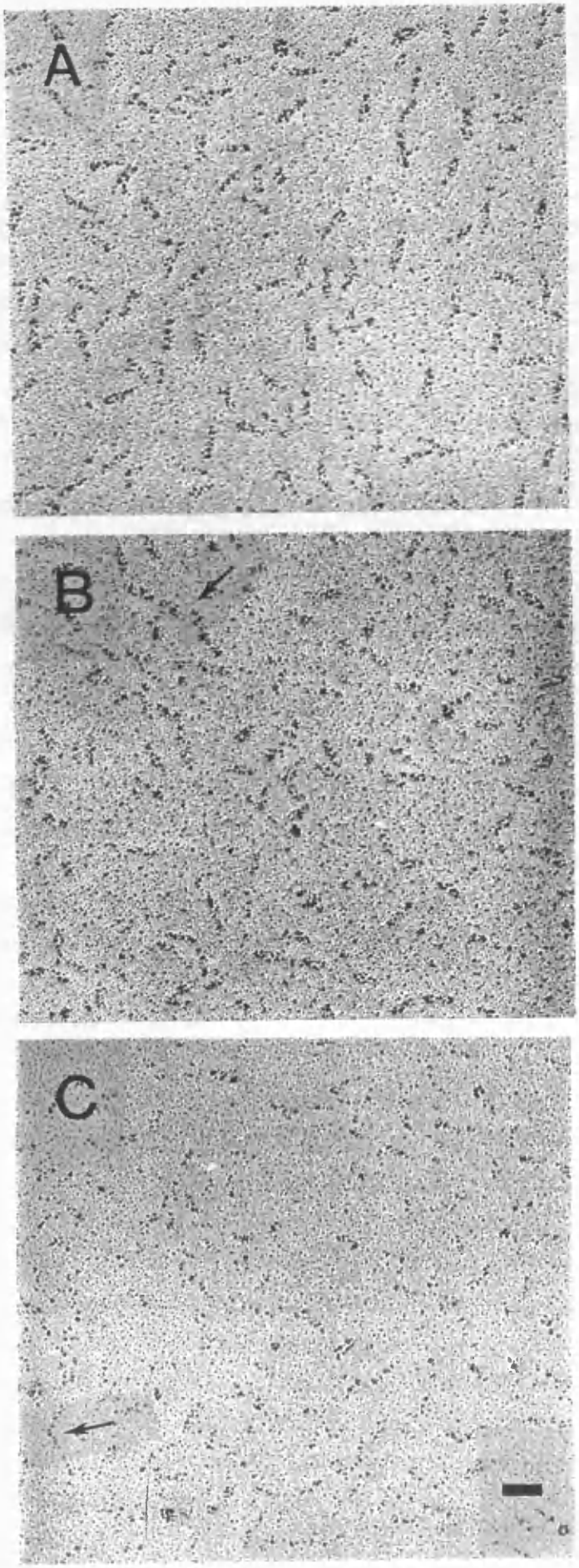
A
B
C

Figure 31: Electron micrographs of rotary shadowed α-actinin polypeptides. **(A)** Repeats 1-4. **(B)** repeats 1-3. **(C)** repeats 2-4. Bar represents 20 nm. Arrows indicate end-to-end association.

are consequently strongly pressure-dependent. Perturbation of the equilibrium by hydrostatic pressure down the liquid column is therefore inescapable (Harrington and Kegeles, 1973). Assuming that the volume change accompanying the self-association of the α-actinin fragment's were the same, our results nevertheless confirm not only that both undergo self-association within the concentration range of these experiments, but also that the propensity of fragment 1-3 to self-associate was stronger than that of fragment 2-4.

3.2.7 Transmission electron microscopy

Examination of the α-actinin polypeptides in the electron microscope after rotary shadowing (Figure 31) revealed that all three were predominantly rod-shaped. A limited degree of end-to-end association of the rods was seen in the truncated polypeptides. The images of the repeat 2-4 polypeptide appeared to have appreciably smaller width than those of the other two polypeptides. In the complete rod domain and the repeat 1-3 polypeptides, many of the particles appeared to contain two laterally aligned components. The average contour length of the intact rod domain was 22.5 ± 2.1 nm, close to that (25 nm) of the equivalent polypeptide liberated from chicken gizzard α-actinin by proteolysis (Imamura et al., 1988). The length of the repeat 1-3 polypeptide was determined to be 20.6 ± 1.7 nm and that of repeat 2-4 was 14.8 ± 2.9 nm (± standard deviation of the mean; N=20 in all cases).

3.3 DISCUSSION

Two-dimensional crystals of chicken gizzard α-actinin have been formed on positively charged lipid layers (Taylor and Taylor, 1993). Low resolution three-dimensional projection images were obtained by optical diffraction from electron micrographs of negatively stained crystals. Interpretation of the molecular boundaries predicted a length of 34 nm and width of 5 nm. The projection image of the molecule lacked 2-fold symmetry, whereas most interpretations of α-actinin structure based upon low resolution images by rotary shadowing or in negative stain have assumed that the molecule is symmetrical with the two polypeptide chains related by a 2-fold rotation axis (Meyer and Aebi, 1990). It is possible that the molecule has 2-fold symmetry but the molecular 2-fold axis is not aligned parallel with the crystallographic axis. Alternatively, the molecule could lack intrinsic 2-fold symmetry, or the symmetry has been disturbed as the result of crystal packing forces.

Each α-actinin molecule in projection consisted of 12 density peaks which arose from variations in the pattern of stain exclusion along the molecule (Taylor and Taylor, 1993). This was interpreted as representing a pattern of protein domains. At the narrow end of the molecule, the two peaks of stain exclusion were dense and compact, while at the wide end the peaks were elongated and less dense, consistent with ellipsoidal domains viewed from two different directions. The interpretation was that domains 1 and 2 constituted the N-terminal actin-binding fragment, due to the following findings. A thermolysin-sensitive cut site is present in chicken skeletal muscle α-actinin near the centre of the actin binding fragment (Hemmings *et al.*, 1992), suggesting the presence of two domains within this fragment. Sequence alignment of the core fragment of chick intestinal fimbrin (De Arruda *et al.*, 1990) revealed a fourfold repeat unit of 125 residues that comprised two homologous ABDs of approximately equal mass, and the ABDs of α-actinin, β-spectrin and dystrophin have an approximately 17% sequence identity to the ABDs of fimbrin.

Eight peaks were observed in the central, rod-shaped region, corresponding to the spectrin-like repeats predicted from the amino acid sequence (Taylor and Taylor, 1993). However, these eight central peaks were not arranged in four pairs but, instead, consisted of three central pairs flanked at either end by a single peak, which appeared larger and denser in projection than the three central pairs. This was interpreted as the unpaired density peak corresponded to repeat 1, and the three pairs of density peaks constituted repeats 2 to 4, which would be paired in reverse order. Chemical cross-linking studies are compatible with this alignment since repeat 4 can be cross-linked to a peptide that contains both repeat 1 and 2 of the other subunit (Imamura *et al.*, 1988). Repeat 1 would then share proximity with the C-terminal domain of the other α-actinin peptide.

Acanthamoeba α-actinin (85-90 kDa) is longer (45 nm) than the smooth muscle isoform while the *Dictyostelium* isoform (97.5 kDa) is shorter (30 nm) (Meyer and Aebi, 1990; Pollard *et al.*, 1986). *Dictyostelium* α-actinin is predicted, based upon the amino acid sequence, to be calcium regulated with respect to actin binding (Noegel *et al.*, 1987) whereas *Acanthamoeba* α-actinin is not (Pollard *et al.*, 1986). Taylor and Taylor (1993) suggested that molecular length might be dependent on the relative alignment of the repeat domains. *Acanthamoeba* α-actinin with a molecular length of 44 nm to 48 nm, might have one or even zero paired repeats. This arrangement would account for the globular domain observed in the centre of the molecule (Pollard *et al.*, 1986). However, as *Acanthamoeba* α-actinin has not been sequenced, an altogether different domain structure cannot be ruled out. *Dictyostelium* α-actinin, with a molecular length of approximately 30 nm, would have four paired repeats. This alignment would place the C-terminal domain with its calcium binding sites, in close proximity to the ABD. Taylor and Taylor (1993) suggested that isoforms that are calcium insensitive occur due to loss of this proximity.

McGough and Josephs (1990) concluded that the central domains of erythrocyte spectrin formed a two-stranded helix with a pitch that varied between 10.4 nm and 16.6 nm depending upon conditions. However, Taylor and Taylor's (1993) reconstruction indicates that α-actinin twists by no more than one-quarter of a turn over a distance of 20 nm. If the molecular twist is a result of interactions between repeats, it may be a function of the degree of pairing of these repeats so that α-actinins might differ not only in length but also twist. α-Actinin isoforms bundle actin filaments differently depending on their molecular lengths (Meyer and Aebi, 1990), and Taylor and Taylor (1993) suggest that this difference is related not just to their molecular lengths but also to the degree of twist.

The thermal denaturation profiles in the present study establish that the bulk of the expressed polypeptide preparations attained their native fold, although a small proportion of unfolded material generally remained, as indicated by the small change in ellipticity in the temperature range below the transition. Rapid spontaneous refolding has been similarly demonstrated for single repeating units from spectrin (Winograd *et al.*, 1991), dystrophin (Kahana and Gratzer, 1995) and α-actinin (Gilmore *et al.*, 1994). The sharp conformational transitions displayed by both three-repeat fragments studied here imply considerable long-range cooperativity of melting along the rod.

The thermal stabilities of both truncated fragments were, however, lower than that of the intact rod domain of four repeats. Whether this is a consequence of an increase in the length of the cooperative unit in the latter or of its much stronger self-association, with $K_d < 10$ pM (Kahana and Gratzer, 1991), is not clear. Certainly the free energy of dimerisation of the native structure would be reflected in the thermal stability of its conformation.

The cross-linking, sedimentation equilibrium, and velocity data show a large difference in the extent of self-association between the intact rod-domain (repeats 1-4) and the deletion mutants containing repeats 1-3 or 2-4. Even though the results for 2-4 must be regarded as only semi-quantitative, in consequence of a tendency of the molecule to aggregate (a process probably precluded in the intact rod domain by formation of the stable dimer), the data argue against a staggered model for the rod dimer, in which there are only three pairwise interactions between the repeats in the constituent chains, while terminal repeat 1 or 4 pairs with the non-homologous EF-hands or ABD as partner (Taylor and Taylor, 1993). The extreme stability of the dimer formed by the isolated rod domain (Imamura *et al.*, 1988; Kahana and Gratzer, 1991) in fact renders it unlikely that either the ABD or the EF-hand domain play any important part in stabilising the α-actinin dimer. Viel and Branton (1994) found that sequences adjoining the four complementary terminal domains of *Drosophila* spectrin contributed to dimer formation, but this was not confirmed in studies on the analogous human erythroid spectrin system (Ursitti *et*

al., 1996). The implication of our results then is that pairwise interactions between all four aligned repeats in the antiparallel orientation contribute to the stability of the dimer.

Speicher *et al.* (1992) have shown that the formation of the antiparallel heterodimer of erythroid spectrin is dependent on pairing of the first four complete repeats at the N-terminal end of the β-chain (β1-β4) with the last four repeats of the α-chain (α18-α21). A characteristic of these strongly associating repeats, shared by their counterparts in *Drosophila* spectrin (Viel and Branton, 1994), is that they all contain an eight-residue insert at their N-terminal ends, although the exact phasing differs in each isoform. Excision of these segments from the sequence resulted in a gross loss in the capacity to associate. Thus for example, the elimination of such an eight-residue insert from β1 of a human erythroid spectrin construct led to a tenfold decrease in affinity of binding to the complementary subunit (Ursitti *et al.*, 1996). The four α-actinin rod repeats display the highest homology (29-47% identity) with the strongly associating spectrin repeats and indeed all contain N-terminal eight-residue inserts (Ursitti *et al.*, 1996). The phasing selected for the truncated rod fragments used here incorporated the eight-residue inserts shown to be essential for *Drosophila* spectrin dimer formation. Hence, because neither of these fragments possessed the complete dimer forming ability of the intact rod domain, or participated in heterodimer formation when mixed, it suggests these inserts alone are not sufficient to allow dimerisation.

The results of electron microscopy are less conclusive. The dimensions of the intact rod domain dimer (Figure 31) correspond to a length of about 5.5 nm per repeat. This is close to the value inferred by Taylor and Taylor (1993) from electron micrograph projections of two-dimensional α-actinin crystals. For erythroid spectrin (Shotton *et al.*, 1979) the dimer contour length is 100 nm, and that of the tetramer 200 nm, which is also the length of the neuronal spectrin tetramer (Glenney *et al.*, 1983); thus with 22 complete repeats in the α-chains and 17 in the β-chain, the lengths per repeat are respectively 4.5 and 5.9 nm, but this makes no allowance for the terminal and other non-homologous elements in the sequences (Sahr *et al.*, 1990; Winkelmann *et al.*, 1990; Wasenius *et al.*, 1989). A further uncertainty is whether the proteins prepared for shadowing electron microscopy in solutions containing 50% glycerol, rising to 100% during drying, attain their maximally extended lengths in these circumstances. This condition is evidently fulfilled in the case of erythroid spectrin, as determined by its extension at low ionic strengths (McGough and Josephs, 1990). By hydrodynamic criteria, α-actinin behaves in the same manner (Kuroda *et al.*, 1994). Particle lengths therefore do not give definitive information on the number of repeats between the ends of the α-actinin rod dimer. On the other hand, the thickness appears uniform from end to end. It is also possible that, if these proteins can be represented as two-stranded helices with variable pitch (McGough and Josephs, 1990), the maximum pitch could be different in spectrin and α-actinin. Meyer and Aebi (1990) have

demonstrated extensibility in α-actinins from two sources (*Dictyostelium* and *Acanthamoeba*): both types change their lengths when they bind to F-actin.

The similar lengths of the intact rod domain polypeptide (22.5 nm ± 2.1) and fragment 1-3 (20.6 nm ± 1.7), taken together with the smaller length (by the equivalent of one repeat) of fragment 2-4, are of course compatible with the staggered model shown in Figure 21B, but in this case a stable antiparallel dimer of repeats 1-3 would need to form through a single paired interaction between repeat 3 of the two chains. This is intrinsically unlikely and in any event the cross-linking and sedimentation data rule out complete dimerisation in any accessible concentration range, as would be implied by this interpretation of the electron microscope observations. The relation of our data to the appearance of the α-actinin dimers in the two-dimensional crystals of Taylor and Taylor (1993) thus remains to be clarified. The possibility of a more complex structure for the rod domain than a contiguous or nested succession of identical repeats cannot be disregarded. The exceptional stability of the isolated rod dimer (Imamura *et al.*, 1988; Kahana and Gratzer, 1991) excludes a dominant contribution from interactions between the N- and C-terminal domains of α-actinin to dimerisation. On the other hand, the remarkable extensibility of the dimer, which reveals itself in the *Acanthamoeba* protein by a 26% increase in length when it binds at both ends to F-actin (Meyer and Aebi, 1990), could reflect slippage of the constituent subunits relative to each other or a change in pitch, if the rod conforms to the helical model put forward by McGough and Josephs (1990) for spectrin. At all events, a structural difference between the molecule in dilute aqueous solution and when constrained in a two-dimensional crystal lattice (or indeed when partially dehydrated in high glycerol concentrations before shadowing) is not unlikely. A difference in the pattern of inter-chain interactions in two conformational states of the dimer in equilibrium with one another could also give rise to distinct cross-linked products on reaction with bifunctional reagents; such a phenomenon is exemplified in actin, which can generate two electrophoretically distinct dimers, representing respectively interactions in the genetic-helix and long-pitch helix modes (Millonig *et al.*, 1988).

The work of Speicher *et al.* (1992) on erythroid spectrin has demonstrated a wide variation in the strengths of pairwise interactions among repeats in the antiparallel αβ-dimer, with strong association between the first four repeats at the N-terminal end of the α-chain and the corresponding repeats at the C-terminus of the β-chain. The complementarity must be assumed to be specific; thus, for example, no hybridisation occurs between the polypeptide chains of erythroid spectrin and the neuronal spectrin, fodrin (Glenney *et al.*, 1983). In α-actinin, if the antiparallel chains are aligned, there can be only two types of interaction - those between repeats 1 and 4 and between repeats 2 and 3. In the aligned structure the absence of one repeat would thus eliminate two paired interactions. That self-association of the truncated rod domains is

much weaker than that of the intact domain is entirely to be expected, since multiple interactions along the polypeptide chains must lead to high co-operativity of binding.

More detailed analysis of subunit interactions, possibly by deleting individual helices, may reveal specific inter-helical interactions between subunits, similar to those observed in tetramer formation for spectrin.

CHAPTER 4.

INVARIANT TRYPTOPHAN AND ITS ROLE IN REPEAT FOLDING AND SUBUNIT INTERACTION

4.1 INTRODUCTION

Current models predict that the repeats in spectrin (Speicher and Marchesi, 1984; Xu *et al.*, 1990; Parry *et al.*, 1992), α-actinin (Parry *et al.*, 1992), and dystrophin (Koenig *et al.*, 1988; Cross *et al.*, 1990) comprise three antiparallel helices, stabilised by electrostatic (Parry *et al.*, 1992) and hydrophobic (Cross *et al.*, 1990) interactions. These occur on correct juxtaposition of repeating heptads of amino acids.

The crystal structure of a single repeat of *Drosophila* spectrin α14 (Yan *et al.*, 1993) has confirmed the accuracy of these predictions. Helices A and B, of the crystallised dimer, formed a hairpin, and helix C was continuous with helix B. Because the intact molecule has an extended structure whose N- and C-termini lie at opposite ends, the C helix of each repeat must fold back against helices A and B. However, unlike a number of the other spectrin repetitive motifs, segment 14 of the *Drosophila* α-chain contains no Pro in the region between helix B and C, so that a continuous BC helix is possible. Furthermore, the BC loop is variable in length from repeat to repeat; in α-spectrin repeat 9, it contains an entire SH3 domain. The three helices interacted with each other over eight turns, forming a left-handed three-helix bundle about 5 nm long and 2 nm in diameter. Helix B was longer by two turns than helix A, and helix C was bent, helix B was slightly bent, and helix A was straight. Each of the three helices exhibited the heptad pattern of residues found in extended α-helical structures, with positions conventionally labelled by the letters *a* to *g* (McLachlan and Stewart, 1975). Residues *a* and *d* are generally hydrophobic and lie on the inward-facing surface of the helix (Cohen and Parry, 1986; Koenig *et al.*, 1988; Cross *et al.*, 1990). The remaining residues tend to be more polar.

The antiparallel A and B helices were in a register such that positions *d* of one helix were at the same level as positions *a* of the other (Figure 32). The *d* sidechains projected into a cavity on the surface of the opposite helix, packing laterally against *a* side chains and bounded axially by *d* side chains of successive heptads. This ridge-to-ridge packing arrangement was similar to that found in coiled-coil proteins (Banner *et al.*, 1987; O'Shea *et al.*, 1991; Lovejoy *et al.*, 1993), except that helix A did not coil around helix B. In contrast, helix C was axially displaced relative to helices B and A so that each turn of helix C ran roughly midway between two adjacent turns in helices B and A, and the side chain packing between helices C and B and between C and A conformed to the ridges-into-grooves arrangment common in globular proteins (Chothia *et al.*, 1977). This model has since been shown to apply equally to a single repeat of chicken brain α-spectrin (Pascual *et al.*, 1996).

An interesting feature of the homologous structural repeats of α- (Speicher and Marchesi, 1984; Wasenius *et al.*, 1989; Dubreil *et al.*, 1989; Sahr *et al.*, 1990) and β- (Byers *et al.*, 1989; Winkelmann *et al.*, 1990; Hu *et al.*, 1992) subunits of erythroid and non-erythroid spectrin, α-

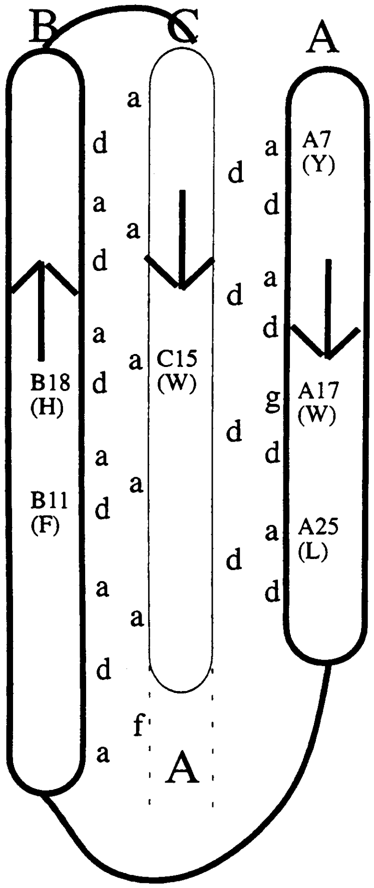

Figure 32: Cartoon view of the three α-helices of *Drosophila* repeat α14. The axial displacement of helix C places the *a* and *d* position residues between the underlying or overlying *a* and *d* residues in helices A and B. Dashed lines extending from the bottom of helix C indicate the proposed position of the next repeat's A helix.

actinin (Witke *et al.*, 1986; Baron *et al.*, 1987), and dystrophin (Koenig *et al.*, 1988) is a single tryptophan in helix A that is conserved to a degree unmatched at any other position (Introduction, Figure 7). Exceptions to the rule include the 10th repeat of human erythroid β-spectrin (Winkelmann *et al.*, 1990), certain repeats of *Drosophila* β-spectrin (Byers *et al.*, 1989), the 15th repeat of erythroid and non-erythroid β-spectrin which exhibits ankyrin-binding activity (Kennedy *et al.*, 1991), and the 4th repeat of *Dictyostelium* α-actinin (Noegel *et al.*, 1987), where it is replaced by a tyrosine, another aromatic residue.

This tryptophan has been reported to promote the conformational stability of one repeat of chicken brain α-spectrin (Macdonald *et al.*, 1994). Four constructs were overexpressed in *E. coli*: two adjacent but separately expressed "conformationally phased" repeats, R16 and R17, one of which (R17) contained a single tryptophan; a mutant, M17, in which the single tryptophan in R17 was substituted with alanine; and a conformationally unphased repeat, 1617, composed of half of each of the phased units. Both the mutant repeat and the unphased repeat

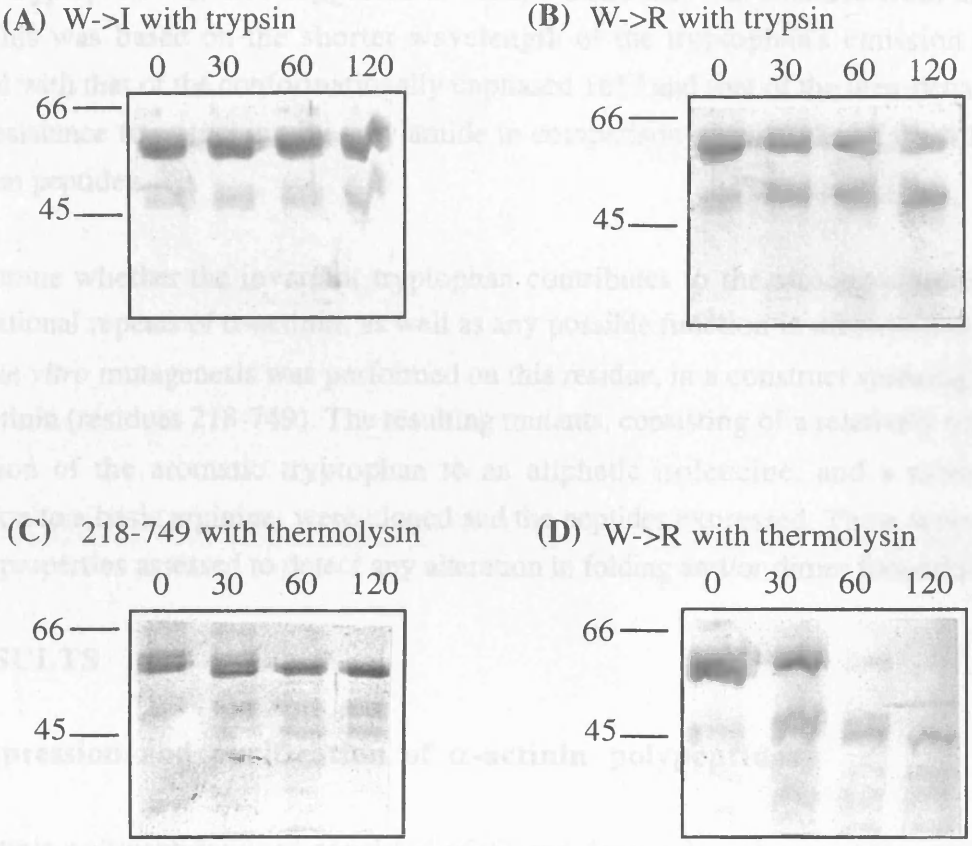

Figure 33: Protease-resistance of the expressed α-actinin repeat domain proteins. Purified α-actinin polypeptides (218-749) were exposed to trypsin or thermolysin (enzyme to substrate ratio 1:1000) for the times shown (mins). Mutant rod domains W->I **(A)** and W->R **(B)** with trypsin. Wild-type **(C)** and mutant W->R **(D)** rod domains with thermolysin. The position of molecular mass standards (kDa) is indicated.

were much more readily digested by proteases than the phased repeats, and exhibited only 38% and 54% as much α-helical structure, respectively, as the phased repeats. Light scattering measurements revealed the folded peptides to be predominantly monomeric in solution, whereas the unfolded, protease-sensitive peptides consisted of dimers and/or trimers. The invariant tryptophan was also suggested to occupy a site that was shielded from the aqueous phase. This was based on the shorter wavelength of the tryptophan's emission maximum compared with that of the conformationally unphased 1617 and that of the urea-denatured R17, and its resistance to quenching by acrylamide in comparison with 1617 and the other single-tryptophan peptides.

To determine whether the invariant tryptophan contributes to the structural stability of the conformational repeats of α-actinin, as well as any possible function in dimerisation of the rod domain, *in vitro* mutagenesis was performed on this residue, in a construct spanning repeats 1-4 of α-actinin (residues 218-749). The resulting mutants, consisting of a relatively conservative substitution of the aromatic tryptophan to an aliphatic isoleucine, and a more dramatic substitution to a basic arginine, were cloned and the peptides expressed. These were examined and their properties assessed to detect any alteration in folding and/or dimer formation.

4.2 RESULTS

4.2.1 Expression and purification of α-actinin polypeptides

The α-actinin polypeptides used consisted of the rod domain based on residues 218-749, and two mutant proteins, each containing a single point mutation at the conserved tryptophan in repeat 1 (W->I, W->R). The chicken smooth muscle cDNAs encoding the polypeptides were generated by amplifying regions of full-length chicken α-actinin cDNA C17 (Baron *et al.*, 1987) by PCR, and the mutagenesis was performed by Andrew Blanchard. The proteins were expressed in *E. coli* as soluble GST-fusion proteins, essentially as described by Smith and Johnson (1988), and purified on glutathione-agarose beads. Successful purification was determined by SDS-PAGE and observed bands corresponded with the expected size of 88 kDa. These were then liberated from GST by proteolytic cleavage with factor Xa. The isolated proteins were shown to be >90% pure by SDS-PAGE, and observed bands again corresponded with the predicted molecular weight of 62 kDa (Figure 33, 34). Yields were determined spectrophotometrically, using calculated absorption coefficients of 1.27, 1.19, and 1.18 cm^{-1} (for 1 mg ml^{-1}) for the wild-type (WT) rod, W->I, and W->R fragments respectively.

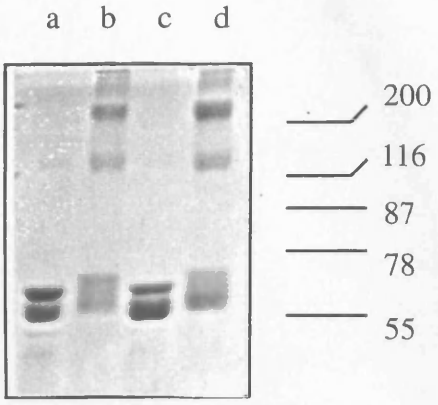

Figure 34: Analysis of the association of α-actinin mutant polypeptides, W->I and W->R, by chemical cross-linking with DMS. W->R, untreated (lane a) and treated at protein concentration of 0.20 mg ml^{-1} (b). W->I, untreated (lane c) and treated at protein concentration of 0.16 mg ml^{-1} (d).

Table VI. Expressed proteins existed as folded dimers as judged by circular dichroism and sedimentation equilibrium.

Construct	Molar residue ellipticity (^{o} cm^2 $dmol^{-1}$) at 222nm	% α-helix	Concentration (mg ml^{-1})	% dimer
W->I rod	-22400	62	1.20	76
			0.60	92
			0.04	97
W->R rod	-23900	66	0.84	100
			0.58	94
			0.10	98

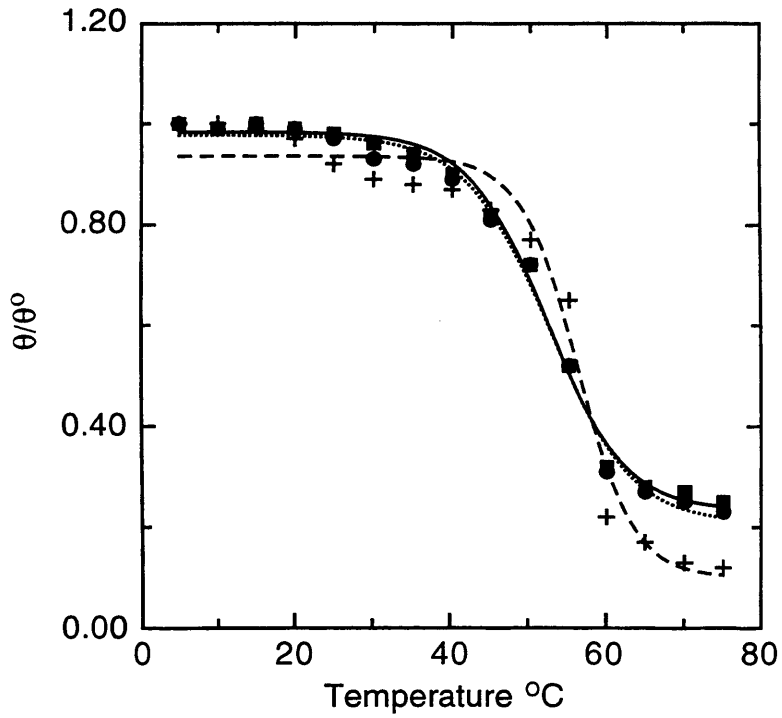

Figure 35: Thermal denaturation profiles of expressed α-actinin rod fragments, determined by circular dichroism. Unfolding is measured by the ellipticity at 222 nm relative to that at 5 °C. Wild-type (218-749) (---, +), and mutant rod domains W->I (···, ●) and W->R (—, ■).

4.2.2 Circular dichroism

To verify native secondary structure, circular dichroism measurements were performed at 20 °C. These showed that the two mutant proteins had a similar CD spectra to that of WT rod (218-749; 66% helix), and also to that of the fragment 1-4 (267-749; 66% helix) (previous chapter), with a high α-helical content (62-66%; Table VI), suggesting that the polypeptides had folded correctly.

4.2.3 Resistance to proteolysis

The ability of rod fragments to enter the native fold has also been assessed for spectrin, dystrophin, and α-actinin (Winograd *et al.*, 1991; Kahana *et al.*, 1994; Gilmore *et al.*, 1994) in terms of resistance to proteolysis. Incubation of the isoleucine mutant polypeptide with trypsin, for up to 2 hours (Figure 33), demonstrated a similar resistance to proteolysis to that of the fragment 1-4 (267-749) (previous chapter), again indicating no significant change in conformation. However, incubation of the arginine mutant demonstrated a reduced resistance to proteolysis, to that of the fragment 1-4 (267-749) (previous chapter) and W->I mutant with trypsin. Since this could be due to the introduction of a new trypsin cut-site, the W->I mutant

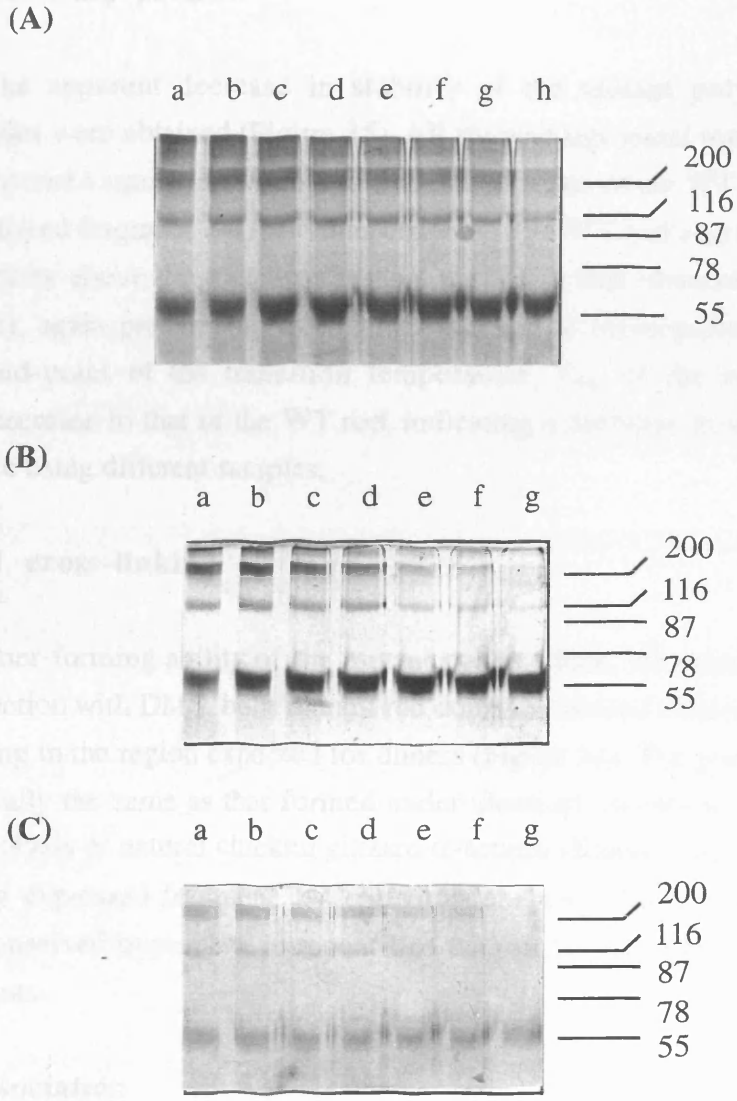

Figure 36. Urea dissociation profiles of expressed α-actinin polypeptides. Wild-type (218-749) (**A**), and mutant rod domains W->I (**B**) and W->R (**C**). Lanes show proteins exposed to DMS in presence of (a) 0.39 M, (b) 0.77 M, (c) 1.54 M, (d) 2.31 M, (e) 3.08 M, (f) 3.85, (g) 4.62, (h) 5.39 M urea. The positions of molecular mass standards (kDa) are indicated.

was also incubated with thermolysin. The mutant again displayed a reduced resistance to proteolysis, to that of the WT rod (218-749) (Figure 33), indicating a change in conformational stability had occurred with this particular mutation.

4.2.4 Thermal melting profiles

To investigate the apparent decrease in stability of the mutant polypeptides, thermal denaturation profiles were obtained (Figure 35). All showed sigmoidal transitions, suggesting the mutants had entered a similar native fold to that characteristic of the WT rod, and also to that of the correctly phased fragment 1-4 (previous chapter). The WT rod also displayed a gradual decrease in ellipticity above the transition region, similar to that observed for fragment 1-4 (previous chapter), again presumably due to the presence of incompletely folded material. However, the mid-point of the transition temperature, T_m, of the mutants showed an approximate 5° decrease to that of the WT rod, indicating a decrease in stability. This result was obtained twice using different samples.

4.2.5 Chemical cross-linking

To investigate dimer-forming ability of the mutant polypeptides, chemical cross-linking was performed. On reaction with DMS, both mutant rod domains showed extensive cross-linking to a doublet, migrating in the region expected for dimers (Figure 34). The proportion of covalent dimer was essentially the same as that formed under identical conditions by the rod domain prepared by proteolysis of natural chicken gizzard α-actinin (Kahana and Gratzer, 1991) and also to that of the expressed fragment 1-4 (previous chapter). These results show that the mutation of the conserved tryptophan in repeat 1 of the rod did not reduce the dimer forming ability of the mutants.

4.2.6 Urea dissociation

The stability of the mutant polypeptides under denaturing conditions was investigated by chemical cross-linking with DMS in the presence of increasing concentrations of urea (Figure 36). Dissociation of the WT rod (218-749) polypeptide into monomers was incomplete upto 5.4 M urea (Figure 36A; lane h). However, the mutant polypeptides appeared less stable with a loss of cross-linking in the presence of 4.6 M urea (Figure 36B and C; lane g).

4.2.7 Sedimentation equilibrium

Analysis of self-association of the expressed mutant polypeptides was performed by sedimentation equilibrium. Molecular weights were determined using calculated values for the

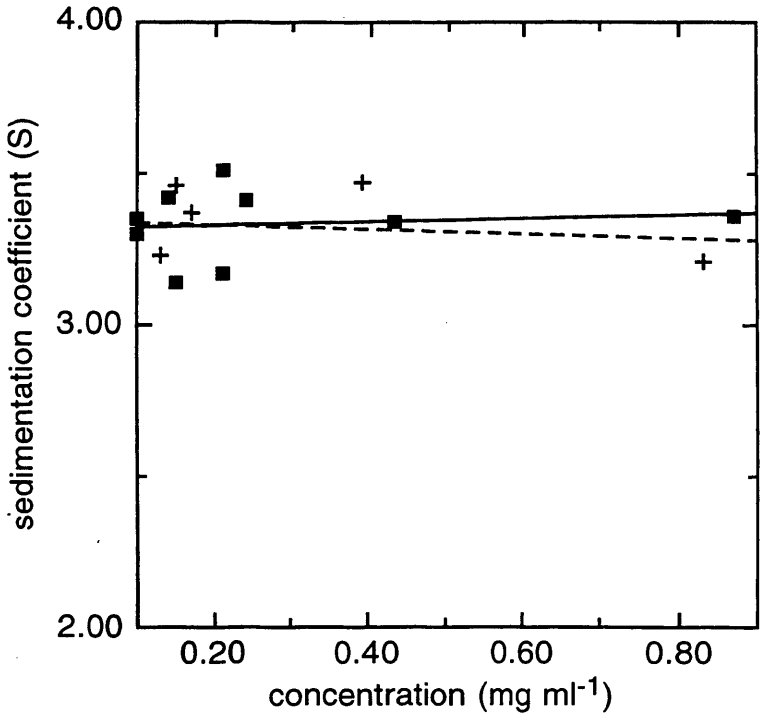

Figure 37: Concentration dependence of sedimentation coefficient for expressed α-actinin mutant polypeptides. Mutant W->I (+, .···); mutant W->R (■, —).

partial specific volume of 0.731 ml g^{-1} for both fragments W->I and W->R. The results indicate that both proteins existed predominantly, or entirely, as dimers, as calculated from weight-average molecular weights (Table VI). The pattern of residuals, as with fragment 1-4 (previous chapter), displayed a random scatter of points around zero indicating a satisfactory fit to the proposed model. There was no obvious concentration-dependent behaviour for values of the molecular mass indicating that there was no association-dissociation equilibrium within the concentration range explored. A negligible concentration-dependence due to the second virial coefficient would be expected at these low protein concentrations, again similar to fragment 1-4 (previous chapter).

4.2.8 Sedimentation velocity

Sedimentation velocity was measured on the expressed polypeptides to investigate size and conformation of the mutant polypeptides, and sedimentation coefficients were obtained as a function of concentration. Both mutants displayed no obvoius concentration-dependent behaviour for values of sedimentation coefficient, again indicative of non-associating systems (Figure 37). Extrapolated values of s^0, corrected to standard conditions of water at 20 °C, were comparable to that obtained for repeats 1-4 (previous chapter) with values of 5.06, 5.23, and

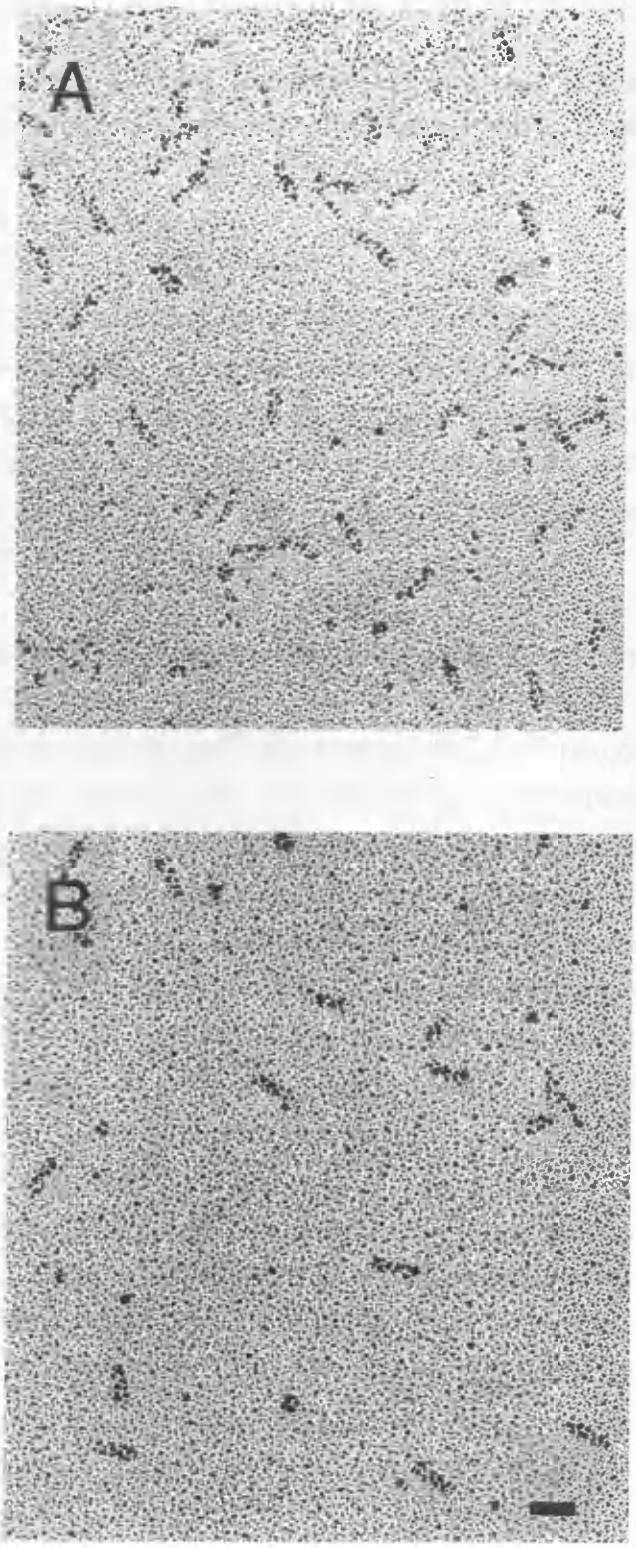

Figure 38. Electron micrographs of rotary platinum shadowed α-actinin polypeptides. Mutant rod domains W->I (**A**) and W->R (**B**). Bar represents 20 nm.

5.20 S for fragments 1-4, W->I, and W->R respectively, indicating the mutants existed in a size and conformation characteristic of rod-shaped α-actinin dimers.

4.2.9 Electron microscopy

Rotary shadowing and visualisation by TEM showed the proteins to be predominantly rod-like, consisting of two laterally associated subunits (Figure 38). Measured mean lengths of the particles were 21.8 (± 2.2) nm for the W->I mutant and 20.2 (± 1.5) nm for the W->R mutant, in good agreement with the fragment 1-4 (previous chapter) and to that of chicken gizzard α-actinin liberated by proteolysis (Imamura et al., 1988) (N=20 for all; ± standard deviation of mean).

4.2.10 Expression of repeat 1 containing conserved tryptophan mutation

Investigation into the stability and dimer forming ability of two constructs spanning repeats 1-4 of the α-actinin rod domain (218-749), containing a tryptophan mutation in repeat 1, to an isoleucine and an arginine residue, indicate a decrease in thermal and urea stability, compared to the WT rod domain. Also, the arginine mutant displayed an increased susceptibility to proteolysis, compared to both the W->I mutant and the WT rod, suggesting a further alteration in subunit stability. To further investigate the role of this invariant tryptophan in stabilising the reapeat unit in α-actinin, plasmid DNA encompassing repeat 1, containing the the more conservative tryptophan to isoleucine mutation, was PCR amplified, ligated into pGEX2-T plasmid vector, and then used to transform *E. coli*.

To establish whether the bacteria had been transformed sucessfully, PCR was performed on 5 µl of an overnight culture. The subsequent reaction was electrophoresed on an agarose gel, and examination under UV light indicated products of the size expected (<0.5 kb) had been formed. Further to this, DNA sequencing was performed to check the ligated insert contained no PCR errors in the sequence surrounding the mutation. The resulting sequence was found to read correctly, as compared to published chicken smooth muscle α-actinin (C17) cDNA (Baron *et al.*, 1987) (Figure 39).

Expression of the GST construct encoding repeat 1 (residues 267-385) alone, containing the tryptophan to isoleucine mutation, resulted in protein which was in inclusion bodies (Figure 40). Since expression of native repeat 1 results in expression of soluble protein (Gilmore *et al.*, 1994), the resultant change in solubility presumably reflects a significant conformational change in the mutant repeat 1.

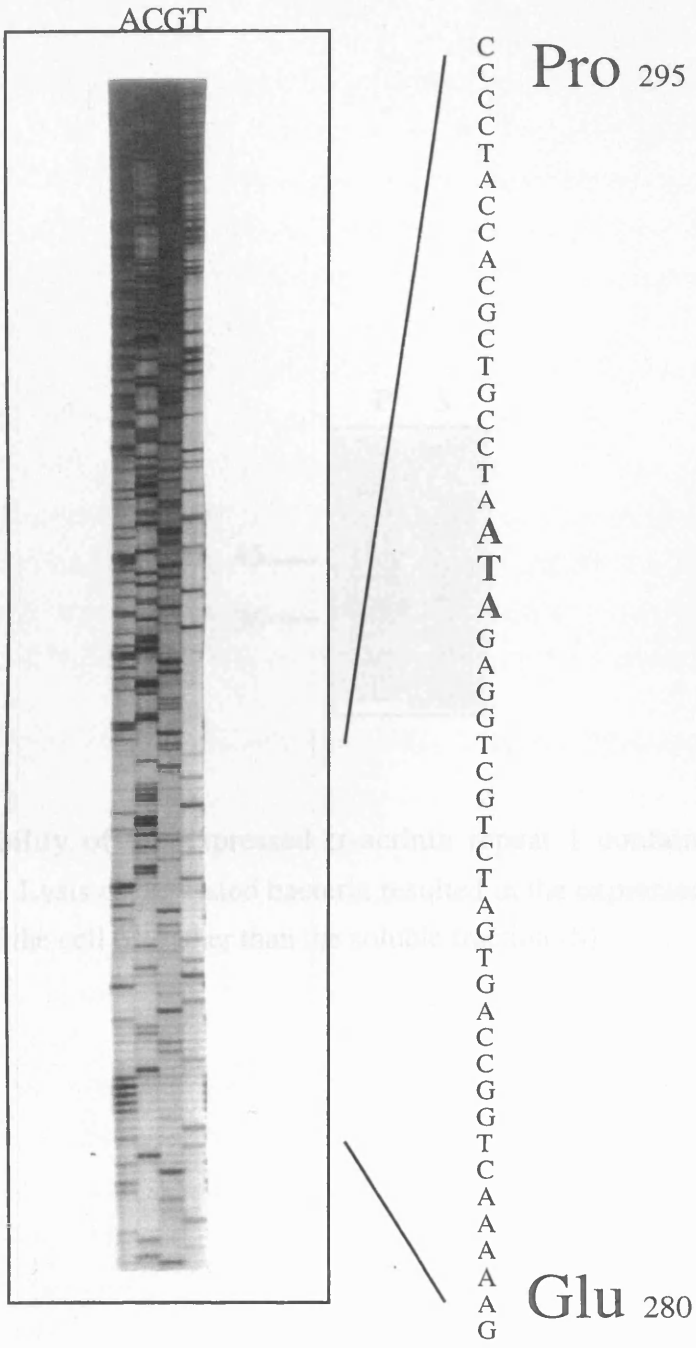

Figure 39: DNA sequence of α-actinin repeat 1 containing a tryptophan to isoleucine mutation. Highlighted sequence encodes from Glu^{280} to Pro^{295}. Replacement codon (ATA) is shown.

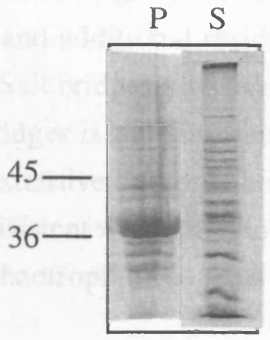

Figure 40: Insolubility of the expressed α-actinin repeat 1 containing a tryptophan to isoleucine mutation. Lysis of harvested bacteria resulted in the expressed protein being in the insoluble fraction of the cell (P) rather than the soluble fraction (S).

4.3 DISCUSSION

The crystal structure of the single *Drosophila* spectrin repeat, α14, which was determined by Yan *et al.* (1993) provides an insight into the overall conformation of spectrins, and also, to a more limited extent, the other members of the spectrin superfamily. The structure determined showed that the spectrin repeat forms a three-helix bundle, similar to the conformational predictions (Figure 32), but also provided much more precise conformational detail.

Between helices A and C, interchain salt bridges were often formed by charged residues, as in conventional coiled-coil structures, and additional residues in helix C were also involved in some ionic interactions (Figure 32). Salt bridges also existed between the antiparallel B and C helices. The large number of salt bridges is not surprising, as a third of the amino-acid side chains in spectrin are charged. The extensive hydrophobic and electrostatic interactions within these relatively small repeats are consistent with spectrin's ability to refold rapidly into native structures after denaturation with chaotrophic reagents such as urea (Speicher and Ursitti, 1994).

In general, the repetitive motifs of spectrin preserve a fixed register between the C helix of one and the A helix of the next, with no prolines or glycines at the segment boundary. It has therefore been proposed that the "two" helices are in fact continuous, with the C helix of the first repeat and the A helix of the next repeat forming a single helix (Figure 6) (Parry and Cohen, 1991; Dubreil *et al.*, 1989). It is not obvious that continuity between helices C and A would lead to a molecular structure consistent with the observed flexibility of these proteins. It seems more likely that at least a kink or a short break in the helix between repeats would be required to explain spectrin's flexibility. The α-helical turns that form the CA boundary are involved in multiple interactions with the two turns of the helix at the N-terminus of B (Figure 32). Because the model predicts that each successive repeat is axially rotated 60° in a right-handed sense with respect to the previous repeat (Yan *et al.*, 1993), it places the first *f* position in the A helix of the next successive repeat between the *a* and *d* residues of the preceding repeat's B helix (Figure 32). This should impart a spiralling or rope-like shape to the molecule, which is consistent with molecular supercoiling seen in electron micrographs (Shotton *et al.*, 1979; McGough and Josephs, 1990). The packing of this hydrophobic residue from helix A of one repeat against the hydrophobic residues from helix B of the previous repeat should confine the repeat-to-repeat flexibility within a limited number of planes. This slight overlapping of adjacent repeats could also explain the unusually strong conservation of most spectrin repeats to a length of precisely 106 residues, despite their overall low degree of sequence similarity. In contrast, the lengths of dystrophin repeats are far more variable, which suggests less extensive interdigitation of adjacent dystrophin repeats; this would allow more freedom for insertions or deletions within individual repeats during evolution (Speicher and Ursitti, 1994).

Among the most conserved of all residues were those that are important for maintaining contacts between the straight helix A and the coiled helices B and C. Near the AB loop, the interaxial distance between helices A and B was relatively large, and open salt bridges between helices A, B, and C replaced the usual hydrophobic contacts. The residue at A7 helped space helix A away from B and C at one end, whereas at the other end the conserved, bulky residue at B11 packed against A25 and A24, the latter exceptionally conserved as a hydrophobic residue (Figure 32). Between these two, near the middle of the helix bundle, the invariant Trp A17 was involved in the way helix A crossed over from B to C, as was the nearly invariant Trp at C15. These two tryptophans were opposite each other, with His B18 between them (Yan *et al.*, 1993) (Figure 32). The same inter-helical contacts were also observed in the NMR structure of chicken brain spectrin α16 (Pascual *et al.*, 1996), where interhelical NOEs (nuclear Overhauser effect) were seen between Trp A22, His B19, and Trp C15.

One repeat that is likely to have a substantially different conformation is β15, which binds to ankyrin, the high-affinity receptor for spectrin (Kennedy *et al.*, 1991). Other repeats that are likely to show substantial conformational variations relative to the α14 repeat are the two C-terminal α-spectrin repeats and the two N-terminal β-spectrin repeats, essential repeats of the nucleation site required for assembly of the spectrin dimer (Speicher *et al.*, 1992), and the most similar in sequence to the α-actinin repeats (Dubreuil *et al.*, 1989; Byers *et al.*, 1989). Although these terminal spectrin and α-actinin repeats are slightly longer than the typical spectrin repeat, they also contain the invariant tryptophan shown to be important for inter-helical contacts in chicken and *Drosophila* α-spectrin (Pascual *et al.*, 1996; Yan *et al.*, 1993). This tryptophan, that occurs midway in helix A, is highly conserved among repeats of spectrin, dystrophin and α-actinin.

The tryptophan rod mutants used in this chapter displayed characteristic CD spectra and thermal denaturation profiles, indicating that the bulk of the expressed polypeptides had attained their native fold. As with the truncated fragments of the previous chapter, the conformational transitions of melting imply long-range cooperativity along the rod. As also observed for the truncated fragments described in the previous chapter, the thermal stabilities of both mutant fragments were lower than that of the WT rod domain. Interestingly, only the W->R mutation displayed a reduced resistance to proteolysis, suggesting that although both fragments have beeen destabilised, the W->I mutant has retained a protease-resistant conformation with sites susceptible from proteolytic attack shielded from the aqueous phase.

The cross-linking, sedimentation equilibrium and velocity, and EM data show that the mutant polypeptides possess dimer-forming ability, comparable to that observed for the intact rod-domain (repeats 1-4, previous chapter), in the concentration range explored. However, the urea dissociation profiles show a decreased stability for both the mutant fragments compared to the

WT rod. The decrease in thermal stability of the truncated fragments, as measured by CD, observed in the previous chapter could be due to a decreased ability to associate, or a reduction in the number of repeats. As the mutant polypeptides studied in this chapter contain the same number of repeats, and associate to essentially the same degree as the native rod, the decrease in thermal and urea stabilities reflect a conformational destabilisation, presumably soley due to the alteration in interhelical contacts mediated by the tryptophan.

This invariant tryptophan was reported to promote the conformational stability of a repeat of chicken brain α-spectrin (Macdonald *et al.*, 1994). Constructs used consisted of two adjacent but separately expressed repeats, R16 and R17, one of which (R17) contains a single tryptophan, a mutant, M17, in which the single tryptophan in R17 is substituted with alanine, and a conformationally unphased repeat, 1617, composed of half of each of the phased repeats. Both the mutant repeat and the unphased repeat were much more readily digested by chymotrypsin and by elastase than the phased repeats, and exhibited only 38% and 54% as much α-helical structure, respectively, as the phased repeats by their far UV CD spectra. If the tryptophan to alanine change in M17 is located in the middle of one of the three, major α-helical regions of the repeating unit, as is predicted by the crystal structure of *Drosophila* α14 (Yan *et al.*, 1993), alanine should stabilise the α-helix because it occurs frequently in the middle of α-helices (Richardson and Richardson, 1988; Blaber *et al.*, 1993) and has been found to stabilise α-helices of model (Padmanabhan *et al.*, 1990; Blaber *et al.*, 1993) and naturally occurring (Blaber *et al.*, 1993) peptides. Likewise, the six N-terminal amino acids and six C-terminal amino acids of 1617 are compatible with helix capping (Richardson and Richardson, 1988) and are unlikely to account for its possessing only 50% of the α-helical content of R16 or R17.

Light scattering measurements revealed the folded repeats to be predominantly monomeric in solution, whereas the unfolded, protease-sensitive repeats consisted of dimers and/or trimers. The shorter wavelength of the tryptophan's flourescence emission maximum compared with that of the conformationally unphased 1617 and that of the urea-denatured R17, and its resistance to quenching by acrylamide in comparison with 1617 and the other single-tryptophan repeats, indicated that the invariant tryptophan occupied a site that was shielded from the aqueous phase. The authors suggested that at this position, the tryptophan may engage in hydrophobic interactions necessary for conformational stability (MacDonald *et al.* 1994).

In the present study, expression of an analogous polypeptide consisting of a single α-actinin repeat containing a tryptophan mutation resulted in the protein being segregated to inclusion bodies. Although no quantitative structural information was obtained for this polypeptide, this drastic decrease in solubility, compared to native repeat, must reflect a significant change in conformation. Therefore, similar to the spectrin study (MacDonald *et al.*, 1994), mutation of

the invariant tryptophan in α-actinin was found to conformationally alter a single repeat, and in addition also to destabilise a polypeptide spanning the rod domain.

MacDonald *et al.* (1994) attributed the primary destabilising effect of the tryptophan to alanine mutation to the cavity created by substituting the small side chain of alanine in mutant M17 for the very large side chain of tryptophan in wild-type R17. Such a cavity would perturb the knob-hole arrangement of non-polar side chains proposed to stabilise the repeating unit of dystrophin (Cross *et al.*, 1990). The putative cavity could also induce some structural strain, as detected in leucine to alanine or phenylalanine to alanine mutants of T4 lysozyme (Eriksson *et al.*, 1992).

A similar explanation is possible in this study since the data shows that a relatively conservative substitution of this conserved apolar bulky tryptophan to a smaller apolar isoleucine results in the destabilisation of the α-actinin dimer and also to a conformational change in a single repeat. The fact that a more drastic substitution to a basic arginine results in a greater reduction in stability of the rod suggests that the charged side chain contributes to the destabilising effects. Interestingly, a more recent mutation of the nearly invariant tryptophan of repeat 16 of α-spectrin to phenylalanine or tyrosine yielded folded polypeptides, but the free energies of unfolding ($\Delta G(H_2O)$) were found to be half that of the wild-type. Similarly, mutation of the moderately conserved tryptophan in the same spectrin repeat (which occurs in position *a* of the third heptad, helix C; Figure 41) to a valine residue also reduced the $\Delta G(H_2O)$ by half (R. I. MacDonald and D. P. Pantazatos, priveliged communication). This suggests that the stability of a repeat depends on moderately conserved, as well as highly conserved, residues. However, since this moderately conserved tryptophan to valine spectrin mutant produced a folded polypeptide, whilst, in the present study, the invariant tryptophan to isoleucine α-actinin mutation resulted in an insoluble repeat, it suggests that the invariant tryptophan is more stringently required for repeat folding. This is probably to be expected as more conserved residues are likely to be more essential than than those that are less conserved. It would be interesting to see if the invariant tryptophan in spectrin was mutated to valine, whether a folded polypeptide would result, or alternatively, if the invariant tryptophan in α-actinin was mutated to tyrosine or phenylalanine, whether a soluble repeat would be produced. Since, in repeat 4 of *Dictyostelium* α-actinin, the invariant tryptophan is replaced by a tyrosine, it suggests that other aromatic residues can replace this tryptophan without drastically compromising the characteristics of the repeat. It would also be interesting to investigate whether a folded repeat could result if both tryptophans were replaced, as at least one may be a minimum requirement for successful folding.

Tetramers of spectrin form by association between the partial repetitive motifs found near the N-terminal region of the spectrin α chain and the C-terminal region of the β-chain (Tse *et al.*,

1990; Speicher *et al.*, 1993) (Figure 9). In all spectrins that have been sequenced, the partial repeat on the α-chain contains only those residues typical of a C helix, whereas the partial repeat on the β-chain contains residues typical of just the A and B helices. If the mode of association in tetramer formation corresponds to the packing seen in the crystallised fragment (helix C of one chain with helices A and B of the second chain) (Figure 10), the observed hydrophobic and ionic interactions should also be those that stabilise the corresponding association between α and β-chains in the tetramer. Hereditory elliptocytosis are subgroups of human hemolytic disorders associated with the defective association of erythroid spectrin heterodimers into tetramers (Palek, 1990). Different point mutations have been found to be responsible for the defect. One of those (Tse *et al.*, 1990), Ala to Pro in the incomplete terminal repeat of the β-chain, would be expected to disrupt the B helix and destabilise the three-helix bundle. Another (Coetzer *et al.*, 1991), Arg to Leu, Ser, Cys, or His in the partial N-terminal segment of the α-chains, could disrupt critical interactions with conserved residues in helices A and B of the β-chain. Thus these observations, along with the results of the spectrin repeat tryptophan mutations (MacDonald *et al.*, 1994; Pantazatos and MacDonald, priveliged communication) and the present α-actinin study, indicate that the triple-helical motifs of the spectrin-like repeats are very sensitive to mutation in a number of positions, and that a strict consensus does apply to achieve the inter-helical contacts needed to stabilise the helical bundles of each repeat.

In the crystal structure of *Drosophila* spectrin α14 (Yan *et al.*, 1993) and the NMR structure of chicken brain α16 (Pascual *et al.*, 1996), the invariant tryptophan (position *g* of the 2nd heptad in helix A) is shown to interact with a tryptophan (position *a* of the 3rd heptad in helix C) and with a histidine (position *d* of the 3rd heptad of helix B) (Figure 32). In chicken smooth muscle α-actinin repeat 1, the conserved tryptophan (also in position *g* of the 2nd heptad of helix A) would probably also interact with a tryptophan (position *a* of the 3rd heptad of helix C), but due to a longer helix B (by one heptad; private communication S. Winder), may interact with a proline residue (position *d* of the 4th heptad in helix B) found in the middle of a conserved motif (Figure 41). Occurrences of prolines within the helical regions will substantially alter the conformation of a specific repeat. The crystal structure of spectrin indicates that helix A was straight for the α14 repeat, but *Drosophila* α-spectrin contains a proline at position 23 of helix A in repeats 8 and 9, which may impart increased molecular flexibility to this region of the molecule. In comparison, human red cell α-spectrin contains six repeats with prolines in the middle of helix B and two motifs with prolines in the midlle of helix C, whereas *Drosophila* α-spectrin has a single occurrence of proline in the helix B region and no occurrences in helix C. Interestingly repeat 1 of all known α-actinins and the homologous repeat β1 in all spectrins, contain this conserved 5 residue motif in the middle of the predicted B helix, that has no homologues in the other α-actinin and spectrin repeats, and which always includes the sequence Lys-Pro-Pro (Figure 7). The two proline residues may either disrupt or distort the α-

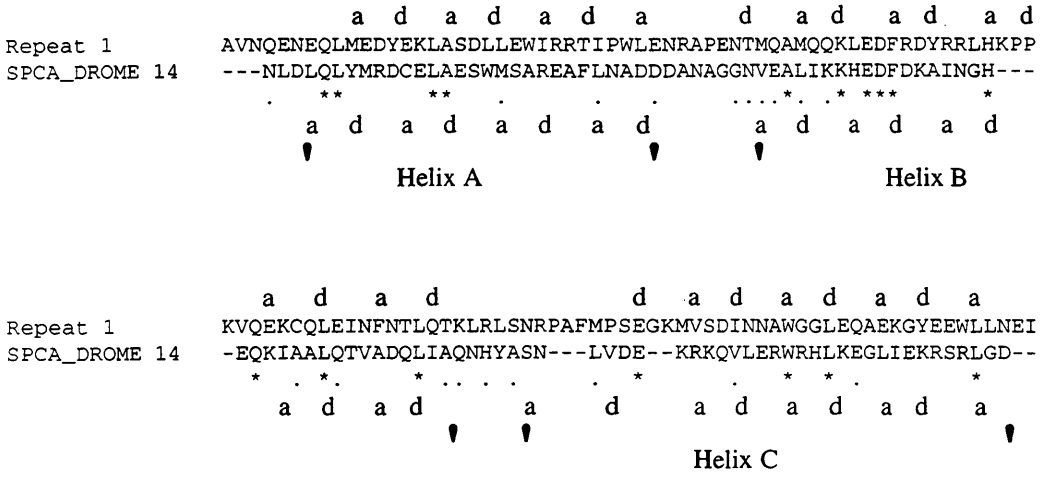

Figure 41: Sequence alignment of chicken smooth muscle α-actinin repeat 1 with *Drosophila* α-spectrin repeat 14. The predicted α-helices and heptad sequence for *Drosophila* repeat 14 are shown (Parry and Cohen, 1991), as are the predicted heptads for α-actinin repeat 1 (S. Winder, personal communication).

helix (Adzhubei and Sternberg, 1993), and clearly introduce a discontinuity of heptad repeats that must differentiate the interface between the three predicted helices of this repeat from that predicted for other α-actinin repeats (Parry and Cohen, 1991; Parry *et al.*, 1992) and that known for *Drosophila* spectrin α14 (Yan *et al.*, 1993) and chicken brain spectrin α16 (Pascual *et al.*, 1996). Such discontinuities have been described as a specific feature of protein domains capable of dynamic coiled-coil interaction (Oas and Endow, 1994), and the di-proline motif, by itself, may be involved in protein-protein interactions (Williamson, 1994). Thus, the association between the two α-actinin subunits may result from a dynamic reorganisation of the coiled-coils in each of the participating segments.

The conserved tryptophan occupies position *g* in the heptad, usually frequented by a hydrophilic residue. For both parallel and antiparallel two-stranded coiled-coils, the residues likely to be involved in interhelix ionic interactions have been specified by McLachlan and Stewart (1975) to be those in the *e* and *g* positions in the heptad, and it has been established that the specificity of the packing of the chains in two-stranded parallel coiled-coils lies with the inter-helix ionic interactions primarily involving residues in the *e* and *g* positions (Conway and Parry, 1990; Cohen and Parry, 1990). Interestingly, the *g* position of helix A in spectrin is predominantly highly acidic, whilst in α-actinin is predominantly basic (Parry *et al.*, 1992). The data in this study shows that the substitution of this apolar bulky tryptophan to a smaller apolar isoleucine results in destabilisation of the dimer and also to a conformational change in a single repeat, and that a more drastic substitution to a basic arginine results in an even greater loss of stability of the rod. This suggests that the mutations do alter optimal knob-hole packing

of the apolar residues, generally occupying *a* and *d* positions (Cohen and Parry, 1986, 1990), by perturbing arrangements of side chains by size and also by charge.

It would be interesting to further investigate these tryptophans in the rod domain of α-actinin, and also in single repeats, by selecting alternative residues as replacement for the conserved tryptophan. This approach could be combined with investigation of the moderately conserved tryptophan, in an endevour to characterise the variations in stringency that are likely to exist with regards to maintenance of native fold and stability.

CHAPTER 5.

FURTHER ANALYSIS OF SUBUNIT INTERACTIONS AND THE ROLE OF 8-RESIDUE INSERTS

5.1 INTRODUCTION

As described in chapter 3, spectrin heterodimer assembly is initiated at a single region of each subunit. This nucleation site includes, but is not limited to, several repeat units that are the most homologous to α-actinin, viz repeats 20 and 21 of the spectrin α-chain and 2 and 3 of the spectrin β-chain, as originally observed by Byers, Dubreil, Branton and coworkers (Dubreil *et al.*, 1989; Byers *et al.*, 1989). A schematic arrangement of the α-actinin molecule and the most homologous spectrin repeats would suggest that the two lateral spectrin pairs, β1-α21 and β2-α20, are responsible for dimer assembly. α-Actinin has two of these unique pairs, and hence the interaction between the subunits would be predicted to be much stronger (Figure 8). Since the isolated α-actinin rod domain exists in solution as a highly stable dimer (Imamura *et al.*, 1988; Kahana and Gratzer, 1991), and defined complementary repeats of the erythroid spectrin α and β-chains also form a stable 1:1 complex (Speicher *et al.*, 1992), it is implied that the structural repeating elements interact specifically by pairs along the rod. Thus in the case of the α-actinin rod, which consists of four repeats, the antiparallel dimer should be stabilised by interactions between repeats 1 and 4 and between 2 and 3. The data from chapter 3 strongly suggests that this aligned model is correct.

In most spectrin repeats, the segment length of 106 residues is very precisely preserved and only a few repeats have insertions or deletions. However, sequence analysis of both *Drosophila* (Dubreil *et al.*, 1989; Byers *et al.*, 1992) and human erythrocyte (Sahr *et al.*, 1990; Winkelmann *et al.*, 1990) spectrins suggested that repeats β2 and α20 and 21 are 8-residues longer than the other motifs, the inserts occurring at the N-terminal region of the repeats (Figure 42). These 8-residue insertions might confer unique, conformational properties upon the nucleation sites which are responsible for the specific initial association (Speicher *et al.*, 1992).

Recently, mapping of the interchain binding at the N- and C-terminal regions of *Drosophila* β- and α-spectrin respectively (Viel and Branton, 1994), using a radioactive immunoprecipitation assay, has revealed that repeats 20 and 21 of the α-chain and 1 and 2 of the β-chain are essential for tail end interchain binding. Although conformation of the peptides used were not assessed, it was also found in this study that the 8-residue inserts of β2 and α21, but not of α20, were also required for heterodimer formation. Interestingly, whilst deletion or duplication of these 8-residue inserts abolished binding, point mutations within the conserved inserts did not.

Mapping experiments in human erythrocyte β-spectrin (Ursitti *et al.*, 1996), using conformational assessment of peptides and a HPLC gel filtration assay, revealed that repeat β1 was essential for dimerisation, and that the minimum dimer assembly site consisted of

Repeat 1 (β1)

```
SPCB_HUMAN 295  DHAIETEKMIEKYSGLASDLLTWIEQTITVLNSRKFANSLTGVQQQLQAFSTYRTVEKPP
SPCB_DROME 291  GIAMENDKMVHDYENFTSDLLKWIETTIQSLGEREFENSLAGVQGQLAQFSNYRTIEKPP
AAC1_HUMAN 267  AVNQENEQLMEDYEKLASDLLEWIRRTIPWLENRVPENTMHAMQQKLEDFRDYRRLHKPP
SP14_DROME 1392 --NLDLQLYMRD-CELAES---WMSAREAFLNADDDANAGGNVEALIKKHEDFDKAINGH
                    .   .     .    *.     *     *.   ..  .     .

SPCB_HUMAN 355  KFQEKGNLEVLLFTIQSRMRANNQKVYTPHDGKLVSDINRAWESLEEAGYRRELALRN
SPCB_DROME 351  KFVEKGNLEVLLFTLQSKMRANNQKPYTPKEGKMISDINKAWERLEKAEHERELALRE
AAC1_HUMAN 327  KVQEKCQLEINFNTLQTKLRLSNRPAFMPSEGRMVSDINNAWGCLEQVEKGYEEWLLN
SP14_DROME 1447 E-QKIAALQ----TVADQLIAQNHYASNLVD-EKRKQVLERWRHLKEGLIEKRSRLGD
                      *.    *.  ..   *.      .      .   *  *          *

Repeat 2 (β2)
SPCB_HUMAN 413  ELIRQEKLEQLARRFDRKAAMRETWLNENQRLVAQ-DNFGYDLAAVEAAKKKHEAIETDT
SPCB_DROME 409  ELIRQEKLEQLAARFDRKASMRETWLSENQRLVSQ-DNFGFDLAAVEAAAKKHEAIETDI
AAC1_HUMAN 385  EIRRLERLDHLAEKFRQKASIHEAWTDGKEAMLRQKDYETATLSEIKALLKKHEAFESDL
SP14_DROME 1392 --------NLDLQLYMRDCELAESWMSAREAFLNA-DDDANAGGNVEALIKKHEDFDKAI
                        . . . . *.*    .  .   *        . *  ****  .

SPCB_HUMAN 473  AAYEERVRALEDLAQELEKENYHDQKRITARKDNILRLWSYLQELLQSRRQRLET
SPCB_DROME 469  FAYEERVQAVVAVCDELESERYHDVKRILLRKDNVMRLWTYLLELLRARRMRLEI
AAC1_HUMAN 445  AAHQDRVEQIAAIAQELNELDYYDSPSVNARCQKICDQWDNLGALTQKRREALER
SP14_DROME 1444 NGHEQKIAALQTVADQLIAQNHYASNLVDEKRKQVLERWRHLKEGLIEKRSRLGD
                   . ..  .  .. .*          .  .   .  *  *      .*  *

Repeat 3 (α20)

SPCA_HUMAN 2033 KQLPLQKAEDLFVEFAHKASALNNWCEKMEENLSEPVHCVSLNEIRQLQKDHEDFLAS
SPCA_DROME 2030 MQEQFRQIEELYLTFAKKASAFNSWFENAEEDLTDPVRCNSIEEIRALRDAHAQFQAS
AAC1_HUMAN 500  TEKLLETIDQLYLEYAKRAAPFNNWMEGAMEDLQDTFIVHTIEEIQGLTTAHEQFKAT
SP14_DROME 1392 --------NLDLQLYMRDCELAESWMSAREAFLNADDDANAGGNVEALIKKHEDFDKA
                        . . .     *       *       .   .  *   *  *  .

SPCA_HUMAN 2091 LARAQADFKCLLELDQQIKALG-------VPSSPYTWLTVEVLERTWKHLSD-IIEEREQ
SPCA_DROME 2089 LSSAEADFKALAALDQKIKSFN-------VGPNPYTWFTMEALEETWRNLQK-IIEERDG
AAC1_HUMAN 558  LPDADKERLAILGIHNEVSKIVQTYHVNMAGTNPYTTITPQEINGKWDHVRQ-LVPRRDQ
SP14_DROME 1443 INGHEQKIAALQTVADQLIAQN------HYASNLVDEKRKQVLER-WRHLKEGLIEKRSR
                .        ..  .   .                        . .   * ..   ..  *

SPCA_HUMAN 2143 ELQ
SPCA_DROME 2140 ELA
AAC1_HUMAN 617  ALT
SP14_DROME 1496 LGD

Repeat 4 (α21)

SPCA_HUMAN 2146 KEEARQVKNFEMCQEFEQNASTFLQWILETRAYFLDGSLLKETGTLESQLEANKRKQKEI
SPCA_DROME 2143 KEAKRQEENDKLRKEFAKHANLFHQWLTETRTSMMEG-----SGSLEQQLEALRVKATEV
AAC1_HUMAN 620  EEHARQQHNESVRKQFGAQANVIGPWIQTKMEEIGRIS-IEMHGTLEDQLSHLRQYEKSI
SP14_DROME 1392 --------NLDL-QLYMRDCELAESWMSAREAFLNADDDANAGGNVEALIKKHEDFDKAI
                      *  . . .   .     *.                 * .*  .        .

SPCA_HUMAN 2206 QAMKRQLTKIVDLGDNLEDALILDIKY---STIGLAQQWDQLYQLGLRMQHNLEQQIQAK
SPCA_DROME 2198 RARRVDLKKIEELGALLEEHLILDNRYTEHSTVGLAQQWDQLDQLSMRMQHNLEQQIQAR
AAC1_HUMAN 679  VNYKPKIDQLEGDHQLIQEALIFDNKHTNYTMEHIRVGWEQLLTTIARTINEVENQILTR
SP14_DROME 1444 NGHEQKIAAL----QTVADQLIAQNHY---ASNLVDEKRKQVLE---RWRHLKEGLIEKR
                      . .      . . **   .    .   .     *.     *  .  *  *  .

SPCA_HUMAN 2263 DIKGV
SPCA_DROME 2258 NHSGV
AAC1_HUMAN 739  DAKGI
SP14_DROME 1494 SRLGD
                   *
```

Figure 42: Sequence alignment of *Drosophila* spectrin α14 (SP14_DROME) with human α-actinin repeats 1-4, and human and *Drosophila* spectrin repeats β1-2 and α20-21 using Clustal V. Human erythroid β-spectrin (SPCB_HUMAN), *Drosophila* β-spectrin (SPCB_DROME), human placental α-actinin (AAC1_HUMAN), human erythroid α-spectrin (SPCA_HUMAN), *Drosophila* α-spectrin (SPCA_DROME). 8-residue inserts shown to be involved in human erythroid (Ursitti *et al.*, 1996) and in *Drosophila* (Viel and Branton, 1994) spectrin dimer formation are in bold and are underlined, whilst those predicted to be involved in spectrin dimer formation are in bold (Ursitti *et al.*, 1996).

repeats 1 and 2. From sequence alignment, Ursitti *et al.* (1996) suggested that repeats β1 of spectrin and repeat 1 of α-actinin, contain 8-residue inserts in their N-terminal regions, and it was demonstrated that deletion of these 8-residues from the spectrin β1 repeat resulted in a nearly 10-fold reduction in binding of a polypeptide containing repeats β1-4 to the complementary subunit.

It has been shown that various isoforms of α-actinin (Bennet *et al.*, 1984; Duhaiman and Bamburg, 1984; Landon *et al.*, 1985), and spectrin (Fowler and Taylor, 1980; Fishkind *et al.*, 1987), are calcium sensitive with respect to actin-binding, due supposedly to interaction between the EF-hands and the ABD (Blanchard *et al.*, 1989; Fishkind *et al.*, 1987) which are thought to be arranged in close proximity in the antiparallel dimer. Calcium sensitivity has been investigated using *Dictyostelium* α-actinin, where mutation of EF-2 resulted in 500-fold more calcium being necessary for inhibition of actin-binding (Witke *et al.*, 1993). This inhibition of binding could be due to a non-specific steric effect (i.e. a physical blocking of the actin-binding sites by the EF-hands), or to a specific interaction between the EF-hands and the ABD. In favour of the latter, it has been demonstrated that utrophin ABD is regulated by calmodulin in a calcium-dependent manner (Winder and Kendrick-Jones, 1995), whilst from sequence alignment it has been shown that EF-hands are calmodulin-like (Trave *et al.*, 1995). Interestingly, it has also been demonstrated that the adjacent EF-hand region on the spectrin α-subunit and the adjacent ABD on the β subunit are also involved in assembly of *Drosophila* spectrin (Viel and Branton, 1994).

To further characterise the subunit interactions between the α-actinin subunits, the following studies were performed:

(A) To further examine subunit interactions of the α-actinin rod, with respect to the aligned or staggered models, single repeats were expressed, and their ability to associate investigated, to locate more precisely the region(s) of α-actinin responsible for dimer formation.

(B) To investigate the role of the 8-residue inserts in α-actinin dimer formation, a mutant of the rod domain of α-actinin lacking the predicted 8-residue insert from the N-terminal region of repeat 1 was expressed, based upon the results of Ursitti *et al.* (1996). Assessment of conformation was followed by investigation of dimer formation.

(C) To further investigate the function of 8-residue inserts, individual repeats lacking predicted 8-residue insertions, were expressed and their abilities to fold and associate investigated.

(D) To investigate if the C-terminal EF-hands and N-terminal ABD are involved in the subunit interaction of α-actinin, these fragments were expressed and their ability to associate evaluated by sedimentation equilibrium.

5.2 RESULTS

(A) SINGLE REPEATS OF α-ACTININ

5.2.1 Expression and purification of α-actinin polypeptides

The proteins used consisted of chicken smooth muscle α-actinin repeat 1 (residues 267-387), repeat 2 (residues 385-499), repeat 3 (residues 497-631), and repeat 4 (residues 614-749), which have previously been shown to constitute stable, folded fragments by the criteria of resistance to proteolysis and high α-helicity (Gilmore *et al.,* 1994). The chicken smooth muscle cDNAs encoding the repeats were generated by amplifying regions of full-length chicken α-actinin cDNA C17 (Baron *et al.*, 1987) by PCR. The proteins were expressed in *E. coli* as soluble GST-fusion proteins and purified on glutathione-agarose beads. Successful purification was determined by SDS-PAGE and molecular weights of the purified polypeptides corresponded with predicted sizes of 40, 39, 42, and 42 kDa respectively. These were then liberated from GST by proteolytic cleavage with factor Xa (repeat 1) or thrombin (repeats 2, 3, and 4). The isolated proteins were shown to be relatively pure by SDS-PAGE, although doublet formation was observable on occasion, and observed bands again corresponded with the predicted molecular weights of 14.5, 13.5, 16.0, and 16.0 kDa respectively (Figure 43; collaboration W. Gratzer, King's College London). Yields were determined spectrophotometrically, using calculated absorption coefficients of 1.88, 1.18, 1.08, and 0.97 cm^{-1} (for 1 mg ml^{-1}).

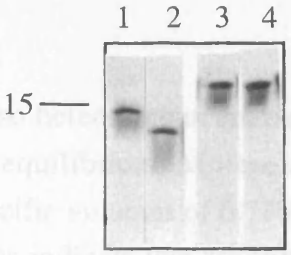

Figure 43: Purity of expressed repeat α-actinin repeat polypeptides, repeats 1, 2. 3, and 4, as assessed by SDS-PAGE. Fragments shown display a smearing below the protein band which may be due to slight degradation. Molecular mass standards (kDa) are shown.

Table VII: Association of expressed individual repeats measured by sedimentation equilibrium.

	Repeat 1	Repeat 2	Repeat 3	Repeat 4
Repeat 1 (14.5 kDa)	19.5 kDa	14.5 kDa	22.5 kDa	29.5 kDa
Repeat 2 (13.5 kDa)		16.5 kDa	20.5 kDa	19.0 kDa
Repeat 3 (16.0 kDa)			20.0 kDa	22.5 kDa
Repeat 4 (16.0 kDa)				22.5 kDa

Predicted molecular weights for each repeat are indicated on the left, and measured apparent weight-average molecular weights are shown for the individual repeats and for molar 1:1 combinations of mixtures.

Table VIII: Association of repeat 1 and repeat 4, as measured by sedimentation velocity.

	$s_{20,w}$
Repeat 1	1.80 S
Repeat 4	1.88 S
Repeat 1+Repeat 4	2.25 S

5.2.2 Sedimentation equilibrium

Analysis of self-association and also heterologous interaction of the expressed polypeptides was performed by sedimentation equilibrium. Molecular weights were determined using calculated values for the partial specific volumes of 0.730, 0.728, 0.731, and 0.728 ml g^{-1} for repeats 1-4 respectively. The results indicate that all polypeptides existed predominantly as monomers, as calculated from weight-average molecular weights (Table VII), with varying degrees of self-association. Self-association constants calculated from the observed weight-average molecular weights were 29, 6, 7, and 21 x 10^3 M^{-1} for repeats 1 to 4 respectively. Upon mixing combinations of individual repeats in a 1:1 molar ratio, only repeats R1 and R4 interacted to any large extent. This result was obtained twice using different samples. The pattern of residuals, as with previous constructs, displayed a random scatter of points around zero indicating a satisfactory fit to the proposed model. Although accurate calculation of an heterologous association constant is difficult, an association constant of approximately 10^7 M^{-1} can be estimated by assuming the mixture to consist of a single component, i.e. a self-association constant, as both species are similar in molar mass.

5.2.3 Sedimentation velocity

In an effort to confirm the sedimentation equilibrium results, which indicated an interaction between α-actinin repeats 1 and 4, sedimentation velocity was performed on individual R1, R4, and a 1:1 molar mixture of the two polypeptides, at concentrations of approximately 15 μM. The observed sedimentation coefficients were corrected to standard conditions of water at 20 °C (Table VIII). Upon mixing samples of R1 and R4, an increase in s value was observed, as compared to those obtained for the individual repeats. That the differences in sedimentation coefficient for the single repeats as compared to the mixture is smaller than might be expected, is taken to be a consequence of the self-association of the individual repeats, as seen by sedimentation equilibrium. Therefore, this result confirmed the equilibrium study suggesting an interaction between α-actinin repeats 1 and 4.

(B) CHARACTERISATION OF A ROD DOMAIN MUTANT CONTAINING AN 8-RESIDUE DELETION FROM REPEAT 1

5.2.4 Expression and purification of α-actinin polypeptide

The protein used consisted of the chicken smooth muscle α-actinin rod domain (residues 267-749) containing an 8-residue deletion from the N-terminal region of repeat 1 (Figure 42; Δ271-278). The chicken smooth muscle cDNAs encoding the polypeptide was generated by

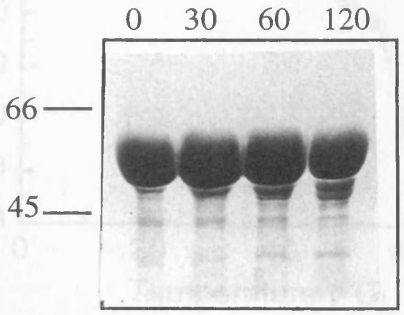

Figure 44: Protease-resistance of the expressed α-actinin repeat domain fragment WT (-Δ8) (267-749). The purifed polypeptide was exposed to trypsin (enzyme to substrate ratio 1:1000) for the time shown (mins). The position of molecular mass standards (kDa) are shown.

Table IX: Investigation of the conformation and dimer-forming ability of the expressed α-actinin polypeptide WT (-Δ8) (267-749) by circular dichroism and sedimentation equilibrium, respectively.

	Molar residue ellipticity (° cm^2 $dmol^{-1}$) at 222 nm	% α-helix	Concentration (mg ml^{-1})	% dimer
WT (-Δ8)	-23900	67	0.49	98
			0.30	93
			0.08	100

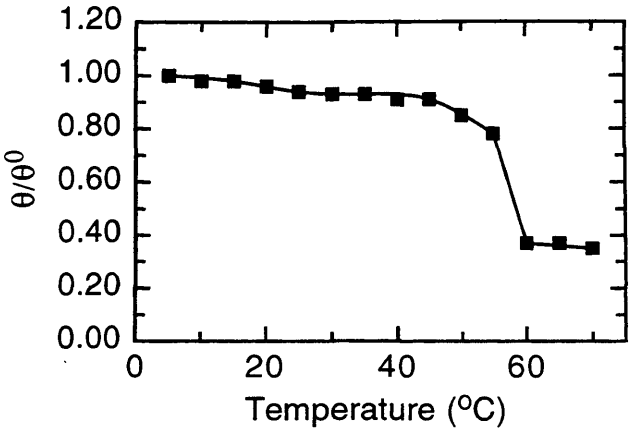

Figure 45: Thermal denaturation profile of expressed α-actinin rod fragment WT (-Δ8) determined by circular dichroism. Unfolding is measured by the ellipticity at 222 nm relative to that at 5 °C.

amplifying the region of full-length chicken α-actinin cDNA C17 (Baron *et al.*, 1987) by PCR. Mutagenesis was performed by Lance Hemmings. The protein was expressed in *E. coli* as a soluble GST-fusion protein and purified on glutathione-agarose beads. Successful purification was determined by SDS-PAGE and the observed band corresponded with the expected size of 82 kDa. This was then liberated from GST by proteolytic cleavage with thrombin. The isolated protein was shown to be >90% pure by SDS-PAGE, and the observed band again corresponded with the predicted molecular weight of 56 kDa (Figure 44). Yield was determined spectrophotometrically, by using a calculated absorption coefficient of 1.36 cm^{-1} (for 1 mg ml^{-1}).

5.2.5 Circular dichroism

To verify native secondary structure, circular dichroism measurements were performed at 20 °C. This showed the mutant protein had a similar CD spectra to that of native rod (66% helix) (chapter 3), with a high α-helical content (67% helix; Table IX), suggesting that the polypeptide had folded correctly.

5.2.6 Resistance to proteolysis

Resistance to proteolysis is also an indication of native secondary structure. Incubation of the deletion mutant with trypsin, for up to 2 hrs, demonstrated a similar resistance to proteolysis to that of the native rod (chapter 3), displaying a slight accumulation of smaller molecular weight species. This again indicates no significant change in folded conformation (Figure 44).

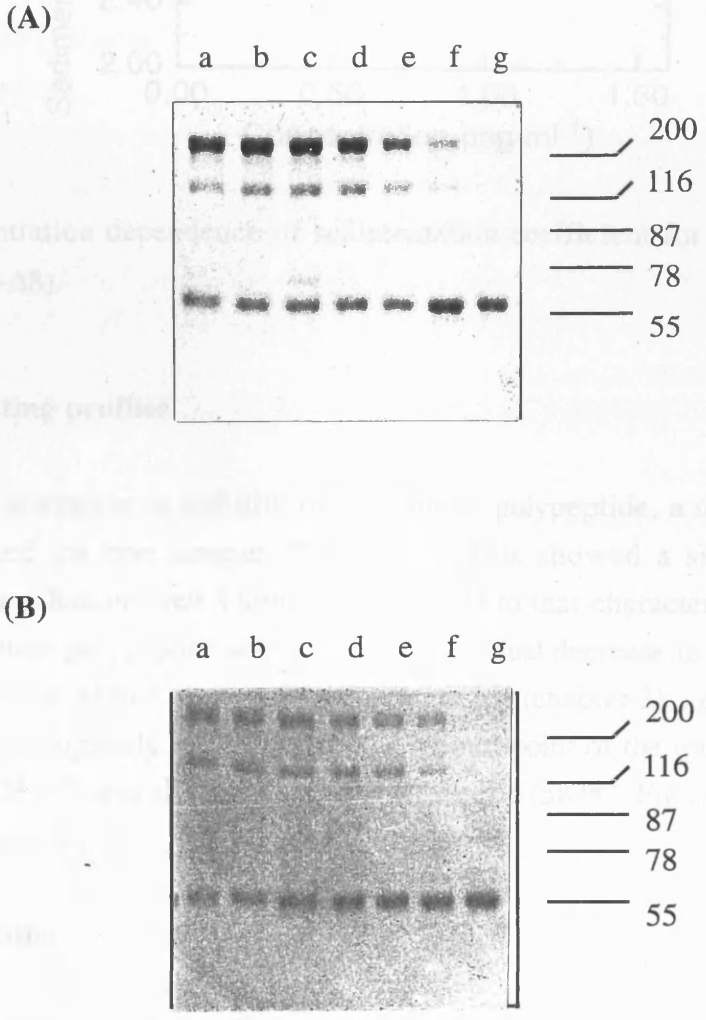

Figure 46: Urea dissociation profiles of expressed α-actinin polypeptides (267-749). **(A)** repeats 1-4 and **(B)** repeats 1-4 (-Δ8) mutant. Lanes show protein exposed to DMS in presence of (a) 0.39 M, (b) 0.77 M, (c) 1.54 M, (d) 2.31 M, (e) 3.08 M, (f) 3.85, (g) 4.62 M urea. The positions of molecular mass standards (kDa) are shown.

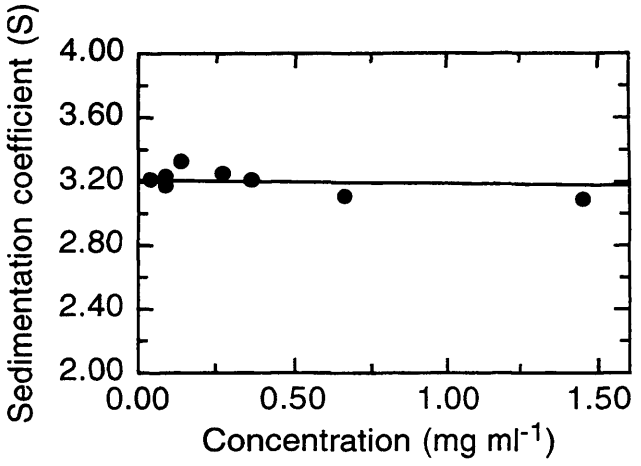

Figure 47: Concentration dependence of sedimentation coefficient for expressed α-actinin rod fragment WT (-Δ8).

5.2.7 Thermal melting profiles

To investigate any alteration in stability of the mutant polypeptide, a thermal denaturation profile was obtained for one sample (Figure 45). This showed a sigmoidal transition, suggesting the mutant had entered a similar native fold to that characteristic of the WT rod (chapter 3). The mutant polypeptide also displayed a gradual decrease in ellipticity above the transition region, similar to that observed for fragment 1-4 (chapter 3), again presumably due to the presence of incompletely folded material. The mid-point of the transition temperature, T_m, of the mutant (58 °C) was also similar to the native rod (58 °C; Figure 26), suggesting no change in thermal stability.

5.2.8 Urea dissociation

The stability of the mutant polypeptide dimer, under denaturing conditions, was investigated by chemical cross-linking with DMS in the presence of increasing urea concentration (Figure 46; collaboration W. Gratzer, King's College London). It can be seen that with the mutant fragment, dissociation into monomers has occurred by 4.6 M urea, similar to that observed for the native rod (267-749) (lane g), indicating no detectable decrease in dimer stability.

5.2.9 Sedimentation equilibrium

Analysis of self-association of the expressed mutant polypeptide was performed by sedimentation equilibrium. Molecular weights were determined using calculated values for the partial specific volume of 0.731 ml g^{-1}. The results indicated that the protein existed predominantly, or entirely, as dimer, as calculated from weight-average molecular weights

(Table IX). The pattern of residuals, as with fragment 1-4 (chapter 3), displayed a random scatter of points around zero indicating a satisfactory fit to the proposed model. There was no obvious concentration-dependent behaviour for values of the molecular mass indicating that there was no association-dissociation equilibrium within the concentration range explored, and a negligible concentration-dependence arising from the second virial coefficient would be expected for this mutant, again similar to fragment 1-4.

5.2.10 Sedimentation velocity

Sedimentation velocity was performed on the expressed polypeptide to investigate size and conformation, and sedimentation coefficients were obtained as a function of concentration (Figure 47). The mutant polypeptide displayed a slight decrease for values of s with increasing concentration, similar to the native rod (chapter 3), indicative of non-associating systems. The plot displayed is based on a theoretical value of k_s, calculated from equation 2 (chapter 3, 3.2.6), which represents the concentration-dependence of the sedimentation coefficient. The experimental results do not differ significantly from this. The extrapolated value of $s^0_{20,w}$, corrected to standard conditions of water at 20 °C, was 5.09 S, comparable to that obtained for repeats 1-4 (5.06 S), indicating the mutant existed in a size and conformation characteristic of rod-shaped dimers.

5.2.11 Electron microscopy

Rotary shadowing with platinum and visualisation by TEM showed the polypeptide to be predominantly rod-like, consisting of two laterally associated subunits (Figure 48). Measured mean lengths of the mutant particle was 20.25 (± 2.2) nm (N=20; ± standard deviation of mean), in good agreement with native rod (Figure 31; chapter 3). As with other polypeptides investigated, some heterogeneity was observable in the electron micrograph.

(C) CHARACTERISATION OF REPEATS 1 AND 4 CONTAINING 8-RESIDUE DELETIONS

Investigation of a construct spanning repeats 1-4 of the α-actinin rod domain (267-749), containing an 8-residue deletion from the N-terminal region of repeat 1, resulted in no detectable decrease in stability or dimer forming ability, compared to the native rod domain.

Due to the finding of an interaction between repeats 1 and 4, by sedimentation equilibrium and velocity, these repeats were expressed, each containing an 8-residue deletion from their N-terminus, based on the alignment of Ursitti *et al.* (1996) (Figure 42). The chicken smooth

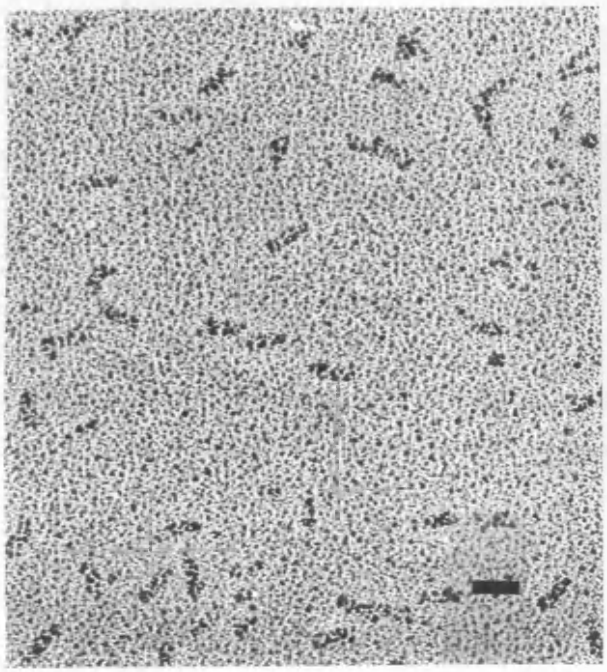

Figure 48: Electron micrograph of rotary platinum shadowed α-actinin fragment WT (-Δ8). Bar represents 20 nm.

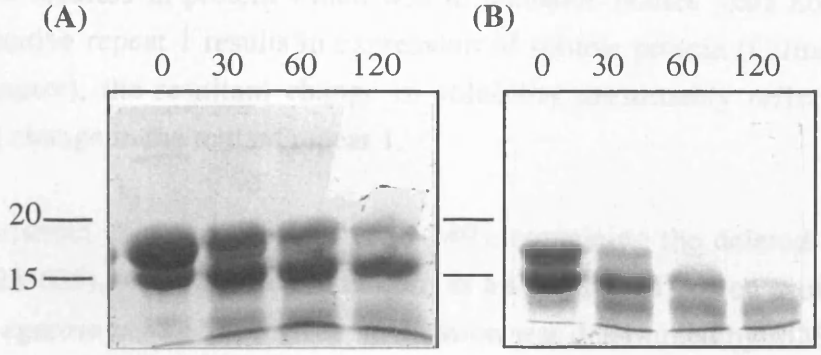

Figure 49: Protease resistance of the expressed α-actinin repeat 4 polypeptides. Purified proteins were exposed to trypsin (enzyme to substrate ratio 1:1000) for the times shown (mins). Repeat 4 **(A)** and 4 (-Δ8) **(B)**. The position of molecular mass standards (kDa) is indicated.

Table X: Analysis of the association of repeat 1 with repeat 4 (-Δ8) by sedimentation equilibrium.

	Repeat 1	Repeat 4 (-Δ8)
Repeat 1 (14.5 kDa)	17.5 kDa	16.0 kDa
Repeat 4 (-Δ8) (15.0 kDa)		15.0 kDa

muscle cDNAs encoding the polypeptides were generated by PCR, and the mutagenesis was performed by Dr Lance Hemmings.

5.2.12 Expression and purification of α-actinin polypeptides

Expression of the GST construct encoding repeat 1 (residues 267-385) containing the 8-residue deletion resulted in protein which was in inclusion bodies (data not shown). Since expression of native repeat 1 results in expression of soluble protein (Gilmore *et al.*, 1994; results this chapter), the resultant change in solubility presumably reflects a significant conformational change in the mutant repeat 1.

The protein construct spanning repeat 4 (614-749), containing the deleted 8-residue insert (Figure 42; Δ628-635), was expressed in *E. coli* as a soluble GST-fusion protein and purified on glutathione-agarose beads. Successful purification was determined by SDS-PAGE and the observed band corresponded with the expected size of 41 kDa. This was then liberated from GST by proteolytic cleavage with thrombin. The isolated protein was shown to be relatively pure by SDS-PAGE, although as seen previously the polypeptide migrated as a doublet. The observed band again corresponded with the predicted molecular weight of 15 kDa (Figure 49). It can be seen for the wild-type repeat 4 that the upper band of the doublet is more prominent than the lower, whilst for the mutant polypeptide the opposite is seen (Figure 49). Interestingly, Gilmore *et al.* (1994) also observed that repeat 4 was the least stable of the expressed α-actinin repeats. Yield was determined spectrophotometrically, using a calculated absorption coefficients of 1.04 cm^{-1} (for 1 mg ml^{-1}).

5.2.13 Circular dichroism

To verify native secondary structure, circular dichroism measurements were performed on one sample at 20 °C. This showed that the mutant protein had a similar CD spectra to that of native repeat 4 (66% helix), characteristic of high α-helical content (60% helix). However, the molar residue ellipticity of the mutant at 222 nm was lower than that of native repeat 4, -21600 compared with -23800 ° cm^2 $dmol^{-1}$.

5.2.14 Resistance to proteolysis

Resistance to proteolysis is also a verification of native secondary structure. Incubation of the mutant polypeptide with trypsin, for up to 2 hours, demonstrated a reduced resistance to proteolysis to that of native repeat 4 (Figure 49), indicating a change in stability had occurred with this deletion.

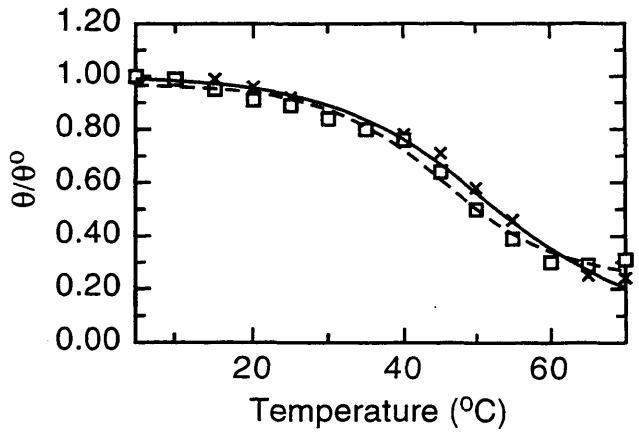

Figure 50: Thermal denaturation profiles of expressed α-actinin repeat 4 fragments, determined by circular dichroism. Unfolding is measured by the ellipticity at 222 nm relative to that at 5 °C. Repeat 4 (x, ---) and 4 (-Δ8) (□, ····).

5.2.15 Thermal melting profiles

To investigate the apparent decrease in stability of the mutant polypeptide, thermal denaturation profiles were obtained on single samples (Figure 50). Both the mutant polypeptide and native repeat 4 showed sigmoidal transitions, suggesting the mutant had entered a similar native fold. However, the mid-point of the transition temperature, T_m, of the mutant showed an approximate 3° decrease to that of native repeat 4, indicating a decrease in thermal stability. Although this experiment was performed only on one sample batch, hence the result may not be greatly significant, it does agree well with the previous observations of a decreased stability with this particular deletion.

5.2.16 Sedimentation equilibrium

Analysis of self-association and also the interaction of the expressed mutant repeat 4 polypeptide with native repeat 1 was performed by sedimentation equilibrium. Molecular weights were determined using a calculated value for the partial specific volumes of 0.729 ml g^{-1}. The results indicated that the mutant protein existed predominantly as a monomer, as calculated from weight-average molecular weight (Table X). Upon mixing with native repeat 1, in a 1:1 molar ratio, performed on one occasion, no increase in molecular weight was observed. The pattern of residuals, as with previous constructs, displayed a random scatter of points around zero indicating a satisfactory fit to the proposed model. This suggests that deletion of the 8-residue insert in repeat 4 does affect the previously shown dimer formation between repeats 1 and 4.

(D) EF-HANDS AND ABD

5.2.17 Expression and purification of α-actinin polypeptides

The proteins used consisted of constructs spanning chicken smooth muscle α-actinin EF-hands (713-888) and ABD (1-269), and also chicken brain α-actinin EF-hands (713-893). The EF-hands cDNAs encoding the polypeptides were generated by David Millake and cloned into the non-cleavable pGEX-1 vector, and the ABD cDNA was generated by Alastair McGregor and cloned into pGEX-2T. These polypeptides were expressed in *E. coli* as soluble GST-fusion proteins and purified on glutathione-agarose beads. Successful purification was determined by SDS-PAGE and the observed bands corresponded with the expected sizes of 46 kDa for the EF-hands and 57 kDa for the ABD (Figure 51). The α-actinin EF-hand fusion proteins were eluted off the beads with an excess of glutathione, and purifed in a Microcon spin purifier. The ABD was liberated from GST by proteolytic cleavage with thrombin. The isolated protein was shown to be >90% pure by SDS-PAGE, and the observed band again corresponded with the predicted molecular weight of 31 kDa. Yields were determined spectrophotometrically, using calculated absorption coefficients of 1.19, 1.20 and 1.49 cm^{-1} (for 1 mg ml^{-1}) for smooth muscle EF-hands, brain EF-hands, and ABD respectively.

5.2.18 Sedimentation equilibrium

Analysis of self-association and also heterologous interaction of the expressed polypeptides was performed by sedimentation equilibrium. Molecular weights were determined using calculated values for the partial specific volumes of 0.736 and 0.740 ml g^{-1} for the EF-hands and ABD respectively. The results indicated that the muscle EF-hands and ABD polypeptide existed predominantly as monomers, as calculated from weight-average molecular weights (Table XI), whilst non-muscle EF-hands were dimeric. Upon mixing, of muscle EF-hands and ABD, in a 1:1 molar ratio, no increase in molecular weight was observed. The pattern of residuals, as with previous constructs, displayed a random scatter of points around zero indicating a satisfactory fit to the proposed model.

5.3 DISCUSSION

Chapter 3 described different models of α-actinin homodimer formation. These consisted of staggered (Taylor and Taylor, 1993) or aligned arrangements of repeats in the interacting subunits. The data presented in that chapter was most easily reconciled with an aligned model. To further investigate these observations, and to ascertain if individual repeats were responsible for dimer formation, sedimentation equilibrium was performed on the expressed

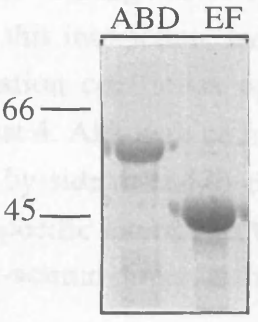

Figure 51: SDS gel showing successful expression and purification of α-actinin EF-hands and ABD polypeptides. The position of molecular mass standards (kDa) is indicated.

Table XI: Analysis of the association of expressed α-actinin ABD with muscle and non-muscle (NM) α-actinin EF-hands by sedimentation equilibrium.

	EF-hands	ABD
EF-hands (Muscle) (45.5 kDa)	47.5 kDa	41.5 kDa
ABD (30.5 kDa)		33.5 kDa
EF-hands (NM) (46.0 kDa)	97.0 kDa	

Predicted molecular weights are shown on the left, and observed apparent weight-averaged molecular weights are indicated for the individual polypeptides and for a molar 1:1 mixture of muscle α-actinin EF-hands and ABD.

individual repeats. The results demonstrated that the individual repeats self-associated ($K_a \sim 10^4$ M^{-1}), but that no significant hetero-interactions occured except for the repeat 1-repeat 4 mixture. An association constant of 10^7 M^{-1} was estimated for this interaction, which is significantly weaker than than estimated for the rod domain of α-actinin (Kahana and Gratzer, 1991). This is to be expected as a high level of cooperativity is observed when all four repeats are present. To confirm this interaction, sedimentation velocity was performed. The increase observed in sedimentation coefficient upon mixing again demonstrated an interaction between repeat 1 and repeat 4. Although no information is available on the type of pairing between the repeats, i.e. side-by-side or end-to-end, the fact that only repeats 1 and 4 do interact significantly, suggests a specific interaction between these repeats. Hence a side-by-side interaction, as occurs in the α-actinin dimer, is the more likely.

In *Drosophila* spectrin, it has been shown that repeats 20 and 21 of the α-chain and 1 and 2 of the β-chain are required for interchain binding *in vitro* (Viel and Branton, 1994). In addition, the 8-residue inserts between β1 and 2 and between α20 and 21 were shown to be essential for tail end interchain binding. Because point mutations within the conserved inserts did not abolish interchain binding, the results suggested that the inserts themselves were unlikely to be distinct binding sites. The facts that both repeats α20 and α21 and β1 and β2 were required for interchain binding and that a tandem duplication of the β2 insert abolished binding were consistent with this conclusion. The results suggest that multiple interactions along the entire length of the α-helical bundles formed by the residues in these repeats are responsible for the high-affinity interaction between α- and β-spectrin (Viel and Branton, 1994).

In human erythrocyte β-spectrin, the minimal region required for association with α-spectrin was determined using recombinant peptides (Ursitti *et al.*, 1996). Based on sequence alignment, and the fact that the other repeats in the spectrin nucleation site and in α-actinin contain an N-terminal 8-residue insertion, the beginning of the first repeat for both β-spectrin and the related dimerisation site of α-actinin is predicted to be approximately 8-residues earlier than most spectrin repeats by Ursitti *et al.* (1996). A four-repeat β-spectrin peptide with this 8-residue insertion bound to full-length α-spectrin with a K_d of about 10 nM, while deletion of these first 8-residues reduced binding nearly 10-fold. It was shown that the first repeat was essential for dimerisation since its deletion abolished binding, but β1 alone could not associate with α-monomers. Interestingly, a truncated form of β1-4 lacking helices A and B of the β1 repeat did show detectable binding to α-monomers, by effectively competing with a larger amount of intact β1-4. The first two repeats represented the minimum lateral dimer assembly site with a K_d of about 230 nM for interaction with full-length α-spectrin or an α-spectrin nucleation site recombinant peptide, α18–21 (Ursitti *et al.*, 1996).

In the present study, repeat 4 of α-actinin contains the N-terminal 8-residue insert shown to be essential for *Drosophila* spectrin dimer formation (Viel and Branton, 1994). However, the phasing of repeat 1 is such that it contains the N-terminal insert, shown to increase the dimer affinity of human erythroid spectrin (Ursitti *et al.*, 1996), but not the C-terminal insert, shown to be essential for *Drosophila* spectrin dimer formation (Figure 42) (Viel and Branton, 1994). Since, repeats 1 and 4 do form heterodimers, it suggests that this C-terminal insert in repeat 1 is not vital for subunit interaction in α-actinin.

Due to the similarity between the repeats in α-actinin and the repeats in spectrin shown to be responsible for initiating subunit assembly (sequence homology and the presence of 8-residue inserts compared to the rest of the spectrin repeats), it is possible that these inserts could be responsible for dimer formation. As the 8-residue insertions in these repeats occur between helix C of one repeat and helix A of the next, it is likely that the insertions alter the inter-repeat contacts by expanding the inter-repeat distance. This could minimise or eliminate the overlap and related twisting of adjacent repeats (Speicher and Ursitti, 1994). Since it has been shown that deletion of a N-terminal insert from human erythroid spectrin β1 reduces the affinity of the β-spectrin nucleation site for the complementary α-spectrin subunit 10-fold (Ursitti *et al.*, 1996), a similar deletion was made from repeat 1 of the α-actinin rod domain. The CD, thermal denaturation profile and susceptibility to proteolysis data suggested a similar confirmation to the native rod, and the sedimentation equilibrium and velocity, electron microscopy and cross-linking results also demonstrated dimer formation, comparable to the native rod. This indicates that the N-terminal insert in repeat 1 is not necessary for dimer formation.

Further 8-residue deletions, based on the phasing of Ursitti *et al.* (1996), were made in the individual repeats 1 and 4 to investigate any alteration in heterologous interaction. Upon deletion of the N-terminal insert from repeat 1, the protein was found to have become insoluble, localising to inclusion bodies, suggesting a conformational change had occurred. Since the same deletion in the rod domain did not alter conformation or dimer formation, it is possible that any alteration in folding of repeat 1 was overcome by steric effects of either the adjacent repeats, or the paired subunit. Deletion of the insert from repeat 4 did not alter solubility, but a conformational change was detected by changes in susceptibility to proteolysis, CD, and thermal melting profile. Mixing of native repeat 1 with mutant repeat 4 resulted in no detectable interaction, as measured by sedimentation equilibrium. This result suggests that the insert in R4 could be necessary for α-actinin dimer formation. However, due to the decrease in stability with this deletion, the change in association behaviour could be due to a change in conformation, rather than the deletion of a specific dimerisation site.

In *Drosophila* spectrin, it has been shown that repeats 20 and 21 of the α chain and 1 and 2 of the β-chain are required for interchain binding *in vitro* (Viel and Branton, 1994). However, domains of the non-repetitive segments, C-terminal domain of α-chain and N-terminal of β-chain, were also shown to be involved in associating the two chains. Required sequences within these non-repetitive segments are interspersed within domains that are known to be involved in associations with other structural proteins, such as actin, and regulatory components, such as protein 4.1 and calcium. The importance of these tail end binding sites has also been demonstrated *in vivo*; *Drosophila* mutations that lack part of the C-terminal region of α-spectrin are lethal (Lee *et al.*, 1993).

The regions within α-C-terminal domain and β-N-terminal domain that are involved in inter-chain binding are located upstream of the first EF-hand motif in the α-subunit C-terminal domain and downstream, immediately following the ABD, in β-spectrin. While none of the well-described structural features within these non-repetitive segments (the EF-hand motifs in α–C-terminal domain and the ABD in β-N-terminal domain) is directly required for inter-chain binding, the interaction between β-N-terminal domain and α-C-terminal domain that brings into apposition the actin binding site on β-spectrin and the EF-hand motifs on α-spectrin may contribute to the calcium regulation of actin binding to spectrin (Fowler and Taylor, 1980; Fishkind *et al.*, 1987) or to α-actinin (Witke *et al.*, 1993). Furthermore, the diminished interchain binding observed when the first EF-hand was deleted suggests that this domain may have a stabilising effect on the interchain binding site in α-C-terminal domain (Viel and Branton, 1994). These results suggest that the lethal defects in the *Drosophila* mutant equivalent to the deletion in α19-22 (rg35), a 37 bp deletion in α-spectrin segment 22 (starting at amino acid residue 2312) (Lee *et al.*, 1993), cannot be directly attributed to failed interchain binding.

In contrast to *Drosophila* spectrin, studies on human erythroid spectrin demonstrated that the adjacent EF-hands and ABD are not essential for spectrin dimer formation (Ursitti *et al.*, 1996). Although these experiments do not rule out a direct interaction of the α-EF-hand motifs with the β-spectrin ABD, this potential interaction was not required for initiation of dimer assembly. In addition, the possible interaction between the EF-hand motifs and the ABD would be expected to be a low affinity interaction since the ABD was quickly cleaved from dimers with trypsin and did not remain covalently bound to the intact α-subunit (Speicher *et al.*, 1992). These differences could reflect a species and/or tissue-specific isoform difference since *Drosophila* spectrin is more closely related to the human brain spectrin (fodrin) isoform than to erythroid spectrin. Also, the *Drosophila* recombinant peptides, which were produced in a reticulocyte lysate system and not purified to homogeneity, had unknown conformational integrity. Lombardo *et al.* (1994) have cited

substantial difficulties in preparing stable, native peptides of brain β-spectrin that contain only a portion of the ABD.

Mixing of chicken smooth muscle α-actinin EF-hands and ABD resulted in no detectable binding, as measured by sedimentation equilibrium. However, it is possible that the GST fused to the EF-hands is blocking any potential binding sites for ABD. Although muscle α-actinins have been shown to be calcium insensitive with respect to actin-binding (Bennet *et al*, 1984; Duhaiman and Bamburg, 1984; Landon *et al.*, 1985) it has been shown that calcium can bind to the EF-hands of chicken gizzard α-actinin, although this effect is eliminated with physiological potassium concentrations (Wenegieme *et al.*, 1994). This suggests that the lack of calcium sensitivity could be due to a potassium-linked alteration in conformation, resulting in elimation of calcium binding. However, it is not immediately clear how this structural change occurs. One possibility is that the ABD of the opposing subunit undergoes a conformational change, which can then either sterically, or through specific interaction, inhibit calcium binding. Since calcium is necessary to mediate the interaction between the EF-hands and ABD, the binding experiments in this study were performed in 2.5 mM calcium.

Since the inhibition of actin-binding by calcium is most likely caused by an alteration in conformation of the EF-hands, resulting in the exposure of hydrophobic residues (Herzberg *et al.*, 1986), it is also possible that only non-muscle isoforms contain the appropriate residues needed for an interaction between the EF-hands and the ABD to occur. A construct consisting of non-muscle EF-hands was available. However, investigation of this construct by sedimentation equilibrium revealed that the construct existed as a dimer. Considering the smooth muscle EF-hands were predominantly monomeric, the dimer state of the non-muscle isoform is interesting. The change in association state could be due to an altered conformation of the non-muscle EF-hands, resulting in either the ability of the fused GST to dimerise (which is known to occur), or the exposure of hydrophobic residues of the EF-hands allowing interaction with other molecules.

It has been demonstrated that the ABD of utrophin is regulated by calmodulin in a calcium-dependent manner, whilst those from dystrophin and chicken smooth muscle α-actinin are not (Winder and Kendrick-Jones, 1995). This was suggested to be due to the utrophin ABD predicted calmodulin-binding site having a high average hydrophobicity and hydrophobic moment, compared to dystrophin and α-actinin. However, since chicken smooth muscle and non-muscle α-actinin ABDs are 100% identical (Figure 3), it is not immediately obvious how chicken non-muscle α-actinin could be regulated by calcium via the EF-hands.

Other conserved motifs in *Drosophila* spectrin have been demonstrated to be essential for heterodimer formation. Repeat 1 of all known α-actinins and the homologous repeat β1 in all spectrins, contain a conserved 5 residue motif in the middle of the predicted B helix, that has no homologues in the other α-actinin and spectrin repeats, and which always includes the sequence Lys-Pro-Pro. Amino acid substitutions within these 5-residues of *Drosophila* spectrin resulted in a loss of interchain binding, indicating that this motif is required in a sequence-specific manner (Viel *et al.*, 1995). Interestingly, amino acid substitutions in the 8-residue inserts, shown to be essential for dimer formation, did not affect interchain binding (Viel and Branton, 1994). A deletion equivalent to that described in the human low expression allele α^{LELY} of red cell spectrin, consisting of 6 residues at the C-terminus of the predicted A helix in repeat 21 (Wilmotte *et al.*, 1993), also resulted in a loss of interchain binding due to a misfolding of repeat 21 in *Drosophila* spectrin (Viel *et al.*, 1995). A similar explanation is also possible for the results of the deletion of the 8-residue inserts (Viel and Branton, 1994), as no analysis of conformation was performed in this study.

Further studies involving these 8-residue inserts could include deletion of the homologous inserts in α-actinin, and possibly also mutation of these residues, to investigate if they also represent important dimer assembly motifs. To this end, other molecular protein techniques could be utilised to investigate the role of these inserts. Peptide synthesis and mimetic studies are possible future techniques for assessment of these putative dimer sites in α-actinin, although it is already clear that these sites alone are unlikely to represent solitary regions responsible for dimerisation.

6. REFERENCES

Adzhubei, A. A., & Steinberg, M. J. E. (1993). Left-handed polyproline-II helices commonly occur in globular-proteins. Journal of Molecular Biology, 229, 472-493.

Ahn, A. H., & Kunkel, L. M. (1993). The structural and functional diversity of dystrophin. Nature Genetics, 3, 283-291.

Albright, D. A., & Williams, J. W. (1967). Sedimentation equilibria in polydisperse nonideal solutions. Journal of Physical Chemistry, 71, 2780-2786.

Arimura, C., Suzuki, T., Yanagisawa, M., Imamura, M., Hamada, Y., & Masaki, T. (1988). Primary structure of chicken skeletal-muscle and fibroblast α-actinins deduced from cDNA sequences. European Journal of Biochemistry, 177, 649-655.

Attri, A. K., Lewis, M. S., & Korn, E. D. (1991). The formation of actin oligomers studied by analytical ultracentrifugation. Journal of Biological Chemistry, 266, 6815-6824.

Babitch, J. A., Wallis, C. J., Wenegieme, E. F., & Naren, A. P. (1994). Calcium-binding to the α-actinin-spectrin-dystrophin superfamily. Journal of Neurochemistry, 62, S64.

Bancroft, F. C., & Freifelder, D. (1970). Molecular weights of coliphages and coliphage DNA. I. Measurement of the molecular weight of bacteriophage T7 by high-speed equilbrium centrifugation. Journal of Molecular Biology, 54, 537-546.

Banner, D. W., Kokkinidis, M., & Tsernoglou, D. (1987). Structure of the CO1E1 ROP protein at 1.7 Å resolution. Journal of Molecular Biology, 196, 657-675.

Baron, M. D., Davison, M. D., Jones, P., & Critchley, D. R. (1987). The sequence Of chick α-actinin reveals homologies to spectrin and calmodulin. Journal of Biological Chemistry, 262, 17623-17629.

Barstead, R. J., Kleiman, L., & Waterston, R. H. (1991). Cloning, sequencing, and mapping of an α-actinin gene from the nematode *Caenorhabditis elegans*. Cell Motility and the Cytoskeleton, 20, 69-78.

Beccerra, S. P., Kumar, A., Lewis, M. S., Widen, S. G., Abbotts, J., Karawya, E. M., Hughes, S. H., Shiloach, J., & Wilson, S. H. (1991). Protein-protein interactions of HIV-1

reverse transcriptase: implication of central and C-terminal regions in subunit binding. Appendix: Ultracentrifugal analysis of mixed associations, by M. S. Lewis. Biochemistry, 30, 11707-11719.

Beck, K. A., Buchanan, J. A., Malhotra, V., & Nelson, W. J. (1994). Golgi spectrin - identification of an erythroid β-spectrin homologue associated with the Golgi-complex. Journal of Cell Biology, 127, 707-723.

Becker, P. S., Tse, W. T., Lux, S. E., & Forget, B. G. (1993). β-Spectrin Kissimmee - a spectrin variant associated with autosomal-dominant hereditary spherocytosis and defective binding to protein 4.1. Journal of Clinical Investigation, 92, 612-616.

Begg, D. A., Rodewald, R., & Rebhun, L. I. (1978). The visualisation of actin filament polarity in thin sections. Evidence for the uniform polarity of membrane-associated filaments. Journal of Cell Biology, 79, 846-852.

Beggs, A. H., Byers, T. J., Knoll, J. H. M., Boyce, F. M., Bruns, G. A. P., & Kunkel, L. M. (1992). Cloning and characterization of 2 human skeletal-muscle α-actinin genes located on chromosome-1 and chromosome-11. Journal of Biological Chemistry, 267, 9281-9288.

Bennett, H., & Condeelis, J. (1988). Isolation of an immunoreactive analogue of brain fodrin that is associated with the cell cortex of *Dictyostelium* amebas. Cell Motility and the Cytoskeleton, 11, 303-317.

Bennett, J. P., Zaner, K. S., & Stossel, T. P. (1984). Isolation and some properties of macrophage α-actinin - evidence that it is not an actin-gelling protein. Biochemistry, 23, 5081-5086.

Bennett, V., & Lambert, S. (1991). The spectrin skeleton - from red-cells to brain. Journal of Clinical Investigation, 87, 1483-1489.

Bennett, V., & Gilligan, D. M. (1993). The spectrin-based membrane skeleton and micron-scale organization of the plasma-membrane. Annual Review of Cell Biology, 9, 27-66.

Ben-Ze'ev, A. (1992). Cytoarchitecture and signal transduction. Critical Review of Eukaryotic Gene Expression, 2, 265-281.

Berridge, M. J., & Irvine, R. F. (1984). Inositol trisphosphate, a novel 2nd messenger in cellular signal transduction. Nature, 312, 315-321.

Berridge, M. J. (1987). Inositol trisphosphate as a 2nd messenger in signal transduction. Annual Review of Biochemistry, 56, 159-193.

Birge, R. B., & Hanafusa, H. (1993). Cloning in on SH2 specificity. Science, 262, 1522-1524.

Blaber, M., Zhang, X.-J., & Matthews, B. W. (1993). α-Helix propensity of amino-acids - response. Science, 260, 1637-1640.

Blanchard, A., Ohanian, V., & Critchley, D. (1989). The structure and function of α-actinin. Journal of Muscle Research and Cell Motility, 10, 280-289.

Bloch, R. J., & Pumplin, D. W. (1992). A model of spectrin as a concertina in the erythrocyte membrane skeleton. Trends in Cell Biology, 2, 186-189.

Bobich, J. A., & Wallis, C. J. (1996). Anomalous migration of horse erythrocyte spectrin dimers in native polyacrylamide gels. Protein and Peptide Letters, 3, 17-22.

Bond, M., & Somlyo, A. V. (1982). Dense bodies and actin polarity in vertebrate smooth-muscle. Journal of Cell Biology, 95, 403-413.

Bonetkerrache, A., Fabbrizio, E., & Mornet, D. (1994). N-terminal domain of dystrophin. FEBS Letters, 355, 49-53.

Bresnick, A. R., Janmey, P. A., & Condeelis, J. (1991). Evidence that a 27-residue sequence is the actin-binding site of ABP-120. Journal of Biological Chemistry, 266, 12989-12993.

Bretscher, A., Vandekerckhove, J., & Weber, K. (1979). α-Actinins from chicken skeletal muscle and smooth muscle show considerable chemical and immunological differences. European Journal of Biochemistry, 100, 237-243.

Bubb, M. R., Lewis, M. S., & Korn, E. D. (1991). The interaction of monomeric actin with two binding sites on *Acanthamoeba* actobindin. Journal of Biological Chemistry, 266, 3820-3826.

Burmeister, M., Monaco, A. P., Gillard, E. F., Vanommen, G. J., B., Affara, N. A., Ferguson-Smith, M. A., & Kunkel, L. M. (1988). A 1-megabase physical map of human XP21, including the Duchenne muscular dystrophy gene. Genomics, 2, 189-202.

Burn, P., Rotman, A., Meyer, R. K., & Burger, M. M. (1985). Diacylglycerol in large α-actinin actin complexes and in the cytoskeleton of activated platelets. Nature, 314, 469-472.

Burridge, K., & Feramisco, J. R. (1981). α-Actinin and vinculin from non-muscle cells - calcium-sensitive interactions with actin. Cold Spring Harbor Symposia on Quantitative Biology, 46, 587-597.

Burridge, K., Turner, C. E., & Romer, L. H. (1992). Tyrosine phosphorylation of paxillin and pp125^{FAK} accompanies cell adhesion to extracellular matrix: a role in cytoskeletal assembly. Journal of Cell Biology, 119, 893-903.

Byers, T. J., & Branton, D. (1985). Visualisation of the protein associations in the erythrocyte-membrane skeleton. Proceedings of the National Academy of Sciences of the United States of America, 82, 6153-6157.

Byers, T. J., Husainchishti, A., Dubreuil, R. R., Branton, D., & Goldstein, L. S. B. (1989). Sequence similarity of the amino-terminal domain of *Drosophila* β-spectrin to α-actinin and dystrophin. Journal of Cell Biology, 109, 1633-1641.

Byers, T. J., Brandin, E., Lue, R. A., Winograd, E., & Branton, D. (1992). The complete sequence of *Drosophila* β-spectrin reveals supra-motifs comprising 8 106-residue segments. Proceedings of the National Academy of Sciences of the United States of America, 89, 6187-6191.

Calvert, R., Kahana, E., & Gratzer, W. B. (1996). Stability of the dystrophin rod domain fold - evidence for nested repeating units. Biophysical Journal, 71, 1605-1610.

Carpen, O., Pallai, P., Staunton, D. E., & Springer, T. A. (1992). Association of intercellular-adhesion molecule-1 (ICAM-1) with actin-containing cytoskeleton and α-actinin. Journal of Cell Biology, 118, 1223-1234.

Castresana, J., & Saraste, M. (1995). Does vav bind to F-actin through a CH domain. FEBS Letters, 374, 149-151.

Chen, B., & Thomas, A. (1980). Recovery of DNA segments from agarose gels. Anals of Biochemistry, 191, 339-341.

Chen, W-L., & Singer, S. J. (1982). Immunoelectron microscopic studies of the sites of substratum and cell-cell contacts in cultured fibroblasts. Journal of Cell Biology, 95, 205-22.

Chothia, C., Levitt, M., & Richardson, D. (1977). Proceedings of the National Academy of Sciences of the United States of America, 74, 4130.

Clerk, A., Morris, G. E., Dubowitz, V., Davies, K. E., & Sewry, C. A. (1993). Dystrophin-related protein, utrophin, in normal and dystrophic human fetal skeletal-muscle. Histochemical Journal, 25, 554-561.

Coetzer, T. L., Sahr, K., Prchal, J., Blacklock, H., Peterson, L., Koler, R., Doyle, J., Manaster, J., & Palek, J. (1991). 4 different mutations in codon 28 of α-spectrin are associated with structurally and functionally abnormal spectrin α-I/74 in hereditary elliptocytosis. Journal of Clinical Investigation, 88, 743-749.

Cohen, C., & Parry, D. A. D. (1986). α-Helical coiled coils; a widespread motif in proteins. Trends in Biochemical Sciences, 11, 245-248.

Cohen, C., & Parry, D. A. D. (1990). α-Helical coiled coils and bundles; how to design an α-helical protein. Proteins Structural Functional Genetics, 7, 1-15.

Cohn, E. J., & Edsall, J. T. (1943). density and apparent specific volume of proteins. Proteins, Amino acids and Peptides as Ions and Dipolar Ions. pp370-381, New York, Reinhold.

Condeelis, J., & Vahey, M. (1982). A calcium and pH-regulated protein from *Dictyostelium discoideum* that cross-links actin filaments. Journal of Cell Biology, 94, 466-471.

Conway, J. F., & Parry, D. A. D. (1990). Structural features in the heptad substructure and longer range repeats of two-stranded α-fibrous proteins. International Journal of Biological Macromolecules, 12, 328-334.

Corrado, K., Mills, P. L., & Chamberlain, J. S. (1994). Deletion analysis of the dystrophin-actin binding domain. FEBS Letters, 344, 255-260.

Correia, J. J., Shire, S., Yphantis, D. A., & Schuster, T. M. (1985). Sedimentation equilbrium measurements of the intermediate-size tobacco mosaic virus protein polymers. Biochemistry, 24, 3292-3297.

Craig, S. W., & Pardo, J. V. (1979). α-Actinin localisation in the junctional complex of intestinal epithelial cells. Journal of Cell Biology, 80, 203-210.

Crawford, A. W., Michelsen, J. W., & Beckerle, M. C. (1992). An interaction between zyxin and α-actinin. Journal of Cell Biology, 116, 1381-1393.

Crawford, L.V., & Waring, M. J. (1967). Supercoiling of polyoma virus DNA measured by its interaction with ethidium bromide. Journal of Molecular Biology, 25, 23-30.

Cross, R. A., Stewart, M., & Kendrick-Jones, J. (1990). Structural predictions for the central domain of dystrophin. FEBS Letters, 262, 87-92.

Dahl, S. C., Geib, R. W., Fox, M. T., Edidin, M., & Branton, D. (1994). Rapid capping in α-spectrin-deficient mel cells from mice afflicted with hereditary hemolytic-anemia. Journal of Cell Biology, 125, 1057-1065.

Davis, G. E., & Stark, G. R. (1970). Use of dimethyl suberimidate, a cross-linking reagent, in studying the subunit structure of oligomeric proteins. Proceedings of the National Academy of Sciences of the United States of America, 66, 651-657.

Davis, L. H., & Bennett, V. (1994). Identification of 2 regions Of β(γ)-spectrin that bind to distinct sites in brain membranes. Journal of Biological Chemistry, 269, 4409-4416.

Davison, M. D., & Critchley, D. R. (1988). α-Actinins and DMD protein contain spectrin-like repeats. Cell, 52, 159-160.

Davison, M. D., Baron, M. D., Critchley, D. R., & Wootton, J. C. (1989). Structural-analysis of homologous repeated domains in α-actinin and spectrin. International Journal of Biological Macromolecules, 11, 81-90.

Desilva, T. M., Peng, K. C., Speicher, K. D., & Speicher, D. W. (1992). Analysis of human red-cell spectrin tetramer (head-to-head) assembly using complementary univalent peptides. Biochemistry, 31, 10872-10878.

Discher, D. E., Winardi, R., Schischmanoff, P. O., Parra, M., Conboy, J. G., & Mohandas, N. (1995). Mechanochemistry of protein 4.1's spectrin-actin-binding domain - ternary

complex interactions, membrane-binding, network integration, structural strengthening. Journal of Cell Biology, 130, 897-907.

Doi, Y., & Frieden, C. (1984). Actin polymerisation. The effect of brevin on filament size and rate of polymerisation. Journal of Biological Chemistry, 259, 11868-11875.

Doi, Y. (1992). Interaction of gelsolin with covalently cross-linked actin dimer. Biochemistry, 31, 10061-10069.

Downes, C. P., & Macphee, C. H. (1990). Myoinositol metabolites as cellular signals. European Journal of Biochemistry, 193, 1-18.

Drenckhahn, D., & Mannherz, H. G. (1983). Distribution of actin and the actin-associated proteins myosin, tropomyosin, α-actinin, vinculin, and villin in rat and bovine exocrine glands. European Journal of Cell Biology, 30, 167-176.

Dubreuil, R. R., Byers, T. J., Sillman, A. L., Barzvi, D., Goldstein, L. S. B., & Branton, D. (1989). The complete sequence of *Drosophila* α-spectrin - conservation of structural domains between α-spectrins and α-actinin. Journal of Cell Biology, 109, 2197-2205.

Dubreuil, R. R., Brandin, E., Reisberg, J. H. S., Goldstein, L. S. B., & Branton, D. (1991). Structure, calmodulin-binding, and calcium-binding properties of recombinant α-spectrin polypeptides. Journal of Biological Chemistry, 266, 7189-7193.

Duchenne, G. B. (1868). Recherches sur la paralysie musculaire pseudo-hypertophique ou paralysie myosclerosique. Archives of General Medicine, 11, 5, 178, 305, 421, 552.

Duhaiman, A. S., & Bamburg, J. R. (1984). Isolation of brain α-actinin - its characterization and a comparison of its properties with those of muscle α-actinins. Biochemistry, 23, 1600-1608.

Durham, A. C. H. (1972). Structures and roles of the polymorphic forms of tobacco mosaic virus protein. I. Sedimentation studies. Journal of Molecular Biology, 67, 289-305.

Ebashi, S., Ebashi, F., & Maryuma, K. (1964). A new protein factor promoting contraction of actomyosin. Nature, 203, 645-646.

Eberle, M., Traynor-Kaplan, A. E., Sklar, L. A., & Norgauer, T. (1990). Is there a relationship between phosphatidylinositol trisphosphate and F-actin polymerisation in human neutrophils. Journal of Biological Chemistry, 265, 16725-16728.

Elliott, G. F., Lowy, J., & Worthington, C. R. (1963). An X-ray and light-diffraction study of the filament lattice of striated muscle in the living state and in rigor. Journal of Molecular Biology, 295-305.

Emes, C. H., & Rowe, A. J. (1978) Hydrodynamic studies on the self association of vertebrate skeletal muscle myosin. Biochimica et Biophysica Acta, 537, 110-124.

Endo, T., & Masaki, T. (1982). Molecular-properties and functions *in vitro* of chicken smooth-muscle α-actinin in comparison with those of striated-muscle α-actinins. Journal of Biochemistry, 92, 1457-1468.

Endo, T., & Masaki, T. (1984). Differential expression and distribution of chicken skeletal-muscle-type and smooth-muscle-type α-actinins during myogenesis in culture. Journal of Cell Biology, 99, 2322-2332.

Eriksson, A. E., Baase, W. A., Zhang, X.-J., Heinz, D. W., Blaber, M., Baldwin, E. P., & Matthews, B. W. (1992). Response of a protein-structure to cavity-creating mutations and its relation to the hydrophobic effect. Science, 255, 178-183.

Ervasti, J. M., Kahl, S. D., & Campbell, K. P. (1991). Purification of dystrophin from skeletal-muscle. Journal of Biological Chemistry, 266, 9161-9165.

Ervasti, J. M., & Campbell, K. P. (1993). A role for the dystrophin-glycoprotein complex as a transmembrane linker between laminin and actin. Journal of Cell Biology, 122, 809-823.

Fabbrizio, E., Bonetkerrache, A., Leger, J. J., & Mornet, D. (1993). Actin-dystrophin interface. Biochemistry, 32, 10457-10463.

Fechheimer, M., Brier, J., Rockwell, M., Luna, E. J., & Taylor, D. L. (1982). A calcium and pH-regulated actin binding protein from *D. discoideum*. Cell Motility, 2, 287-308.

Feener, C. A., Koenig, M., & Kunkel, L. M. (1989). Alternative splicing of human dystrophin messenger-RNA generates isoforms at the carboxy-terminus. Nature, 338, 509-511.

Fishkind, D. J., Bosder, E. M., & Bmgg, D. A. (1987). Isolation and characterization of sea-urchin egg Spectrin - calcium Modulation of the spectrin-actin interaction. Cell Motility and the Cytoskeleton, 7, 304-314.

Fowler, V., & Bennett, V. (1984). Erythrocyte membrane tropomyosin: Purification and properties. Journal of Biological Chemistry, 259, 5978-5989.

Fowler, V., & Taylor, D. L. (1980). Spectrin plus band 4.1 cross-link actin. Regulation by micromolar calcium. Journal of Cell Biology, 85, 361-376.

Francis, G. R., & Waterston, R. H. (1985). Muscle organisation in *Caenorhabditis elegans*: localisation of proteins implicated in thin filament attachment and I-band organisation. Journal of Cell Biology, 101, 1532-1549.

Freifelder, D., & Davison, P. F. (1963). Physicochemical studies on the reaction between formaldehyde and DNA. Biophysical Journal, 3, 49-63.

Fujimori, T., & Takeichi, M. (1993). Disruption of epithelial cell-cell adhesion by exogenous expression of a mutated non-functional N-cadherin. Molecular Biology of the Cell, 4, 37-47.

Fukami, K, Furuhashi, K, Inagaki, M, Endo, T, Hatano, S, Takenawa, T (1992). Requirement of phosphatidylinositol 4,5-bisphosphate for α-actinin function. Nature, 359, 150-152.

Fukami, K., Endo, T., Imamura, M., & Takenawa, T. (1994). α-Actinin and vinculin are PIP_2-binding proteins involved in signaling by tyrosine kinase. Journal of Biological Chemistry, 269, 1518-1522.

Fukami, K., Sawada, N., Endo, T., & Takenawa, T. (1996). Identification of a phosphatidylinositol-4,5-bisphosphate-binding site in chicken skeletal-muscle α-actinin. Journal of Biological Chemistry, 271, 2646-2650.

Fyrberg, E., Kelly, M., Ball, E., Fyrberg, C., & Reedy, M. C. (1990). Molecular-genetics of *Drosophila* α-actinin - mutant alleles disrupt Z-disk integrity and muscle insertions. Journal of Cell Biology, 110, 1999-2011.

Gache, Y., Landon, F., & Olomucki, A. (1984). Polymorphism of α-actinin from human-blood platelets - homodimeric and heterodimeric forms. European Journal of Biochemistry, 141, 57-61.

Gardner, K., & Bennett, V. (1987). Modulation of spectrin actin assembly by erythrocyte adducin. Nature, 328, 359-362.

Geiger, B., Tokuyashi, K. T., & Singer, S. J. (1979). Immunocytochemical localisation of α-actinin in intestinal epithelial cells. Proceedings of the National Academy of Sciences of the United States of America, 76, 2833-7.

Geiger, B., Dutton, A. H., Tokuyasu, K. T., & Singer, S. J. (1981). Immunoelectron microscope studies of membrane-microfilament interactions - distributions of α-actinin, tropomyosin, and vinculin in intestinal epithelial brush-border and chicken gizzard smooth-muscle cells. Journal of Cell Biology, 91, 614-628.

Geiger, B., Avnur, Z., & Schlessinger, J. (1982). Restricted mobility of membrane constituents in cell substrate focal contacts of chicken fibroblasts. Journal of Cell Biology, 93, 495-500.

Geiger, B., Avnur, Z., Kreis, T.E., & Schlessinger, J. (1984). The dynamics of cytoskeletal organisation in areas of cell contact. Cell Muscle Motility, 5, 195-234.

Geiger, B., Volk, T., Volberg, T., & Bendori, R. (1987). Molecular interactions in adherens-type contacts. Journal of Cell Science Supplement, 8, 251-272.

Geiger, B., Volk, T., Ginsberg, D., Bitzur, S., Sabanay, I., & Hynes, R. O. (1990). Broad spectrum pan-cadherin antibodies, reactive with the C-terminal 24 amino acid residues of N-cadherin. Journal of Cell Science, 97, 607-614.

Geiger, B., & Ayalon, O. (1992). Cadherins. Annual Review of Cell Biology, 8, 307-332.

Geiger, B., Ayalon, O., Ginsberg, D., Volberg, T., Rodriguez Fernandez, J. L., Yarden, Y., & Ben-Ze'ev, A. (1992). Cytoplasmic control of cell adhesion. Cold Spring Harbor Symposium on Quantitative Biology, 57, 631-642.

Gilbert, L. M., & Gilbert, G. A. (1973). Sedimentation velocity measurement of protein association. Methods in Enzymology, 27D, 273-296.

Gilmore, A. P., Parr, T., Patel, B., Gratzer, W. B., & Critchley, D. R. (1994). Analysis of the phasing of 4 spectrin-like repeats in α-actinin. European Journal of Biochemistry, 225, 235-242.

Gluck, U., Rodriguez Fernandez, J. L., Pankov, R., & Benzeev, A. (1992). Regulation of adherens junction protein expression in growth-activated 3T3 cells and in regenerating liver. Experimental Cell Research, 202, 477-486.

Gluck, U., Kwiatkowski, D. J., & Benzeev, A. (1993). Suppression of tumorigenicity in simian-virus 40-transformed 3T3 cells transfected with α-actinin cDNA. Proceedings of the National Academy of Sciences of the United States of America, 90, 383-387.

Gluck, U., & Benzeev, A. (1994). Modulation of α-actinin levels affects cell motility and confers tumorigenicity on 3T3 cells. Journal of Cell Science, 107, 1773-1782.

Goll, D. E., Suzuki, A., Temple, J., & Holmes, G. R. (1972). Studies on purified α-actinin. Effect of temperature and tropomyosin on the α-actinin/F-actin interaction. Journal of Molecular Biology, 67, 469-488.

Goll, D. E., Dayton, W. R., Singh, I., & Robson, R. M. (1991). Studies of the α-actinin actin interaction in the Z-disk by using calpain. Journal of Biological Chemistry, 266, 8501-8510.

Graf, E., Filoteo, A. G., & Penniston, J. T. (1980). Preparation of ^{125}I-calmodulin with retention of full biological activity: its binding to human erythrocyte ghosts. Archives of Biochemistry and Biophysics, 203, 719-726.

Greenfield, N., & Fasman, G. D. (1969). Computed circular dichroism spectra for the evaluation of protein conformation. Biochemistry, 8, 4108-4116.

Griffith, I. P. (1972). The effect of cross-links on the mobility of proteins in dodecyl sulphate-polyacrylamide gels. Biochemical Journal, 126, 553-560.

Guan, J.-L., & Shalloway, D. (1992). Regulation of focal adhesion-associated protein tyrosine kinase by both cellular adhesion and oncogenic transformation. Nature, 358, 690-692.

Haiech, J., Kilhoffer, M. C., Lukas, T. J., Craig, T. A., Roberts, D. M., & Watterson, D. M. (1991). Restoration of the calcium-binding activity of mutant calmodulins toward normal by the presence of a calmodulin binding structure. Journal of Biological Chemistry, 266, 3427-3431.

Hammonds, R. G. (1987). Protein-sequence Of DMD gene is related to actin-binding domain of α-actinin. Cell, 51, 1-1.

Harrington, W. F., & Kegeles, G. (1973). Pressure effects in ultracentrifugation of interacting systems. Methods in Enzymology, 27D, 306-345.

Harlan, J. E., Hajduk, P. J., Yoon, H. S., & Fesik, S. W. (1994). Pleckstrin homology domains bind to phosphatidyinositol-4,5-bisphosphate. Nature, 371, 168-170.

Harris, A. S., & Morrow, J. S. (1988). Proteolytic processing of human-brain α-spectrin (fodrin) - identification of a hypersensitive site. Journal of Neuroscience, 8, 2640-2651.

Harris, A. S., Corall, D. E., & Morrow, J. S. (1988). The calmodulin-binding site in α-fodrin is near the calcium-dependent protease-I cleavage site. Journal of Biological Chemistry, 263, 15754-61.

Harris, A. S., & Morrow, J. S. (1990). Calmodulin and calcium-dependent protease-1 coordinately regulate the interaction of fodrin with actin. Proceedings of the National Academy of Sciences of the United States of America, 87, 3009-3013.

Harris, H. W., & Lux, S. E. (1980). Structural characterisation of the phosphorylation sites of human erythrocyte spectrin. Journal of Biological Chemistry, 255, 11512-20.

Hartwig, J. H. (1995). Actin-binding proteins 1 - spectrin superfamily. Protein Profile, 2, 703-800.

Heaysman, J. E. M., & Pegrum, S. M. (1973). Early contacts between fibroblasts: An ultrastructural study. Experimental Cell Research, 78, 71-78.

Heiska, L., Kantor, C., Parr, T., Critchley, D. R., Vilja, P., Gahmberg, C. G., & Carpen, O. (1996). Binding of the cytoplasmic domain of intercellular-adhesion molecule-2 (ICAM-2) to α-actinin. Journal of Biological Chemistry, 271, 26214-26219.

Heizmann, C. W., & Hunziker, W. (1991). Intracellular calcium binding proteins; more sites than insights. Trends in Biochemical Sciences, 16, 98-103.

Helliwell, T. R., Ellis, J. M., Mountford, R. C., Appleton, R. E., & Morris, G. E. (1992). A truncated dystrophin lacking the C-terminal domains is localized at the muscle membrane. American Journal of Human Genetics, 50, 508-514.

Hemmings, L., Kuhlman, P. A., & Critchley, D. R. (1992). Analysis of the actin-binding domain of α-actinin by mutagenesis and demonstration that dystrophin contains a functionally homologous domain. Journal of Cell Biology, 116, 1369-1380.

Herskovits, T. T., Otero, R. M., & Hamilton, M. G. (1990). The hemocyanin of the ramshorn snail, *Marisa cornuarietis* (Linne). Computational Biochemistry and Physiology, 97B, 623-629.

Herzberg, O., Moult, J., & James, M. N. G. (1986). A model for the calcium-induced conformational transition of tropinin C. Journal of Biological Chemistry, 261, 2638-2644.

Higuchi, R. (1990) in: PCR protocols: A guide to methods and applications, (Innis, M. A., Gelfand, D. H., Sninsky, J. J., & White, T. J. eds.) pp177-183, Academic, San Diego.

Hoessli, D., Rungger-Brandle, E., Jockusch, B. M., & Gabbiani, G. (1980). Relationship to cell membrane and co-capping with surface receptors. Journal of Cell Biology, 84, 305-314.

Hoffman, E. P., Brown, R. H., & Kunkel, L. M. (1987). Dystrophin - the protein product of the Duchenne muscular-dystrophy locus. Cell, 51, 919-928.

Hoffman, E. P., Watkins, S. C., Slayter, H. S., & Kunkel, L. M. (1989). Detection of a specific isoform of α-actinin with antisera directed against dystrophin. Journal of Cell Biology, 108, 503-510.

Holmes, G. R., Goll, D. E., & Suzuki, A. (1971). Effect of α-actinin on actin viscosity. Biochimica et Biophysica Acta, 253, 240-253.

Howard, T. H., & Oresajo, C. O. (1985). The kinetic of chemotactic peptide induced change in F-actin content, F-actin distribution, and the shape of neutrophils. Journal of Cell Biology, 101, 1078-1085.

Hu, R. J., Moorthy, S., & Bennett, V. (1995). Expression of functional domains of $\beta_{(G)}$-spectrin disrupts epithelial morphology in cultured-cells. Journal of Cell Biology, 128, 1069-1080.

Hutter, O. F., Burton, F. L., & Bovell, D. L. (1991). Mechanical properties of normal and *mdx* mouse sarcolemma; bearing on function of dystrophin. Journal of Muscle Research and Cell Motility, 12, 585-589.

Huxley, H. E. (1953). Proceedings of the Royal Society of Biology, 141, 59-62.

Iida, N., Lokeshwar, V. B., & Bourguignon, L. Y. W. (1994). Mapping the fodrin binding domain in CD45, a leukocyte membrane-associated tyrosine phosphatase. Journal of Biological Chemistry, 269, 28576-28583.

Ikura, M., Clore, G. M., Gronenberg, A., Zhu, G., Klee, C. B., & Bax, A. (1992). Solution structure of a calmodulin-target peptide complex by multidimensional NMR. Science, 256, 632-638.

Imamura, M., Endo, T., Kuroda, M., Tanaka, T., & Masaki, T. (1988). Substructure and higher structure of chicken smooth-muscle α-actinin molecule. Journal of Biological Chemistry, 263, 7800-7805.

Imamura, M., & Masaki, T. (1992). A novel nonmuscle α-Actinin - purification and characterization of chicken lung α-actinin. Journal of Biological Chemistry, 267, 25927-25933.

Imamura, M., Sakurai, T., Ogawa, Y., Ishikawa, T., Goto, K., & Masaki, T. (1994). Molecular-cloning of low-calcium-sensitive-type nonmuscle α-actinin. European Journal of Biochemistry, 223, 395-401.

Imamura, M., & Masaki, T. (1994). Identification of a 115-kDa protein from muscle tissues - expression of a novel nonmuscle α-actinin in vascular endothelial-cells. Experimental Cell Research, 211, 380-390.

Isobe, Y., Warner, F. D., & Lemanski, L. F. (1988). 3-Dimensional immunogold localization of α-actinin within the cytoskeletal networks of cultured cardiac-muscle and nonmuscle cells. Proceedings of the National Academy of Sciences of the United States of America, 85, 6758-6762.

Jackson, P., Smith, G., & Critchley, D. R. (1989). Expression of a muscle-type α-actinin cDNA clone in non-muscle cells. European Journal of Cell Biology, 50, 162-169.

Jacob, R., Merritt, J. E., Hallam, T. J., & Rink, T. J. (1988). Repetitive spikes in cytoplasmic calcium evoked by histamine in human-endothelial cells. Nature, 335, 40-45.

Janssen, K. P., Eichinger, L., Janmey, P. A., Noegel, A. A., Schliwa, M., Witke, W., & Schleicher, M. (1996). Viscoelastic properties of F-actin solutions in the presence of normal and mutated actin-binding proteins. Archives of Biochemistry and Biophysics, 325, 183-189.

Jarrett, H. W., & Madhavan, R. (1991). Calmodulin-binding proteins also have a calmodulin-like binding-site within their structure - the flip-flop model. Journal of Biological Chemistry, 266, 362-371.

Jarrett, H. W., & Foster, J. L. (1995). Alternate binding of actin and calmodulin to multiple sites on dystrophin. Journal of Biological Chemistry, 270, 5578-5586.

Johnson, M. L. (1992). Analysis of ligand-binding data with experimental uncertainties in independent variables. Methods in Enzymology, 210, 106-117.

Jockusch, B. M., Burger, M. M., Prada, M. D., Richards, J. G., Chaponnier, C., & Gabbiani, G. (1977). α-Actinin attached to membranes of secretory vesicles. Nature, 270, 628-629.

Jokhadze, G. G., Oleinikov, A. V., Alakhov, Y. B., Nadirashvili, N. S., & Zaalishvili, M. M. (1991). Primary structure of the cDNA 5'-terminal region encoding the N- terminal domain of the rabbit muscle α-actinin subunit. FEBS Letters, 289, 190-192.

Juliano, R. L., & Haskill, S. (1993). Signal transduction from the extracellular matrix. Journal of Cell Biology, 120, 577-585.

Kahana, E., & Gratzer, W. B. (1991). Properties of the spectrin-like structural element of smooth-muscle α-actinin. Cell Motility and the Cytoskeleton, 20, 242-248.

Kahana, E., Marsh, P. J., Henry, A. J., Way, M., & Gratzer, W. B. (1994). Conformation and phasing of dystrophin structural repeats. Journal of Molecular Biology, 235, 1271-1277.

Kahana, E., & Gratzer, W. B. (1995). Minimun folding unit of dystrophin rod domain. Biochemistry, 34, 8110-8114.

Kahana, E., Flood, G., & Gratzer, W. B. (1996). Physical properties of dystrophin rod fragment. In press.

Kake, T., Spissinger, T., Sato, O., Kimura, S., & Maruyama, K. (1994). Molecular shape of dystrophin with special reference to type-VI collagen. Proceedings of Japan Academy of Sciences Series B, Physical Biological Science, 71, 24, 26.

Kakiuchi, S., Sobue, K., & Fujita, M. (1981). Purification of a 240000 MR calmodulin-binding protein from a microsomal fraction of brain. FEBS Letters, 132, 144-148.

Kam, Z., Josephs, R., Eisenberg, H., & Gratzer, W. B. (1977). Structural study of spectrin from human erythrocyte membranes. Biochemistry, 16, 5568-5572.

Karpati, G., & Carpenter, S. (1986). Small-caliber skeletal-muscle fibers do not suffer deleterious consequences of dystrophic gene-expression. American Journal of Medical Genetics, 25, 653-658.

Karpati, G., Carpenter, S., & Prescott, S. (1988). Small-caliber skeletal-muscle fibers do not suffer necrosis in *mdx* mouse dystrophy. Muscle & Nerve, 11, 795-803.

Kawasaki, H., & Kretsinger, R. (1994). Calcium-binding proteins 1: EF-hands. Protein Profile, 1.

Keller, H. U., & Niggli, V. (1993). Colchicine-induced stimulation of PMN motility related to cytoskeletal changes in actin, α-actinin, and myosin. Cell Motility and the Cytoskeleton, 25, 10-18.

Kennedy, S. P., Weed, S. A., Forget, B. G., & Morrow, J. S. (1994). A partial structural repeat forms the heterodimer self-association site of all β-spectrins. Journal of Biological Chemistry, 269, 11400-11408.

Khurana, T. S., Byers, T. J., Kunkel, L. M., Sancho, S., Tanji, K., & Miranda, A. F. (1991). Dystrophin detection in freeze-dried tissue. Lancet, 338, 448-448.

Khurana, T. S., Watkins, S. C., & Kunkel, L. M. (1992). The subcellular-distribution of chromosome 6-encoded dystrophin-related protein in the brain. Journal of Cell Biology, 119, 357-366.

Kirschner, M. W., & Schachman, H. K. (1971). Conformational changes in proteins as measured by difference sedimentation studies. II. Effect of stereospecific ligands on the catalytic subunit of aspartate transcarbamylase. Biochemistry, 10, 1919-1926.

Knecht, D. A., & Loomis, W. F. (1988). Developmental consequences of the lack of myosin heavy chain in *Dictyostelium discoideum*. Developmental Biology, 128, 178-184.

Knudsen, K. A., Soler, A. P., Johnson, K. R., & Wheelock, M. J. (1995). Interaction of α-actinin with the cadherin catenin cell-cell adhesion complex via α-catenin. Journal of Cell Biology, 130, 67-77.

Koch, C. A., Anderson, D., Moran, M. F., Ellis, C., & Pawson, T. (1991). SH2 and SH3 domains - elements that control interactions of cytoplasmic signaling proteins. Science, 252, 668-674.

Koenig, M. *et al.* (1987). Complete cloning of the Duchenne muscular-dystrophy (DMD) cDNA and preliminary genomic organisation of the DMD gene in normal and affected individuals. Cell, 50, 509-517.

Koenig, M., Monaco, A. P., & Kunkel, L. M. (1988). The complete sequence of dystrophin predicts a rod-shaped cytoskeletal protein. Cell, 53, 219-228.

Koenig, M., & Kunkel, L. M. (1990). Detailed analysis of the repeat domain of dystrophin reveals 4 potential hinge segments that may confer flexibility. Journal of Biological Chemistry, 265, 4560-4566.

Kotula, L., Desilva, T. M., Speicher, D. W., & Curtis, P. J. (1993). Functional-characterization of recombinant human red-cell α-spectrin polypeptides containing the tetramer binding-site. Journal of Biological Chemistry, 268, 14788-14793.

Kratky, O., Leopold, H., & Stabinger, H. (1973). The determination of the partial specific volumes of proteins by the mechanical oscillator technique. Methods in Enzymology, Vol. 27, pp. 98-110. Edited by C. H. W. Hirs and S. N. Timasheff. New York, Academic Press.

Kreis, T. E., Avnur, Z., Schlessinger, J., & Geiger, B. (1984) in Molecular Biology of the Cytoskeleton, eds. Borisy, G., Cleveland, D., & Murphy, D. (Cold Spring Harbor Laboratory, Cold Spring Harbor, New York), pp 45-47.

Kretsinger, R. H. (1980). Crystallographic studies of calmodulin and homologues. Annual New York Academy of Sciences, 356, 14-19.

Kuhlman, P. A., Hemmings, L., & Critchley, D. R. (1992). The identification and characterization of an actin-binding site in α-actinin by mutagenesis. FEBS Letters, 304, 201-206.

Kuhlman, P. A., Ellis, J., Critchley, D. R., & Bagshaw, C. R. (1994). The kinetics of the interaction between the actin-binding domain of α-actinin and F-actin. FEBS Letters, 339, 297-301.

Kuo, P. F., Mimura, N., & Asano, A. (1982). Purification and characterisation of actinogelin, a calcium-sensitive actin-accessory protein, from rat-liver. European Journal of Biochemistry, 125, 277-282.

Kuroda, M., Kohira, Y., & Sasaki, M. (1994). Conformational change of skeletal-muscle α-actinin induced by salt. Biochimica et Biophysica Acta Protein Structure and Molecular Enzymology, 1205, 97-104.

Laemmli, U. K. (1970). Cleavage of structural proteins during the assembly of bacteriophage T4. Nature, 227, 680-685.

LaFlamme, S. E., Akiyama, S. K., & Yamada, K. M. (1992). Regulation of fibronectin receptor distribution. Journal of Cell Biology, 117, 437-447.

Laing, N. G., Majda, B. T., Akkari, P. A., Layton, M. G., Mulley, J. C., Phillips, H., Haan, E. A., White, S. J., Beggs, A. H., Kunkel, L. M., Groth, D. M., Boundy, K. L., Kneebone, C. S., Blumberg, P. C., Wilton, S. D., Speer, M. C., & Kakulas, B. A. (1992). Assignment of a gene (nemi) for autosomal dominant nemaline myopathy to chromosome-I. American Journal Of Human Genetics, 50, 576-583.

Lakatos, S., & Minton, A. P. (1991). Interactions between globular proteins and F-actin in isotonic saline solution. Journal of Biological Chemistry, 266, 18707-18713.

Lakey, A., Labeit, S., Gautel, M., Ferguson, C., Barlow, D. P., Leonard, K., & Bullard, B. (1993). Kettin, a large modular protein in the Z-disc of insect muscles. EMBO Journal, 12, 2863-2871.

Lamm, O. (1929). Die differentialgleichung der ultrazentrifugierung. Ark. Mat., Astron. Fys., 21B: 2, 1-4.

Landon, F., Gache, Y., Touitou, H., & Olomucki, A. (1985). Properties of 2 isoforms of human-blood platelet α-actinin. European Journal of Biochemistry, 153, 231-237.

Laposata, M., Downarsky, D. K., & Shin, H. S. (1983). Thrombin-induced gap formation in confluent endothelial-cell monolayers *in vitro*. Blood, 62, 549-556.

Lazarides, E., & Burridge, K. (1975). α-Actinin: Immunmofluorescent localisation of a muscle structural protein in non-muscle cells. Cell, 6, 289-98.

Lazarides, E., & Granger, B. L. (1978). Fluorescent localisation of membrane sites in glycerinated chicken skeletal muscle fibers and the relationship of these sites to the protein composition of the Z disc. Proceedings of the National Academy of Sciences of the United States of America, 75, 3683-3687.

Lee, J. K., Coyne, R. S., Dubreuil, R. R., Goldstein, L. S. B., & Branton, D. (1993). Cell-shape and interaction defects in α-spectrin mutants of *Drosophila*-melanogaster. Journal of Cell Biology, 123, 1797-1809.

Lemaire, C., Heilig, R., & Mandel, J. L. (1988). Nucleotide-sequence of chicken dystrophin cDNA. Nucleic Acids Research, 16, 11815-11816.

Leto, T. L., Pleasic, S., Forget, B. G., Benz, E. J., & Marchesi, V. T. (1989). Characterization of the calmodulin-binding site of non-erythroid α-spectrin - recombinant protein and model peptide studies. Journal of Biological Chemistry, 264, 5826-5830.

Levine, B. A., Moir, A. J. G., Patchell, V. B., & Perry, S. V. (1990). The interaction of actin with dystrophin. FEBS Letters, 263, 159-162.

Levine, B. A., Moir, A. J. G., Patchell, V. B., & Perry, S. V. (1992). Binding-sites involved in the interaction of actin with the N-terminal region of dystrophin. FEBS Letters, 298, 44-48.

Liu, S. C., Derick, L. H., & Palek, J. (1987). Visualisation of the hexagonal lattice in the erythrocyte-membrane skeleton. Journal of Cell Biology, 104, 527-536.

Lohman, T. M., Wensley, C. G., Cina, J., Burgess, R. R., Record, M. T., Jr. (1980). Use of difference boundary sedimentation velocity to investigate nonspecific protein-nucleic acid interactions. Biochemistry, 19, 3516-3522.

Lombardo, C. R., Weed, S. A., Kennedy, S. P., Forget, B. G., & Morrow, J. S. (1994). β-Ii-Spectrin (fodrin) and β-I-σ-2-spectrin (muscle) contain NH_2-terminal and COOH-terminal membrane association domains (MAD1 and MAD2). Journal of Biological Chemistry, 269, 29212-29219.

Love, D. R., Hill, D. F., Dickson, G., Spurr, N. K., Byth, B. C., Marsden, R. F., Walsh, F. S., Edwards, Y. H., & Davies, K. E. (1989). An autosomal transcript in skeletal-muscle with homology to dystrophin. Nature, 339, 55-58.

Love, D. R., England, S. B., Speer, A., Marsden, R. F., Bloomfield, J. F., Roche, A. L., Cross, G. S., Mountford, R. C., Smith, T. J., & Davies, K. E. (1991). Sequences of junction fragments in the deletion-prone region of the dystrophin gene. Genomics, 10, 57-67.

Macdonald, R. I., Musacchio, A., Holmgren, R. A., & Saraste, M. (1994). Invariant tryptophan at a shielded site promotes folding of the conformational unit of spectrin. Proceedings of the National Academy of Sciences of the United States of America, 91, 1299-1303.

Macdonald, R. I., & Pantazatos, D. P. (1995). Mutation of nearly invariant tryptophan of repeating unit of spectrin to histidine or tyrosine but not phenylalanine yields little change in $\Delta G(H_2O)$ of urea-induced unfolding. Faseb Journal, 9, A1431-A1431.

Madhavan, R., Massom, L. R., & Jarrett, H. W. (1992). Calmodulin specifically binds 3 proteins of the dystrophin-glycoprotein complex. Biochemical and Biophysical Research Communications, 185, 753-759.

Madhavan, R., & Jarrett, H. W. (1995). Interactions between dystrophin-glycoprotein complex proteins. Biochemistry, 34, 12204-12209.

Man, N. T., Ellis, J. M., Love, D. R., Davies, K. E., Gatter, K. C., Dickson, G., & Morris, G. E. (1991). Localization of the DMDl dene-encoded dystrophin-related protein using a panel of 19 monoclonal-antibodies - presence at neuromuscular-junctions, in the sarcolemma of dystrophic skeletal-muscle, in vascular and other smooth muscles, and in proliferating brain-cell lines. Journal of Cell Biology, 115, 1695-1700.

Man, N. T., Le Thiet Thank, Blake, D. J., Davies, K. E., & Morris, G. E. (1992). Utrophin, the autosomal homologue of dystrophin, is widely-expressed and membrane-associated in cultured cell lines. FEBS letters, 313, 19-22.

Man, N. T., Ginjaar, I. B., Vanommen, G. J. B., & Morris, G. E. (1992). Monoclonal-antibodies for dystrophin analysis - epitope mapping and improved binding to SDS-treated muscle sections. Biochemical Journal, 288, 663-668.

Mark, A. E., Nichol, L. W., & Jeffrey, P. D. (1987). The self-association of zinc-free bovine insulin. A single model based on interactions in the crystal that describes the association pattern in solution at pH 2, 7 and 10. Biophysical Chemistry, 27, 103-117.

Maruyama, K. (1976). Actinins, regulatory proteins of muscle. Advances in Biophysics, 9, 157-185.

Masaki, T., Endo, M., & Ebashi, S. (1967). Localisation of the 6 S component of α-actinin in the Z-band. Journal of Biochemistry, 62, 630-632.

Matsudaira, P. (1991). Modular organization of actin cross-linking proteins. Trends in Biochemical Sciences, 16, 87-92.

Matsumura, K., Ervasti, J. M., Ohlendieck, K., Kahl, S. D., & Campbell, K. P. (1992). Association of dystrophin-related protein with dystrophin-associated proteins in *mdx* mouse muscle. Nature, 360, 588-591.

Maude, D., Guillet,. G., Rogers, P. A., & Charest, P. M. (1991). Identification of a 220 kDa membrane-associated plant cell protein immunologically related to human β-spectrin. FEBS Letters, 294, 77-80.

McGough, A. M., & Josephs, R. (1990). On the structure of erythrocyte spectrin in partially expanded membrane skeletons. Proceedings of the National Academy of Sciences of the United States of America, 87, 5208-5212.

McGough, A., Way, M., & Derosier, D. (1994). Determination of the α-actinin-binding site on actin-filaments by cryoelectron microscopy and image-analysis. Journal of Cell Biology, 126, 433-443.

McGregor, A., Blanchard, A. D., Rowe, A. J., & Critchley, D. R. (1994). Identification of the vinculin-binding site in the cytoskeletal protein α-actinin. Biochemical Journal, 301, 225-233.

McKenna, N. M., Meigs, J. B., & Wang, Y. L. (1985). Exchangeability of α-actinin in living cardiac fibroblasts and muscle-cells. Journal of Cell Biology, 101, 2223-2232.

McLachlan, A. D., & Stewart, M. (1975). Tropomyosin coiled-coil interactions: evidence for an unstaggered structure. Journal of Molecular Biology, 97, 293-304.

McLachlan, A. D., & Karn, J. (1983). Periodic features in the amino-acid-sequence of nematode myosin rod. Journal of Molecular Biology, 164, 605-626.

McLaughlan, P. J., Gooch, J. T., Mannherz, H.-G, & Weeds, A. G. (1993). Structure of gelsolin segment 1-actin complex and the mechanism of filament severing. Nature, 364, 685-692.

Meador, W. E., Means, A. R., & Quiocho, F. A. (1992). Target enzyme recognition by calmodulin: 2.4 Å structure of a calmodulin-peptide complex. Science, 257, 1251-1255.

Meigs, J. B., & Wang, Y. L. (1986). Reorganization of α-actinin and vinculin induced by a phorbol ester in living cells. Journal of Cell Biology, 102, 1430-1438.

Merisko, E. M., Welch, J. K., Chen, T. Y., & Chen, M. (1988). α-Actinin and calmodulin interact with distinct sites on the arms of the clathrin trimer. Journal of Biological Chemistry, 263, 15705-15712.

Meryon, E. (1852). On granular and fatty degeneration of the voluntary muscles. Medico-Chirurgical Transactions, 35, 73.

Meyer, R. K., Schindler, H., & Burger, M. M. (1982). α-Actinin interacts specifically with model membranes containing glycerides and fatty-acids. Proceedings of the National Academy of Sciences of the United States of America-Biological Sciences, 79, 4280-4284.

Meyer, R. K., & Aebi, U. (1990). Bundling of actin-filaments by α-actinin depends on its molecular length. Journal of Cell Biology, 110, 2013-2024.

Millake, D. B., Blanchard, A. D., Patel, B., & Critchley, D. R. (1989). The cDNA sequence of a human placental α-actinin. Nucleic Acids Research, 17, 6725-6725.

Millonig, R., Salvo, H., & Aebi, U. (1988). Probing actin polymerization by intermolecular cross-linking. Journal of Cell Biology, 106, 785-796.

Minura, N., & Asano, A. (1986). Isolation and characterisation of a conserved actin-binding domain from rat hepatic actinogelin, rat skeletal-muscle, and chicken gizzard α-actinins. Journal of Biological Chemistry, 261, 680-687.

Mimura, N., & Asano, A. (1987). Further characterisation of a conserved actin-binding 27 kDa fragment of actinogelin and α-actinins and mapping of their binding sites on the actin molecule by chemical cross-linking. Journal of Biological Chemistry, 262, 4717-23.

Minton, A. P. (1990). Quantitative characterisation of reversible molecular associations via analytical centrifugation. Anals of Biochemistry, 190, 1-6.

Mooseker, M. S., & Tilney, L. G. (1975). Organisation of an actin-filament-membrane complex: filament polarity and membrane attachment in the microvilli of intestinal epithelial cells. Journal of Cell Biology, 67, 725-743.

Morrow, J. S., Speicher, D. W., Knowles, W. J., Hsu, C .J., & Marchesi, V. (1980). Proceedings of the National Academy of Sciences of the United States of America, 77, 6592-96.

Morrow, J. S., & Marchesi, V. T. (1981). Self-assembly of spectrin oligomers *in vitro* - a basis for a dynamic cytoskeleton. Journal of Cell Biology, 88, 463-468.

Morrow, J. S. (1989). The spectrin membrane skeleton: emerging concepts. Current Opinion in Cell Biology, 1, 23-29.

Moser, H. (1984). Duchenne muscular dystrophy: pathogenic aspects and genetic prevention. Human Genetics, 66, 17-40.

Mulzer, K., Kampmann, L., Petrasch, P., & Schubert, D. (1990). Complex associations between membrane proteins analysed by analytical ultracentrifugation: studies on the erythrocyte membrane proteins band 3 and ankyrin. Colloid Polymer Science, 268, 60-64.

Nakamura, S., Sakurai, T., & Nonomura, T. (1991). Determination of the native subunit pattern of gizzard tropomyosin using antibodies specific to each subunit. Journal of Biochemistry, 109, 758-762.

Narvanen, O., Narvanen, A., Wasenius, V. M., Partanen, P., & Virtanen, I. (1987). A monoclonal-antibody against a synthetic peptide reveals common structures among spectrins and α-actinin. FEBS Letters, 224, 156-160.

Newell, J. O., & Schachman, H.K. (1990). amino acid substitutions which stabilise aspartate transcarbamoylase in the R state disrupt both homotropic and heterotropic effects. Biophysical Chemistry, 37, 183-196.

Niggli, V., & Gimona, M. (1993). Evidence for a ternary interaction between α-actinin, (meta)vinculin and acidic-phospholipid bilayers. European Journal of Biochemistry, 213, 1009-1015.

Nishizuka, Y. (1984). The role of protein kinase-C in cell-surface signal transduction and tumor promotion. Nature, 308, 693-698.

Noegel, A., Witke, W., & Schleicher, M. (1987). Calcium-sensitive non-muscle α-actinin contains EF-hand structures and highly conserved regions. FEBS Letters, 221, 391-396.

Nudel, V., Zuk, D., Einat, P., Zeelon, E., Levy, Z., Nevman, S., & Yaffe, D. (1989). Duchenne muscular-dystrophy gene-product is not identical in muscle and brain. Nature, 337, 76-78.

Oas, T. G., & Endow, S. A. (1994). Springs and hinges - dynamic coiled coils and discontinuities. Trends in Biochemical Sciences, 19, 51-54.

Ohlendieck, K., & Campbell, K. P. (1991). Dystrophin-associated proteins are greatly reduced in skeletal-muscle from *mdx* mice. Journal of Cell Biology, 115, 1685-1694.

Ohlendieck, K., Ervasti, J. M., Matsumura, K., Kahl, S. D., Leveille, C. J., & Campbell, K. P. (1991). Dystrophin-related protein is localized to neuromuscular-junctions of adult skeletal-muscle. Neuron, 7, 499-508.

Ohlendieck, K. (1996). Characterisation of the dystrophin-related protein utrophin in highly purified skeletal-muscle sarcolemma vesicles. Biochimica et Biophysica Acta-Biomembranes, 1283, 215-222.

Ohtaki, T., Tsukita, S., Mimura, N., Tsukita, S., & Asano, A. (1985). Interaction of actinogelin with actin - no nucleation but high gelation activity. European Journal of Biochemistry, 153, 609-620.

Omann, G. M., Allen, R. A., Bokoch, G. M., Painter, R. G., Traynor, A. E., & Sklar, L. A. (1987). Signal transduction and cytoskeletal activation in the neutrophil. Physiological Research, 67, 285-322.

O'Shea, E. K., Klemm, J. D., Kim, T., & Alber, T. (1991). X-ray structure of the GCN4 leucine zipper, a 2-stranded, parallel coiled coil. Science, 254, 539.

Otey, C. A., Pavalko, F. M., & Burridge, K. (1990). An interaction between α-actinin and the β-1 integrin subunit *in vitro*. Journal of Cell Biology, 111, 721-729.

Pacaud, M., & Harricane, M. C. (1987). Calcium control of macrophage cytoplasmic gelation - evidence for the involvement of the 7000 MR actin-bundling protein. Journal of Cell Science, 88, 81-94.

Pacaud, M., & Harricane, M. C. (1993). Macrophage α-actinin is not a calcium-modulated actin-binding protein. Biochemistry, 32, 363-374.

Pace, C. N., & Laurents, D. V. (1989). A new method for determining the heat capacity change for protein folding. Biochemistry, 28, 2520-2525.

Padmanabhan, S., Marqusee, S., Ridgeway, T., Laue, T. M., & Baldwin, R. L. (1990). relative helix-forming tendencies of non-polar amino-acids. Nature, 344, 268-270.

Palek, J. (1990). Hematology. W. Williams, E. Beutler, A. Erslev, & M. Lichtman, Eds. McGraw-Hill, New York, ed. 4, pp 569-581.

Parr, T., Waites, G. T., Patel, B., Millake, D. B., & Critchley, D. R. (1992). A chick skeletal-muscle α-actinin gene gives rise to 2 alternatively spliced isoforms which differ in the EF-hand calcium-binding domain. European Journal of Biochemistry, 210, 801-809.

Parry, D. A. N., & Cohen, C. (1991). Structure of the spectrin superfamily: a three-a-helix motif. In The Living Cell in Four Dimensions (G Paillotin, ed.), AIP Conference Proceedings 226, American Institute of Physics, New York, pp. 367-377.

Parry, D. A. D., Dixon, T. W., & Cohen, C. (1992). Analysis of the 3-α-helix motif in the spectrin superfamily of proteins. Biophysical Journal, 61, 858-867.

Pascual, J., Pfuhl, M., Rivas, G., Pastore, A., & Saraste, M. (1996). The spectrin repeat folds into a 3-helix bundle in solution. FEBS Letters, 383, 201-207.

Pasternak, C., Bischoff, R., Roberds, S. L., Cox, G. A., Campbell, K. P., Chamberlain, J., & Elson, E. L. (1995). Components of the dystrophin linkage system contribute to the mechanical reinforcement of the muscle-cell membrane. Molecular Biology of the Cell, 6, 883-883.

Pavalko, F. M., & Laroche, S. M. (1993). Activation of human neutrophils induces an interaction between the integrin-β-2-subunit (CD18) and the actin-binding protein α-actinin. Journal of Immunology, 151, 3795-3807.

Pavalko, F. M., Walker, D. M., Graham, L., Goheen, M., Doerschuk, C. M., & Kansas, G. S. (1995). The cytoplasmic domain of l-selectin interacts with cytoskeletal proteins via α-actinin - receptor positioning in microvilli does not require interaction with α-actinin. Journal of Cell Biology, 29, 1155-1164.

Pawson, T., & Gish, G. D. (1992). SH2 and SH3 domains - from structure to function. Cell, 71, 359-362.

Perkins, S. J. (1986). Protein volumes and hydration effects. The calculation of partial specific volumes, neutron scattering matchpoints and 280-nm absorption coefficients for proteins and glycoproteins from amino acid sequences. European Journal of Biochemistry, 157, 169-180.

Petrof, B. J., Shrager, J. B., Stedman, H. H., Kelly, A. M., & Sweeney, H. L. (1993). Dystrophin protects the sarcolemma from stresses developed during muscle-contraction. Proceedings of the National Academy of Sciences of the United States of America, 90, 3710-3714.

Podlubnaya, Z. A., Tskhovrebova, L. A., Zaalishvili, M. M., & Stefanenko, G. A. (1975). Electron microscopic study of α-actinin. Journal of Molecular Biology, 92, 357-359.

Pollard, T. D., Tseng, P. C. H., Rimm, D. L., Bichell, D. P., Williams, R. C., Sinard, J., & Sato, M. (1986). Characterization of α-actinin from *Acanthamoeba*. Cell Motility and the Cytoskeleton, 6, 649-661.

Pollerberg, G. E., Burridge, K., Krebs, K. E., Goodman, S. R., & Schachner, M. (1987). The 180 kD component of the neural cell adhesion molecule N-CAM is involved in cell-cell contacts and cytoskeleton-membrane interactions. Cell Tissue Research, 250, 227-236.

Pons, F., Augier, N., Heilig, R., Leger, J., Mornet, D., & Leger, J. J. (1990). Isolated dystrophin molecules as seen by electron-microscopy. Proceedings of the National Academy of Sciences of the United States of America, 87, 7851-7855.

Pons, F., Augier, N., Leger, J. O. C., Robert, A., Tome, F. M. S., Fardeau, M., Voit, T., Nicholson, L. V. B., Mornet, D., & Leger, J. J. (1991). A homologue of dystrophin is expressed at the neuromuscular-junctions of normal individuals and DMD patients, and of normal and *mdx* mice - immunological evidence. FEBS Letters, 282, 161-165.

Porter, G. A., Dmytrenko, G. M., Winkelmann, J. C., & Bloch, R. J. (1992). Dystrophin colocalizes with β-Spectrin in distinct subsarcolemmal domains in mammalian skeletal-muscle. Journal of Cell Biology, 117, 997-1005.

Rallison, J. M., & Harding, S. E. (1985). Excluded volume for pairs of triaxial ellipsoids at dominant brownian motion. Journal of Colloid Interface Science, 103, 284-289.

Ralston, G. B. (1975). The isolation of aggregates of spectrin from bovine erythrocyte membranes. Australian Journal of Biological Science, 28, 259-266.

Ren, R., Mayer, B. J., Cicchetti, P., & Baltimore, D. (1994). Identification of a 10-amino acid proline-rich SH3 binding-site. Science, 259, 1157-1161.

Richards, E. G., & Schachman, H. K. (1959). Ultracentrifuge studies with Rayleigh interference optics. I. General applications. Journal of Physical Chemistry, 63, 1578-1591.

Richardson, J. S., & Richardson, D. C. (1988). Amino-acid preferences for specific locations at the ends of α-helices. Science, 240, 1648-1652.

Rimm, D. L., Kebriaei, P., & Morrow, J. S. (1994). Molecular-cloning reveals alternative splice forms of human α(E)-catenin. Biochemical and Biophysical Research Communications, 203, 1691-1699.

Rosenberg, S., & Stracher, A. (1981). Isolation and characterization of an α-actinin-like protein from human-platelet cytoskeletons. Journal of Cell Biology, 91, A290-A290.

Ross, P. D., Howard, F. B., & Lewis, M. S. (1991). Thermodynamics of antiparallel hairpin-double helix equilibria in DNA oligonucleotides from equilibrium ultracentrifugation. Biochemistry, 30, 6269-6275.

Rost, B., & Sander, C. (1994). Combining evolutionary information and neural networks to predict protein secondary structure. Proteins-Structure Function and Genetics, 19, 55-72.

Roulier, E. M., Fyrberg, C., & Fyrberg, E. (1992). Perturbations of *Drosophila* α-actinin cause muscle paralysis, weakness, and atrophy but do not confer obvious nonmuscle phenotypes. Journal of Cell Biology, 116, 911-922.

Rowe, A. J. (1977). The concentration dependence of transport processes: A general description applicable to sedimentation translational diffusion and viscosity coefficients of macromolecular solutes. Biopolymers, 16, 2595-2611.

Ruoslahti, E., & Pierschbacher, M. D. (1987). New Perspectives in cell-adhesion - RGD and integrins. Science, 238, 491-7.

Sadler, I., Crawford, A. W., Michelson, J. W., & Beckerle, M. C. (1992). Zyxin and cCRP: two interactive LIM domain proteins associated with the cytoskeleton. Journal of Cell Biology, 119, 1573-1587.

Sahr, K. E., Laurila, P., Kotula, L., Scarpa, A. L., Coupal, E., Leto, T. L., Linnenbach, A. J., Winkelmann, J. C., Speicher, D. W., Marchesi, V. T., Curtis, P. J., & Forget, B. G. (1990). The complete cDNA and polypeptide sequences of human erythroid α-spectrin. Journal of Biological Chemistry, 265, 4434-4443.

Sanger, J. W., Mittal, B., & Sanger, J. M. (1984). Analysis of myofibrillar structure and assembly using fluorescently labeled conractile proteins. Journal of Cell Biology, 98, 825-833.

Sato, O., Nonomura, Y., Kimura, S., & Maruyama, K. (1992). Molecular shape of dystrophin. Journal of Biochemistry, 112, 631-636.

Schachman, H. K. (1959). Ultracentrifugation in Biochemistry. New York, Academic Press.

Schleicher, M., Noegel, A., Schwarz, T., Wallraff, E., Brink, M., Faix, J., Gerisch, G., & Isenberg, G. (1988). A *Dictyostelium* mutant with severe defects in α-actinin - its

characterization using cDNA probes and monoclonal-antibodies. Journal of Cell Science, 90, 59-71.

Schollmeyer, J. E., Furcht, L. T., Goll, D. E., Robson, R. M., & Stromer, M. H. (1976). Localisation of contractile proteins in smooth muscle cells and in normal and transformed fibroblasts, in Cell Motility, Vol. A. R. Golgman, T. Pollard, & J. Rosenbaum editors. Cold Spring Harbor Laboratory, Cold Spring Harbor, New York, 361-388.

Schwartz, M. A. (1992). Transmembrane signaling by integrins. Trends in Cell Biology, 2, 304-307.

Sealock, R., & Froehner, S. C. (1994). Dystrophin-associated proteins and synapse formation - is α-dystroglycan the agrin receptor. Cell, 77, 617-619.

Senter, L., Luise, M., Presotto, C., Betto, R., Teresi, A., Ceoldo, S., & Salviati, G. (1993). Interaction of dystrophin with cytoskeletal proteins - binding to talin and actin. Biochemical and Biophysical Research Communications, 192, 899-904.

Shen, B. W., Josephs, R., & Steck, T. L. (1986). Ultrastructure of the intact skeleton of the human-erythrocyte membrane. Journal of Cell Biology, 102, 997-1006.

Sheterline, P., Clayton, J., & Sparrow, J. C. (1995). Actin. Protein Profile, 2, 1.

Shibasaki, F., Fukami, K., Fukui, Y., & Takenawa, T. (1994). Phosphatidylinositol 3-kinase binds to α-actinin through the p85 subunit. Biochemical Journal, 302, 551-557.

Shotton, D. M., Burke, B., & Branton, D. (1979). The molecular structure of human erythocyte spectrin. Biophysical and electron microscopic studies. Journal of Molecular Biology, 130, 303-329.

Singh, I., Goll, D. E., Robson, R. M., & Stromer, M. H. (1977). N- and C-terminal amino acids of purified α-actinin. Biochimica et Biophysica Acta, 491, 29-45.

Sklar, G. C., Omann, G. M., & Painter, R. G. (1985). Relationship of actin polmerisation and depolymerisation to light-scattering in human-neutrophils - dependence on receptor occupancy and intracellular calcium. Journal of Cell Biology, 101, 1161-1166.

Small, J. V., Isenberg, G., & Celis, J. E. (1978). Polarity of actin at the leading edge of cultured cells. Nature, 272, 638-639.

Small, V., Furst, D. O., & Thurnell, L-E. (1992). The cytoskeletal lattice of muscle-cells. Journal of Biochemistry, 208, 559-572.

Smith, D. B., & Johnson, K. S. (1988). Single step purification of proteins expressed in *E. coli* as fusion proteins with glutathione-S-transferase. Gene, 67, 31-40.

Smith, G. D., & Schachman, H. K. (1973). Effect of D_2O and nicotinamide adenine dinucleotide on the sedimentation properties and structure of glyceride phosphate dehydrogenase. Biochemistry, 12, 3789-3801.

Smith, G. P. (1973). Unequal crossover and the evolution of multigene families. Cold Spring Harbor Symposium on Quantitative Biology, 38, 507-513.

Sobue, K., Muramoto, Y., Fujita, M., & Kakiuchi, S. (1981). Calmodulin-binding protein of erythrocyte cytoskeleton. Biochemical and Biophysical Research Communications, 100, 1063-1070.

Soucek, D. A., & Adams, E. T. (1976). Molecular weight distributions from sedimentation equilbrium of nonideal solutions. Journal of Colloids and Interface Science, 55, 571-582.

Speicher, D. W., Weglarz, L., & Desilva, T. M. (1992). Properties of human red-cell spectrin heterodimer (side-to-side) assembly and identification of an essential nucleation site. Journal of Biological Chemistry, 267, 14775-14782.

Speicher, D. W., Morrow, J. S., Knowles, W. J., & Marchesi, V. T. (1982). A structural model of human-erythrocyte spectrin - alignment of chemical and functional domains. Journal of Biological Chemistry, 257, 9093-9101.

Speicher, D. W., & Marchesi, V. T. (1984). Erythrocyte spectrin is comprised of many homologous triple helical segments. Nature, 311, 177-180.

Speicher, D.W. (1985). The present status of erythrocyte spectrin structure - the 106-residue repetitive structure is a basic feature of an entire class of proteins. Journal of Cellular Biochemistry, 30, 245-58.

Speicher, D. W., Desilva, T. M., Speicher, K. D., Ursitti, J. A., Hembach, P., & Weglarz, L. (1993). Location of the human red-cell spectrin tetramer binding-site and detection of a related closed hairpin loop dimer using proteolytic footprinting. Journal of Biological Chemistry, 268, 4227-4235.

Speicher, D. W., & Ursitti, J. A. (1994). Conformation of a mammoth protein. Current Biology, 4, 154-157.

Stedman, H. H., Sweeney, H. L., Shrager, J. B., Maguire, H. C., Pannettieri, R. A., Petrof, B. J., Narusawa, M., Leferovich, J., Sladky, J. T., & Kelly, A.M. (1991). The *mdx* mouse diaphragm reproduces the degenerative changes of Duchenne muscular-dystrophy. Nature, 352, 536-539.

Steinberg, I. Z., & Schachman, H. K. (1966). Ultracentrifuge studies with absorption optics. V. Analysis of interacting systems involving macromolecules and small molecules. Biochemistry, 5, 3728-3747.

Stewart, M., & McLachlan, A. D. (1975). Fourteen actin-binding sites on tropomyosin? Nature, 257, 331-333.

Stickel, S. K., & Wang, Y. L. (1987). α-Actinin containing aggregates in transformed-cells are highly dynamic structures. Journal of Cell Biology, 104, 1521-1526.

Stickel, S. K., & Wang, Y. (1988). Synthetic peptide GRGDS induces dissociation of α-actinin and vinculin from the sites of focal contacts. Journal of Cell Biology, 107, 1231-1239.

Straub, V., Bittner, R. E., Leger, J. J., & Voit, T. (1992). Direct visualization of the dystrophin network on skeletal-muscle fiber membrane. Journal of Cell Biology, 119, 1183-1191.

Strynadka, N. C. J., & James, M. N. J. (1989). Crystal structures of the helix-loop-helix calcium-binding proteins. Annual Review of Biochemistry, 58, 951-998.

Strynadka, N. C. J., & James, M. N. J. (1991). Towards the understanding of the effects of calcium on protein structure and function. Current Opinion in Structural Biology, 1, 905-914.

Takeda, T., & Yamamoto, M. (1987). Analysis and *in vivo* disruption of the gene coding for calmodulin in *Schizosaccharomyces pombe*. Proceedings of the National Academy of Sciences of the United States of America, 84, 3580-3584.

Takeichi, M., Hirano, S., Matsuyoshi, N., & Fujimori, T. (1992). Cytoplasmic control of cadherin-mediated cell-cell adhesion. Cold Spring Harbor Symposium on Quantitative Biology, 57, 327-334.

Takemitsu, M., Ishiura, S., Koga, R., Kamakura, K., Arahata, K., Nonaka, I., & Sugita, H. (1991). Dystrophin-related protein in the fetal and denervated skeletal- muscles of normal and *mdx* mice. Biochemical and Biophysical Research Communications, 180, 1179-1186.

Tanford, C. (1961). Physical Chemistry of Macromolecules. New York, Wiley.

Taylor, K. A., & Taylor, D. W. (1993). Projection image of smooth-muscle α-actinin from 2-dimensional crystals formed on positively charged lipid layers. Journal of Molecular Biology, 230, 196-205.

Taylor, K. A., & Taylor, D. W. (1994). Formation of 2-dimensional complexes of F-actin and cross-linking proteins on lipid monolayers - demonstration of unipolar α-actinin-F-actin cross-linking. Biophysical Journal, 67, 1976-1983.

Tidball, J. G. (1987). α-Actinin is absent from the terminal segments of myofibrils and from subsarcolemmal densities in frog skeletal-muscle. Experimental Cell Research, 170, 469-482.

Tinsley, J. M., Blake, D. J., Roche, A., Fairbrother, U., Riss, J., Byth, B. C., Knight, A. E., Kendrick-Jones, J., Suthers, G. K., Love, D. R., Edwards, Y. H., & Davies, K. E. (1992). Primary structure of dystrophin-related protein. Nature, 360, 591-593.

Tinsley, J. M., Potter, A. C., Phelps, S. R., Fisher, R., Trickett, J. I., & Davies, K. E. (1996). Amelioration of the dystrophic phenotype of *mdx* mice using a truncated utrophin transgene. Nature, 384, 349-353.

Touhara, K., Inglese, J., Pitcher, J. A., Shaw, G., & Lefkowitz, R. J. (1994). Binding of G-protein β-γ-subunits to pleckstrin homology domains. Journal of Biological Chemistry, 269, 10217-10220.

Trave, G., Lacombe, P. J., Pfuhl, M., Saraste, M., & Pastore, A. (1995). Molecular mechanism of the calcium-induced conformational change in the spectrin EF-hands. EMBO Journal, 14, 4922-4931.

Tse, W. T., Lecomte, M. C., Costa, F. F., Garbarz, M., Feo, C., Boivin, P., Dhermy, D., & Forget, B. G. (1990). Point mutation in the β-spectrin gene associated with α-I/74 hereditary elliptocytosis - implications for the mechanism of spectrin dimer self-association. Journal of Clinical Investigation, 86, 909-916.

Tsukada, S., Simon, M. I., Witte, O. N., & Katz, A. (1994). Binding of β-γ-subunits of heterotrimeric G-proteins to the PH domain of Bruton tyrosine kinase. Proceedings of the National Academy of Sciences of the United States of America, 91, 11256-11260.

Tsukita, S., Tsukita, S., & Ishikawa, H. (1983). Association of actin and 10 nm filaments with the dense body in smooth muscle cells of the chicken gizzard. Cell Tissue Research, 229, 233-242.

Tsukita, S., Itoh, M., Nagafuchi, A., Yonemura, S., & Tsukita, S. (1993). Submembranous junctional plaque proteins include potential tomor suppressor molecules. Journal of Cell Biology, 123, 1049-1053.

Tufty, R. M., & Kretsinger, R. H. (1975). Tropinin and parvalbumin calcium binding regions predicted in myosin light chain and T4 lysozyme. Science, 185, 167-169.

Ungewickell, E., & Gratzer, W. (1978). Self-association of human spectrin. European Journal of Biochemistry, 88, 379-385.

Ursitti, J. A., Pumplin, D. W., Wade, J. B., & Bloch, R. J. (1991). Ultrastructure of the human erythrocyte cytoskeleton and its attachment to the membrane. Cell Motility and the Cytoskeleton, 19, 227-243.

Ursitti, J. A., Kotula, L., Desilva, T. M., Curtis, P. J., & Speicher, D. W. (1996). Mapping the human erythrocyte β-spectrin dimer initiation site using recombinant peptides and correlation of its phasing with the α-actinin dimer site. Journal of Biological Chemistry, 271, 6636-6644.

Vancompernolle, K., Gimona, M., Herzog, M., Vandamne, J., Vandekerckhqve, J., & Small, V. (1990). Isolation and sequence of a tropomyosin-binding fragment of turkey gizzard calponin. FEBS Letters, 274, 146-150.

Van Holde, K. E., & Baldwin, R. L. (1958). Rapid attainment of sedimentation equilibrium. Journal of Physical Chemistry, 62, 734-743.

Van Holde, K. E., Miller, K., Schabtach, E., & Libertini, L. (1991). Assembly of *Octopus dofleini* hemocyanin. A study of the kinetics by sedimentation, light scattering and electron microscopy. Journal of Molecular Biology, 217, 307-321.

Van Ommen, G. J. B., Bertelson, C., ginjaar, H. B., den Dunnen, J. T., Bakker, E., Chelly, J., Matton, M., Van Essen, A. J., Bartley, J., Kunkel, L. M., & Pearson, P. L. (1987). Long-range genomic map of the Duchenne muscular dystrophy (DMD) gene: Isolation and use of J66 (DXS268), a distal intragenic marker. Genomics, 1, 329-336.

Viel, A., & Branton, D. (1994). Interchain binding at the tail end of the *Drosophila* spectrin molecule. Proceedings of the National Academy of Sciences of the United States of America, 91, 10839-10843.

Viel, A., Gee, M., & Branton, D. (1995). Molecular analysis of interchain binding at the tail end of *Drosophila* spectrin. Molecular Biology of the Cell, 6, 1565-1565.

Viel, A., & Branton, D. (1996). Spectrin - on the path from structure to function. Current Opinion in Cell Biology, 8, 49-55.

Vogelstein, B., & Gillespie, D. (1979). Preparative and analytical purification of DNA from agarose. Proceedings of the National Academy of Sciences of the United States of America, 76, 615-619.

Volberg, T., Zick, Y., Dror, R., Sabanay, L., Gilon, C., Levitzki, A., & Geiger, B. (1992). The effect of tyrosine-specific protein phosphorylation on the assembly of adherens-type junctions. EMBO Journal, 11, 1733-1742.

Volk, T., & Geiger, B. (1984). A 135-kD-membrane protein of intercellular adherens junctions. EMBO Journal, 3, 2249-2260.

Wachsstock, D. H., Schwarz, W. H., & Pollard, T. D. (1993). Affinity of α-actinin for actin determines the structure and mechanical-properties of actin filament gels. Biophysical Journal, 65, 205-214.

Waites, G. T., Graham, I. R., Jackson, P., Millake, D. B., Patel, B., Blanchard, A. D., Weller, P. A., Eperon, I. C., & Critchley, D. R. (1992). Mutually exclusive splicing of calcium-

binding domain exons in chick α-actinin. Journal of Biological Chemistry, 267, 6263-6271.

Wallis, C. J., Wenegieme, E. F., & Babitch, J. A. (1992). Characterization of calcium-binding to brain spectrin. Journal of Biological Chemistry, 267, 4333-4337.

Wallis, C. J., Babitch, J. A., & Wenegieme, E. F. (1993). Divalent-cation binding to erythrocyte spectrin. Biochemistry, 32, 5045-5050.

Wallraff, E., Schleicher, M., Modersitzki, M., Rieger, D., Isenberg, G., & Gerisch, G. (1986). Selection of *Dictyostelium* mutants defective in cytoskeletal proteins - use of an antibody that binds to the ends of α-actinin rods. EMBO Journal, 5, 61-67.

Wasenius, V. M., Narvanen, O., Lehto, V. P., & Saraste, M. (1987). α-Actinin and spectrin have common structural domains. FEBS Letters, 221, 73-76.

Wasenius, V. M., Saraste, M., Salven, P., Eramaa, M., Holm, L., & Lehto, V. P. (1989). Primary structure of the brain α-spectrin. Journal of Cell Biology, 108, 79-93.

Watterson, D. M., Sharief, F., & Vanaman, T. C. (1980). The complete amino acid sequence of the calcium-dependent modulator protein (calmodulin) of bovine brain. Journal of Biological Chemistry, 255, 962-975.

Way, M., Pope, B., & Weeds, A. G. (1992). Evidence for functional homology in the F-actin binding domains of gelsolin and α-actinin - implications for the requirements of severing and capping. Journal of Cell Biology, 119, 835-842.

Wenegieme, E. F., Babitch, J. A., & Naren, A. P. (1994). Cation-binding to chicken gizzard α-actinin. Biochimica et Biophysica Acta Protein Structure and Molecular Enzymology, 1205, 308-316.

Wenegieme, E. F., Naren, A. P., & Bobich, J. A. (1996). Cation effects on the conformations of muscle and nonmuscle α-actinins. Biometals, 9, 259-265.

Wessel, G. M., & Chen, S. M. W. (1993). Transient, localized accumulation of α-spectrin during sea-urchin morphogenesis. Developmental Biology, 155, 161-171.

Williamson, M. P. (1994). The structure and function of proline-rich regions in proteins. Biochemical Journal, 297, 249-260.

Wilmotte, R., Marechal, J., Morle, L., Baklouti, F., Philippe, N., Kastally, R., Kotula, L., Delaunay, J., & Alloisio, N. (1993). Low expression allele-α(^{LELY}) of red-cell spectrin is associated with mutations in exon-40 (α(V/41)-polymorphism) and intron-45 and with partial skipping of exon-46. Journal of Clinical Investigation, 91, 2091-2096.

Winder, S. J., Hemmings, L., Maciver, S. K., Bolton, S. J., Tinsley, J. M., Davies, K. E., Critchley, D. R., & Kendrick-Jones, J. (1995). Utrophin actin-binding domain - analysis of actin-binding and cellular targeting. Journal of Cell Science, 108, 63-71.

Winder, S. J., & Kendrick-Jones, J. (1995). Calcium/calmodulin-dependent regulation of the NH2-terminal F-actin binding domain of utrophin. FEBS Letters, 357, 125-128.

Winder, S. J., Gibson, T. J., & Kendrick-Jones, J. (1995). Dystrophin and utrophin - the missing links. FEBS Letters, 369, 27-33.

Winder, S. J., Gibson, T. J., & Kendrick-Jones, J. (1996). Low probability of dystrophin and utrophin coiled coil regions forming dimers. Biochemical Society Transactions, 24, 280S.

Winkelmann, J. C., Chang, J. G., Tse, W. T., Scarpa, A. L., Marchesi, V. T., & Forget, B. G. (1990). Full-length sequence of the cDNA for human erythroid β-spectrin. Journal of Biological Chemistry, 265, 11827-11832.

Winograd, E., Hume, D., & Branton, D. (1991). Phasing the conformational unit of spectrin. Proceedings of the National Academy of Sciences of the United States of America, 88, 10788-10791.

Witke, W., Schleicher, M., Lottspeich, F., & Noegel, A. (1986). Studies on the transcription, translation, and structure of α-actinin in *Dictyostelium discoideum*. Journal of Cell Biology, 103, 969-975.

Witke, W., Schleicher, M., & Noegel, A. A. (1992). Redundancy in the microfilament system - abnormal-development of *Dictyostelium* cells lacking 2 F-actin cross-linking proteins. Cell, 68, 53-62.

Witke, W., Hofmann, A., Koppel, B., Schleicher, M., & Noegel, A. A. (1993). The calcium-binding domains in nonmuscle type α-actinin - biochemical and genetic-analysis. Journal of Cell Biology, 121, 599-606.

Wysolmerski, R. B., & Lagunoff, D. (1988). Inhibition of endothelial-cell retraction by ATP depletion. American Journal of Pathology, 132, 28-37.

Wysolmerski, R. B., & Lagunoff, D. (1990). Involvement of myosin light-chain kinase in endothelial-cell retraction. Proceedings of the National Academy of Sciences of the United States of America, 87, 16-20.

Wyszynski, M., Lin, J., Rao, A., Nigh, E., Beggs, A. H., Craig, A. M., & Sheng, M. (1997). Competitive binding of α-actinin and calmodulin to the NMDA receptor. Nature, 385, 439-442.

Xu, Y., Prabhakaran, M., Johnson, M. E., & Fung, L. W. M. (1990). Secondary structure prediction for the spectrin 106-amino acid segment, and a proposed model for tertiary structure. Journal of Biomolecular Structure and Dynamics, 8, 55-62.

Yan, Y., Winograd, E., Viel, A., Cronin, T., Harrison, S. C., & Branton, D. (1993). Crystal structure of the repetitive segments of spectrin. Science, 262, 2027-2030.

Yao, L., Kawakami, Y., & Kawakami, T. (1994). The pleckstrin homology domain of Bruton tyrosine kinase interacts with protein-kinase-C. Proceedings of the National Academy of Sciences of the United States of America, 91, 9175-9179.

Youssoufian, H., McAfee, M., & Kwiatkowski, D. J. (1990). Cloning and chromosomal localization of the human cytoskeletal α-actinin gene reveals linkage to the β-spectrin gene. American Journal of Human Genetics, 47, 62-72.

Yu, H., Chen, J. K., Feng, S., Dalgarno, D. C., Brauer, A., & Schreiber, S. L. (1994). Structural basis for the binding of proline-rich peptides to SH3 domains. Cell, 76, 933-945.

Zellweger, H., & Hanson, J. W. (1967). Psychometric studies in muscular dystrophy type IIIa (Duchenne). Developmental Medical Child Neurology, 9, 576-581.

Zhang, J., Fry, M., Waterfield, M. D., Jaken, S., Liao, L., Fox, J. E. B., & Rittenhous, S. E. (1992). Activated phosphoinositide 3-kinase associates with membrane skeleton in thrombin-exposed platelets. Journal of Biological Chemistry, 267, 4686-4692.

7. PUBLICATION LIST

Flood, G., Kahana, E., Gilmore, A. P., Rowe, A. J., Gratzer, W. B., and Critchley, D. R. (1995). Asoociation of structural repeats in the α-actinin rod domain. Alignment of inter-subunit interactions. Journal of Molecular Biology, 252, 227-234.

Flood, G. J., Gratzer, W. B., Kahana, E., Rowe, A. J., and Critchley, D. R. (1995). Association of structural repeats in α-actinin. Biochemical Society Transactions, 23, 399S.

Flood, G., Rowe, A. J., Critchley, D. R., and Gratzer, W. B. (1997). Further analysis of the role of spectrin repeat motifs in α-actinin dimer formation. European Biophysical Journal. In Press.

Kahana, E., Flood, G., and Gratzer, W. B. (1997). Physical properties of dystrophin rod domain. Cell Motility and the Cytoskeleton. In Press.